Functional dissection of recurrent feedback signaling within the mushroom body network of the *Drosophila* larva

Funktionelle Analyse einer Rückkopplungsschleife innerhalb der Pilzkörper von *Drosophila* Larven

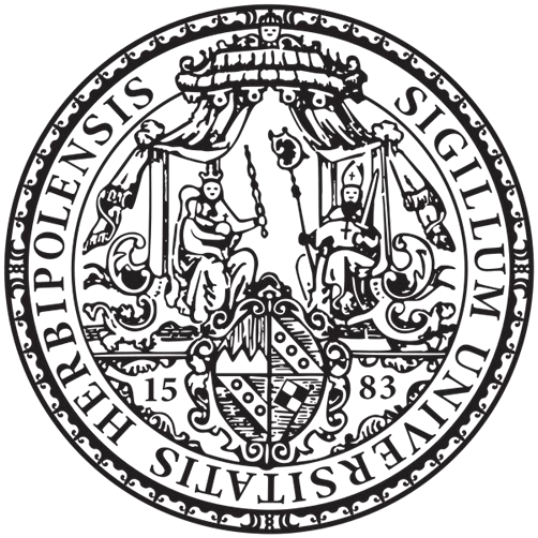

Doctoral thesis for a doctoral degree

at the Graduate School of Life Sciences,

Julius-Maximilians-Universität Würzburg,

Section Neurosciences

Submitted by

Radostina Lyutova

From Varna

Würzburg, 2019

The present work was accomplished at the Chair of Neurobiology and Genetics, Theodor-Boveri-Institute, Biocenter, at the University of Würzburg.

Submitted on: 15.05.2019

Members of the *Promotionskomitee*:

Chairperson: Prof. Dr. med. Manfred Gessler

Primary Supervisor: Dr. Dennis Pauls

Supervisor (Second): Prof. Dr. Thomas Raabe

Supervisor (Third): Prof. Dr. Christian Wegener

Supervisor (Fourth): Prof. Dr. Björn Brembs

Date of Public Defense: ……..

Date of Receipt of Certificates: ……..

Table of contents

Index of figures and tables

List of abbreviations

A

AC: adenylyl cyclase

ACh: acetylcholine

AChR: acetylcholine receptor

AEL: after egg laying

AL: antennal lobe

AM: amyl acetate

AN: antennal nerve

ARM: anesthesia-resistent memory

B

BA: benzaledyde

BAC: bacterial artificial chromosome

BL: blue light

Brp: Bruchpilot

C

cAMP: cyclic adenosine 3’5’-monophosphate

ChR: Chennelrhodopsin

CNS: central nervous system

CR: conditioned responce

CS: conditioned stimulus

D

DA: dopamine

DAG: diacylglycerol

DAN: dopaminergic neuron

dcr2: dicer2

DCSO: dorsal cibarial sense organ

Dilp: *Drosophila* insulin like peptide

DMSO: dimethyl sulfoxide

dnc: dunce

DO: dorsal organ

DOG: dorsal organ ganglion

DPSO: dorsal pharyngeal sense organ

DS: dark side

dTRPA1: *Drosophila* transient receptor potential A1

E

EM: electron microscopy

F

FIM: FTIR-based Imaging Method

FLP-FRT: flipase-flipase recognition target

G

GC: genetic construct

GFP: green fluorescent protein

GR: gustatory receptor

GRN: gustatory receptor neuron

I

InR: insulin receptor

IP3: inositol triphosphate

K

KC: Kenyon cell

L

LAL: larval antennal lobe

LBN: labial nerve

LED: light-emitting diodes

LH: lateral horn

LN: labral nerve

LSO: labral sense organ

LTM: long-term memory

M

MARCM: mosaic analysis with a repressible cell marker

MB: mushroom body

MBIN: mushroom body input neuron

MBON: mushroom body output neuron

MN: maxillary nerve

mPN: multiglomerular PN

MTM: middle-term memory

N

NS: nervous system

O

OAN: octopaminergic neuron

OCT: octanol

OI: olfactory index

OR: olfactory receptor

ORN: olfactory receptor neuron

P

PI: performance index

PKA: protein kinase A

PKC: protein kinase C

PLC: phospholipase C

PN: projection neuron

pPAM: primary-lineage protocerebral anterior medial

PPSO: posterior pharyngeal sense organ

PREF: preference index

R

RL: red light

rpr: reaper

Rsh: radish

RT: retention time

rut: rutabaga

S

SEZ: subesophageal zone

sNPF: short neuropeptide F

STM: short-term memory

T

TNT: tetanus toxin

TO: terminal organ

TOG: terminal organ ganglion

U

UAS: upstream activation sequence

uPN: uniglomerular PN

UR: unconditioned response

US: unconditioned stimulus

V

VCSO: ventral cibarial sense organ

VO: ventral organ

VOG: ventral organ ganglion

VPSO: ventral pharyngeal sense organ

Abstract

Behavioral adaptation to environmental changes is crucial for animals' survival. The prediction of the outcome of one owns action, like finding reward or avoiding punishment, requires recollection of past experiences and comparison with current situation, and adjustment of behavioral responses. The process of memory acquisition is called learning, and the *Drosophila* larva came up to be an excellent model organism for studying the neural mechanisms of memory formation. In *Drosophila*, associative memories are formed, stored and expressed in the mushroom bodies. In the last years, great progress has been made in uncovering the anatomical architecture of these brain structures, however there is still a lack of knowledge about the functional connectivity.

Dopamine plays essential roles in learning processes, as dopaminergic neurons mediate information about the presence of rewarding and punishing stimuli to the mushroom bodies. In the following work, the function of a newly identified anatomical connection from the mushroom bodies to rewarding dopaminergic neurons was dissected. A recurrent feedback signaling within the neuronal network was analyzed by simultaneous genetic manipulation of the mushroom body Kenyon cells and dopaminergic neurons from the primary protocerebral anterior (pPAM) cluster, and learning assays were performed in order to unravel the impact of the Kenyon cells-to-pPAM neurons feedback loop on larval memory formation.

In a substitution learning assay, simultaneous odor exposure paired with optogenetic activation of Kenyon cells in fruit fly larvae in absence of a rewarding stimulus resulted in formation of an appetitive memory, whereas no learning behavior was observed when pPAM neurons were ablated in addition to the KC activation. I argue that the activation of Kenyon cells may induce an internal signal that mimics reward exposure by feedback activation of the rewarding dopaminergic neurons. My data further suggests that the Kenyon

cells-to-pPAM communication relies on peptidergic signaling via short neuropeptide F and underlies memory stabilization.

Zusammenfassung

Eine Anpassung des eigenen Verhaltens an Veränderungen der Umwelt ist unerlässlich für das Überleben der Tiere. Vorhersage über die Konsequenzen der eigenen Handlungen, z.B. belohnt oder bestraft zu werden, erfordert den Vergleich von gemachten Erfahrungen und der aktuellen Situation. Eine solche Vorhersage kann zu einer Verhaltensanpassung führen. Der Prozess der Gedächtnisbildung ist auch bekannt als Lernen. Als hervorragender Modellorganismus zum Erforschen der Lernverhaltensmechanismen hat sich die *Drosophila* Larve etabliert. In *Drosophila* werden olfaktorische Gedächtnisse in einer bilateralen Struktur des Protozerebrums gespeichert, den Pilzkörpern. In den letzten Jahren sind erhebliche Fortschritte in der Beschreibung der anatomischen Strukturen der Pilzkörper gemacht worden. Allerdings ist die funktionelle Konnektivität dieser Gehirnstrukturen noch unzureichend verstanden.

Dopamin spielt eine essentielle Rolle in Lernprozessen. Dopaminerge Neurone vermitteln Informationen über das Vorliegen belohnender oder bestrafender Stimuli. Die Funktion einer vor kurzem beschriebenen anatomischen Verbindung von den Pilzkörpern zu belohnenden dopaminergen pPAM Neuronen wurde in der folgenden Arbeit untersucht, und der rückläufige Signalweg innerhalb des neuronalen Netzwerks wurde mittels simultaner genetischer Manipulation der Pilzkörperneurone, die sog. Kenyon Zellen, und der pPAM Neuronen analysiert. Der Einfluss der Rückkopplungsschleife zwischen Kenyon Zellen und pPAM Neuronen auf das larvale Verhalten wurde durch verschiedene Verhaltensexperimente getestet.

In dieser Arbeit wurden *Drosophila* Larven darauf trainiert, einen Duft mit optogenetischer Aktivierung der Pilzkörper Neurone zu assoziieren. Dabei konnte die Ausbildung eines positiven Gedächtnisses in Abwesenheit einer physischen Belohnung beobachtet werden. Wurden aber zusätzlich die dopaminergen Neurone des pPAM Clusters ablatiert, so zeigten die Larven keine Expression des Gedächtnisses mehr. Meine Daten zeigten, dass die

Aktivierung der Kenyon Zellen in einer Aktivierung der dopaminergen Neurone über der Rückkopplungsschleife resultiert, und dementsprechend einen internen Belohnungssignalweg einleitet. Dadurch wird das Vorhandensein einer „echten“ Belohnung nachgeahmt. Es konnte weiterhin gezeigt werden, dass die Rückkopplung von den Kenyon Zellen zu den pPAM Neurone von peptiderger Natur ist. Die Kenyon Zellen exprimieren das Neuropeptid short neuropeptide F, das an Rezeptoren in den pPAM Neurone bindet und das Lernverhalten beeinflusst. Darüber hinaus konnte gezeigt werden, dass die Aktivierung der Rückkopplungsschleife eine Auswirkung auf die Stabilität des positiven Gedächtnisses in Richtung nachhaltiger Erinnerungen hat.

I. General Introduction

1. A historical overview of *Drosophila* research

It is more than 100 years that *Drosophila melanogaster* is used as a genetic model organism [Stephenson and Metcalfe 2013; Bellen et al. 2010]. In 1901, the fruit fly, cheap and fast breading, was first introduced in the lab of William Ernest Castle (1867 - 1962), a professor at Harvard University to work on the genetics of coat-color in mice and guinea pigs. Following his advice, in 1903 Professor William J Moenkhaus (1871 - 1947) at Indiana University Medical School incorporated *Drosophila* in his work. Later, Moenkhaus convinced the entomologist Frank E Lutz (1879 - 1943) at the Station for Experimental Evolution at the Carnegie Institution (Cold Spring Harbor) of the advantages of *Drosophila* as a model organism for studying development and evolution [Kohler 1993; Stephenson and Metcalfe 2013]. The key event in establishing the fruit fly as a common model organism in genetic research was the work of Thomas Hunt Morgan (1866 - 1945) and the setup of “the fly room” at Columbia University, New York in 1906. Morgan bred a culture of *Drosophila* with red eyes for around one year as he found a white-eyed male fly. After further inbreeding and a series of crossings of red- and white-eyed flies he suggested that the white color of the eyes is carried on the X chromosome and laid the foundation for research on sex-linked inheritance [Morgan 1910, 1911]. For his theory of inheritance Morgan won the Nobel Prize in 1933. Based on Morgan’s work one of his students, Alfred Henry Sturtevant (1891 - 1970), assembled the first genetic map of six sex-linked mutations and described the process of cross-over, the interchange of sections of homologous non-sister chromatids [Sturtevant 1913]. Another student of Morgan, Hermann Joseph Muller (1890 - 1967), discovered the balancer chromosomes in 1918 [Muller 1918]. While working at the University of Texas he did observations on genetic mutations produced by ionizing radiation and described X-rays produced mutations in a dose-response relationship as well as inversions, translocations and fragmentations within chromosomes [Muller 1927]. For his discoveries Muller received the Nobel Prize in 1946.

Besides genetic studies, *Drosophila* became an important model organism in developmental neuroscience. Already in 1915 mutations in *Notch* were identified to cause wing malformations [Morgan and Bridges 1916]. Later, Donald F Poulson linked *Notch* and neuronal development [Poulson 1937]. In the 1980s, *Notch* and its ligand *Delta* were cloned [Artavanis-Tsakonas et al. 1983; Vassin et al. 1987; Wharton et al. 1985]. Further research on the *Notch* signaling pathway resulted in identification of other key players and their role in neurogenesis and neuronal differentiation [Artavanis-Tsakonas et al. 1995; Artavanis-Tsakonas et al. 1999]. A milestone in developmental biology was the discovery of *homeotic (Hox)* genes in the 1950-80s. Mutations in genes affecting the segmentation in *Drosophila* during development were studied by Lewis and Sanchez-Herrero and the *bithorax* complex, including the three genes *Ultrabithorax*, *Abdominal-A* and *Abdominal-B*, was identified to be crucial for the segmental identity of thorax and abdomen of larvae and flies [Lewis 1978; Sanchez-Herrero et al. 1985]. In the 1970s and 1980s Nüsslein-Volhard and Wieschaus performed a systematical chemical mutagenesis screen and identified 139 genes (incl. *Hedgehog*, *Wingless* and *Tumor growth factor-β*) involved in larval development [Jurgens et al. 1984; Nusslein-Volhard and Wieschaus 1980; Nusslein-Volhard et al. 1984; Wieschaus et al. 1984]. In 1995 Nüsslein-Volhard, Wieschaus and Lewis won the Nobel Prize for their work on genetic control of early embryonic development. The characterization of developmental genes as well as complexes of *Hox* genes in *Drosophila* revealed similarities to those in other organisms resulting in the identification of conserved signaling pathways involved in neurogenesis and development from fruit flies to higher vertebrates [Charron and Tessier-Lavigne 2007; Duboule 2007; Ho and Scott 2002].

The groundwork in the field of behavioral neurogenetics was laid by Seymour Benzer in the 1960-70s. He reasoned that genes controlling neuronal function can be identified by combining chemical mutagenesis and genetic analysis of fly's behavior. After the first studies on rhythmic behavior in flies in the 1930s - 50s by Bünning, Kalmus, and Pittendrigh [Bünning 1935; Kalmus 1935, 1938, 1940; Pittendrigh 1954], Benzer established a behavioral assay to observe circadian rhythms in *Drosophila*: the light countercurrent assay [Benzer 1967]. In 1971 Benzer and Konopka described three different mutations in a gene that affects eclosion rhythm and locomotor activity and called this gene *period* (*per*) [Konopka and Benzer 1971]. 13 years later the group of Rosbash and Hall dissected the function of *per* and the concept of the molecular clock was introduced [Reddy et al. 1984; Zehring et al. 1984]. In 1994 forward

genetic screens in the group of Young led to the isolation of the *timeless* gene, another key player in the molecular mechanism of circadian rhythm in *Drosophila* [Sehgal et al. 1994]. Hall, Rosbash and Young received the Nobel Prize in Physiology or Medicine "*for their discoveries of molecular mechanisms controlling the circadian rhythm*" in 2017. In the 1970s, another behavioral assay was established in Benzer's laboratory, an olfactory shock-avoidance learning assay [Quinn et al. 1974]. Performing this assay allowed Benzer's group to study the mechanisms of learning behavior and memory formation in flies. The establishment of a robust behavioral assays resulted in the identification of the first learning mutant, *dunce* (*dnc*) [Dudai et al. 1976] and in 1979 first results were published on learning behavior in wild type and mutant *Drosophila* larvae [Aceves-Pina and Quinn 1979]. In the following years it was shown that *dnc* encodes a cAMP phosphodiesterase, a crucial enzyme for learning [Byers et al. 1981; Chen et al. 1986; Davis and Kiger 1981]. At the same time, a second gene involved in cAMP signaling and learning behavior, respectively, was identified. *rutabaga* (*rut*) was shown to encode an adenylate cyclase, an enzyme that produces cAMP [Livingstone et al. 1984]. These findings laid the basis for the identification of many other genes involved in learning processes, and memory formation and storage.

A major milestone in fruit fly research was the sequencing of the *Drosophila* genome [Adams et al. 2000], the first application of a whole-genome shot-gun approach. To accomplish this huge challenge, a joint effort of 40 experimental and computational biologists from 20 institutions in five countries was required [Rubin and Lewis 2000].

Today, *Drosophila* appears to be a powerful model organism for fundamental research in the field of neurobiology. *Drosophila* shows a high degree of accessibility on the physiological and behavioral level in combination with a huge genetic toolbox for sophisticated manipulations, a diverse behavioral repertoire, relative small number of neurons, and short life cycle.

2. The life cycle of *Drosophila melanogaster*

The short life cycle of the fruit fly, the possibilities to manipulate the developmental period as well as the large number of offspring are main advantages of the animal as a model organism. First to describe *Drosophila*'s life cycle (Fig. 1) in a textbook were Demerec and Kaufman in 1940 and is later summarized in different handbooks and protocols.

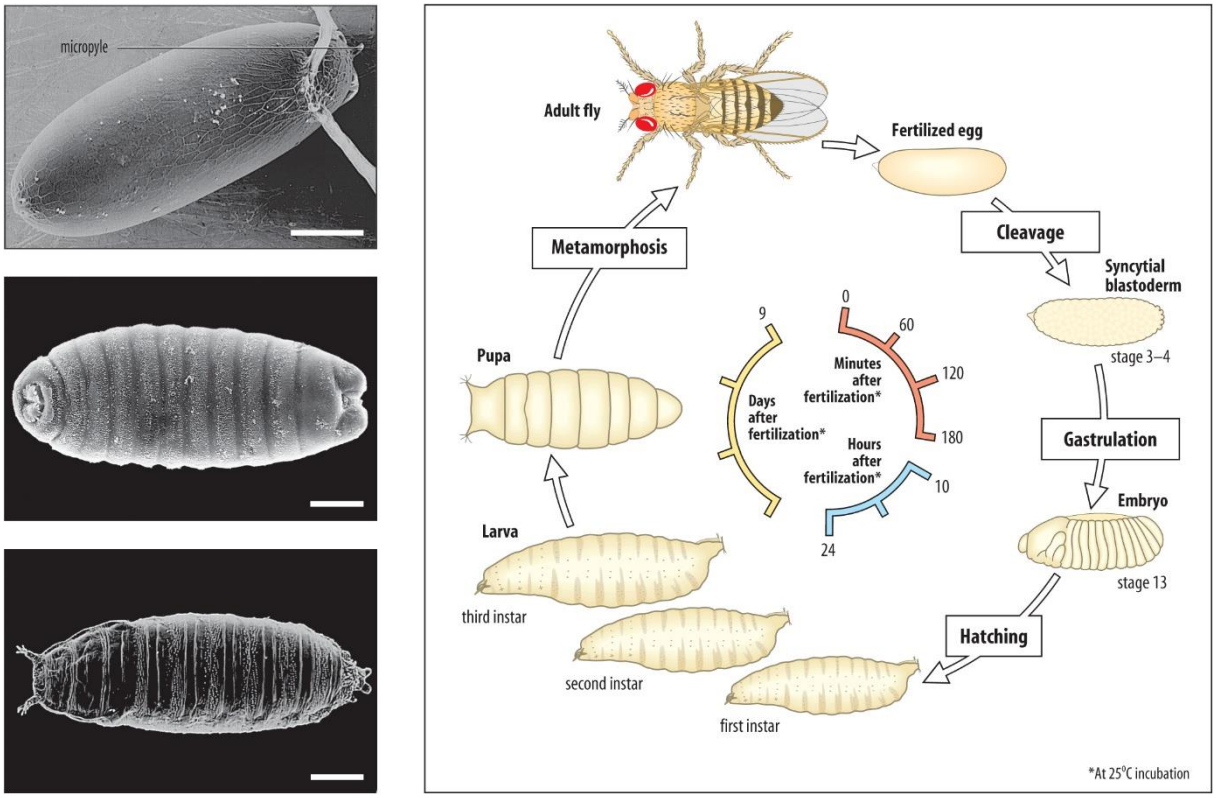

Figure 1: *Life cycle of the fruit fly under culture conditions 25°C and 60% humidity. From http://www.mun.ca/biology/desmid/brian/BIOL3530/DEVO_02/ch02f01.jpg (last access 12.04.2019)*

Briefly, the fruit fly's development consists of four stages (egg, larva, pupa and adult) and its duration is highly dependent on the surrounding temperature. At 25°C the cycle from egg laying to eclosion of the imago is completed in approximately 10 days. This time span is prolonged at lower and shortened at higher temperatures [Demerec and Kaufman 1976]. The

embryonic development starts directly after fertilization around the time point of egg laying. 24 hours after egg laying (AEL) first instar larva hatches from the egg. *Drosophila* larva undergoes two more molts: 48 hours and 72 hours AEL when second and third instar larva hatches [Demerec and Kaufman 1976]. After reaching a critical size (around 96 hour AEL) third instar larvae stop feeding, become "wandering larvae" and prepare to puparate. Pupation starts at 120 hours AEL within the last stage skin. During the pupal stage (4-5 days) metamorphosis takes place and adult structures are formed [Demerec and Kaufman 1976]. Approximately 10 days AEL an imago ecloses through the operculum of the puparium [Ashburner and Thompson 1978; Demerec and Kaufman 1976; Sullivan et al. 2000; Ashburner et al. 2005]. Female flies become receptive 8 to 12 hours after eclosion and start mating. Female *Drosophila* produce around 100 eggs per day and lay around 2000 eggs in a lifetime [Pitnick 1996; Sang 2001]. Thus, the rapid generation time and the high number of offspring provide the feasibility of performing large scale systematic genetic and/or behavioral screens.

3. Tools for genetic manipulation in *Drosophila melanogaster*

The genetic accessibility of the fruit fly as well as the fast development of technologies for gene manipulation make *Drosophila* one of the most powerful model organisms. In 1968, chemical mutagenesis was first described as genes can be randomly mutated by feeding the animals with ethyl methane sulfonate [Lewis and Bacher 1968]. In 1982, a method for gene insertion using *P* transposable element-mediated transformation was developed [Rubin and Spradling 1982]. This technology was later improved (e.g. P[acman] technology, bacteriophage *ΦC31* integrase) for insertions of large DNA fragments in specific docking sites using a bacterial artificial chromosome (BAC) platform [Groth et al. 2014; Groth and Calos 2004; Venken et al. 2006]. The development of *P* element-mediated transformation led to the generation of the flipase-flipase recognition target (FLP/FRT) system, allowing site-specific recombination catalyzed by a heat-induced recombinase [Golic 1991; Golic and Lindquist 1989]. Modification of the FLP/FRT system resulted later in the development of the mosaic analysis with a repressible cell marker (MARCM) for specific gene knockout in neurons and tissues, and mutated cell marking [Lee and Luo 2001]. However, probably the highest impact on *Drosophila* research has the development of binary expression systems: GAL4/UAS, LexA/LexAop and QF/QUAS. The QF/QUAS system is the newest binary expression system in flies. It is based on regulatory gene cluster from *Neurospora crassa* [Potter et al. 2010]. As this system is not applied for the experiments in this work, it will not be explained in detail. The most used binary system for targeted gene expression is the GAL4-UAS system. In 1988, Fisher and colleagues could first report that a transcriptional activator GAL4 from the yeast *Saccharomyces cerevisiae* can induce the transcription of a gene of interest under the control of an upstream activation sequence (UAS) as a GAL4 binding site in *Drosophila melanogaster* [Fischer et al. 1988]. Few years later, Brand and Perrimon described the GAL4/UAS system as a binary system with its features of targeted cell- and/or tissue-specific expression of genes of interest (Fig. 2). Transgenic fly lines are generated by fusing a genomic enhancer to the GAL4 construct (driver line) and by cloning a gene of interest behind the UA sequence (effector line). When both parental (driver and effector) lines are crossed, GAL4 is expressed under the

control of the endogenous enhancer in the F1 generation, and binds to the UAS to elicit so cell-specific expression of a target gene [Brand and Perrimon 1993; Duffy 2002].

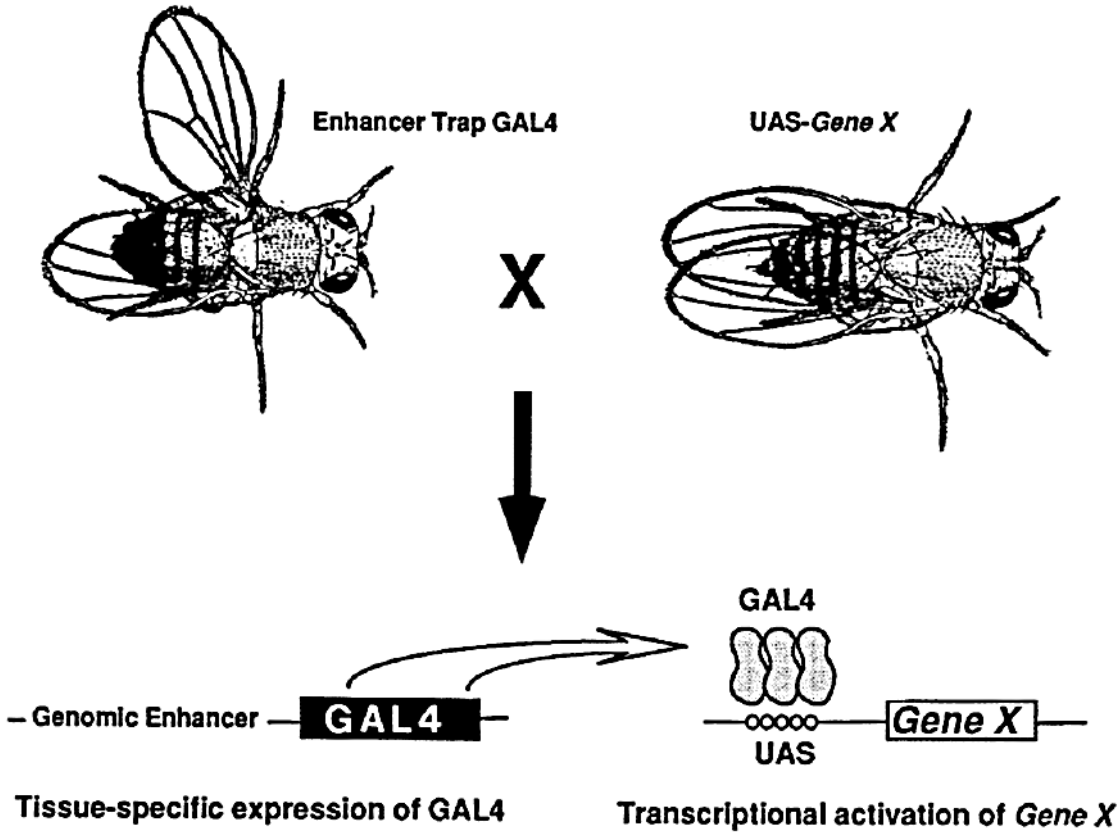

Figure 2: *GAL4/UAS system for targeted gene expression and selective cell-specific manipulation. From [Brand and Perrimon 1993]*

Later, a second binary expression system for genetic manipulations in *Drosophila*, the LexA/LexAop system, was developed [Lai and Lee 2006]. LexA is a transcriptional activator expressed in *Escherichia coli* that contains a DNA-binding domain and binds to the LexA DNA-binding motif (LexAop/LexA operator) upstream of a target gene [Little and Mount 1982]. If an activation domain, i.e. VP-16 from the *Herpes simplex* virus [Triezenberg et al. 1988] or GAL4 [Brent and Ptashne 1985] is fused to the C-terminus of LexA, *in vivo* transcription of genes with LexAop motifs containing promoters is elicited [Lai and Lee 2006; Szuts and Bienz 2000] (Fig. 3). This system allows, similar to the GAL4/UAS system, the separate maintenance of parental driver (LexA) and effector (LexAop) lines and by that the spatial and temporal control over gene expression.

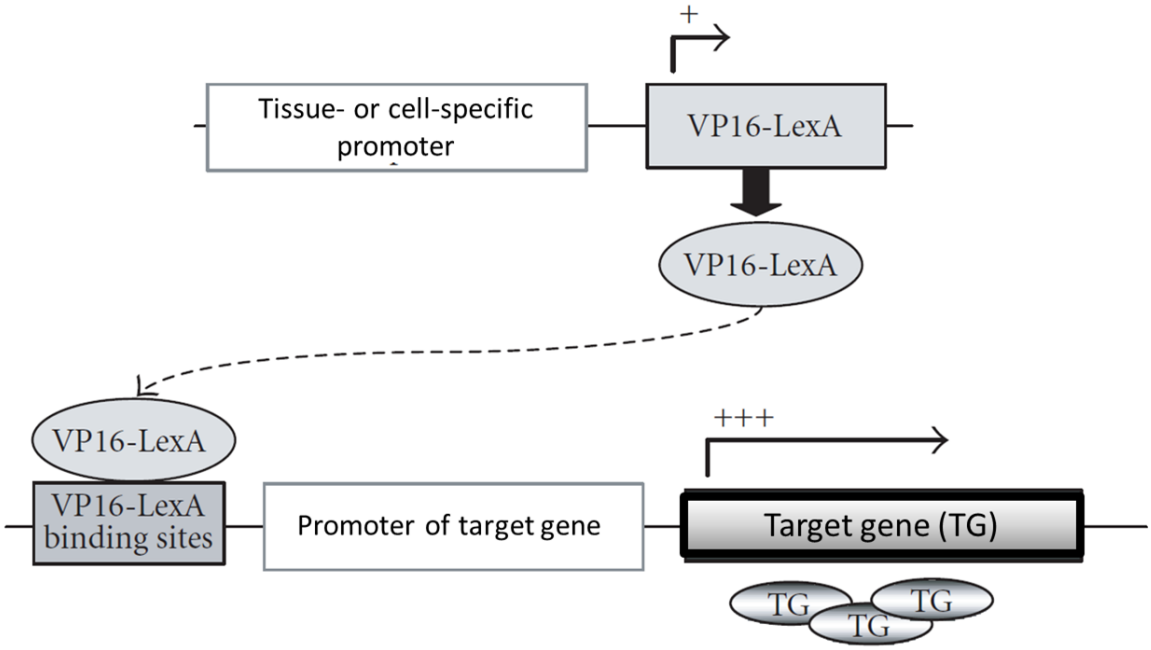

Figure 3: *LexA/LexAop system for targeted gene expression and selective cell-specific manipulation. Modified from [Robson and Hirst 2003]*

The development of different independent binary expression systems was a milestone in the *Drosophila* research, allowing simultaneous genetic manipulation of neuronal network components, e.g. GRASP for GFP reconstruction for visualization of synaptic partners [Feinberg et al. 2008; Gordon and Scott 2009]. Since the introduction of binary expression systems as powerful neurogenetics tools, more and more effector lines were generated to selectively manipulate the functions of neuronal cells. Meanwhile the activity of a neuron can be silenced by using different effector genes like *shibire^{ts}* [Kitamoto 2001], *TeTxLC* [Sweeney et al. 1995] or *Kir2.1* [Baines et al. 2001]. Neurons can be further artificially activated via transgenic expression of temperature-dependent (e.g. TRPM8 [Peabody et al. 2009] and TRPA1 [Rosenzweig et al. 2005]) or light-dependent (e.g. Channelrhodopsin-2 [Dawydow et al. 2014; Nagel et al. 2003] and Chrimson [Klapoetke et al. 2014]) ion channels. Ablation of neurons can be achieved by expressing apoptotic genes like *reaper* and/or *head involution defective* [Zhou et al. 1997]. However, as previous research showed that different effector lines vary in their efficiency to affect one and the same behavior, it is crucial to select appropriate effectors [Pauls et al. 2015].

Today, thousands of driver and effector lines are available in different stock centers, such as Bloomington Drosophila Stock Center (70.970 stocks), Kyoto Stock Center and Vienna Drosophila Resource Center (>31.000 stocks). Besides the possibility of ordering a line needed for a certain experiment, researchers have the opportunity to share stocks at first hand which is of high benefit for the *Drosophila* community and a major advantage for the progress in fruit fly research.

4. References

Aceves-Pina EO, Quinn WG (1979) Learning in normal and mutant *Drosophila* larvae. Science 206:93-96.

Adams MD, Celniker SE, Holt RA, Evans CA, Gocayne JD, Amanatides PG, Scherer SE, Li PW, Hoskins RA, Galle RF, George RA, Lewis SE, Richards S, Ashburner M, Henderson SN, Sutton GG, Wortman JR, Yandell MD, Zhang Q, Chen LX, Brandon RC, Rogers YH, Blazej RG, Champe M, Pfeiffer BD, Wan KH, Doyle C, Baxter EG, Helt G, Nelson CR, Gabor GL, Abril JF, Agbayani A, An HJ, Andrews-Pfannkoch C, Baldwin D, Ballew RM, Basu A, Baxendale J, Bayraktaroglu L, Beasley EM, Beeson KY, Benos PV, Berman BP, Bhandari D, Bolshakov S, Borkova D, Botchan MR, Bouck J, Brokstein P, Brottier P, Burtis KC, Busam DA, Butler H, Cadieu E, Center A, Chandra I, Cherry JM, Cawley S, Dahlke C, Davenport LB, Davies P, de Pablos B, Delcher A, Deng Z, Mays AD, Dew I, Dietz SM, Dodson K, Doup LE, Downes M, Dugan-Rocha S, Dunkov BC, Dunn P, Durbin KJ, Evangelista CC, Ferraz C, Ferriera S, Fleischmann W, Fosler C, Gabrielian AE, Garg NS, Gelbart WM, Glasser K, Glodek A, Gong F, Gorrell JH, Gu Z, Guan P, Harris M, Harris NL, Harvey D, Heiman TJ, Hernandez JR, Houck J, Hostin D, Houston KA, Howland TJ, Wei MH, Ibegwam C, Jalali M, Kalush F, Karpen GH, Ke Z, Kennison JA, Ketchum KA, Kimmel BE, Kodira CD, Kraft C, Kravitz S, Kulp D, Lai Z, Lasko P, Lei Y, Levitsky AA, Li J, Li Z, Liang Y, Lin X, Liu X, Mattei B, McIntosh TC, McLeod MP, McPherson D, Merkulov G, Milshina NV, Mobarry C, Morris J, Moshrefi A, Mount SM, Moy M, Murphy B, Murphy L, Muzny DM, Nelson DL, Nelson DR, Nelson KA, Nixon K, Nusskern DR, Pacleb JM, Palazzolo M, Pittman GS, Pan S, Pollard J, Puri V, Reese MG, Reinert K, Remington K, Saunders RD, Scheeler F, Shen H, Shue BC, Siden-Kiamos I, Simpson M, Skupski MP, Smith T, Spier E, Spradling AC, Stapleton M, Strong R, Sun E, Svirskas R, Tector C, Turner R, Venter E, Wang AH, Wang X, Wang ZY, Wassarman DA, Weinstock GM, Weissenbach J, Williams SM, WoodageT, Worley KC, Wu D, Yang S, Yao QA, Ye J, Yeh RF, Zaveri JS, Zhan M, Zhang G, Zhao Q, Zheng L, Zheng XH, Zhong FN, Zhong W, Zhou X, Zhu S, Zhu X, Smith HO, Gibbs RA, Myers EW, Rubin GM, Venter JC (2000) The genome sequence of *Drosophila* melanogaster. Science 287:2185-2195.

Artavanis-Tsakonas S, Muskavitch MA, Yedvobnick B (1983) Molecular cloning of *Notch*, a locus affecting neurogenesis in *Drosophila melanogaster*. Proc Natl Acad Sci U S A 80:1977-1981.

Artavanis-Tsakonas S, Matsuno K, Fortini ME (1995) *Notch* signaling. Science 268:225-232.

Artavanis-Tsakonas S, Rand MD, Lake RJ (1999) *Notch* signaling: cell fate control and signal integration in development. Science 284:770-776.

Ashburner M, Thompson JN (1978) "The laboratory culture of *Drosophila*". In Ashburner M, Wright TRF. The genetics and biology of Drosophila. 2A. Academic Press. 1–81.

Ashburner M, Golic KG, Hawley RS (2005) *Drosophila*: A Laboratory Handbook (2nd ed.). Cold Spring Harbor Laboratory Press. pp. 162–4. ISBN 978-0-87969-706-8.

Baines RA, Uhler JP, Thompson A, Sweeney ST, Bate M (2001) Altered electrical properties in *Drosophila* neurons developing without synaptic transmission. J Neurosci 21:1523-1531.

Bellen HJ, Tong C, Tsuda H (2010) 100 years of *Drosophila* research and its impact on vertebrate neuroscience: a history lesson for the future. Nat Rev Neurosci 11(7): 514-522

Benzer S (1967) Behavioral mutants of *Drosophila* isolated by countercurrent distribution. Proc Natl Acad Sci U S A 58:1112-1119.

Brand AH, Perrimon N (1993) Targeted gene expression as a means of altering cell fates and generating dominant phenotypes. Development 118:401-415.

Brent R, Ptashne M (1985) A eukaryotic transcriptional activator bearing the DNA specificity of a prokaryotic repressor. Cell 43:729-736.

Bünning E (1935) Zur Kenntnis der endogenen Tagesrhythmik bei Insekten und Pflanzen. Berichte der Deutschen Botanischen Gesellschaft 53:594–623

Byers D, Davis RL, Kiger JA, Jr. (1981) Defect in cyclic AMP phosphodiesterase due to the *dunce* mutation of learning in *Drosophila* melanogaster. Nature 289:79-81.

Charron F, Tessier-Lavigne M (2007) The *Hedgehog*, *TGF-beta*/*BMP* and *Wnt* families of morphogens in axon guidance. Adv Exp Med Biol 621:116-133.

Chen CN, Denome S, Davis RL (1986) Molecular analysis of cDNA clones and the corresponding genomic coding sequences of the *Drosophila dunce+* gene, the structural gene for cAMP phosphodiesterase. Proc Natl Acad Sci U S A 83:9313-9317.

Davis RL, Kiger JA, Jr. (1981) *Dunce* mutants of *Drosophila melanogaster*: mutants defective in the cyclic AMP phosphodiesterase enzyme system. J Cell Biol 90:101-107.

Dawydow A, Gueta R, Ljaschenko D, Ullrich S, Hermann M, Ehmann N, Gao S, Fiala A, Langenhan T, Nagel G, Kittel RJ (2014) Channelrhodopsin-2-XXL, a powerful optogenetic tool for low-light applications. Proc Natl Acad Sci U S A 111:13972-13977.

Demerec, and Kaufman (Tenth edition 1996) *Drosophila* Guide. Carnegie Institution of Washington, Washington D.C.

Duboule D (2007) The rise and fall of *Hox* gene clusters. Development 134:2549-2560.

Dudai Y, Jan YN, Byers D, Quinn WG, Benzer S (1976) *dunce*, a mutant of *Drosophila* deficient in learning. Proc Natl Acad Sci U S A 73:1684-1688.

Duffy JB (2002) GAL4 system in *Drosophila*: a fly geneticist's Swiss army knife. Genesis 34:1-15.

Feinberg EH, Vanhoven MK, Bendesky A, Wang G, Fetter RD, Shen K, Bargmann CI (2008) GFP Reconstitution Across Synaptic Partners (GRASP) defines cell contacts and synapses in living nervous systems. Neuron 57:353-363.

Fischer JA, Giniger E, Maniatis T, Ptashne M (1988) GAL4 activates transcription in *Drosophila*. Nature 332:853-856.

Golic KG, Lindquist S (1989) The FLP recombinase of yeast catalyzes site-specific recombination in the *Drosophila* genome. Cell 59:499-509.

Golic KG (1991) Site-specific recombination between homologous chromosomes in *Drosophila*. Science 252:958-961.

Gordon MD, Scott K (2009) Motor control in a *Drosophila* taste circuit. Neuron 61:373-384.

Groth AC, Calos MP (2004) Phage integrases: biology and applications. J Mol Biol 335:667-678.

Ho KS, Scott MP (2002) Sonic hedgehog in the nervous system: functions, modifications and mechanisms. Curr Opin Neurobiol 12:57-63.

Jurgens G, Wieschaus E, Nusslein-Volhard C, Kluding H (1984) Mutations affecting the pattern of the larval cuticle in *Drosophila melanogaster*: II. Zygotic loci on the third chromosome. Wilehm Roux Arch Dev Biol 193:283-295.

Kalmus, H. (1935) Periodizität und Autochronie (Ideochronie) als zeitregelnde Eigenschaften der Organismen. Biol Gen 11:93-114.

Kalmus, H. (1938) Die Lage des Aufnahmeorgans für die Schlupfperiodik von *Drosophila*. Zeitschrift für Vergleichende Physiologie 26:362-365

Kalmus, H. (1940) Diurnal rhythms in the Axolotl larvae and in *Drosophila*. Nature 145:72-73

Kitamoto T (2001) Conditional modification of behavior in *Drosophila* by targeted expression of a temperature-sensitive *shibire* allele in defined neurons. J Neurobiol 47:81-92.

Klapoetke NC, Murata Y, Kim SS, Pulver SR, Birdsey-Benson A, Cho YK, Morimoto TK, Chuong AS, Carpenter EJ, Tian Z, Wang J, Xie Y, Yan Z, Zhang Y, Chow BY, Surek B, Melkonian M, Jayaraman V, Constantine-Paton M, Wong GK, Boyden ES (2014) Independent optical excitation of distinct neural populations. Nat Methods 11:338-346.

Kohler RE (1993) *Drosophila*: a life in the laboratory. J Hist Biol 26:281-310.

Konopka RJ, Benzer S (1971) Clock mutants of *Drosophila melanogaster*. Proc Natl Acad Sci U S A 68:2112-2116.

Lai SL, Lee T (2006) Genetic mosaic with dual binary transcriptional systems in *Drosophila*. Nat Neurosci 9:703-709.

Lee T, Luo L (2001) Mosaic analysis with a repressible cell marker (MARCM) for *Drosophila* neural development. Trends Neurosci 24:251-254.

Lewis EB, Bacher F. (1968) Methods of feeding ethyl methane sulfonate (EMS) to *Drosophila* males. Dros Inf Serv. 43:193

Lewis EB (1978) A gene complex controlling segmentation in *Drosophila*. Nature 276:565-570.

Little JW, Mount DW (1982) The SOS regulatory system of *Escherichia coli*. Cell 29:11-22.

Livingstone MS, Sziber PP, Quinn WG (1984) Loss of calcium/calmodulin responsiveness in adenylate cyclase of *rutabaga*, a *Drosophila* learning mutant. Cell 37:205-215.

Morgan TH (1910) Sex Limited Inheritance in *Drosophila*. Science 32:120-122.

Morgan TH (1911) The origin of five mutations in eye color in *Drosophila* and their modes of inheritance. Science 33:534-537.

Morgan TH, Bridges CB (1916) Sex-linked inheritance in *Drosophila*. Carnegie Institute of Washington Publication. 237:1-88.

Muller HJ (1918) Genetic variability, twin hybrids and constant hybrids, in a case of balanced lethal factors. Genetics 3:422-499.

Muller HJ (1927) Artificial transmutation of the gene. Science 66:84-87.

Nagel G, Szellas T, Huhn W, Kateriya S, Adeishvili N, Berthold P, Ollig D, Hegemann P, Bamberg E (2003) Channelrhodopsin-2, a directly light-gated cation-selective membrane channel. Proc Natl Acad Sci U S A 100:13940-13945.

Nusslein-Volhard C, Wieschaus E (1980) Mutations affecting segment number and polarity in *Drosophila*. Nature 287:795-801.

Nusslein-Volhard C, Wieschaus E, Kluding H (1984) Mutations affecting the pattern of the larval cuticle in *Drosophila melanogaster*: I. Zygotic loci on the second chromosome. Wilehm Roux Arch Dev Biol 193:267-282.

Pauls D, von Essen A, Lyutova R, van Giesen L, Rosner R, Wegener C, Sprecher SG (2015) Potency of transgenic effectors for neurogenetic manipulation in *Drosophila* larvae. Genetics 199:25-37.

Peabody NC, Pohl JB, Diao F, Vreede AP, Sandstrom DJ, Wang H, Zelensky PK, White BH (2009) Characterization of the decision network for wing expansion in *Drosophila* using targeted expression of the TRPM8 channel. J Neurosci 29:3343-3353.

Pittendrigh CS (1954) On temperature independence in the clock system controlling emergence time in *Drosophila*. Proc Nat Acad Sci USA 40:1018–1029

Potter CJ, Tasic B, Russler EV, Liang L, Luo L (2010) The Q system: a repressible binary system for transgene expression, lineage tracing, and mosaic analysis. Cell 141:536-548.

Poulson DF (1937) Chromosomal deficiencies and the embryonic development of *Drosophila melanogaster*. Proc Natl Acad Sci U S A 23:133-137.

Quinn WG, Harris WA, Benzer S (1974) Conditioned behavior in *Drosophila melanogaster.* Proc Natl Acad Sci U S A 71:708-712.

Reddy P, Zehring WA, Wheeler DA, Pirrotta V, Hadfield C, Hall JC, Rosbash M (1984) Molecular analysis of the *period* locus in *Drosophila melanogaster* and identification of a transcript involved in biological rhythms. Cell 38:701-710.

Pitnick S (1996) Investment in testes and the cost of making long sperm in *Drosophila*. American Naturalist. 148: 57–80. doi:10.1086/285911

Robson T, Hirst DG (2003) Transcriptional targeting in cancer gene therapy. J Biomed Biotechnol 2003:110-137.

Rosenzweig M, Brennan KM, Tayler TD, Phelps PO, Patapoutian A, Garrity PA (2005) The *Drosophila* ortholog of vertebrate TRPA1 regulates thermotaxis. Genes Dev 19:419-424.

Rubin GM, Spradling AC (1982) Genetic transformation of *Drosophila* with transposable element vectors. Science 218:348-353.

Rubin GM, Lewis EB (2000) A brief history of *Drosophila*'s contributions to genome research. Science 287:2216-2218.

Sang JH (2001). *Drosophila melanogaster*: The Fruit Fly. In Reeve EC. Encyclopedia of genetics. USA: Fitzroy Dearborn Publishers, I. p. 157. ISBN 978-1-884964-34-3. Retrieved 2009-07-01

Sanchez-Herrero E, Vernos I, Marco R, Morata G (1985) Genetic organization of *Drosophila bithorax* complex. Nature 313:108-113.

Sehgal A, Price JL, Man B, Young MW (1994) Loss of circadian behavioral rhythms and *per* RNA oscillations in the *Drosophila* mutant *timeless*. Science 263:1603-1606.

Stephenson R, Metcalfe NH (2013) *Drosophila melanogaster*: a fly through its history and current use. J R Coll Physicians Edinb 43:70-75.

Sturtevant AH. (1923) The linear arrangement of six sex-linked factors in *Drosophila*, as shown by their mode of association. Journal of Experimental Zoology 14:43-59.

Sullivan W, Ashburner M, Hawley R. (2000) *Drosophila* protocols. Cold Spring Harbor Laboratory Press, Cold Spring Harbor, NY.

Sweeney ST, Broadie K, Keane J, Niemann H, O'Kane CJ (1995) Targeted expression of tetanus toxin light chain in *Drosophila* specifically eliminates synaptic transmission and causes behavioral defects. Neuron 14:341-351.

Szuts D, Bienz M (2000) LexA chimeras reveal the function of *Drosophila Fos* as a context-dependent transcriptional activator. Proc Natl Acad Sci U S A 97:5351-5356.

Triezenberg SJ, Kingsbury RC, McKnight SL (1988) Functional dissection of VP16, the trans-activator of *Herpes simplex* virus immediate early gene expression. Genes Dev 2:718-729.

Vassin H, Bremer KA, Knust E, Campos-Ortega JA (1987) The neurogenic gene *Delta* of *Drosophila melanogaster* is expressed in neurogenic territories and encodes a putative transmembrane protein with EGF-like repeats. EMBO J 6:3431-3440.

Venken KJ, He Y, Hoskins RA, Bellen HJ (2006) P[acman]: a BAC transgenic platform for targeted insertion of large DNA fragments in *D. melanogaster*. Science 314:1747-1751.

Wharton KA, Johansen KM, Xu T, Artavanis-Tsakonas S (1985) Nucleotide sequence from the neurogenic locus *notch* implies a gene product that shares homology with proteins containing EGF-like repeats. Cell 43:567-581.

Wieschaus E, Nusslein-Volhard C, Jurgens G (1984) Mutations affecting the pattern of the larval cuticle in *Drosophila melanogaster*: III. Zygotic loci on the X-chromosome and fourth chromosome. Wilehm Roux Arch Dev Biol 193:296-307.

Zehring WA, Wheeler DA, Reddy P, Konopka RJ, Kyriacou CP, Rosbash M, Hall JC (1984) P-element transformation with period locus DNA restores rhythmicity to mutant, arrhythmic *Drosophila melanogaster*. Cell 39:369-376.

Zhou L, Schnitzler A, Agapite J, Schwartz LM, Steller H, Nambu JR (1997) Cooperative functions of the *reaper* and *head involution defective* genes in the programmed cell death of *Drosophila* central nervous system midline cells. Proc Natl Acad Sci U S A 94:5131-5136.

II. Generation of combined transgenic lines for multiple manipulation of neuronal networks

1. Introduction

One of the greatest advantages of *Drosophila* as model organism is the availability of tools for genetic manipulations. The generation of transgenic lines for overexpression of genes and controlled silencing, ablation or activation of neurons is a fundament for structural and functional analyses in *Drosophila* neuroscientific research. The breakthrough of transgenesis was achieved in 1982 with the introduction of the *P* element transposon [Rubin and Spradling 1982]. A transgene is an exogenous DNA introduced into a host's genome. There are two methods for integration of transgenes in *Drosophila*, transposon-mediated (e.g. *P* element-based transformation) and site-specific transgenesis, respectively. *P* element-based transformation involves a transgene and a particular marker (usually *white* mini-gene) inside a transposon-based vector on a transformation plasmid, and a helper plasmid which codes for transposase. Both are injected into an embryo usually with mutated *white* (e.g. w^{1118}) genetic background to reliably track the integration event as the progeny of the transformed flies should have red eyes due to expression of the *white* mini-gene fused to the *P* element [Castro and Carareto 2004; Klemenz et al. 1987; Rubin and Spradling 1982, 1983; Spradling and Rubin 1982]. This method for generation of transgenic flies was widely used in the 80's and 90', however it has several limitations. Transformation with large DNA fragments is problematic, and the location of integration cannot be manipulated allowing position effects and biased phenotypic analysis, respectively [Venken and Bellen 2007]. These limitations are addressed by site-directed recombination-based transformation. This technique was pioneered in *Drosophila* by the introduction of the bacteriophage *ΦC31* integrase [Groth et al. 2004]. The *ΦC31* integrase mediates recombination between *attP* and *attB* sites with cognate sequences [Thorpe and Smith 1998]. In the fruit fly, an *attP* docking site is integrated with a transposon

into the genome, while *attB* is delivered by injecting a *pUASTB* plasmid containing an additional marker, e.g. *mini-white*. The *ΦC31* Int RNA is coinjected in order to elicit recombination between *attP* and *attB* sites and integration of a transgene into the genome, respectively [Groth et al. 2004]. Groth and colleagues described initially two different *attP* docking sites (*attP1* and *attP2*). Later, numerous docking sites were generated using other backbones such as *piggyBac* or *Mariner* [Bischof et al. 2007; Venken et al. 2006]. Site-specific transgenesis ensures precise insertions of transgenes at defined docking sites. Therefore, it is widely used for generation of transgenic driver and effector lines used by the binary expression systems.

The development of independent binary expression systems (GAL4/UAS, LexA/LexAop) allows disparate manipulations of different components of a neuronal network so that the functions of communicating neurons within the network can be dissected. The combination of driver and/or effector constructs in one parental line is therefore essential for investigating the functional connectivity of the *Drosophila* nervous system. Generation of combined transgenic lines depends on the location of the constructs. In case both constructs are located on different chromosomes, balancer chromosomes are introduced into the genome of the transgenic lines to reliably identify flies carrying the transgenes. Balancer chromosomes suppress recombination, are homozygous lethal, or cause sterility, and are characterized by dominant visible markers. The first balanced lethal mutation (*Beaded* (*Ser^{Bd-1}*)) was described by Muller in 1918. Balancer chromosomes are inverted rearranged chromosomes used for maintenance of deleterious mutations, complex stock constructions and tracing of chromosomes throughout crossing schemes [Hentges and Justice 2004; Muller 1918; Sturtevant 1921]. That is why transgenic lines are first to be balanced to obtain stable combinations of transgenes on different chromosomes.

In contrast, classical genetic recombination is required if both transgenes are located on the same chromosome. Genetic recombination implies exchange of genetic material between homologous chromosomes during meiosis. It is enabled by chromosomal crossing over, first described in 1909 and called 'chiasmatypie' [Janssens et al. 2012]. Later, the physical basis of crossover was described in maize by McClintock and Creighton [Creighton and McClintock 1931; Sharp 1934; Clancy 2008; Pray and Zhaurova 2008]. In brief, during meiosis between prophase I and metaphase I non-sister chromatids of homologous chromosomes align with

each other. The chromatids are cut at identical sites followed by invasion of the homologous chromosome, base pairing with the complementary strand and formation of a Holiday junction. The Holiday junction migrates along the chromosome creating a heteroduplex region, a process called branch migration. Branch migration is terminated with a resolution of the Holiday structure resulting in recombinant chromosomes carrying maternal as well as paternal genetic information [Griffiths et al. 2000].

In my thesis, both approaches were applied to generate combined driver and effector lines used in experiments for functional dissection of a neuronal circuit.

2. Materials and methods

Investigation of complex neuronal networks and interactions between partners within such circuits requires in many cases elaborate simultaneous manipulations of more than one population of neurons. This can be achieved by the combination of binary expression systems in one organism. As most of the single driver and effector lines are available with individual constructs it is therefore crucial to generate fly lines carrying at least two transgenes for genetic manipulation.

2.1. Fly stocks

All fly strains were raised at 25°C, 60% humidity and 12:12 hours light:dark cycle in vials containing nutrient solution. Driver and effector lines used for the generation of combined fly strains are listed in Table 1. Each line of interest was crossed to one of these balancer lines: *w^{1118};Cyo/sco;MKRS/TM6b*, or *w^{1118};Cyo/sp;TM2/TM6b*, respectively. Thus, all lines would have the same genetic background, particularly *w^{1118}* genetic background, as usually *w^{1118}* is crossed with transgenic lines as genetic control for e.g. behavioral experiments. Further, using balancer chromosomes, crossing schemes can be easily tracked to obtain reliable combination of transgenic constructs within one animal.

Table 1: *Drosophila melanogaster transgenic strains (GAL4/UAS, LexA/LexAop) used for combination of drivers or effectors, respectively.*

Stock	Genotype	Chr	Source	Reference
H24-GAL4	P{w[+mW.hs]=GawB}H24	3	Andreas Thum	
R58E02-LexA	w[1118]; P{y[+t7.7] w[+mC]=GMR58E02-lexA}attP40	2	Andreas Thum	

R58E02-GAL4	w[1118]; P{y[+t7.7] w[+mC]=GMR58E02-GAL4}attP2	2	Andreas Thum	
UAS-dicer2	w[1118]; P{GD11429}v24666	2	VDRC #24666	
UAS-dicer2	w[1118]; P{GD11429}v24667	3	VDRC #24667	
UAS-ChR2-XXL	y[1] w[1118]; PBac{y[+mDint2] w[+mC]=UAS-ChR2.XXL}VK00018	2	Robert Kittel, Tobias Langenhan	[Dawydow et al. 2014]
UAS-Dop1R1-RNAi	P{TRiP.HM04077}attP2	3	Bloomington #31765	
UAS-amon-RNAi^{28b}	P{UAS-amon-RNAi}28b	2	Jeanne Rhea, Michael Bender	[Rhea et al. 2010]
UAS-amon-RNAi^{78b}	w[*]; P{w[+mC]=UAS-amon-RNAi}78b	3	Bloomington #29009	
LexAop-reaper		3	Hector Herranz	[Herranz et al. 2014]
LexAop-GCamp6m	w[1118]; P{y[+t7.7] w[+mC]=13XLexAop2-IVS-GCaMP6m-SV40}su(Hw)attP1	3	Bloomington #44588	
UAS-Chrimson, LexAop-GCamp6m	w; CyO/Sp; 13XLexAop2-IVS-p10-GCaMP6m,20xUAS-CsChrimson-mCherry	3	Katharina Eichler Vivek Jayaraman	
LexAop-Kir2.1^{260b}	P{lexAop-EGFP-Kir2.1} w;pSW921[260b]	2	Katharina Eichler	[Prieto-Godino et al. 2012]
LexAop-TNT^{49b}	w;pSW922[49b]	2	Katharina Eichler	
LexAop-TNT^{260b}	w;pSW922[260b]	2	Katharina Eichler	

2.2. Combination of transgenes located on different chromosomes

First, all stocks were balanced by crossing each one with a double-balancer line. For balancing transgenic lines with genetic constructs (GC) on the second chromosome the following example crossing scheme was used:

P:	$\male \frac{GC\ A}{GC\ A};\frac{+}{+}$	X	$\female\ w^{1118};\frac{CyO}{Sco};\frac{MKRS}{TM6b}$
F1:	$\male\ w^{1118};\frac{GC\ A}{CyO};\frac{MKRS}{+}$	X	$\female\ w^{1118};\frac{GC\ A}{CyO};\frac{TM6b}{+}$
F2:	$\male\ w^{1118};\frac{GC\ A}{CyO};\frac{MKRS}{TM6b}$	X	$\female\ w^{1118};\frac{GC\ A}{CyO};\frac{MKRS}{TM6b}$

Figure 4: *Crossing scheme for balancing transgenic lines with transgenes located on the second chromosome. P: parental lines – transgenic line is crossed with double-balancer line; F1: virgin females are crossed with males carrying the same balancer on the second chromosome and different balancer on the third chromosome; F2: virgin females and males are crossed with respect to completely balanced third chromosome*

The F3 offspring was then tracked for several generations to verify the presence of both balancers on the third chromosome. For balancing transgenic lines with GCs on the third chromosome the following example crossing scheme was used:

P:	♂ $\frac{+}{+};\frac{GC\ B}{GC\ B}$	X	♀ $w^{1118};\frac{CyO}{Sco};\frac{MKRS}{TM6b}$
F1:	♂ $w^{1118};\frac{CyO}{+};\frac{GC\ B}{MKRS}$	X	♀ $w^{1118};\frac{Sco}{+};\frac{GC\ B}{MKRS}$
F2:	♂ $w^{1118};\frac{CyO}{Sco};\frac{GC\ B}{MKRS}$	X	♀ $w^{1118};\frac{CyO}{Sco};\frac{GC\ B}{MKRS}$

Figure 5: *Crossing scheme for balancing transgenic lines with transgenes located on the third chromosome. P: parental lines – transgenic line is crossed with double-balancer line; F1: virgin females are crossed with males carrying the same balancer on the third chromosome and different balancer on the second chromosome; F2: virgin females and males are crossed with respect to completely balanced second chromosome*

The F3 offspring was then tracked for several generations to verify the presence of both balancers on the third chromosome. To combine both transgenes within one strain the following example crossing scheme was used:

P:	♀ $w^{1118};\frac{GC\ A}{CyO};\frac{MKRS}{TM6b}$	X	♂ $w^{1118};\frac{CyO}{sco};\frac{GC\ B}{MKRS}$
F1:	♀ $w^{1118};\frac{GC\ A}{CyO};\frac{GC\ B}{MKRS}$	X	♂ $w^{1118};\frac{GC\ A}{CyO};\frac{GC\ B}{MKRS}$

Figure 6: *Crossing scheme for combining two transgenic lines with transgenes located on different chromosomes. P: parental lines – two balanced transgenic lines are crossed with each other; F1: virgin females are crossed with males with respect to the balancers on the second and third chromosome. Attention should be payed that none of the chromosomes is double balanced.*

The F2 generation was then assumed as stable stock carrying two transgenes on the second and third chromosome, respectively.

2.3. Recombination of transgenes located on the same chromosome

Classical genetic recombination is then provided if two transgenes are located on the same chromosome. In this case, once more crossing with a double-balancer line is required to reliably track the presence of both constructs within the generated recombined stock. The first step in the recombination process was the crossing of the two transgenic lines as follows:

$$\male \frac{GC\ A}{GC\ A};\frac{+}{+} \quad \text{X} \quad \female \frac{GC\ B}{GC\ B};\frac{+}{+}$$

Figure 7: *Parental cross for classical genetic recombination of transgenes located on the second chromosome.*

The F1 generation consisted of heterozygous flies carrying both genetic constructs. As homologous recombination following crossing over occurs in female flies during meiosis, single virgin females were collected from the F1 generation and were crossed with single double-balancer males:

$$\female \frac{GC\ A}{GC\ B};\frac{+}{+} \quad \text{X} \quad \male w^{1118};\frac{CyO}{Sp};\frac{TM2}{TM6b}$$

Figure 8: *F1 singe flies cross (1 virgin female (F1):1 double-balancer male).*

In the F2 generation three types of progeny with different genetic combinations on the second chromosome were possible: heterozygous flies carrying either *GC A* or *GC B* (e.g. w^{1118}*;GC A/CyO;TM6b/+* or w^{1118}*;GC B/CyO;TM6b/+*), and heterozygous flies with recombined *GC A* and *GC B* (e.g. w^{1118}*;GC A,GC B/CyO;TM6b/+*). As transgenes are usually inserted into the genome together with the *white* mini-gene it is consequential that the level of expression of this gene would result in flies with considerably darker eyes in comparison to flies carrying only one

transgene. Therefore, vials consisting of bright eyed F2 progeny were discarded. From the single-cross vials consisting only of dark eyed progeny, virgin female and male flies were collected and crossed. For that step it was crucial to cross flies with the same balancer on the second chromosome (either *CyO* or *sp*). The progeny from the F2 crossings was then monitored for several generations to verify the presence of both constructs on the second chromosome. Vials in which flies did not display homogenous dark red color of the eyes were discarded.

2.4. Verification of recombination events

As genetic recombination is a random process, every potential recombinant line had to be tested for the integration of both transgenes into the genome. For this study, *UAS-ChR2-XXL* was recombined with three different LexAop constructs (*LexAop-Kir2.1*^{260b}, *LexAop-TNT*^{49b} and *LexAop-TNT*^{260b}).

2.4.1. Behavioral pre-screen

First, a behavioral pre-screen was performed to prove whether *ChR2-XXL* is expressed in the potential recombination lines. Channelrhodopsin2 is a light-sensitive cation channel, which opens upon blue light illumination resulting in depolarization of the expressing neuron and in activation of the latter, respectively [Dawydow et al. 2014]. Recombinant lines were crossed with *sNPF-GAL4* driver line. From previous work in the laboratory it was known that artificial optogenetic activation of *sNPF-GAL4* positive neurons results in a typical nociceptive response, in that larvae show a rolling behavior while flies are paralyzed or at least impaired in climbing (R. Lyutova, Master thesis). For the test, five days AEL ten 3rd instar larvae from each cross were transferred on a Petri dish covered by a thin layer of 1.5% agarose gel under blue light. Larval behavior was recorded and analyzed for nociceptive responses. Seven days later (12 days AEL), adult F1 flies from the same crosses were transferred under blue light. It was monitored whether the flies exhibit a typical paralysis or inability to climb. Recombinant lines without behavioral phenotype were discarded. Lines showing larval nociceptive and adult paralysis behavior were then tested at molecular level.

2.4.2. Molecular screen

After the behavioral pre-screen, all potential recombinant lines were examined molecularly. From each stock ten flies were collected and single fly DNA extraction was performed. Single flies were transferred into PCR tubes. 25 µl Squishing buffer was pipetted into each tube and the fly within was smashed with a pipette tip. 25 µl Squishing buffer and 5 µl proteinase K were added. After mixing by pipetting up and down the tubes were transferred in a PCR machine and a program was run:

1. 56°C for 30 minutes
2. 93°C for 3 minutes
3. 4°C forever.

After the DNA was extracted, a PCR for each sample was carried out. Master PCR mix was prepared (per DNA Sample): 12.5 µl PCR Mix, 1 µl F Primer, 1 µl R Primer, 8.5 µl H_2O. 2 µl of each DNA sample was diluted in 23 µl of the master mix. The PCR tubes were put in a PCR machine and the following program was run:

1. 94°C for 2 minutes
2. 94°C for 30 seconds
3. MT for 30 seconds
4. 72°C for 2 minutes
5. steps 2 to 4 repeated in total 35 times
6. 72°C for 5 minutes
7. 4°C forever.

The sequences for the *ChR2-XXL* primers were kindly provided by Gao Shiqiang: ChR2-XXL_210_F: 5'-gcttatgttttacgcctacca-3', ChR2-XXL_610_R: 5'-gtgtggtaaccctcgatgt-3'; MT: 60°C; expected PCR product: 400 bp. *Kir2.1* primers were designed in Primer3 (https://primer3plus.com/) and synthesized by Sigma-Aldrich (Munich, Germany): eGFP_Kir2.1_1_F: 5'-aagagggcaaagcttgtgtg-3', eGFP_Kir2.1_1_R: 5'-catgactgcgccaatgatga-3'; MT: 66°C; expected PCR product: 200 bp. *TNT* could not be tested, as the exact sequence was unknown. Thus, *TNT* primers could not be designed. Besides the DNA samples, positive

controls were prepared by extracting DNA from the original transgenic lines (either *UAS-ChR2-XXL* or *LexAop-Kir2.1*) and a negative control was prepared by adding ddH_2O to the master mix. 20 µl of each PCR-amplified sample were loaded on a 1.5% agarose gel (1.5 g agarose, 100 ml TEA, 5 µl Midori green) and electrophoresis was run at 80 V for 40 to 50 minutes. A GeneRuler® 100 bp Plus DNA ladder was used as a reference for DNA fragment length. Images of the gels were taken using E-Box version 15.05 via E-Capt version 15.06 and edited with Gimp 2.10.8. Reagents and hardware are listed in Table 2.

Table 2: *Reagents and devices used for molecular verification of recombinant transgenic lines.*

Reagents	Manufacturer
GeneRuler® 100 bp Plus DNA ladder	ThermoFischer Scientific; Waltham, USA
JumpStart™ REDTaq® ReadyMix™ Reaction Mix	Sigma-Aldrich; Missouri, USA
Midori Green Advance DNA Stain	Nippon Genetics, Europe GmbH, Germany
MJ Mini thermocycler	Bio-Rad, Hercules, USA
E-Box	Vilber Lourmat; Eberhardzell, Germany

A recombination event was only considered as successful if ten out of ten (100%) DNA samples were positive for the tested transgene.

3. Results

The use of binary expression systems requires awareness of the expression pattern of driver lines. Further, the choice of appropriate effector is crucial for the experimental outcome.

Eight combined lines were generated as described above: *w^{1118};R58E02-LexA/CyO;H24-GAL4/TM6b, w^{1118};R58E02-GAL4/CyO;UAS-dicer2/TM6b, w^{1118};UAS-dicer2/CyO;H24-GAL4/TM6b, w^{1118};UAS-ChR2-XXL/CyO;UAS-amon-RNAi^{78b}/TM6b, w^{1118};UAS-ChR2-XXL/CyO; LexAop-GCamp6m/TM6b, w^{1118};UAS-ChR2-XXL/CyO;LexAop-reaper/TM6b, w^{1118};UAS-ChR2-XXL/CyO;UAS-Dop1R1-RNAi/TM6b, and w^{1118};UAS-amon-RNAi^{28b}/CyO;UAS-Chrimson,LexAop-GCamp6m/MKRS*. For further experiments balancer chromosomes were outcrossed and the stocks were used as homozygous transgenic lines.

Occasionally, the expression of effector genes has to be confirmed in case there are no visible markers as proof for successful transgenesis. This also applies for recombinant lines which are supposed to carry two different transgenes on one chromosome.

The aim of the classical genetic recombination performed here was the generation of recombinant fly stocks expressing *ChR2-XXL* and *Kir2.1^{260b}*, *ChR2-XXL* and *TNT^{49b}*, and *ChR2-XXL* and *TNT^{260b}*, respectively. After crossing both transgenic lines (parental crossing) single virgin F1 females were crossed with single double-balancer males. For each combination of transgenes 80 to 100 single fly crosses were raised. First preselection of possible recombinant lines was performed due to eye color. In 31 stocks *UAS-ChR2-XXL* likely recombined with *LexAop-Kir2.1^{260b}*. The number of possible *UAS-ChR2-XXL/LexAop-TNT^{49b}* and *UAS-ChR2-XXL/LexAop-TNT^{260b}* recombinants was 20 and 63, respectively. Next, a behavioral nociceptive pre-screen was performed to further narrow down the number of potential recombinant lines. Artificial optogenetic activation of *sNPF-GAL4* positive neurons results in a typical nociceptive response, in that larvae show a rolling behavior while flies are paralyzed or at least impaired in climbing (R. Lyutova, Master thesis). Therefore, the generated lines were crossed to *sNPF-GAL4* and the nociceptive behavior in larvae and

paralysis in adults was observed. Out of the 31 *UAS-ChR2-XXL,LexAop-Kir2.1*^{260b} stocks, 19 stocks showed no nociceptive response, four stocks showed adult and three larval phenotype, and in five lines larval as well as adult phenotype could be observed (Fig. 9A). In 9 *UAS-ChR2-XXL,LexAop-TNT*^{49b} stocks no nociceptive behavior could be monitored, three lines showed an adult phenotype, in one line only the larval phenotype was observed, and in seven lines both phenotypes were observed (Fig. 9B). Out of the 71 *UAS-ChR2-XXL,LexAop-TNT*^{260b} potential recombinants, 16 lines showed an adult-specific effect, 9 lines a larval-specific effect, while 22 lines showed an effect in both larva and adult (Fig. 9C).

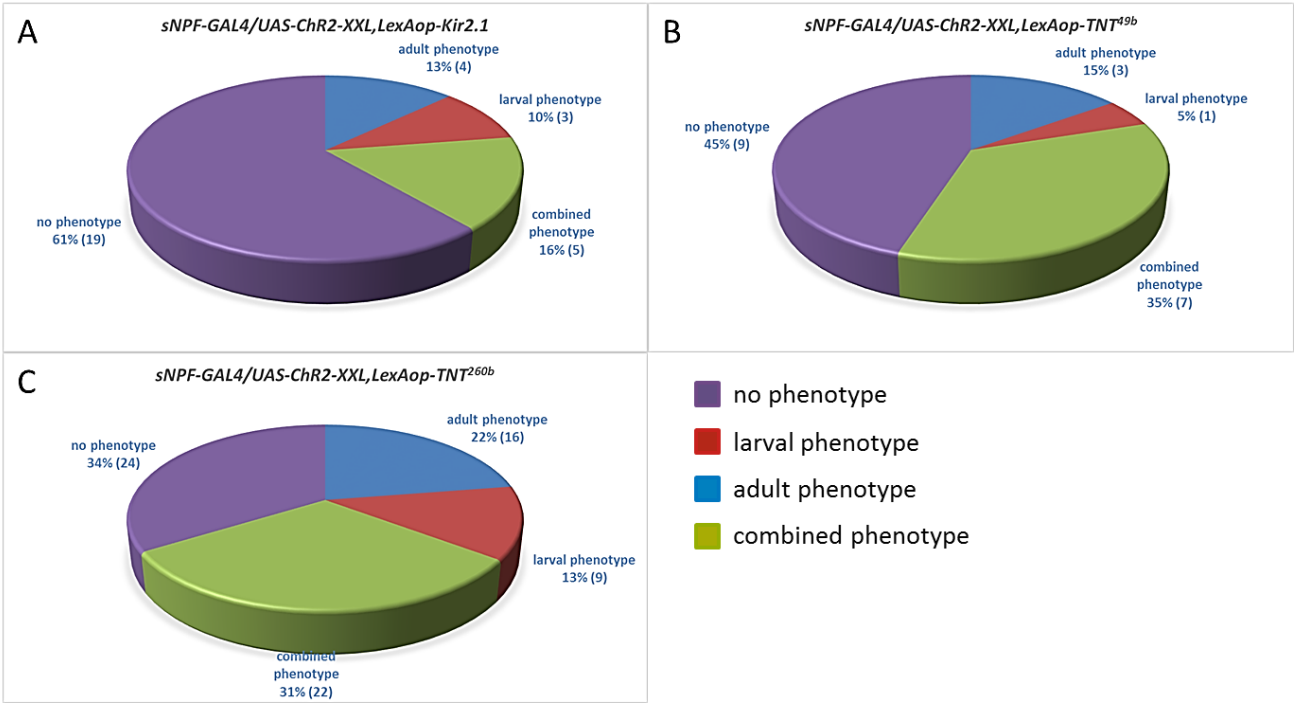

Figure 9: *Behavioral pre-screen of potential recombinant transgenic lines. The potential recombinant lines were crossed with sNPF-GAL4. It was monitored whether nociception behavior is elicited by blue light illumination. A: UAS-ChR2-XXL,LexAop-Kir2.1*^{260b} *potential recombinants showed variable nociceptive response. Only five of the tested stocks responded with robust phenotype during larval and adult stages; B: In seven of the tested UAS-ChR2-XXL,LexAop-TNT*^{49b} *stocks combined (larval and adult) phenotype was observed; C: In 22 UAS-ChR2-XXL,LexAop-TNT*^{260b} *potential recombinants nociceptive and paralysis responses were elicited in larvae and adults, respectively.*

As there was a variation in the manifestation of nociception, all lines showing a nociceptive response or paralysis during only larval or adult stage were discarded and molecular tests were only performed for lines with robust nociceptive behavior (larval and adult phenotype).

Five *UAS-ChR2-XXL,LexAop-Kir2.1*^{260b} lines were tested for the presence of both constructs via PCR. In two of the lines 100% of the tested flies were positive for *ChR2-XXL* as well as for *Kir2.1* (Fig 10A, B). In all other stocks the percentage of *ChR2-XXL* positive flies ranged from 60% to 90% whereas the *Kir2.1* construct was present in all tested flies (Appendix, Figures S1 - S3).

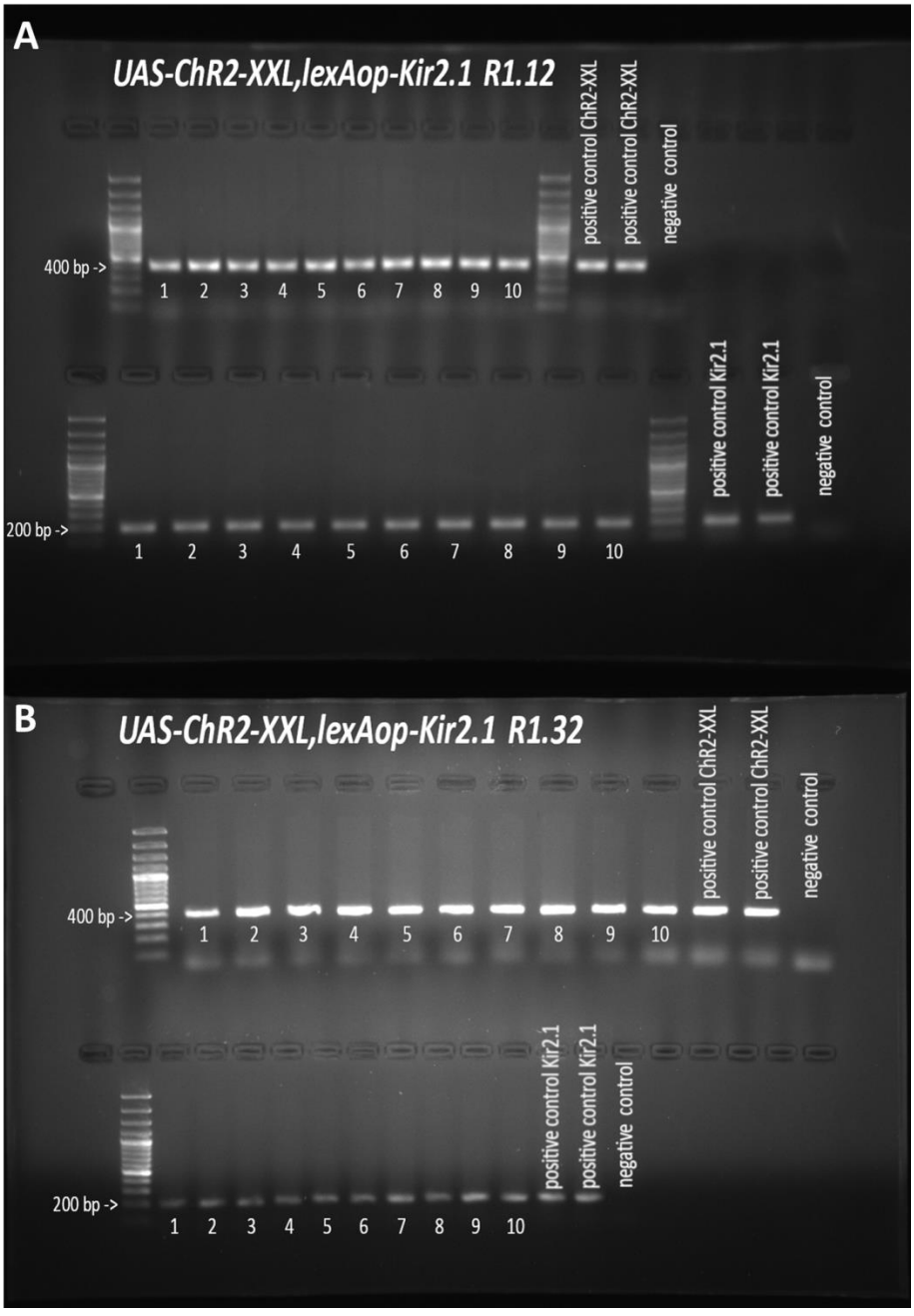

Figure 10: *PCR verification of the transgenes UAS-ChR2-XXL and lexAop-Kir2.1. In both tested recombinant lines (A: R1.12, B: R1.32) 100% of the flies were ChR2-XXL positive (upper 1 to 10 lanes in A and B).The presence of Kir2.1 was also proven in all tested flies (lower 1 to 10 lanes in A and B).*

In none of the *UAS-ChR2-XXL,LexAop-TNT^{49b}* lines *ChR2-XXL* could be found with 100% frequency (Appendix, Figures S4 – S7).

In three *UAS-ChR2-XXL,LexAop-TNT^{260b}* lines 100% of the tested flies were *ChR2-XXL* positive (Fig. 11A-C). All other stocks with 0% - 90% positive flies (Appendix, Figures S7 – S18) were discarded.

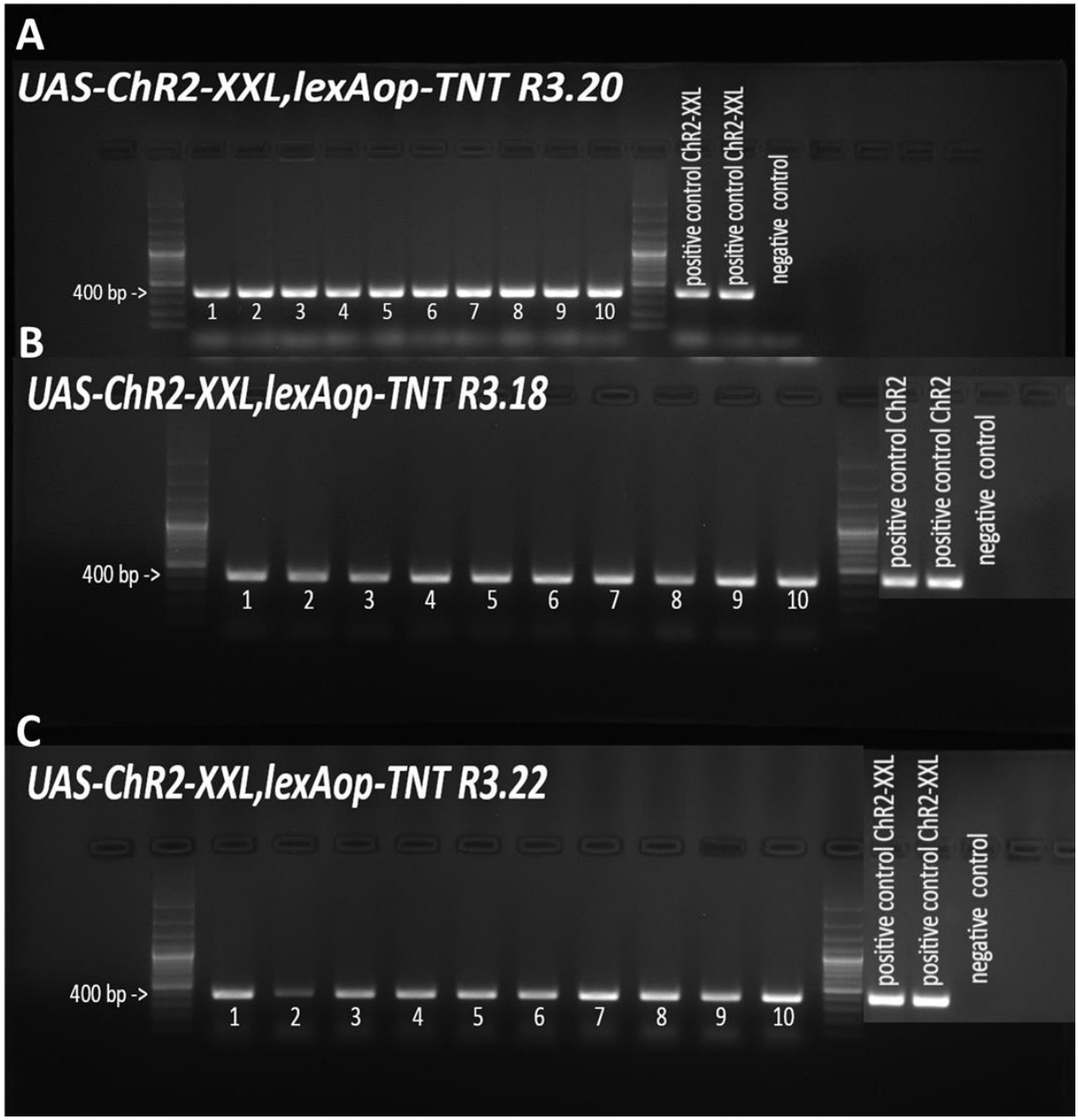

Figure 11: *PCR verification of the UAS-ChR2-XXL transgene expression. In three of the tested recombinant lines (A: R3.20, B: R3.18, C: R3.22) 100% of the flies were ChR2-XXL positive.*

4. Discussion

One of the main goals in the field of neurobiology is to dissect the functions of the nervous system (NS). Due to the "simplicity", e.g. small number of neurons, *Drosophila melanogaster* acts as an excellent model organism in basic research. By the use of approaches like electron microscopy (EM), working groups across the world collaborate in the FlyLight Project to produce and analyze the connectivity of the fruit fly NS and to describe the anatomy of every single neuron at synaptic level. Thus, the connectome of different brain areas of *Drosophila* larvae is described and publicly available, e.g. mushroom body [Eichler et al. 2017] and the feeding [Miroschnikow et al. 2018] connectome. However, the anatomical circuit architecture of brain structures gives only hints about the functions of the single components within these neuronal networks. Therefore, it is indispensable to analyze the role of communication between neurons for behavioral processes and output. To study complex connections between neurons, simultaneous manipulations of diverse neuronal populations are often required involving at least two different expression systems. Here, the GAL4/UAS and the LexA/LexAop systems were combined to generate transgenic lines for such complex genetic manipulations.

4.1. Combined lines

A prerequisite for simultaneous manipulation of different neurons is the expression of at least four transgenes within one animal. This is achieved by the crossing of combined driver and combined effector lines. Here, a GAL4/LexA driver line was generated to elicit the expression of two different effectors in the target cell populations, in order to investigate the functional connectivity of different neurons within the mushroom body (MB) circuit. In the stock *w^{1118};R58E02-LexA/CyO;H24-GAL4/TM6b* LexA is expressed in three dopaminergic neurons from the primary-lineage protocerebral anterior medial (pPAM) cluster. GAL4 is expressed in most of the MB intrinsic neurons, the Kenyon cells (KCs). The connectome

reconstruction of the MB revealed synaptic connections between KCs and pPAM neurons, however at that time point the function was still unknown. To achieve coincident genetic manipulation of KCs and pPAM neurons, three effector lines were generated. *w^{1118};UAS-ChR2-XXL/CyO;LexAop-reaper/TM6b* allows optogenetic activation of one neuronal population and simultaneous ablation of a second cluster of cells. Channelrhodopsin2 (ChR2) is a light-sensitive cation channel consisting of seven transmembrane domains and an all-trans-retinal chromophore. Upon photon absorption (blue light illumination, 480nm) the retinal changes its conformation resulting in cation influx and cell depolarization [Dawydow et al. 2014; Nagel et al. 2002; Nagel et al. 2003]. *reaper* (*rpr*) is an apoptosis regulating gene and its expression results in cell death [White et al. 1994; Zhou et al. 1997]. After simultaneous expression of both transgenes fused to UAS and LexAop, respectively, under the control of *H24-GAL4* and *R58E02-LexA*, KCs would be artificially activated and dopaminergic pPAM neurons - ablated. Thus, such orthogonal expression system during behavioral experiments allows a verification of the importance of synaptic connections for behavioral output. Besides the impact on behavior, a second aspect of anatomical circuit architecture is whether synapses between neurons are functional. This can be proven by activating presynaptic neurons and simultaneous recording of the activity of corresponding candidate postsynaptic cells. To apply this strategy, a *w^{1118};UAS-ChR2-XXL/CyO;LexAop-GCamp6m/TM6b* line was generated. GCaMP consists of the Green Fluorescent Protein (GFP) and the calcium-binding protein Calmodulin. Upon cell activation followed by respective intracellular Ca^{2+} increase, GFP and Calmodulin rearrange resulting in increased fluorescence output [Nakai et al. 2001]. In this manner, crossing *w^{1118};R58E02-LexA/CyO;H24-GAL4/TM6b* with *w^{1118};UAS-ChR2-XXL/CyO;LexAop-GCamp6m/TM6* allows recording the pPAM neurons' response to KC activation. If an anatomical connection is verified to be functional, it is crucial to examine the type of intercellular communication as most of the neurons express more than one neurotransmitter and/or neuropeptide. Peptidergic signaling can be manipulated by expression of *amon-RNAi*. The *amontillado* (*amon*) gene encodes a homolog of the mammalian PC2 and is required for peptide processing in *Drosophila* [Wegener et al. 2011; Rhea et al. 2010; Siekhaus and Fuller 1999; Pauls et al. 2014]. The combined effector line *w^{1118};UAS-amon-RNAi^{28b}/CyO;UAS-Chrimson,LexAop-GCamp6m/MKRS* was generated in order to simultaneously block

neuropeptide maturation in the artificially activated cells and record the response in downstream neurons. As for the generation of the latter stock it was necessary to integrate three transgenic constructs into the genome, a previously recombined *UAS-Chrimson,LexAop-GCamp6m* line was used. Here, the optogenetic activation is achieved by expression of Chrimson, a light-sensitive cation channel that opens upon red light illumination (590 nm) [Klapoetke et al. 2014]. By crossing the newly generated triple line with a respective driver line it is possible to be observed whether a functional synaptic connection relies on peptidergic signaling.

The combination of transgenic effector lines allows further manipulation of two different aspects of neuronal activity in the same cell. Therefore, two additional combined effector stocks were generated. Crossing *w^{1118};UAS-ChR2-XXL/CyO;UAS-amon-RNAi^{78b}/TM6b* with a single driver line results in a simultaneous optogenetic activation of a neuronal cluster, and knock down of *amon* and impaired neuropeptide maturation within the same neurons, respectively. Thereby, the function of a neuronal population with respect to peptidergic signaling can be examined. Generating the line *w^{1118};UAS-ChR2-XXL/CyO;UAS-Dop1R1-RNAi/TM6b* ensures optogenetic activation of neurons with coincident knock down of the dopaminergic R1 receptor (Dop1R1) in the latter. By that, the dopaminergic input to the respective cells is disturbed. If a behavioral output, usually triggered by activation of certain cells, is impaired upon Dop1R1 knock down in the same cells, it is reasonable that dopaminergic input from upstream neurons as consequence of e.g. feedback loops is necessary for eliciting the behavior.

All lines described here were used for functional dissection of an anatomical KC-to-pPAM feedback loop (Chapter III). However, crossing the recombined effector lines to other recombined driver lines could provide basis for investigating the function of many other neuronal circuits.

The examples of combined transgenic lines for sophisticated genetic manipulations outlines the great potential of the genetic tools available in *Drosophila*. The described crossing scheme for combination of transgenes within one organism can be used for any two transgenic constructs located on different (second and third) chromosomes.

4.2. Homologous recombination

To date, a wide range of transgenic effector lines is available. Nevertheless, one of the limitations in generating variants of the stocks is the restriction in the chromosome number of *Drosophila* (four chromosomes [Metz 1914]) and integration sites, respectively. As many of the effector lines are available in one variant as insertion in a certain chromosome, it becomes problematic if two transgenic constructs are located on the same chromosome, but should be combined within one transgenic line. Here, a crossing scheme for classical homologous recombination of transgenes was provided. UAS and LexAop constructs were recombined in order to generate a double effector line.

Genetic recombination upon crossing over of homologous chromosomes was extensively studied in the last 100 years. The terms “genetic recombination” and “crossing over” are mutually used, however they describe two aspects of chromosomal genetic material exchange. Crossing over refers to the physical mechanism whereas recombination is the empirical trackable read-out of crossover [Schweitzer 1935]. Thus, both processes depend on different factors. The number and position of crossovers depend on external factors, e.g. temperature [Plough 1917] and maternal age [Bridges 1927]. Further, crossing over occurs only in *Drosophila* females, as fruit fly males do not develop synaptonemal complex and chiasmata during prophase I of meiosis [Morgan 1914]. Therefore, while performing genetic recombination according to crossing scheme it should be always kept in mind collecting virgin females from F1 generation of parental lines carrying the recombining genes. Another concern should be the location of the genes within the genome as gene distance is pivotal. The probability of gene recombination increases with lengthening the distance between the genes. In case of transgenic constructs, it should be considered that different insertion sites were used for generation of the transgenic stocks. If this is not the case, both transgenes will be exchanged against each other during crossover. Here, a protocol for generation of stocks with recombined transgenes on the second chromosome was provided. Homologous recombination was performed to combine *UAS-ChR2-XXL* with either *LexAop-Kir2.1*^{260b}, *LexAop-TNT*^{49b}, or *LexAop-TNT*^{260b}. *Kir2.1* is human inward rectifying K^+ channel. Its overexpression decreases the excitability of neurons due to hyperpolarization resulting in

silencing of the cells and reduced probability of neurotransmitter release [Baines et al. 2001]. Tetanus toxin (*TNT*) inhibits neurotransmitter release as it cleaves neuronal Synaptobrevin, a synaptic vesicle protein [Sweeney et al. 1995]. Recombination of *ChR2-XXL* and *Kir2.1* or *TNT*, respectively, would allow optogenetic activation of a neuronal population and simultaneous silencing of distinct cluster of neurons without complete ablation of the target cells.

UAS-ChR2-XXL is inserted in chromosome 2 at position 2R:16298254..16298254 (landing site *attP-9A[VK18]*) [Dawydow et al. 2014]. As all three LexAop lines were kindly provided by Katharina Eichler and are not officially published yet, the exact position of the constructs on the second chromosome was unknown. Still, it was assumed that the landing sites do not overlap, as the LexAop stocks were generated at Janelia Research Campus of the Howard Hughes Medical Institute. So far, all published transgenic effector lines from the Janelia stock collection were inserted using the landing sites *attP1*, *attP2*, *attP8*, *attP18* and *attP40* (https://www.janelia.org/open-science/rubin-lab-fly-stocks, state: 21.01.2019). Indeed, five positive recombination effects were verified: two recombinant *UAS-ChR2-XXL,LexAop-Kir2.1^{260b}* lines and three recombinant *UAS-ChR2-XXL,LexAop-TNT^{260b}* lines. *UAS-ChR2-XXL* could not recombine with *lexAop-TNT^{49b}*. It is possible that both transgenes are integrated at neighboring positions within the second chromosome. If so, homologous recombination of these transgenes would be exceptional, as usually the exchange of genetic material occurs in blocks [Sturtevant 1913, 1915; Morgan et al. 1925]. The successful recombination in the *UAS-ChR2-XXL,LexAop-Kir2.1^{260b}* stocks was proved via PCR amplification of both transgenes and represents a frequency of recombination events of 2-2.5%. In the *UAS-ChR2-XXL,LexAop-TNT^{260b}* recombinant lines, the integration of *UAS-ChR2-XXL* was verified via PCR. However, as *TNT* primers were not available, the integration of *LexAop-TNT^{260b}* in the recombinant line could only be suggested by the dark eye color of the flies. Thus, it is indispensable to prove the expression of *TNT* using another approach. Crossing *UAS-ChR2-XXL,LexAop-TNT^{260b}* with class IV multidendritic neurons (MD) specific driver *R38A10-LexA* would cause significant change in nociceptive behavior in case of successful recombination, and *TNT* expression in cIV MD neurons, respectively. Class IV MD neurons are responsible for the characteristic rolling behavior during nociceptive responses [Hwang et al. 2007]. If neurotransmitter release is inhibited in the cIV MD neurons, e.g. due to *TNT* expression, larvae will not be able

to perform rolling. Such behavioral tests are suited for fast and easy analysis of transgenic effectors' expression.

One recombinant *UAS-ChR2-XXL,LexAop-Kir2.1*^{260b} line was further used for functional dissection of an anatomical KC-to-pPAM feedback loop (Chapter III). Nevertheless, as *Kir2.1* and *TNT* affect neuronal activity in different ways (hyperpolarization and neurotransmitter release inhibition, respectively), it could be reasonable to reproduce the experiment by using a *UAS-ChR2-XXL,LexAop-TNT*^{260b} recombinant line.

Yet, similar to the previously described combined effector lines, *UAS-ChR2-XXL,LexAop-Kir2.1*^{260b} and *UAS-ChR2-XXL,LexAop-TNT*^{260b} can be crossed to any desired recombined driver line, and by that be used for investigating the functions of other neuronal networks.

5. Summary

Here, two protocols with crossing schemes for combining different transgenes within one animal are provided. Combining transgenic lines into one stock allows multiple manipulations of diverse neuronal network components. In this work, new lines were produced, in order to investigate the function of an anatomical feedback loop within the MB circuit. By simultaneous expression of *ChR2-XXL* and a second effector gene, it is possible to activate one subset of neurons and genetically manipulate a distinct population of cells. For example, crossing *w^{1118};UAS-ChR2-XXL/CyO;LexAop-reaper/TM6b*, *UAS-ChR2-XXL,LexAop-Kir2.1^{260b}*, or *UAS-ChR2-XXL,LexAop-TNT^{260b}* to a recombined driver line can be useful to observe the functional relationship of communicating neurons with respect to behavioral output. Other recombined lines (*w^{1118};UAS-ChR2-XXL/CyO;LexAop-GCamp6m/TM6b and w^{1118};UAS-amon-RNAi^{28b}/CyO;UAS-Chrimson,LexAop-GCamp6m/MKRS*) allow the investigation of the functionality of anatomical connections between different neurons. Finally, the *w^{1118};UAS-ChR2-XXL/CyO;UAS-Dop1R1-RNAi/TM6b* and *w^{1118};UAS-ChR2-XXL/CyO;UAS-amon-RNAi^{78b}/TM6b* stocks can be used for multiple genetic manipulations of one population of neurons. By using these effector lines, the function of an anatomical KC-to-pPAM signaling within the memory circuitry was dissected (Chapter III). However, all produced effector lines can find broader application in research that targets neuronal networks.

6. References

Baines RA, Uhler JP, Thompson A, Sweeney ST, Bate M (2001) Altered electrical properties in *Drosophila* neurons developing without synaptic transmission. J Neurosci 21:1523-1531.

Bischof J, Maeda RK, Hediger M, Karch F, Basler K (2007) An optimized transgenesis system for *Drosophila* using germ-line-specific phiC31 integrases. Proc Natl Acad Sci U S A 104:3312-3317.

Bridges CB (1927) The relation of the age of the female to crossing over in the third chromosome of *Drosophila melanogaster*. J. Gen. Physiol. 8: 689-700.

Castro JP, Carareto CM (2004) *Drosophila melanogaster* P transposable elements: mechanisms of transposition and regulation. Genetica 121:107-118.

Clancy, S (2008) Genetic recombination. Nature Education 1(1):40

Creighton HB, McClintock B (1931) A correlation of cytological and genetical crossing-over in zea mays. Proc Natl Acad Sci U S A 17:492-497.

Dawydow A, Gueta R, Ljaschenko D, Ullrich S, Hermann M, Ehmann N, Gao S, Fiala A, Langenhan T, Nagel G, Kittel RJ (2014) Channelrhodopsin-2-XXL, a powerful optogenetic tool for low-light applications. Proc Natl Acad Sci U S A 111:13972-13977.

Eichler K, Li F, Litwin-Kumar A, Park Y, Andrade I, Schneider-Mizell CM, Saumweber T, Huser A, Eschbach C, Gerber B, Fetter RD, Truman JW, Priebe CE, Abbott LF, Thum AS, Zlatic M, Cardona A (2017) The complete connectome of a learning and memory centre in an insect brain. Nature 548:175-182.

Griffiths AJF, Miller JH, Suzuki DT, Lewontin RC, Gelbart WM (2000) An introduction to genetic analysis, 7th edition, New York: W. H. Freeman

Groth AC, Fish M, Nusse R, Calos MP (2004) Construction of transgenic *Drosophila* by using the site-specific integrase from phage phiC31. Genetics 166:1775-1782.

Hentges KE, Justice MJ (2004) Checks and balancers: balancer chromosomes to facilitate genome annotation. Trends Genet 20:252-259.

Herranz H, Weng RF, Cohen SM (2014) Crosstalk between epithelial and mesenchymal tissues in tumorigenesis and imaginal disc development. Current Biology 24:1476-1484.

Hwang RY, Zhong L, Xu Y, Johnson T, Zhang F, Deisseroth K, Tracey WD (2007) Nociceptive neurons protect *Drosophila* larvae from parasitoid wasps. Curr Biol 17:2105-2116.

Janssens FA, Koszul R, Zickler D (2012) The chiasmatype theory. A new interpretation of the maturation divisions. 1909. Genetics 191:319-346.

Klapoetke NC, Murata Y, Kim SS, Pulver SR, Birdsey-Benson A, Cho YK, Morimoto TK, Chuong AS, Carpenter EJ, Tian Z, Wang J, Xie Y, Yan Z, Zhang Y, Chow BY, Surek B, Melkonian M, Jayaraman V, Constantine-Paton M, Wong GK, Boyden ES (2014) Independent optical excitation of distinct neural populations. Nat Methods 11:338-346.

Klemenz R, Weber U, Gehring WJ (1987) The *white* gene as a marker in a new P-element vector for gene transfer in *Drosophila*. Nucleic Acids Res 15:3947-3959.

Lyutova, R (2015) Manipulation of sNPF signaling reveals pleiotropic functions in *Drosophila* larvae. Master thesis

Metz CW (1914) Chromosome studies in the Diptera. I. A preliminary survey of five different types of chromosome groups in the genus *Drosophila*. J. exp. Zool. 17(1): 45--59.

Miroschnikow A, Schlegel P, Schoofs A, Hueckesfeld S, Li F, Schneider-Mizell CM, Fetter RD, Truman JW, Cardona A, Pankratz MJ (2018) Convergence of monosynaptic and polysynaptic sensory paths onto common motor outputs in a *Drosophila* feeding connectome. Elife 7.

Morgan TH (1914) No crossing over in the male of *Drosophila* of genes in the second and third pairs of chromosomes. Biol Bull 26:195-204; http://dx.doi.org/10.2307/1536193

Morgan TH, Bridges CB and Sturtevant AH (1925) The genetics of *Drosophila*. Bibliogr. Genet. 2: 1-262.

Muller HJ (1918) Genetic variability, twin hybrids and constant hybrids, in a case of balanced lethal factors. Genetics 3:422-499.

Nagel G, Ollig D, Fuhrmann M, Kateriya S, Musti AM, Bamberg E, Hegemann P (2002) Channelrhodopsin-1: a light-gated proton channel in green algae. Science 296:2395-2398.

Nagel G, Szellas T, Huhn W, Kateriya S, Adeishvili N, Berthold P, Ollig D, Hegemann P, Bamberg E (2003) Channelrhodopsin-2, a directly light-gated cation-selective membrane channel. Proc Natl Acad Sci U S A 100:13940-13945.

Nakai J, Ohkura M, Imoto K (2001) A high signal-to-noise Ca(2+) probe composed of a single green fluorescent protein. Nat Biotechnol 19:137-141.

Pauls D, Chen J, Reiher W, Vanselow JT, Schlosser A, Kahnt J, and Wegener C (2014) Peptidomics and processing of regulatory peptides in the fruit fly *Drosophila*, EuPA Open Proteomics 3, 114-127

Plough HH (1917) Effect of temperature on crossing-over in *Drosophila*. Baltimore.

Pray L & Zhaurova K (2008) Barbara McClintock and the discovery of jumping genes (transposons). Nature Education 1(1):169

Prieto-Godino LL, Diegelmann S, Bate M (2012) Embryonic origin of olfactory circuitry in *Drosophila*: contact and activity-mediated interactions pattern connectivity in the antennal lobe. PLoS Biol 10:e1001400.

Rhea JM, Wegener C, Bender M (2010) The proprotein convertase encoded by *amontillado* (*amon*) is required in *Drosophila* corpora cardiaca endocrine cells producing the glucose regulatory hormone AKH. PLoS Genet 6:e1000967.

Rubin GM, Spradling AC (1982) Genetic transformation of *Drosophila* with transposable element vectors. Science 218:348-353.

Rubin GM, Spradling AC (1983) Vectors for P element-mediated gene transfer in *Drosophila*. Nucleic Acids Res 11:6341-6351.

Schweitzer MD (1935) An analytical study of crossing over in *Drosophila melanogaster*. In, pp 1 p. l., p. 497 -527, 491 l. Brooklyn,: Columbia university.

Sharp, L (1934) Introduction to Cytology (McGraw–Hill, New York), pp. 303, 330, 333

Siekhaus DE, Fuller RS (1999) A role for *amontillado*, the *Drosophila* homolog of the neuropeptide precursor processing protease PC2, in triggering hatching behavior. J Neurosci 19:6942-6954.

Spradling AC, Rubin GM (1982) Transposition of cloned P elements into *Drosophila* germ line chromosomes. Science 218:341-347.

Sturtevant AH (1913) The linear arrangement of six sex-linked factors in *Drosophila* as shown by their mode of association. J. Exp. Zool. 14: 43-59.

Sturtevant AH (1915) The behavior of the chromosomes as studied through linkage. Z.I.A.V. 13: 238-287.

Sturtevant AH (1921) A case of rearrangement of genes in *Drosophila*. Proc Natl Acad Sci U S A 7:235-237.

Sweeney ST, Broadie K, Keane J, Niemann H, O'Kane CJ (1995) Targeted expression of tetanus toxin light chain in *Drosophila* specifically eliminates synaptic transmission and causes behavioral defects. Neuron 14:341-351.

Thorpe HM, Smith MC (1998) In vitro site-specific integration of bacteriophage DNA catalyzed by a recombinase of the resolvase/invertase family. Proc Natl Acad Sci U S A 95:5505-5510.

Venken KJ, He Y, Hoskins RA, Bellen HJ (2006) P[acman]: a BAC transgenic platform for targeted insertion of large DNA fragments in *D. melanogaster*. Science 314:1747-1751.

Venken KJ, Bellen HJ (2007) Transgenesis upgrades for *Drosophila melanogaster*. Development 134:3571-3584.

Wegener C, Herbert H, Kahnt J, et al (2011) Deficiency of prohormone convertase dPC2 (AMONTILLADO) results in impaired production of bioactive neuropeptide hormones in *Drosophila*. J Neurochem 118:581–595.

White K, Grether ME, Abrams JM, Young L, Farrell K, Steller H (1994) Genetic control of programmed cell death in *Drosophila*. Science 264:677-683.

Zhou L, Schnitzler A, Agapite J, Schwartz LM, Steller H, Nambu JR (1997) Cooperative functions of the *reaper* and *head involution defective* genes in the programmed cell death of *Drosophila* central nervous system midline cells. Proc Natl Acad Sci U S A 94:5131-5136.

III. Reward signaling in a recurrent circuit of dopaminergic neurons and peptidergic Kenyon cells

1. Introduction

Memory can be defined as stored and later retrieved knowledge and skills. The knowledge is gained during the process of learning that changes behavior due to previous experience and allows adaptation to environmental changes. A huge effort was done to unravel the mechanisms of memory formation, and the underlying principles of learning behavior. Two types of learning were extensively studied from the very late 19th century. In 1898, Edgar Thorndike postulated the theory of "trial-and-error learning" or the so-called operant conditioning. His work was later continued by Burrhus Frederic Skinner, who developed the famous "Skinner box". During operant conditioning an animal learns to associate its own action with a certain outcome, resulting in either expression of behavior in order to receive reward, or suppressing a behavior to avoid punishment [Skinner 1950; Thorndike 1898; Kandell, 5th ed., 1556-1557]. In the late 20s, the Russian physiologist Ivan Petrovich Pavlov described a second paradigm of associative conditioning, the classical conditioning. During this type of training an animal associates an unconditioned stimulus (US) with a conditioned stimulus (CS). After the training, in a test situation, the animal responds to the CS with a conditioned response (CR), equivalent to the unconditioned response (UR) to the US [Pavlov and Anrep 1927; Kandell, 5th ed., 1555-1556].

Research in the field of memory formation in *Drosophila* was initiated by Seymour Benzer's group in the 70s. An assay for operant conditioning of flies was established and it was shown that *Drosophila* indeed reliably learns to prevent electric shock punishment (outcome) by avoiding approach behavior towards an odor (action) [Quinn et al. 1974]. The setup of this learning assay led to identification of memory phases and first learning mutants, e.g. *dunce*

and *amnesiac* [Dudai et al. 1976; Quinn and Dudai 1976; Quinn et al. 1979]. Later, a classical conditioning assay was developed in order to overcome some limitations of the operant conditioning trials. In the first approach of Tully and Quinn, flies were trained to associate electric shock (US) with odor exposure (CS). In a subsequent test, flies were thought to predict punishment due to the presence of the associated odor [Tully and Quinn 1985]. The ability of *Drosophil*a larvae to associate an odor with an US was shown in the 70s and 80s [Aceves-Pina and Quinn 1979; Heisenberg et al. 1985]. Since then, researchers from all over the world are using *Drosophila* as model organism to investigate the basics of learning and memory.

Diverse learning assays for formation of different kinds of memory were established for adult flies. Similar to other insects, fruit flies are capable of visual learning in a flight simulator [Brembs and Heisenberg 2000; Wolf and Heisenberg 1991], spatial learning in a heat box [Putz and Heisenberg 2002; Wustmann et al. 1996], and visual place learning in a heat maze [Ofstad et al. 2011]. However, studies on olfactory learning have provided the most extensive insights into the neuronal mechanisms underlying learning behavior and memory formation. Further, except few works applying light as CS [Gerber et al. 2004; von Essen et al. 2011], most research on learning in *Drosophila* larvae was done using odors as CS. It is also notable, that meanwhile gustatory stimuli (i.e. sugar, salt or amino acids) are mostly used as US for olfactory learning assays in larvae as these flavors are by definition appetitive or aversive for naïve animals and represent natural reward or punishment.

The aim of this work was to investigate in detail the function of an anatomical feedback loop within the circuitry of the *Drosophila* memory center, the mushroom bodies, with regard to learning behavior as well as naïve behaviors, e.g. olfaction and gustation.

1.1. The olfactory system of *Drosophila melanogaster*

Olfaction can be determined as "the sense of smell". It involves perception of volatile compounds and plays significant role in regulating different behavioral aspects, such as navigation, predator avoidance, and finding mating partners or oviposition sites [Stocker 1994]. Interestingly, the chemosensory system of *Drosophila* evinces a prominent degree of similarity with that of higher animals, e.g. the organization of the olfactory pathway from olfactory receptor neurons (ORNs) through olfactory primary centers with glomerular organization to higher brain areas.

In adult *Drosophila*, the olfactory receptor neurons (ORNs) are situated in sensilla located in the 3rd segment of the antenna (funiculus) and maxillary palp (Fig. 12) [Shanbhag et al. 1999]. There are three types of sensilla – basiconic, trichoid and coelonic, differing in the type of odors they respond to – food odors, fly odors, and humidity, respectively [de Bruyne et al. 1999; de Bruyne et al. 2001; Shanbhag et al. 1999; van der Goes van Naters and Carlson 2007; Yao et al. 2005]. The antennal lobe, a vetrebrates' olfactory bulb analog, receives mostly bilateral input from 1100-1250 sensory neurons from the antennae and 120 sensory neurons from the palps [Gerber et al. 2009; Stocker 2001]. ORNs express specific olfactory receptors (ORs) and project to specific glomeruli in the antennal lobe (AL) [Gao et al. 2000; Vosshall et al. 2000]. The AL glomeruli are interconnected via GABAergic inhibitory and cholinergic excitatory interneurons, improving the signal-to-noise ratio [Olsen et al. 2007; Silbering and Galizia 2007; Wilson and Laurent 2005]. Cholinergic projection neurons (PNs) project in a divergent combinatorial manner from the AL to higher brain centers, the lateral horn (LH) and the mushroom bodies (MBs) (Fig. 13) [Marin et al. 2002; Yasuyama et al. 2003; Yusuyama et al. 2002]. Both brain structures were shown to play a role in regulating behavior. The LH is known to be involved in naïve odor responses whereas the MBs are brain centers required for olfactory learning [Debelle and Heisenberg 1994; Heimbeck et al. 2001; Jefferis et al. 2007; Tanaka et al. 2004].

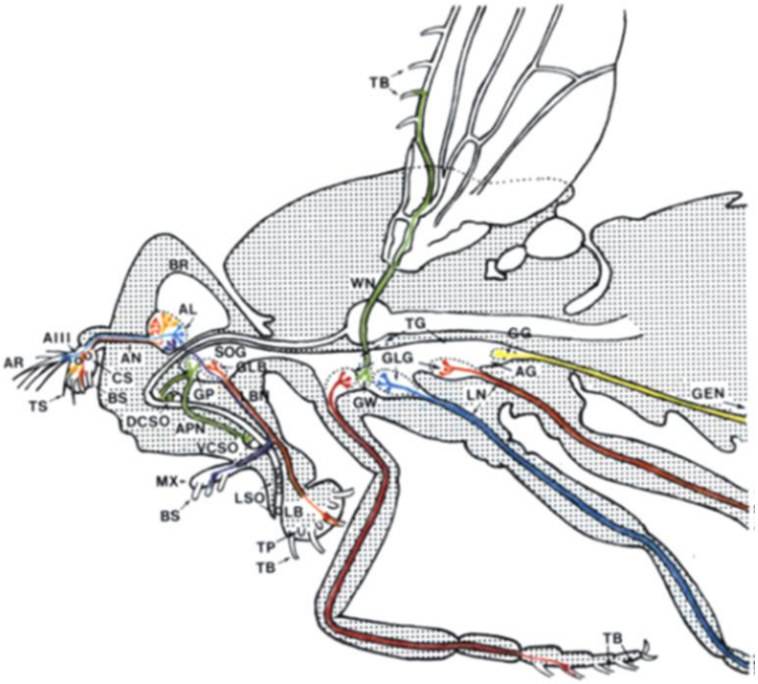

***Figure 12**: Illustration of the olfactory and gustatory system of Drosophila melanogaster and their main targets. AIII: 3rd antennal segment (funiculus); AG: abdominal ganglia; AL: antennal lobe; AN: antennal nerve; APN: accessory pharyngeal nerve; AR: arista, BR: supraoesophageal ganglion (brain); BS basiconic sensillum; CS: coeloconic sensillum; DCSO: dorsal cibarial sense organ; GEN: female genitalia; GG: gustatory center of genitalia; GLB: gustatory center of the labellum; GLG: gustatory centers of the legs; GP: gustatory center of the pharynx; GW: gustatory center of the wing; LB: labellum (labial palps); LBN: labial nerve; LN: leg nerves; LSO: labral sense organ; MX: maxillary palps; SOG: suboesophageal ganglion (meanwhile SEZ); TB: taste bristle; TG: thoracic ganglia; TP: taste peg; TS: trichoid sensillum; VCSO: ventral cibarial sense organ; WN: wing nerve. From [Jefferis et al. 2007; Stocker 1994]*

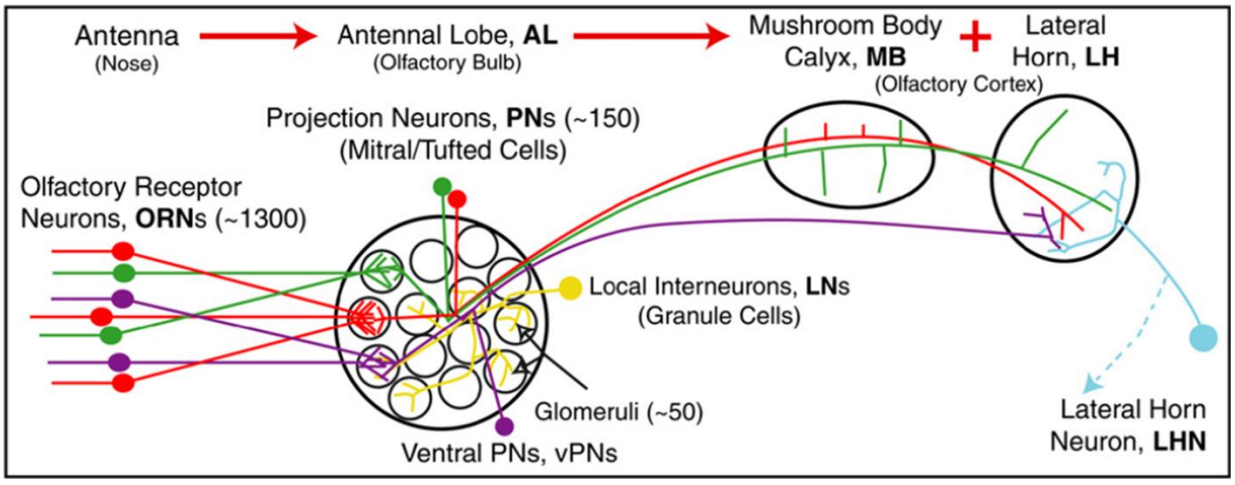

***Figure 13:** Olfactory pathway of Drosophila melanogaster. The color-coded signaling pathway shows ORNs expressing certain olfactory receptor, their target glomeruli within the AL and the projections to the MBs and LH. From [Jefferis et al. 2007; Stocker 1994]*

In *Drosophila* larvae 21 ORNs are situated in the dorsal organ (DO), a mixed olfactory and gustatory chemosensory organ (Fig. 14) housing an olfactory "dome" sensillum. The ORNs are bundled in seven triplets and project via the antennal nerve to the ipsilateral larval antennal lobe (LAL). Conversely to the wiring in the fly, there is no convergence of ORN dendrites at the level of the 21 LAL glomeruli [Fishilevich et al. 2005; Fishilevich and Vosshall 2005; Heimbeck et al. 1999; Kreher et al. 2005]. As in adults, LAL glomeruli are interconnected by local interneurons, however each glomerulus is innervated by only one to few projection neurons [Ramaekers et al. 2005]. Indeed, EM reconstruction of the glomerular olfactory system in *Drosophila* larvae revealed two types of signaling to higher brain areas. The uniglomerular system consists of 21 uniglomerular PNs (uPNs) receiving exclusive input from single ORNs and mostly projecting to both LH and MBs [Berck et al. 2016]. The multiglomerular system consists of 14 multiglomerular PNs (mPNs) which receive input from multiple neurons, either only from ORNs or from one ORN and non-ORN sensory neurons in the suboesophageal zone (SEZ) [Berck et al. 2016]. The mPNs project to the LH, MB calyx, vertical lobe of the MB and regions around the MB calyx (Fig. 14) [Berck et al. 2016; Marin et al. 2005; Ramaekers et al. 2005].

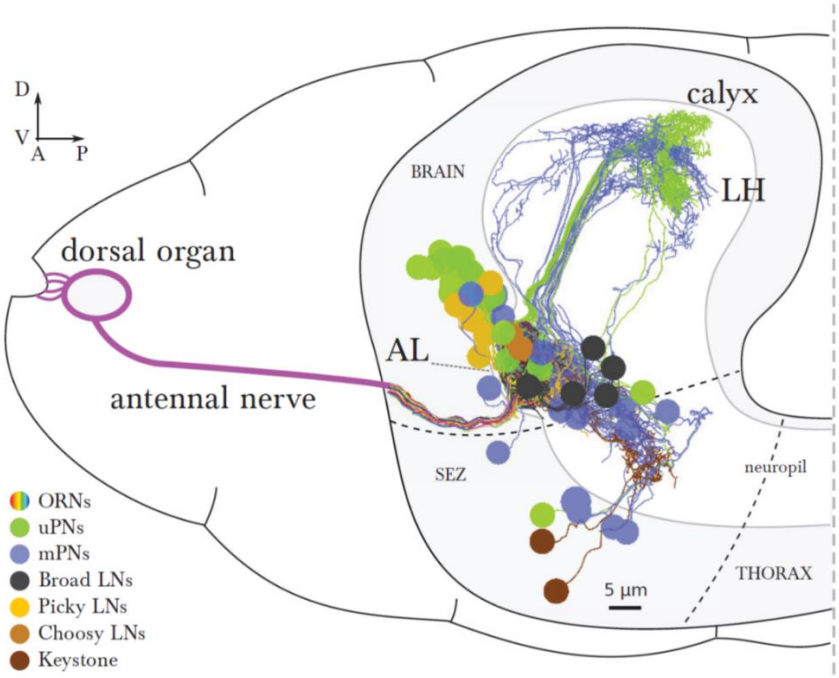

Figure 14: *Illustration of the olfactory system of the Drosophila larva. AL: antennal lobe; LH: lateral horn; LN: lateral neuron; ORN: olfactory receptor neuron; PN: projection neuron; SEZ: suboesophageal zone. The major local neurons and two classes of projection neurons with the respective targets are color-coded. From [Berck et al. 2016]*

Besides the similarities in the cellular architecture, a common principle of olfaction in both vertebrates and fruit flies is that each glomerulus is innervated by a single class of ORNs. The ORN classes are defined by the olfactory receptor (OR) situated in the membrane, as characteristic for olfactory sensory systems is the exclusive expression of only one OR per ORN [Hildebrand and Shepherd 1997; Vosshall et al. 1999]. Although observations on olfactory behavior in *Drosophila* flies and larvae were done already in the 70s and 80s [Aceves-Pina and Quinn 1979; Monte et al. 1989; Rodrigues 1980], the first genes encoding for ORs were identified in the late 90s. In total 60 genes (*Or*s) encode for 62 ORs [Clyne et al. 1999; Gao and Chess 1999; Robertson et al. 2003; Vosshall et al. 1999]. 12 ORs are expressed in adult and larva, 48 are expressed exclusively in flies, and 25 only in larvae (Fig. 15). Besides the ligand-specific ORs expressed in defined subpopulation of ORNs, an atypical OR – *Or83b* - is expressed in all ORNs and forms a dimer with conventional ORs [Benton et al. 2006; Fishilevich et al. 2005; Larsson et al. 2004; Vosshall et al. 1999].

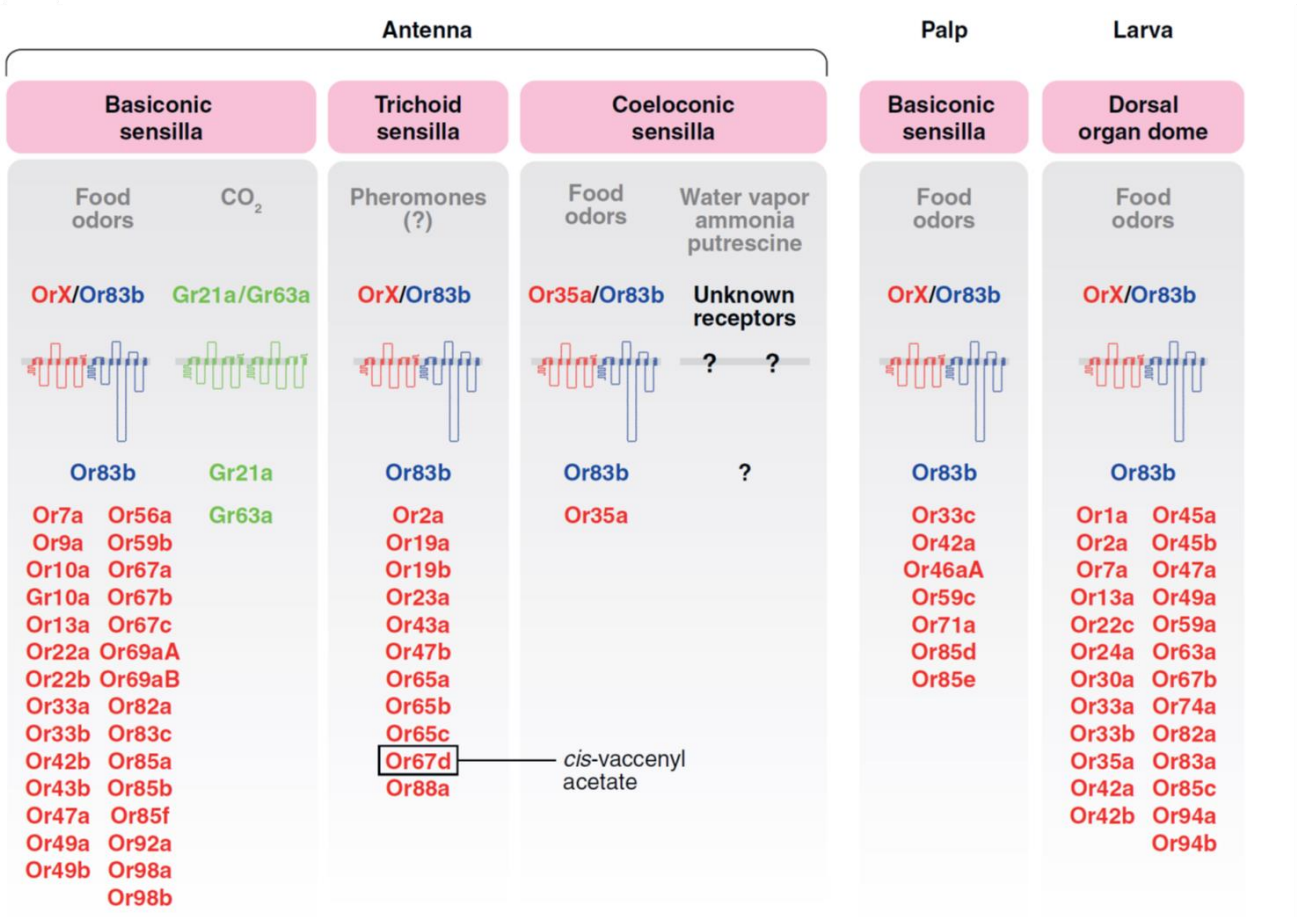

Figure 15: *List of the larval and adult olfactory receptors in Drosophila melanogaster. Olfactory receptors (ORs) are subdivided due to sensillum type and function. Or83b forms coreceptor dimers with all ORs. From [Vosshall and Stocker 2007]*

Based on the expression patterns of ORs, OR-to-glomerulus maps were established and the molecular basis of odor coding in the adult AL was investigated [Couto et al. 2005; Fishilevich and Vosshall 2005]. Furthermore, a spatial map of odor representation in larvae was generated and the response properties of the ORs were investigated, showing that functionally related ORNs target related spatial positions of the LAL. In the larval olfactory system sensitivity is achieved via overlapping response spectra, and combinatorial coding ensures odor discrimination [Kreher et al. 2005].

1.2. The gustatory system of *Drosophila melanogaster*

Besides olfaction, gustation is crucial for food quality evaluation and adequate responses (appetitive or aversive) to solid compounds, and organizes feeding behavior. Unlike the olfactory system, the gustatory system of insects does not resemble the one of vertebrates in terms of the cellular architecture. In adult *Drosophila* external gustatory organs are distributed over different body parts – labial palps part of the proboscis, legs, wings and vaginal plate, ensuring initial contact with and examination of the food, and initiating ingestion [Kraliz and Singh 1997; Stocker 1994; Vosshall and Stocker 2007]. Further, three internal taste organs with embryonic origin are located along the pharynx – ventral (VCSO) and dorsal cibarial (DCSO), and labral (LSO) sense organs, monitoring the quality of the food [Gendre et al. 2004; Nayak and Singh 1983; Stocker 1994]. Gustatory receptor neurons (GRNs) are primary sensory neurons. Two to four GRNs are located within a taste sensillum, a cuticular hair-like structure. They extend their dendrites to a pore at the tip of the sensillum and project to different areas of the SEZ (Fig. 12) [Nayak and Singh 1985; Stocker and Schorderet 1981; Thorne et al. 2004; Wang et al. 2004]. The number of sensilla varies within taste organs and within sexes (for the tarsi taste organs) [Meunier et al. 2000]. Due to the length and the substance they respond to, the labellar sensilla are subdivided in three types: long (l-type), short (s-type), and intermediate (i-type). Each of the two GRNs in the i-type sensilla respond to either attractive or aversive stimuli. The l- and s-type sensilla contain each four GRNs: S cell responding to sugar, W cell responding to water, and L1 and L2 cells responding to low and high salt concentrations respectively [Hiroi et al. 2002; Hiroi et al. 2004; Meunier et al. 2003]. Besides classical taste sensilla, 30-40 taste pegs are located in pseudotrachea in the labellum. Taste

pegs trigger pumping behavior and ingestion and each taste peg is innervated by two sensory neurons, a mechanosensory and a gustatory [Shanbhag et al. 2001]. In adults, 60 gustatory receptor (*Gr*) genes encode 68 GRs [Clyne et al. 2000; Robertson et al. 2003; Scott et al. 2001]. The expression pattern of GRs is highly variable. They can be expressed either in only one or in different tissues or gustatory organs, respectively. Further, they differ in their expression pattern among sensilla and in their projection pattern to regions of the SEZ [Dunipace et al. 2001; Robertson et al. 2003; Scott et al. 2001; Stocker and Schorderet 1981; Thorne et al. 2004; Wang et al. 2004] suggesting combinatorial coding of chemosensory information from the different gustatory organs. In *Drosophila* larvae, 43 GRs are expressed, 39 of which are expressed in the chemosensory organs of the head [Kwon et al. 2011]. The gustatory system of larvae consists of three external – dorsal (DO), terminal (TO), and ventral (VO) organs, and three internal – dorsal pharyngeal (DPSO), ventral pharyngeal (VPSO) and posterior pharyngeal (PPSO) sense organs (Fig. 16a) [Gendre et al. 2004; Singh and Singh 1984]. The cell bodies of the gustatory neurons are organized in ganglia: DO (DOG), TO (TOG) and VO (VOG) ganglion [Stocker 1994]. The neurons extend their dendrites to sensilla within the gustatory organs characterized by a distal pore, and project to the central pattern generator for food intake in the SEZ via the antennal nerve (AN), the maxillary nerve (MN), and the labral (LN) and labial (LBN) nerves (Fig. 16a, b) [Huckesfeld et al. 2015; Miroschnikow et al. 2018; Python and Stocker 2002; Schoofs et al. 2010; Stocker 1994].

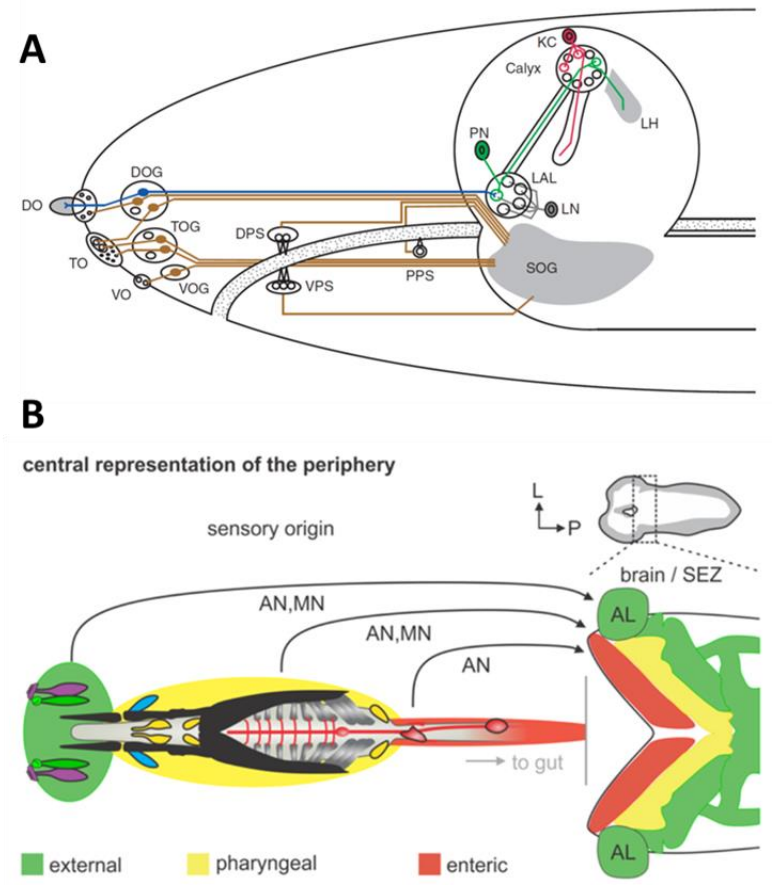

Figure 16: *A: The gustatory and olfactory system of the Drosophila larva. DO: dorsal organ; DOG: dorsal organ ganglion; DPS dorsal pharyngeal sense organ; KC: Kenyon cell; LAL: larval antennal lobe; LH: lateral horn; LN: local interneurons; PN: projection neuron; PPS: posterior pharyngeal sense organ; SOG: suboesophageal ganglion (meanwhile SEZ); TO: terminal organ; TOG: terminal organ ganglion; VO: ventral organ; VOG: ventral organ ganglion; VPS: ventral pharyngeal sense organ. B: The peripheral origin of chemosensory information. Topographical target regions of the external, pharyngeal, and enteric/internal sensory organs within the SEZ are color-coded. AL: antennal lobe; AN: antennal nerve; MN: maxillary nerve; SEZ: suboesophageal zone. From [Gerber and Stocker 2007; Miroschnikow et al. 2018; Stocker 1994]*

Like in adults, the SEZ can be divided in four target regions mainly by the respective nerve that innervates the consequent area and not by the *Gr* gene expressed in the projecting GRNs [Colomb et al. 2007; Miroschnikow et al. 2018]. The chemosensory system has second order neuronal connections to neurosecretory cells, the ring gland, the protocerebrum near the MB calyces, pharyngeal muscles, and ventral nerve cord via 20 *hugin* expressing cells in the SEZ [Bader et al. 2007; Melcher and Pankratz 2005]. Last year, the feeding connectome was reconstructed at EM level providing a synaptic map of sensory and motor output neurons underlying feeding behavior, and outlining monosynaptic and polysynaptic connections between sensory neurons, endocrine organs, and higher brain centers [Miroschnikow et al. 2018].

1.3. The mushroom bodies

The MBs are prominent brain structures in the central nervous system (CNS) of insects. They are found in annelids and all arthropods except for crustaceans [Campbell and Turner 2010]. The MBs were first described in 1850 by Dujardin [Dujardin 1850; Campbell and Turner 2010]. They are high-order integration centers required for olfactory learning and memory formation, and organization of complex behaviors [Davis 1993; Heisenberg 1998, 2003; Zars 2000]. The MBs are paired structures in the CNS and consist of calyces, pedunculi, and lobes. In adult flies, the MBs comprise around 2000 intrinsic neurons per hemisphere, the so-called Kenyon cells (KCs) [Aso et al. 2014b]. The calyx is formed by the dendritic branches of the KCs. The KCs are classified due to the projection and gene expression patterns in α/β-, α'/β'- and γ-type [Crittenden et al. 1998; Lee et al. 1999]. KCs' axons bundle through the pedunculus and bifurcate to form the lobes: vertical α and α' and medial β, β', and γ lobes (Fig. 17) [Crittenden et al. 1998; Heisenberg 1980; Ito et al. 1997; Tanaka et al. 2008; Technau 1984].

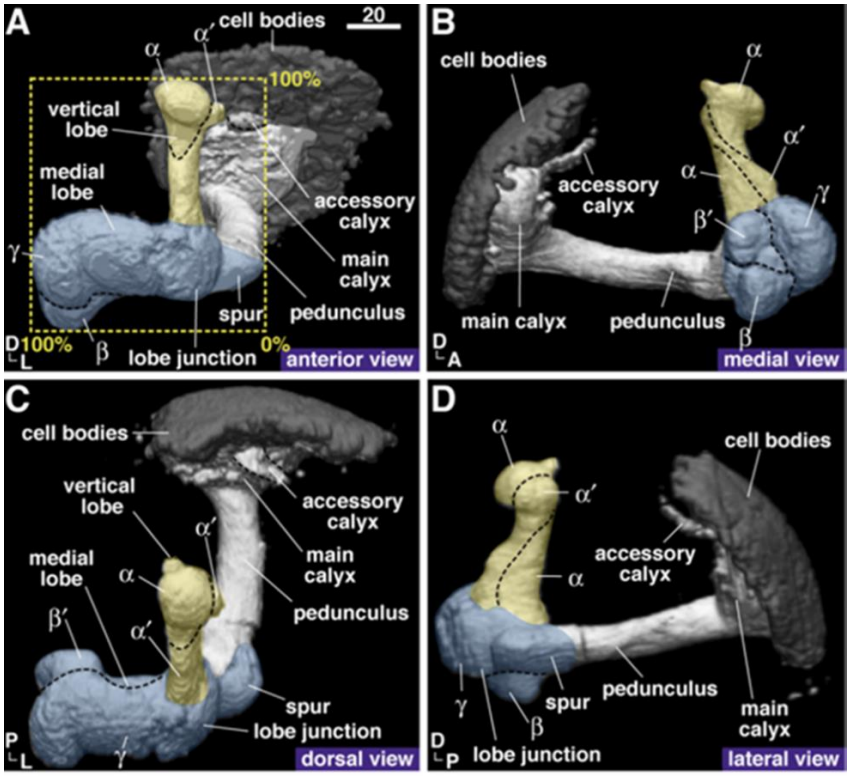

Figure 17: *Three-dimensional reconstruction of the mushroom body of Drosophila melanogaster. Different compartments of the MB (cell bodies of Kenyon cells – dark grey, calyx and pedunculus – light grey, vertical lobes – yellow, medial lobes - blue) are illustrated from anterior (A), medial (B), dorsal (C) and lateral (D) view. From [Tanaka et al. 2008]*

The architecture of the larval MBs resembles that of adult flies yet consisting of a significant smaller number of cells [Pauls et al. 2010]. In first instar larvae EM reconstruction revealed in total 223 KCs which number increases throughout larval development to ca. 800 in third instar larvae [Eichler et al. 2017; Ito and Hotta 1992; Masuda-Nakagawa et al. 2005; Pauls et al. 2010]. The KCs can be subdivided into three groups: embryonic-born γ and larval-born α'/β' type Kenyon cells [Ito and Hotta 1992; Technau and Heisenberg 1982] which form the larval vertical and medial (Fig. 18) lobes [Lee et al. 1999; Pauls et al. 2010].

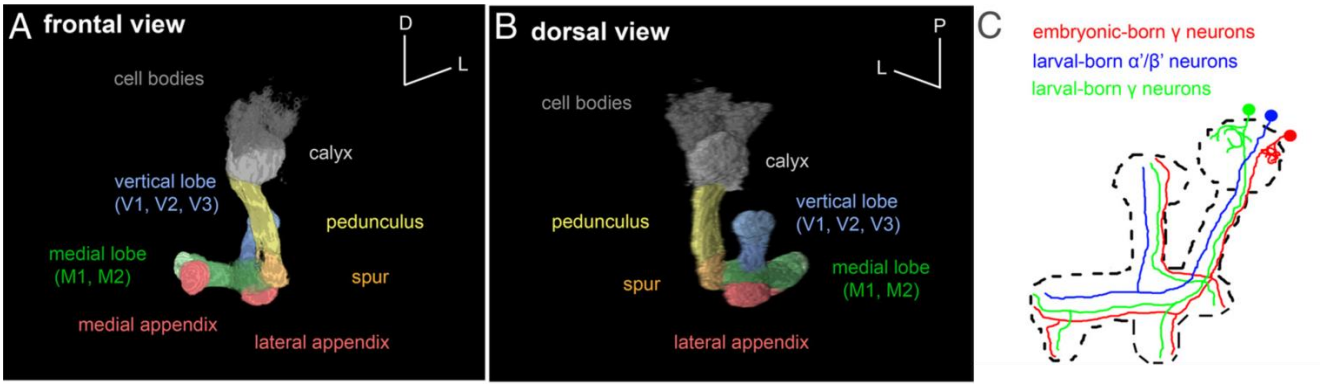

Figure 18: *Three-dimensional reconstruction of the mushroom body of the Drosophila larva. Different compartments of the MB (cell bodies of Kenyon cells – dark grey, calyx – light grey, pedunculus – yellow, vertical lobe - blue, medial lobe – green, spur – orange, lateral appendix - apricot) are illustrated from anterior (A) and dorsal (B) view. C: Color-coded projection patterns of the three types of Kenyon cells. From [Pauls et al. 2010]*

For adults as well as for larvae functional differences are claimed for the different lobes. In adult *Drosophila*, the α/α' lobes play role in long-term memory whereas the γ lobe is involved in short-term memory [Pascual and Preat 2001; Zars et al. 2000]. Further, α/β KCs are required for memory retrieval whereas α'/β' KCs are necessary for memory acquisition [Dubnau et al. 2001; Krashes et al. 2007]. In both larvae and adults, functional differences of the lobes are additionally suggested at the stimulus quality level (appetitive or aversive). Regarding the connectivity, the larval and adult MBs feature also similarities. The MB calyx receives odor information from the ORNs via AL PNs in a random fashion [Caron et al. 2013; Eichler et al. 2017; Honegger et al. 2011; Marin et al. 2002; Masuda-Nakagawa et al. 2005; Murthy et al. 2008; Ramaekers et al. 2005; Wong et al. 2002]. However, odor coding and discrimination can be observed at the level of adult and larval MB calyx [Campbell et al. 2013; Lin et al. 2014; Louis et al. 2018; Ludke et al. 2018; Masuda-Nakagawa et al. 2009]. The MB lobes in both adults and larvae are innervated by modulatory MB input neurons (MBINs) which provide

rewarding or punishing signals. Rewarding signals are transferred via octopaminergic MBINs (OANs) whereas dopaminergic MBINs (DANs) transmit information about rewarding and punishing stimuli [Busch et al. 2009; Eichler et al. 2017; Mao and Davis 2009; Nassel and Elekes 1992]. Due to sensory integration in the MBs, behavioral output via glutamatergic, GABAergic, or cholinergic MB output neurons (MBONs) is elicited. In adult *Drosophila*, the MB lobes consist of 15 compartments due to the innervation pattern of the MBONs. Following similar reasoning, the complete larval MB is defined by 11 compartments according to the overlapping MBINs' and MBONs' innervation pattern (Fig. 19, 20) [Aso et al. 2014b; Aso et al. 2014a; Saumweber et al. 2018].

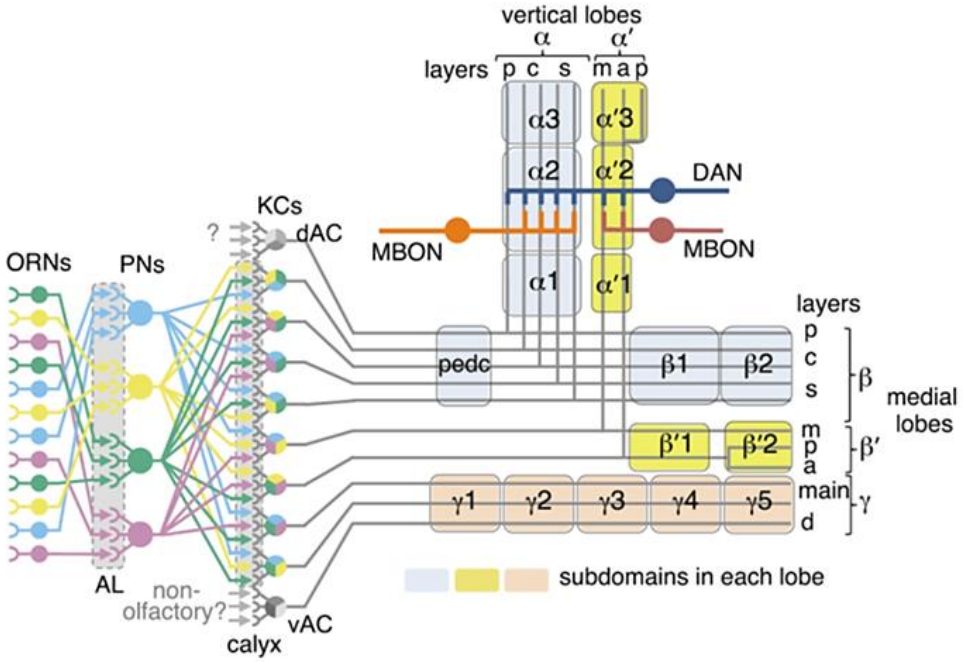

Figure 19: *Illustration of the information flow from olfactory receptor neurons to the mushroom body in Drosophila melanogaster. ORNs expressing certain olfactory receptor, their target glomeruli within the AL, and the projections to the calyx region of the MB are color-coded. The lobes are subdivided on one hand in distinct layers: posterior (p), core (c), surface (s), medial (m) anterior (a) and dorsal (d). On the other hand, the lobes are subdivided in 15 compartments due to the MBON innervation pattern. From [Aso et al. 2014b]*

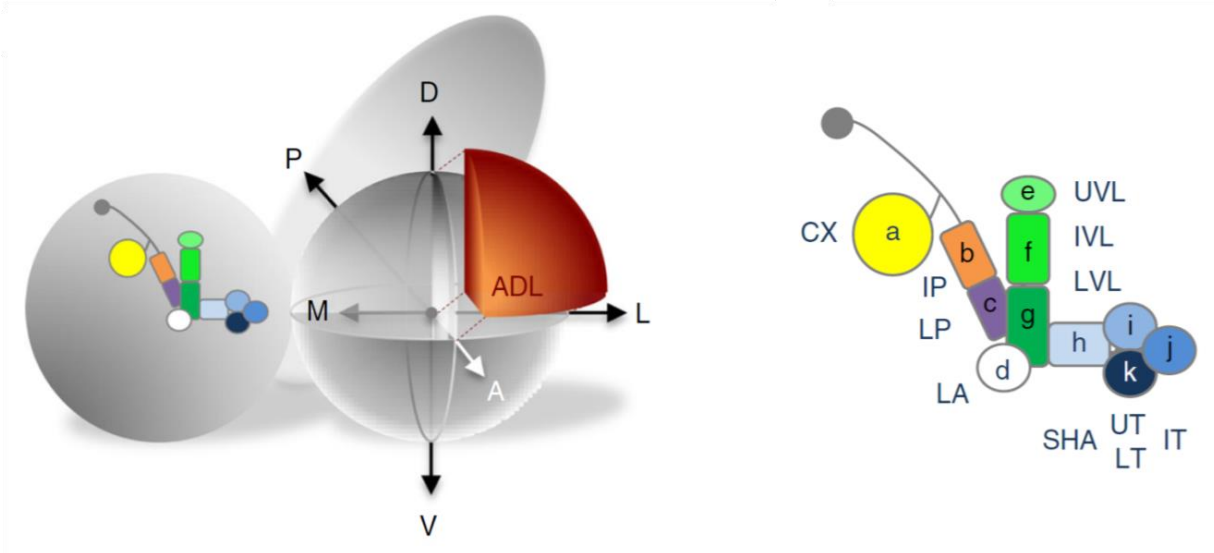

Figure 20: *Illustration of the location and orientation of the larval mushroom body. The larval MB consists of 11 compartments (a-k) determined by the MBIN/MBON innervation pattern. Some of the compartments are color-coded due to the type of information they receive (i.e. green shades – aversive stimuli, blue shades – appetitive stimuli, yellow – olfactory information). From [Saumweber et al. 2018]*

Besides investigations on the anatomical architecture and functions of the *Drosophila* MBs, two neurotransmitters expressed in the KCs were identified in the last decades. Single cell transcriptomics and immunostainings of the MBs revealed acetylcholine (ACh) and short neuropeptide F (sNPF) as neurotransmitters in adult *Drosophila* [Croset et al. 2018; Johard et al. 2008] and the role of both, ACh and sNPF in KCs, was investigated [Barnstedt et al. 2016; Cervantes-Sandoval et al. 2017; Knapek et al. 2013]. However, comparable studies lack for *Drosophila* larvae and the effect of ACh and sNPF expressed in the MBs on larval behavior has to be investigated.

1.4. Learning behavior and memory formation in *Drosophila melanogaster* larvae

The MB is the memory center in *Drosophila* [Heisenberg 2003; Heisenberg et al. 1985]. It integrates sensory information and is required for olfactory learning. The classical synaptic connections ("Heisenberg model") thought to be involved in olfactory associative conditioning are: i) cholinergic PNs to KCs providing odor information [Masuda-Nakagawa et al. 2005; Ramaekers et al. 2005], ii) modulatory MBINs (DANs, OANs) to KCs providing rewarding and punishing information [Rohwedder et al. 2016; Selcho et al. 2009; Selcho et al. 2014; Honjo and Furukubo-Tokunaga 2009], and iii) KCs to MBONs triggering behavioral output after conditioning [Eichler et al. 2017; Honjo and Furukubo-Tokunaga 2005] (Fig. 21). EM reconstruction of the MB neurons in first instar larva revealed even higher complexity of the larval MB: i) KCs communicate with each other via KC>KC synapses, ii) DANs form synaptic connections with MBONs, iii) KCs synapse onto DANs, and iv) MBINs connect to MBONs [Eichler et al. 2017] (Fig. 21). However, the function of many of these newly identified synaptic connections within the larval memory circuit is still elusive.

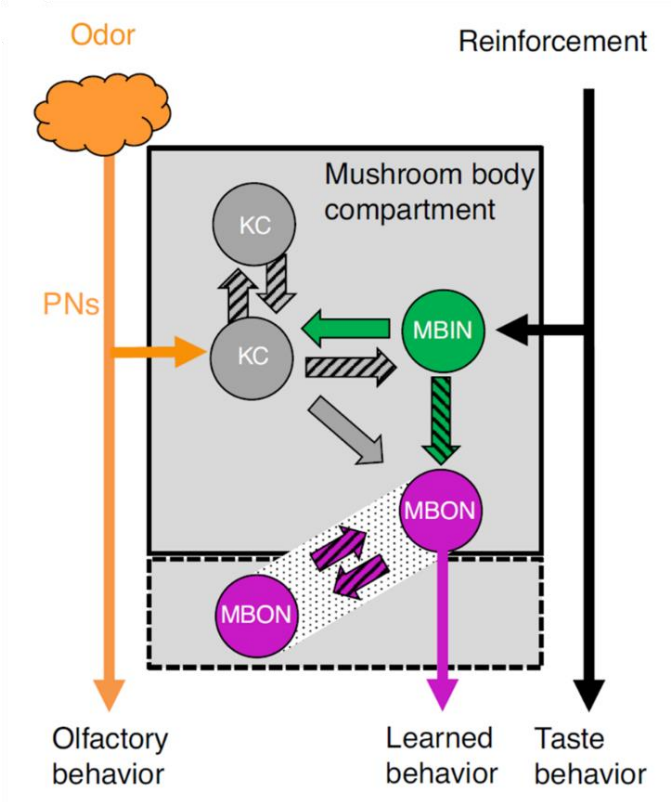

Figure 21: *'Canonical' mushroom body compartment. Full-colored arrows indicate already known connections ("Heisenberg model"). Hatched arrows show newly identified connections. Except for the MBON-MBON connections, all connections are local within one compartment. From [Thum and Gerber 2018]*

During olfactory associative conditioning the animals are simultaneously exposed to an odor (CS; via cholinergic AL PNs) and a gustatory stimulus, either appetitive or aversive (US; e.g. via DANs). Binding of acetylcholine (ACh) to the respective receptors in the KCs results in Ca^{2+} influx via voltage-gated calcium channels [Honjo and Furukubo-Tokunaga 2009; Ramaekers et al. 2005; Widmann et al. 2018]. Simultaneous binding of dopamine (DA) to G-coupled receptors [Kim et al. 2003; Selcho et al. 2009] and their activation together with endogenous Ca^{2+}/Calmodulin increase leads to activation of *rutabaga* (*rut*) encoded type I adenylyl cyclase (AC). AC acts within this cellular mechanism as a coincidence detector for the US/CS occurrence and its activation results in an increase of cyclic adenosine 3’5’-monophosphate (cAMP) level in the KCs. cAMP is a positive regulator of protein kinase A (PKA), which in turn phosphorylates Synapsin, K^+ channels and other proteins within the cells (Fig. 22). This cascade induces cellular or synaptic plasticity [Dudai et al. 1988; Gervasi et al. 2010; Honjo and Furukubo-Tokunaga 2009; Levin et al. 1992; Livingstone et al. 1984; Tomchik and Davis 2009]. Notably, there is a second signaling cascade suggested to be involved in memory formation: phospholipase C (PLC)-inositol triphosphate (IP3), diacylglycerol (DAG)-protein kinase C (PKC) (Fig. 22). Phosphorylation of the potential downstream targets of PKC *Radish* (*Rsh*) and *Bruchpilot* (*Brp*) could then facilitate synaptic plasticity [Folkers et al. 2006; Khurana et al. 2009; Widmann et al. 2016]. However, the exact role of PKC signaling in memory formation has to be further studied in detail.

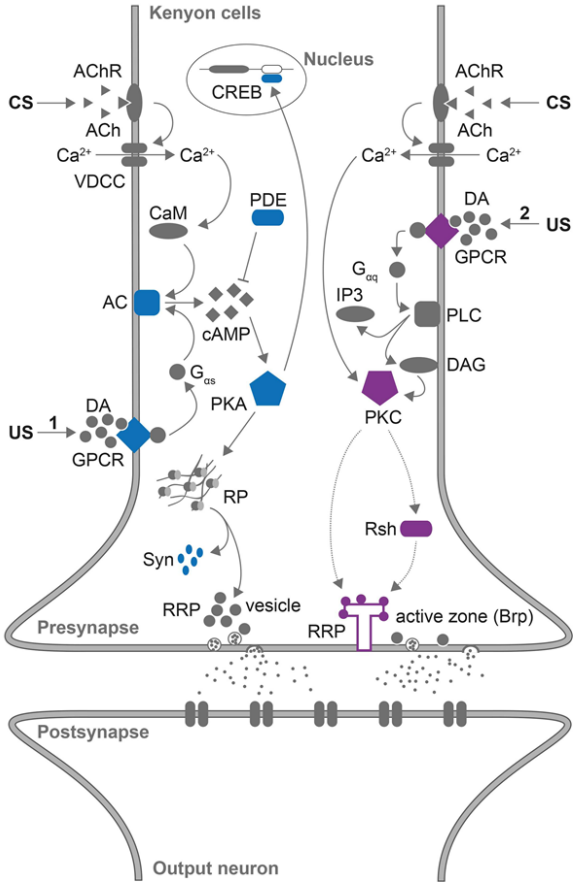

Figure 22: *Cellular mechanism underlying memory formation in Drosophila. Key players within the PKA signaling cascade are depicted in blue. Key players within the PKC signaling cascade are depicted in violet. AC: adenylyl cyclase, ACh: acetylcholine, AChR: acetylcholine receptor, Brp: Bruchpilot CaM: calmodulin, cAMP: cyclic adenosine 3'5'-monophosphate, CS: conditioned stimulus, DA: dopamine, DAG: diacylglycerol, GPCR: G-protein coupled receptor, IP3: inositol triphosphate, PKA: protein kinase A, PKC: protein kinase C, PLC: phospholipase C, RP: reserve pool, RRP: readily releasable pool, Rsh: Radish, Syn: Synapsin, US: unconditioned stimulus, VDCC: voltage-dependent calcium channel. From [Widmann et al. 2016]*

Indeed, huge efforts towards unraveling the neuronal and molecular circuits of learning behavior and memory formation in *Drosophila* larvae were made. In the last few years the connectivity of the larval MB was described on EM level [Eichler et al. 2017], the functional architecture of MB extrinsic neurons was characterized at single cell level [Saumweber et al. 2018], and the ability of fruit fly larvae to form nuanced memories about the value and quality of a gustatory stimulus was shown [Schleyer et al. 2015]. But still,

"having the synaptic connectome now available makes one wonder how one could have ever hoped to understand mushroom body function without it. Significantly, however, the 'pre-connectome' accounts of mushroom body function were surprisingly correct — though, as we know now, distressingly incomplete. Readers working on brain structures for which a synaptic connectome is not yet available should therefore expect the unexpected."

From Thum and Gerber, 2018

2. Materials and methods

2.1. Fly stocks and general information

All fly strains were raised at 25°C, 60% humidity, and 12:12 light:dark cycle in vials containing nutrient solution. Driver and effector lines used in this study are listed in Table 3.

Table 3: *Drosophila melanogaster transgenic strains (GAL4/UAS, LexA/LexAop) used for the experiments described below.*

Stock	Genotype	Chr	Source	Reference
	Driver lines			
H24-GAL4	P{w[+mW.hs]=GawB}H24	3	Andreas Thum	[Pauls et al. 2010]
OK107-GAL4	w*; P{GawB}OK107 eyOK107	4		[Pauls et al. 2010]
MB247-GAL4	P{Mef2-GAL4.247}	3		[Pauls et al. 2010]
201y-GAL4	w^{1118}; P{GawB}Tab2^{201Y}	2		[Pauls et al. 2010]
NP1131-GAL4	y* w*; P{GawB}NP1131 / CyO, P{UAS-lacZ.UW14}UW14	2	Johannes Felsenberg	[Pauls et al. 2010]
R58E02-LexA	w[1118]; P{y[+t7.7] w[+mC]=GMR58E02-lexA}attP40	2	Andreas Thum	[Liu et al. 2012]
R58E02-GAL4	w[1118]; P{y[+t7.7] w[+mC]=GMR58E02-GAL4}attP2	2	Andreas Thum	[Rohwedder et al. 2016]

Effector lines

10xUAS-IVS-myr::GFP		2		
UAS-mCD8::GFP		2		
UAS-ChR2-XXL	y[1] w[1118]; PBac{y[+mDint2] w[+mC]=UAS-ChR2.XXL}VK00018	2	Robert Kittel, Tobias Langenhan	[Dawydow et al. 2014]
20xUAS-Chrimson	w^{1118},P{20XUAS-IVS-CsChrimson.mVenus}attP18	X	Katharina Eichler	[Klapoetke et al. 2014]
UAS-dTRPA1	w[*]; P{w[+mC]=UAS-TrpA1.K}attP2/TM6B, Tb[1]	3	Bloomington #26264	[Rosenzweig et al. 2005]
UAS-nAChRα1-RNAi	y[1] v[1]; P{y[+t7.7] v[+t1.8]=TRiP.JF03103}attP2	3	Bloomington #28688	[Perkins et al. 2015]
UAS-nAChRα4-RNAi	y[1] v[1]; P{y[+t7.7] v[+t1.8]=TRiP.JF03419}attP2	3	Bloomington #31985	[Perkins et al. 2015]
UAS-nAChRα5-RNAi	y[1] v[1]; P{y[+t7.7] v[+t1.8]=TRiP.JF01963}attP2	3	Bloomington #25943	[Perkins et al. 2015]
UAS-nAChRα6-RNAi	y[1] v[1]; P{y[+t7.7] v[+t1.8]=TRiP.JF01853}attP2	3	Bloomington #25835	[Perkins et al. 2015]
UAS-sNPFR-RNAi		3		
UAS-Chrimson, LexAop-GCamp6m	w; CyO/Sp; 13XLexAop2-IVS-p10-GCaMP6m,20xUAS-CsChrimson-mCherry	3	Katharina Eichler	

Combined lines generated for this study

w^{1118};UAS-ChR2-XXL,LexAop-Kir2.1;+
w^{1118};R58E02-LexA/CyO;H24-GAL4/TM6b
w^{1118};R58E02-GAL4/CyO;UAS-dicer2/TM6b
w^{1118};UAS-dicer2/CyO;H24-GAL4/TM6b
w^{1118};UAS-ChR2-XXL/CyO;UAS-amon-RNAi^{78b}/TM6b
w^{1118};UAS-ChR2-XXL/CyO; LexAop-GCamp6m/TM6b
w^{1118};UAS-ChR2-XXL/CyO;LexAop-reaper/TM6b
w^{1118};UAS-ChR2-XXL/CyO;UAS-Dop1R1-RNAi/TM6b
w^{1118};UAS-amon-RNAi^{28b}/CyO;UAS-Chrimson,LexAop-GCamp6m/MKRS

In case, it was expected that genetic manipulation would induce a behavioral phenotype, negative genetic controls were obtained by crossing the respective driver and effector lines to w^{1118} flies. For experiments, where phenotypic suppression was expected due to combination of the GAL4/UAS and LexA/LexAop systems, lines lacking either the LexA or LexAop construct were crossed to obtain positive genetic controls.

For optogenetic experiments, larvae were raised in darkness covered with aluminum foil to prevent constant activation of the neurons expressing the respective optogenetic tool. Larvae expressing the XXL variant of Channelrhodopsin2 were raised on standard food as ChR2-XXL was shown to elicit efficient activation without supplement of retinal, whereas larvae expressing Chrimson were fed additionally with all-trans retinal (500µM) as previously described [Dawydow et al. 2014; Pauls et al. 2015; Ullrich et al. 2013]. For optogenetic activation with ChR2-XXL, 475nm light-emitting diodes (LED) with light intensity of ~ 1300 µW/cm^2 were used. For artificial activation with Chrimson, larvae were exposed to 620nm light-emitting diodes (LED) with light intensity of ~ 50 µW/cm^2. The LEDs were placed ~ 45 cm

above the Petri dish to induce activation, while all other steps of the experimental procedure were done under red light.

2.2. Behavioral experiments

2.2.1. Associative conditioning

Substitution learning

Substitution experiments were performed after slightly modified protocol described previously [Apostolopoulou et al. 2013; Widmann et al. 2018] at room temperature (22°C) and ~ 25% humidity. Petri dishes (diameter: 88mm) were covered by a thin 1.5% agarose layer. 10 µl pure 1-octanol (OCT) were pipetted into homemade Teflon container with a porous lid and used as CS. Instead of gustatory US, the larvae were exposed to blue light in order to artificially activate different populations of cells defined by the driver line used in each experiment. Cell activation was achieved by expression of the XXL variant of Channelrhodopsin2 in the respective neurons. 30 naïve larvae from each genotype were placed in the middle of a Petri dish with two odor containers on both sides and transferred under blue light (OCT+). Five minutes later larvae were transferred on a second Petri dish under red light without odor exposure (NONE-). By that, the odor was associated with cell activation during the first half of the training cycle (from here on CS1). This training regime (OCT+ -> NONE-) was performed three times in total. To test whether a memory was formed during the training and whether it is recalled during the test situation, larvae were placed in the middle of a Petri dish under red light containing only one odor container on one side of the Petri dish. The animals had three minutes to crawl either towards the odor or away from it, respectively (Fig. 23).

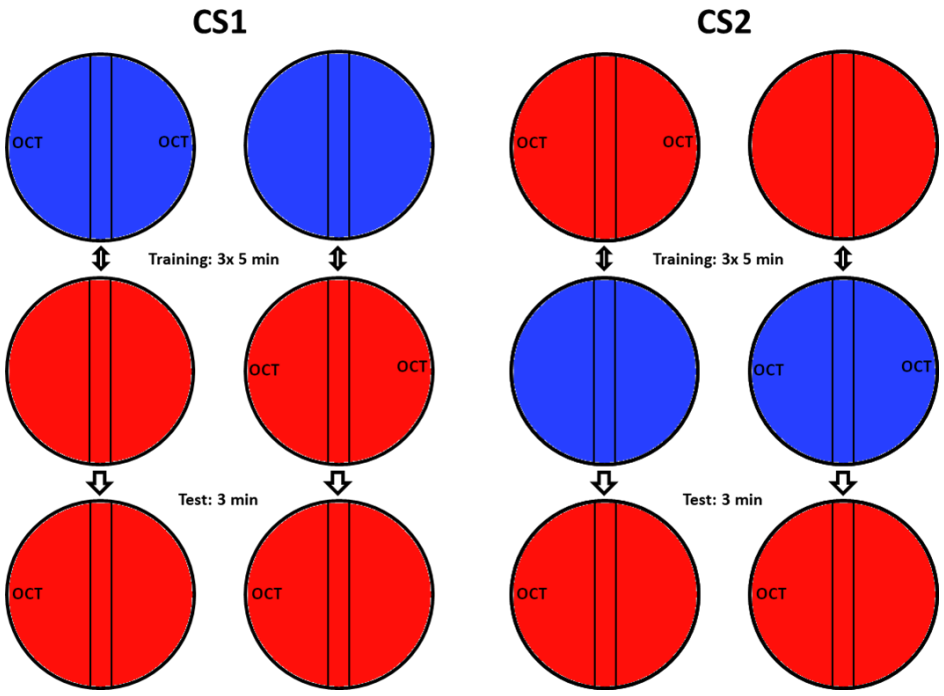

Figure 23: *Experimental setup for associative conditioning. Color of the Petri dishes corresponds to the type of illumination (either blue or red light). CS1 and CS2 depict both experimental sequences.*

At the end of this test situation the number of larvae in each sector (OCT, neutral zone, NONE) of the Petri dish were counted and an olfactory index (OI [-1;+1]) was calculated as follows:

$$OI(OCT+/NONE-) = \frac{\#OCT - \#NONE}{\#TOTAL} \quad (1)$$

#TOTAL = #OCT + #NONE + #neutral zone

#: number of larvae

To exclude an impact of a naïve odor preference on the learning performance a reciprocal experiment was performed simultaneously, whereby the odor container was present under red light (OCT-) and the activation of the cells was associated with “no odor” information (NONE+) (Fig. 23). A reciprocal OI was determined as follows:

$$OI(NONE+/OCT-) = \frac{\#NONE - \#OCT}{\#TOTAL} \quad (2)$$

The learning performance of the larvae was defined as a performance index (PI [-1;+1]) and was calculated as follows:

$$PI = \frac{OI(OCT+/NONE-)+(NONE+/OCT-)}{2} \quad (3)$$

In the course of the assays, the experimental sequence was changed by associating the CS with the cell activation during the second part of a training cycle (from here on CS2, Fig. 23). Thereby, the time between last exposure of larvae to blue light and test situation could be excluded as a factor that might influence the learning performance.

Substitution learning assay was also performed using the two-odor reciprocal training design, where 10 µl amyl acetate (AM, 1:40) was used as second odor opposing OCT.

As the recall of memory depends on the test situation and the presence of rewarding or punishing stimuli, in an experimental series larvae were tested on 2M fructose, 1.5M sodium chloride, and 10 mM aspartic acid test plates, and on pure test plates under blue light, respectively.

Additionally, a two-odor substitution learning experiment was performed activating KCs thermogenetically. Thermogenetic cell activation was achieved by expression of the temperature-sensitive cation channel dTRPA1 in the respective neurons. For thermogenic activation, larvae were placed on a Petri dish with bottom temperature of 31.5°C (±1°C) and lid temperature of 29.5°C (±1°C) and were trained under constant red light according to the protocol described above.

Odor-sugar learning

For odor-sugar learning, the CS was associated during training with fructose as a gustatory US. The experiment was performed under red light and according to the protocol described above, except for the blue light exposure.

2.2.2. Preference tests

Olfactory preference tests

To test larvae for their naïve odor response, 30 larvae were placed on a Petri dish covered by a thin 1.5% agarose layer containing one odor container on one side. After 3 minutes larvae on the odor side (#ODOR), on the no odor side (#NO) and in the neutral zone were counted and a preference index ($PREF_{odor}$) was calculated as follows:

$$PREF_{odor} = \frac{\#ODOR - \#NO}{\#TOTAL} \quad (4)$$

#TOTAL = #ODOR + #NO + #neutral zone

#: number of larvae

Gustatory preference tests

To test the naïve gustatory behavior of larvae, one half of a Petri dish was filled with 1.5% pure agarose. The other half was covered by a layer of 1.5% agarose containing 2M fructose. A group of 30 larvae was placed on the Petri dish and the number of larvae on the sugar side (#Sugar), on the no sugar side (#NS) and in the neutral zone was counted after 3 minutes. A preference index ($PREF_{sugar}$) was calculated as follows:

$$PREF_{sugar} = \frac{\#Sugar - \#NS}{\#TOTAL} \quad (5)$$

#TOTAL = #Sugar + #NS + #neutral zone

#: number of larvae

For both, olfactory and gustatory preference tests positive PREF values indicate approach (appetitive) behavior, whereas negative PREF values represent avoidance (aversive) behavior. Further, naïve olfactory and gustatory responses were tested upon optogenetic activation under blue light as well as under red light as control.

Compound choice assays

Larvae were put to a test, where they had to choose between two different conditions: 1) odor + darkness, and 2) no odor + blue light (optogenetic activation of neurons). A Petri dish containing 1.5% agarose was covered by a lid, divided in a transparent and a shaded half, respectively. One odor container filled with 10 µl of the respective odor was placed in the darkend half. The non-shaded half was illuminated with blue light. 30 larvae were tested for 3 minutes. After counting the number of larvae on the dark side ($\#Odor_{DS}$), in the neutral zone, and on the blue light side ($\#NO_{BL}$) a preference index ($PREF_{Odor/BL}$) was calculated as follows:

$$PREF_{Odor/BL} = \frac{\#Odor_{DS} - \#NO_{BL}}{\#TOTAL} \quad (6)$$

#TOTAL = #Odor + #NO + #neutral zone

#: number of larvae

Negative PREF values indicate approach towards the illuminated side/odor avoidance, whereas positive PREF values represent light avoidance/odor approach.

Darkness preference tests

To test larvae for their response to blue light (and by that to optogenetic manipulation), a Petri dish containing 1.5% agarose was covered by a lid, divided in two transparent and two shaded quarters, respectively. 30 larvae were placed on a Petri dish exposed to blue light. During the 3 minutes of testing, the number of larvae on the dark side (#DS) and the number of larvae on the blue light side (#BL) was counted every 30 seconds. A preference index ($PREF_{DS}$) was calculated as follows:

$$PREF_{DS} = \frac{\#DS - \#BL}{\#TOTAL} \quad (7)$$

#TOTAL = #DS + #BL

#: number of larvae

Positive PREF values indicate light avoidance, whereas negative PREF values represent approach towards the illuminated site.

2.2.3. Locomotion assay

For the locomotion assay, the FIM (FTIR-based Imaging Method) tracking system was used as described in [Risse et al. 2013]. Recordings were made by a monochrome industrial camera with a Pentax objective and infrared pass filter, and the IC capture software. 10 larvae were simultaneously recorded on 1.5% agarose for two minutes. During the first minute, larvae were exposed to red light. For the second minute, they were exposed to blue light. Accumulated distance, velocity, number of stops, and number of bendings were analyzed using the FIM software.

2.3. Immunofluorescence

Immunofluorescence studies were performed as described previously [Selcho and Wegener 2015]. Briefly, 5-6 day old larvae were dissected in phosphate buffer saline (PBS) or HL3.1 (pH 7.2), fixated in 4% paraformaldehyde in PBS for 40min, washed in PBS with 0.3% Triton-X 100 (PBT), and afterwards blocked in 5% normal goat serum in PBT. Specimens were incubated in primary antibody solution containing polyclonal rabbit anti-GFP antibody (1:1000) or combined monoclonal mouse anti-GFP (1:250), polyclonal rabbit anti-sNPFp (1:1000 [Johard et al. 2008; Nassel et al. 2008]) and 3% normal goat serum for one to two nights at 4°C. Then brains were washed six times in PBT and incubated for one night at 4°C in secondary antibody solution containing goat anti-rabbit Alexa 488 (1:250) or combined goat anti-mouse DyLight 488 (1:250) and goat anti-rabbit Alexa 635 (1:250). Finally, specimens were rinsed six times in PBT and mounted in 80% glycerol or Vectashield mounting medium in PBS. Until scanning with a Leica SP8 confocal light scanning microscope, brains were stored in darkness at 4°C. Image processing was performed with Fiji and Adobe Photoshop CS6.

2.4. Functional imaging

To monitor intracellular Ca^{2+} levels in potential target neurons of optogenetically activated cells, *LexAop-GCaMP6m* was expressed for Ca^{2+} detection and *UAS-ChR2-XXL* for artificial activation. 1-2 larval brains were dissected and subsequently put in a Petri dish containing 405µl hemolymph-like HL3.1 saline solution. Before the experiment, brains maintained for around 30min for settling. Specimens were imaged with an AXIO Examiner D1 upright microscope with a Zeiss W Plan-Apochromat x20/1.0 or x40/1.0 water immersion objective and a SPECTRA-4 hybrid solid state LED source (Lumencor, USA). Images were taken with a PCO.edge 4.2m sCMOS camera at a frame rate of 0.5Hz using a Chroma ET-GFP emission filter, and analyzed by VisiView 2.0.

During monitoring, brains were first excited with 475nm light and an exposure time of 60ms at 4x binning with an intensity of around 700µW/cm2. After 5min, light intensity was increased to around 3800µW/cm2 for optogenetic activation of MB KCs. Monitoring of Ca^{2+} levels was continued for 5min. For Chrimson experiment, Ca^{2+} levels were only monitored for 5min.

For sNPF peptide application, brains of 5-6 days old *R58E02>GCamp6m* larvae were dissected and mounted in HL3.1 Ringer solution. sNPF (sNPF-1: AQRSPSLRLRFamide) was dissolved to concentration of 10^{-5}M in HL3.1 containing 0.1% DMSO (dimethyl sulfoxide) and applied manually onto dissected brains during acquisition. Respectively, HL3.1 containing 0.1% DMSO was applied as vehicle control. To analyze differences between corresponding groups in the imaging experiments, the maximum values ($\Delta F/F_0$) and the area under the curve after normalization were calculated.

2.5. Statistical methods

Data was analyzed for normal distribution using the Shapiro-Wilk Normality test. To test against chance level, a t-test was used for normally distributed data, a Wilcoxon Signed Rank test for not normally distributed data. For the comparison between genotypes, a pairwise t-test was used for normally distributed data, a pairwise Wilcoxon Rank Sum test was used for not normally distributed data. Pairwise tests included the Bonferroni-Holm correction. All statistical analyses were done with R version 3.3.0 (www.r-project.org). Data plots were done with R version 3.3.0 and OriginPro 2016G, b9.3.226 (www.originlab.com). Data is mainly presented as box plots, with 50% of the values of a given genotype being located within the box, and whiskers represent the entire set of data. No data was excluded. Outliers are indicated as open circles. The median performance index is indicated as a thick line within the box plot. For the persistence of memory, data is also presented as a line chart, with mean values and the standard error of the mean. Significance levels between genotypes shown in the figures refer to the raw p-values obtained in the statistical tests. P-values are summarized in Table S1.

2.6. Chemicals and devices

Table 4: *Chemicals used for behavioral assays and functional imaging.*

Chemicals	Manufacturer	CAS
Agarose Standard	Carl Roth GmbH, Germany	9012-36-6
D(-)-Fructose	Carl Roth GmbH, Germany	57-48-7
L-Aspartic acid	Carl Roth GmbH, Germany	56-84-8
Sodium chloride	Carl Roth GmbH, Germany	7647-14-5
1-Octanol	Sigma-Aldrich, Germany	111-87-5
n-Amyl acetate	Merck Schuchardt OHG, Germany	628-63-7
Benzaldehyde	Fluka Analytical, Germany	100-52-7
sNPF-1: AQRSPSLRLRFamide	Iris Biotech GmbH; Germany	
dimethyl sulfoxide (DMSO)	Carl Roth GmbH, Germany	67-68-5

Table 5: *Antibodies used for immunohistochemical preparations.*

Antibodies	Manufacturer	Catalog Nr.
polyclonal rabbit anti-GFP antibody	Molecular Probes	A6455
monoclonal mouse anti-GFP	Molecular Probes	A11120
polyclonal rabbit anti-sNPFp	[Johard et al. 2008; Nassel et al. 2008]	
goat anti-rabbit Alexa 488	Molecular Probes	R37116
goat anti-mouse DyLight 488	Jackson ImmunoResearch	115-485-146
goat anti-rabbit Alexa 635	Molecular Probes	A31577

Table 6: *Chemicals used for immunohistochemical preparations.*

Chemical	Manufacturer	CAS
Triton-X 100	Carl Roth GmbH, Germany	9036-19-5
paraformaldehyde	Polysciences, Inc.	30525-89-4
normal goat serum	Jackson ImmunoResearch	005-000-121
Vectashield mounting medium	Vector Laboratories, USA	
glycerol	Carl Roth GmbH, Germany	56-81-5

Table 7: *Hardware and software used for conducting this work.*

Hardware/Software	Manufacturer
Monochrome industrial camera DMK27BUP031	
Pentax C2514-M objective	Ricon Imaging Company, Japan
Infrared pass filter	Schneider Kreuznach, Germany
Confocal light scanning microscope Leica SP8	Leica Microsystems, Germany
AXIO Examiner D1 upright microscope	Carl Zeiss AG, Germany
W Plan-Apochromat objectives x20/1.0 and x40/1.0 water immersion	Carl Zeiss AG, Germany
SPECTRA-4 hybrid solid state LED source	Lumencor, USA
Camera PCO.edge 4.2m sCMOS	PCO AG, Germany
Chroma ET-GFP emission filter	
FIM (FTIR-based Imaging Method) tracking system	
IC capture	www.theimagingsource.com
Fiji	www.imagej.net/Fiji/
Adobe Photoshop CS6	Adobe Systems, USA
GNU Image Manipulation Program (GIMP) 2.10.8	www.gimp.org
VisiView 2.0	
R Studio version 0.99.896	www.r-project.org
OriginPro 2016G, b9.3.226	www.originlab.com

3. Results

3.1. Does artificial activation of mushroom body Kenyon cells affect learning and memory formation in *Drosophila* larvae?

It was previously shown that artificial activation of dopaminergic or octopaminergic neurons respectively is sufficient to substitute physical unconditioned stimulus during olfactory learning in *Drosophila* larvae [Schroll et al. 2006; Honda et al. 2016; Rohwedder et al. 2016]. Further, odor exposure during associative conditioning can be substituted by optogenetic activation of olfactory receptor neurons [Honda et al. 2016]. Previous results (R. Lyutova, Master thesis) revealed that optogenetic activation of *sNPF-GAL4* positive neurons results in a robust nociceptive behavior consisting of a corkscrew roll and accordion-like behavior (twitching) (Fig. S19). To investigate whether the optogenetically-induced nociceptive response can be used as a negative US during associative conditioning, *Drosophila* larvae were trained to associate an odor with artificial activation of *sNPF-GAL4* positive neurons as a substitution for an aversive stimulus. It was assumed that by that, larvae would form aversive memory. Surprisingly, appetitive and not aversive memory expression was observed in experimental larvae (Fig. S20). As sNPF is expressed in the MB KCs, it was assumed that not the activation of sNPF expressing neurons resulted in the appetitive memory formation *per se*, but the consequential activation of the MB KCs covered by the *sNPF-GAL4* driver line. To prove whether the artificial optogenetic activation of KCs indeed elicits the observed appetitive learning behavior, a one-odor learning paradigm [Schleyer et al. 2011] was used, in that the larvae did not experience a physical US, but an odor (CS) that was associated with blue light activation of the KCs instead. A XXL variant of the blue light sensitive Channelrhodopsin2 (*ChR2-XXL*) [Dawydow et al. 2014] was expressed in different subsets of KCs in order to optogenetically activate the neurons (substitution learning) (Fig. 24A). In total, five driver lines were used: *OK107-GAL4* (all KCs), *H24-GAL4* (almost all KCs), *MB247-GAL4* (341 KCs), *201y-GAL4* (315 KCs) and *NP1131-GAL4* (27 KCs) (Fig. 24B, C, D, E, F) [Pauls et al. 2010]. Artificial activation of four of these KC populations resulted in a significant appetitive

learning of the larvae from the experimental groups (*201y*, *MB247*, *OK107*, and *H24-GAL4*) in contrast to the genetic controls (Fig. 24C', D', E', F'). Interestingly, *NP1131>ChR2-XXL* experimental larvae did not show learning behavior (Fig. 24B'), suggesting that either the neurons of this small population of KCs is not involved in the processes during this type of substitution learning, or artificial activation of only 27 neurons is not sufficient to induce appetitive memory expression.

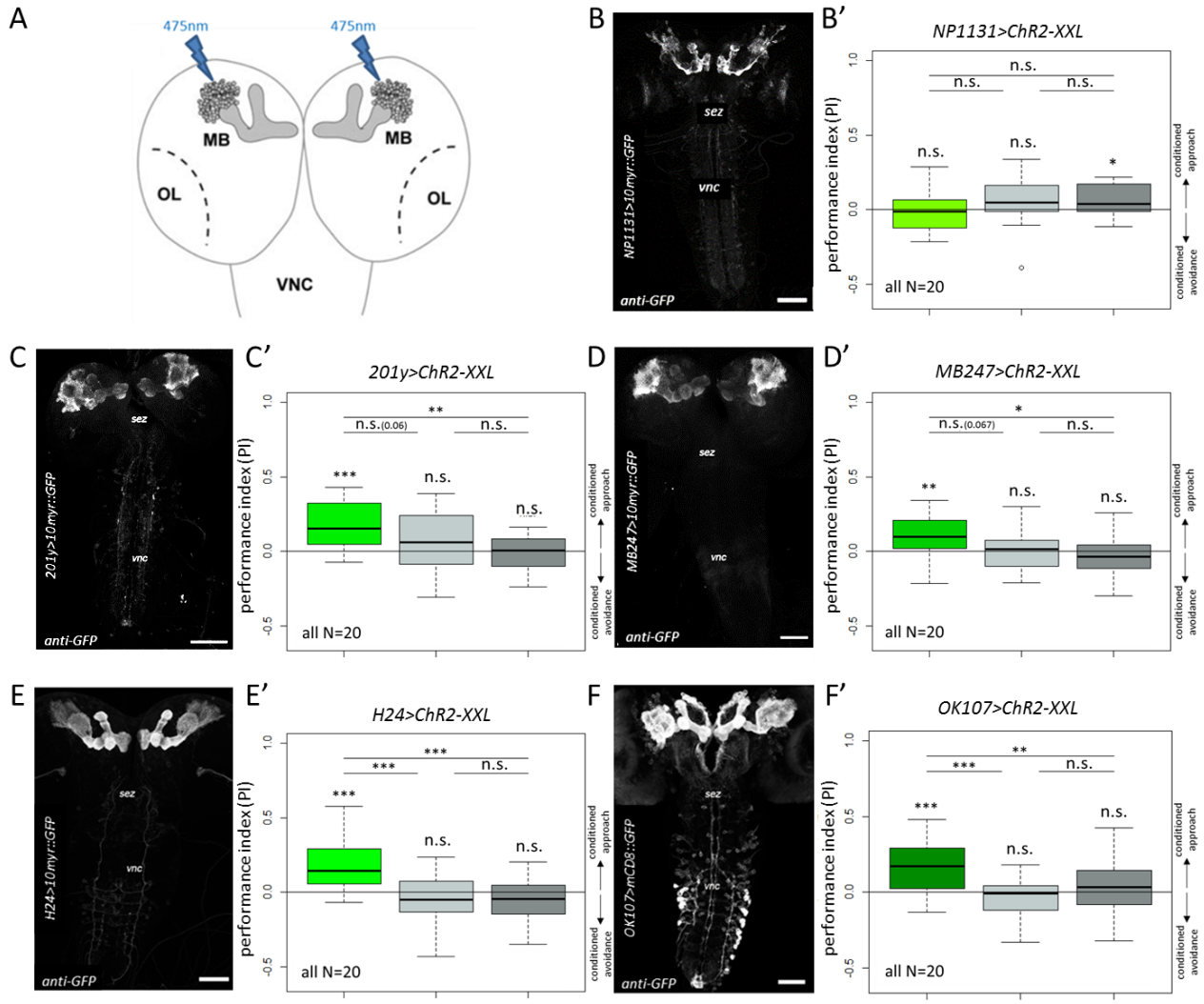

Figure 24: *Artificial activation of MB KCs results in appetitive memory formation. A: Optogenetic activation of KCs using 475nm blue light LEDs; B: Activation of 27 KCs was not sufficient to induce memory formation in Drosophila larvae; C-F: Artificial activation of 314 or more KCs paired with odor during substitution learning assay resulted in significant learning behavior and formation of appetitive memory. Green shaded boxes show learning performance of experimental larvae. Light gray and dark grey boxes depict performance indices of genetic GAL4 and UAS control larvae, respectively. Immunostainings by M. Selcho (B, C, D, E) and A.S. Thum (F)*

No difference in learning performance between different regimes (CS1 and CS2, Fig. 23 and Fig. S21) could be observed. Since the expression pattern of the tested driver lines overlaps only in the MB, it is conclusive that the observed learning behavior is an outcome of pairing odor information with an optogenetic acivation of the respective KCs. As *H24>ChR2-XXL* experimental larvae performed most robust and least scattering and the *H24-GAL4* expresses almost exclusively in the MBs, all further experiments were performed using this driver line.

3.2. Does optogenetic activation of mushroom body Kenyon cells affect locomotor activity of *Drosophila* larvae?

The locomotion behavior of *Drosophila* larvae is characterized by a stereotyped crawling involving series of muscle contractions from posterior to anterior followed by stops and had swings/turns in order to reorientate and change crawling direction. To exclude that activation of the KCs impairs locomotor behavior of larvae and thus affects learning, *H24>ChR2-XXL* larvae were tested in a locomotion assay. Larvae were first monitored using the FIM tracking system [Risse et al. 2013] for one minute under red light followed by one minute of blue light illumination and KC activation, respectively. General locomotor parameters (e.g. velocity and crawled distance) were not affected by KC activation (Fig. 25A-D). Interestingly, larvae from the experimental group showed significantly decreased number of stops as well as turns upon blue light illumination (Fig. 25E, 25F), suggesting a change in orientation/searching behavior.

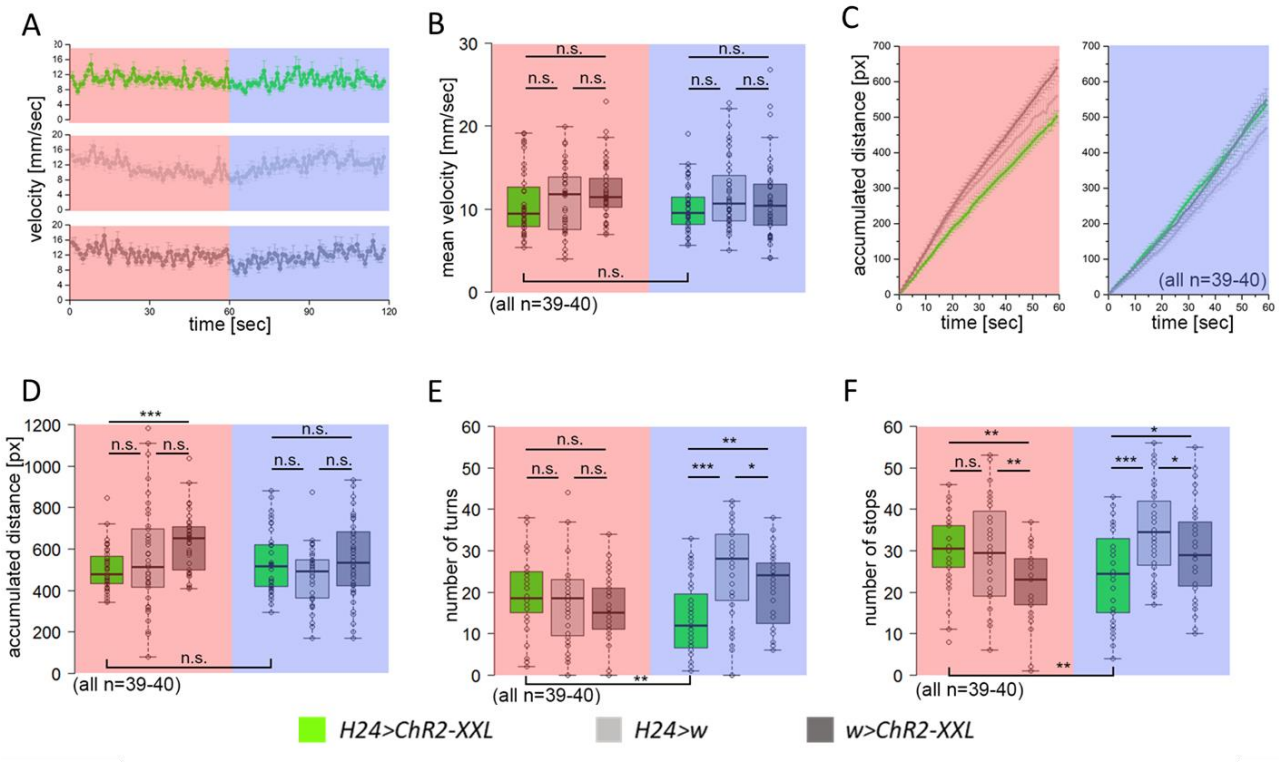

Figure 25: *Optogenetic activation of MB KCs does not affect general locomotion. A, B: Artificial activation of KCs did not impair larval velocity; C,D: Experimental larvae did not differ in accumulated distance from control groups. E: Upon blue light illumination experimental larvae showed significantly reduced number of turns; F: Optogenetic activation of KCs resulted in significant reduction of stops. Data and figures by D. Pauls*

3.3. Does optogenetic activation of mushroom body Kenyon cells affect naïve odor responses in *Drosophila* larvae?

During classical conditioning *Drosophila* larvae associate an US with a CS (usually an odor). Therefore, unbiased odor perception is crucial for memory formation. To exclude that KC activation impairs olfactory processing as the MB is known to be an integration center for sensory information [Heisenberg 2003], *H24>ChR2-XXL* larvae were tested for their naïve odor responses. An odor preference test using OCT was performed under red and blue light respectively and the naïve preference of larvae was monitored. In both conditions larvae from the experimental group did not differ in their odor response from the genetic controls (Fig. 26), suggesting that optogenetic activation of KCs does not impair naïve olfaction.

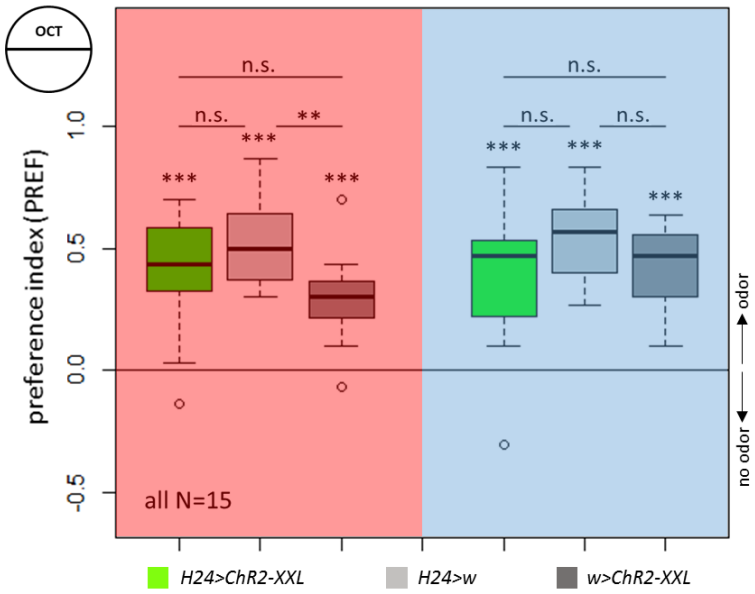

Figure 26: *Optogenetic activation of Kenyon cells does not affect naïve odor preference. Upon blue light illumination experimental larvae showed unbiased approach behavior towards OCT.*

This experiment verifies that larvae show unaffected approach towards an attractive odor. However, it could not be excluded that the quality of the used odor is changed to an unspecific odor and that larvae would not be able to discriminate different volutiles while KCs are active.

3.4. Are *Drosophila* larvae able to discriminate different odors upon Kenyon cell activation in a substitution assay?

Since odor discrimination occurs at the level of the MBs [Masuda-Nakagawa et al. 2009], and odor coding and intracellular Ca^{2+} increase in the KCs due to incoming signals from the AL PNs [Ramaekers et al. 2005] during associative conditioning are essential for olfactory memory formation, it was important to investigate whether larvae are able to discriminate different odors while KCs are artificially activated. The naïve odor response of *H24>ChR2-XXL* larvae was therefore tested using two other volatiles, benzaldehyde (BA) and amylacetate (AM), as these odors were previously used as a CS in larval olfactory conditioning [Pauls et al. 2010; Schleyer et al. 2011; Apostolopoulou et al. 2013]. Spatial map of odor representation at the level of ORNs and LAL shows that BA and OCT are coded by different *Ors* and are represented in distinct areas of the LAL [Kreher et al. 2005]. Thus, larvae were monitored for their naïve BA

preference (M. Pfeuffer, Bachelor thesis). Under red light, experimental larvae showed no impairment in the naïve response. However, a significant decrease in the approach towards BA upon blue light illumination was observed (Fig. 27A), suggesting that KC activation impairs the larval naïve preference for BA. Next, it was tested whether the naïve AM preference is affected by KC activation (M. Pfeuffer, Bachelor thesis). AM shows similarities with OCT in the coding pattern. Both odorants activate ORNs expressing *Or85c* and show comparable representation in the LAL [Kreher et al. 2005]. Larval preference for AM in dilution 1:40 (usually used in larval associative conditioning) was tested (M. Pfeuffer, Bachelor thesis). Under red as well as under blue light *H24>ChR2-XXL* larvae showed unaffected approach behavior towards AM (Fig. 27B). To further test whether KC activation changes the odor quality from specific to unspecific, OCT was opposed to undiluted and diluted AM respectively (M. Pfeuffer, Bachelor thesis), as it was previously shown that undiluted AM is more attractive for larvae than OCT, while 1:40 diluted AM and OCT should be equally attractive. Indeed, under both conditions (KC activation and control red light exposure) experimental as well as control larvae showed preference for undiluted AM (Fig. 27C) whereas exposure to OCT and diluted AM decreased the approach behavior towards AM (Fig. 27D).

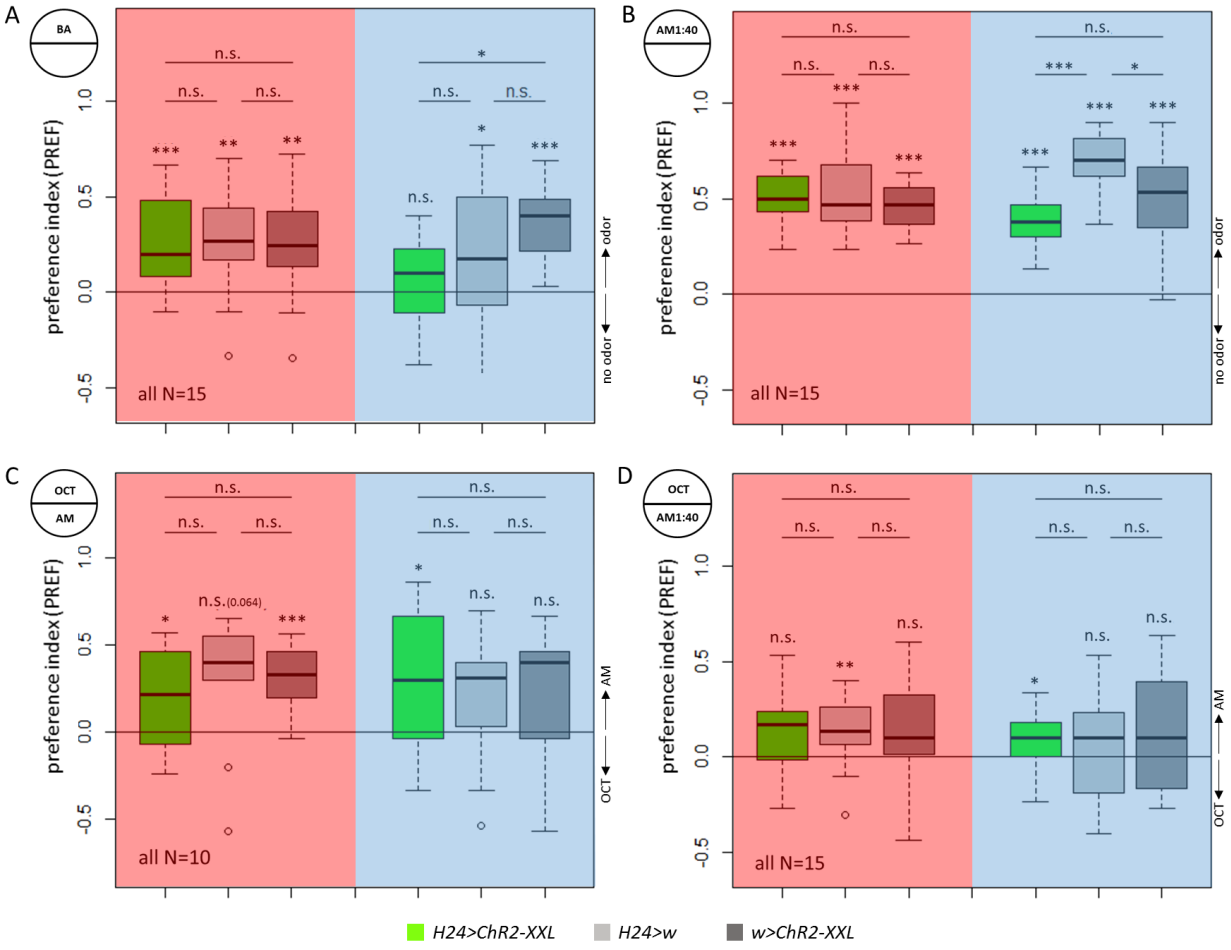

Figure 27: *Optogenetic activation of Kenyon cells does not affect concentration dependent odor discrimination. A: Upon blue light illumination experimental larvae showed biased approach behavior towards BA; B: Larval naïve preference for AM was not affected by optogenetic activation of KCs; C: Drosophila larvae showed preference for undiluted AM over OCT independent of KC activation; D: OCT and diluted AM (1:40) were balanced in their attractiveness independent of KC activation. Data by Maximilian Pfeuffer*

The preference tests showed that optogenetic activation of MB KCs does not impair larval naïve OCT and AM responses. However, it was still elusive whether odor coding at the level of the MBs would also be unaffected. To prove whether the activation of KCs impairs odor discrimination during substitution learning, two independent substitution experiments with different driver lines (*H24-GAL4* (M. Pfeuffer, Bachelor thesis) and *OK107-GAL4*) were performed using the two-odor reciprocal design [Scherer et al. 2003; Schleyer et al. 2011] with OCT and AM(1:40). Corresponding to the one-odor learning paradigm, *H24>ChR2-XXL* (Fig. 28A, S22A) as well as *OK107>ChR2-XXL* (Fig. 28B, S22B) experimental larvae showed significant

appetitive memory formation in contrast to both genetic controls, suggesting that optogenetic activation of KCs does not impair odor discrimination at the MB level, at least for OCT and AM.

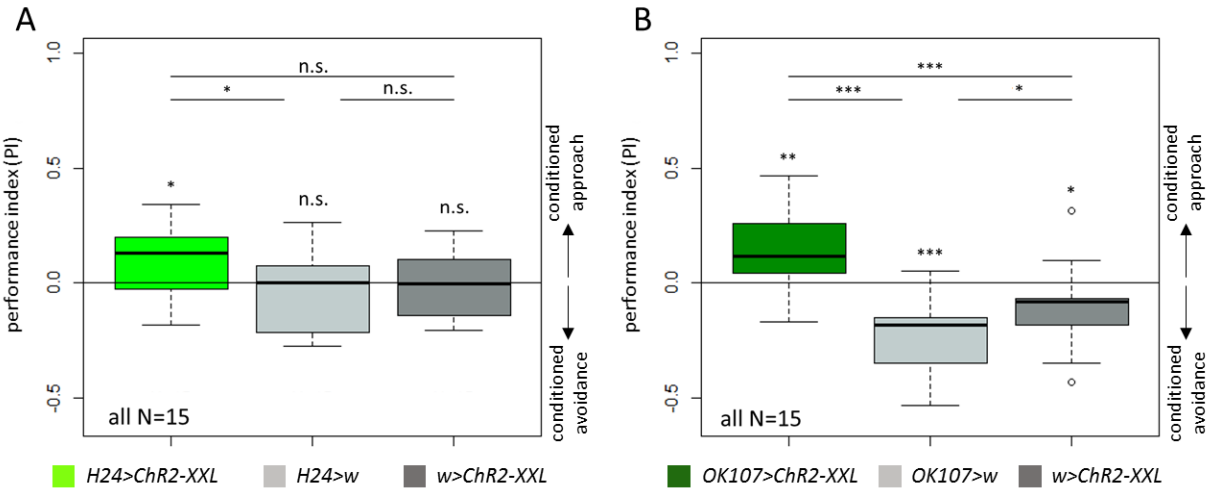

Figure 28: *Artificial activation of MB KCs results in appetitive memory formation in a two-odor (OCT vs. AM (1:40)) substitution paradigm. A: Optogenetic activation of H24-GAL4 positive KCs induced appetitive memory; B: OK107>ChR2-XXL experimental larvae showed significant learning behavior after optogenetic activation of all KCs.*

As already mentioned, Ca^{2+} increase in the somata of KCs underlies odor coding in the MBs [Lin et al. 2014; Ludke et al. 2018; Masuda-Nakagawa et al. 2009]. ChR2 is a cation channel permeable for sodium and potassium and to a much lesser extent for calcium. It is further, at least in motor neurons, expressed axonically and not somatically [Dawydow et al. 2014]. Consequently, optogenetic activation using *ChR2-XXL* consitutes of axonix action potentials and synaptic output respectively, but not of intrasomatic Ca^{2+} increase. Thus, activation of KCs using genetic tool that increases intracelular Ca^{2+} within the KC somata may disrupt odor discrimination. To test this hypothesis, the activating *Drosophila* transient receptor potential A1 (dTRPA1) cation channel was expressed in the KCs and the two-odor substitution learning was performed. dTRPA1 is temperature sensitive channel that opens at temperatures above 25°C and is mainly permeable for Ca^{2+} [Rosenzweig et al. 2005; Viswanath et al. 2003]. For thermogenic activation, larvae were placed on a Petri dish with bottom temperature of 31.5°C (±1°C) and lid temperature of 29.5°C (±1°C). Interestingly, experimental *H24>dTRPA1* larvae as well as control larvae showed significant learning behavior and formation of an appetitive memory (Fig. 29, S23).

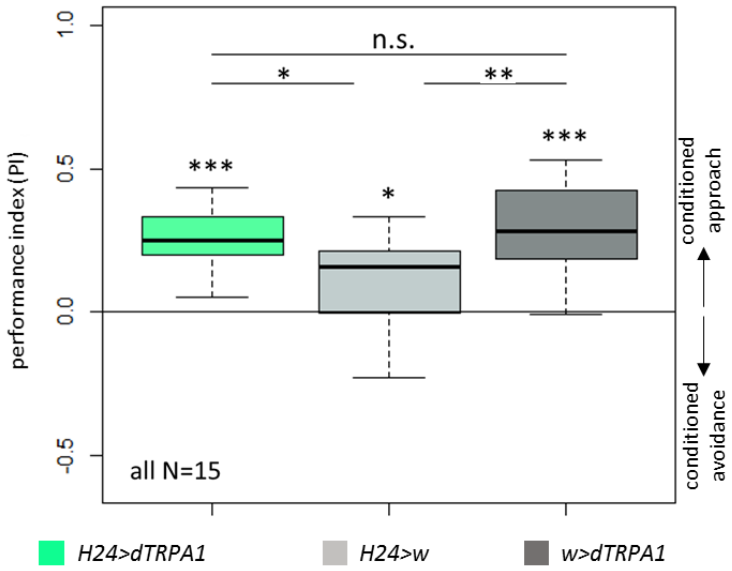

Figure 29: *Odor discrimination at MB level is not disrupted by thermogenetic activation of KCs. In a two-odor (OCT vs. AM (1:40)) substitution paradigm using dTRPA1 for thermogenetic activation of KCs experimental H24>dTRPA1 larvae showed significant learning performance. Appetitive memory formation was further observed in both genetic controls, however w>H24 control larvae showed significantly decreased learning performance compared to H24>dTRPA1 as well as w>dTRPA1 larvae.*

This result indicates, that i) Ca^{2+} increase-based activation of KCs does not affect odor coding at the level of the MBs and ii) high temperature is used by the animals as appetitive US during conditioning independent of KC activation. However, it remains unclear to which extent temperature as US and KC activation contribute to the observed learning behavior of experimental larvae, as *H24>dTRPA1* showed significantly higher performance index than *w>H24* control larvae and in *w>dTRPA1* larvae leaky expression of the channel cannot be excluded.

3.5. Do *Drosophila* larvae form different types of memory during substitution learning?

After substitution learning, experimental larvae showed appetitive memory expression during a test situation (Fig. 24C-F). However, memory expression is highly dependent on the test situation, as the outcome expectation of larvae is based on the value (how much) and the quality (what) of the stimulus present during test [Schleyer et al. 2015; Schleyer et al. 2011]. On one hand, an aversive memory is expressed during test only in the presence of the trained aversive gustatory US. On the other hand, an appetitive memory cannot be recalled if larvae are exposed to the matching appetitive US in the test situation. For instance, sugar memory is not expressed in the presence of sugar during test, but its recall is not affected if larvae are tested on amino acids [Schleyer et al. 2015]. To test whether different types of memory are formed during substitution learning, larvae were tested on different plates. When tested on sugar plates, *H24>ChR2-XXL* larvae lacked memory expression (Fig. 30A, S24A) which was not the case when tested on amino acid plates (Fig. 30B, S24B), suggesting that the optogenetically-induced memory in *H24>ChR2-XXL* larvae is sugar specific. However, it could not be excluded that larvae do not form aversive memory during training, as animals were not exposed to aversive stimuli during the different test situations. Therefore, larvae were tested on salt plates. Here, experimental larvae showed no memory expression (Fig. 30C, S24C). Thus, one can speculate that an aversive salt memory is formed during training and in this test situation aversive memory is expressed due to presence of salt but it is overwritten by simultaneous recall of appetitive memory due to the absence of sugar.

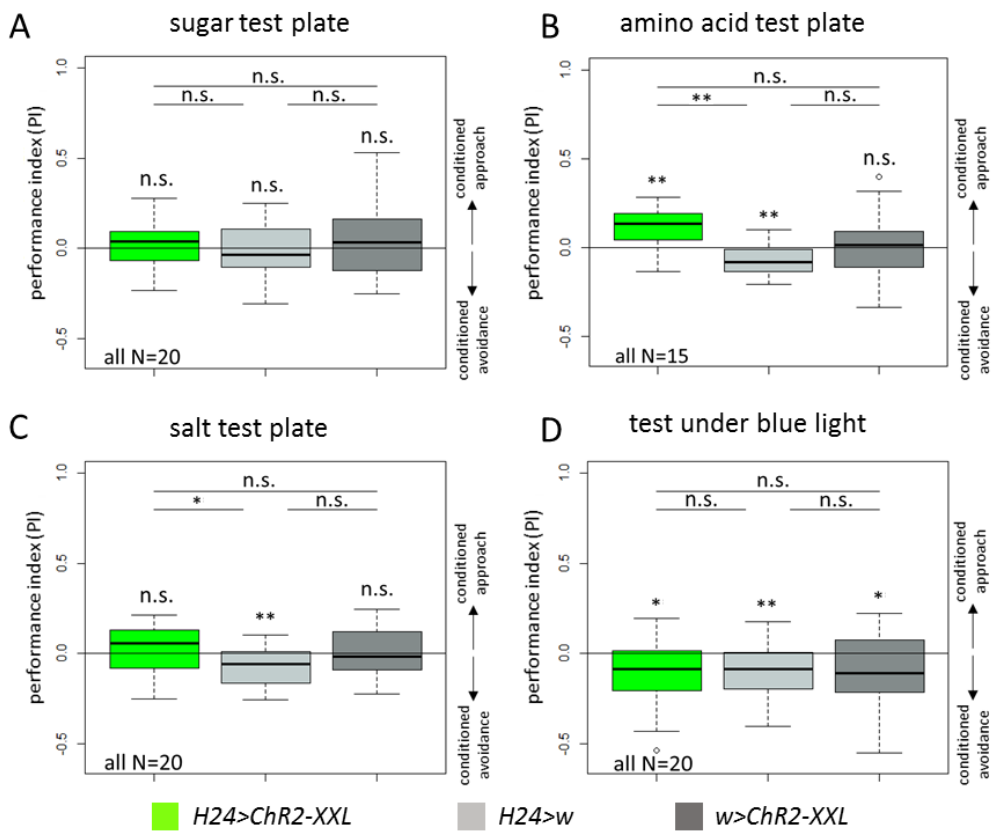

Figure 30: *Optogenetic activation of KCs induces sugar memory formation. A: Sugar exposure of larvae during test abolished appetitive memory expression; B: Amino acid exposure during test did not affect recall appetitive memory; C: Salt exposure of larvae during test inhibited appetitive memory expression; D: When exposed to blue light in a test situation experimental as well as control larvae expressed aversive memory.*

Drosophila larvae are characterised by robust negative phototaxis and it was shown that light can be used as aversive US during conditioning [Sawin-McCormack et al. 1995; von Essen et al. 2011]. As in the substitution assay larvae are exposed to blue light in order to optogenetically activate KCs, it had to be tested whether the light exposure is used by the animals as an additional aversive US. To do so, larvae were tested on pure plates under blue light. Indeed, experimental larvae as well as control larvae expressed significant aversive memory (Fig. 30D, S24D). However, the observed aversive learning behavior was not induced by KC activation, as there was no diference in the performance between the tested groups.

Lastly, it can be claimed that during substitution learning i) a sugar memory and ii) probably an aversive memory are simultaneously formed, and iii) larvae perceive blue light as an aversive US independent of KC activation. Thus, to conclusively demonstrate aversive memory formation, a test situation eliminating appetitive memory expression should be offered to the larvae, e.g. by concurrent adding of salt and sugar to the agar substrate.

3.6. Does KC activation induce an internal reward signal?

The formation of appetitive memory requires the presence of CS associated with a positive US. In the substitution learning assay, instead of exposing larvae to a physical reward, MB KCs were optogenetically activated resulting in expression of appetitive memory (Fig. 24). This raised the question, whether KC activation substitutes an appetitive US by mimicking an internal reward signal. To test this hypothesis, naïve *H24>ChR2-XXL* larvae were first tested for 3 minutes in a light avoidance assay for their preference for darkness opposed to blue light exposure. Assuming that KC activation induces an internal reward signal, it was suggested that experimental larvae would exhibit reduced negative phototaxis behavior. Indeed, after 1 minute experimantal larvae were randomly distributed throughout the Petri dish whereas control larvae showed significant light avoidance behavior. After two minutes, the darkness preference of *H24>ChR2-XXL* larvae was still significantly decreased compared to genetic controls. By the end of the experiment (minute 3) no significant difference in the light avoidance behavior between experimental and control larvae was observed (Fig. 31A). To verify the rewarding effect of KC activation under elimination of the aversive light stimulation, the assay was repeated by using red light, which is assumed to be not aversive for *Drosophila* larvae [Warrick et al. 1999]. Here, the activating red-light sensitive channel Chrimson [Klapoetke et al. 2014] was expressed in KCs. Throughout the assay control larvae were randomly distributed on the Petri dish showing no active phototaxis. Corresponding to the previous results, experimental larvae actively crowled towards the illuminated site of the Petri dish within the first two minutes while after 3 minutes no difference between the groups was observed (Fig. 31B). Extended data on 30 seconds measurements is depicted in Figures S25 and S26.

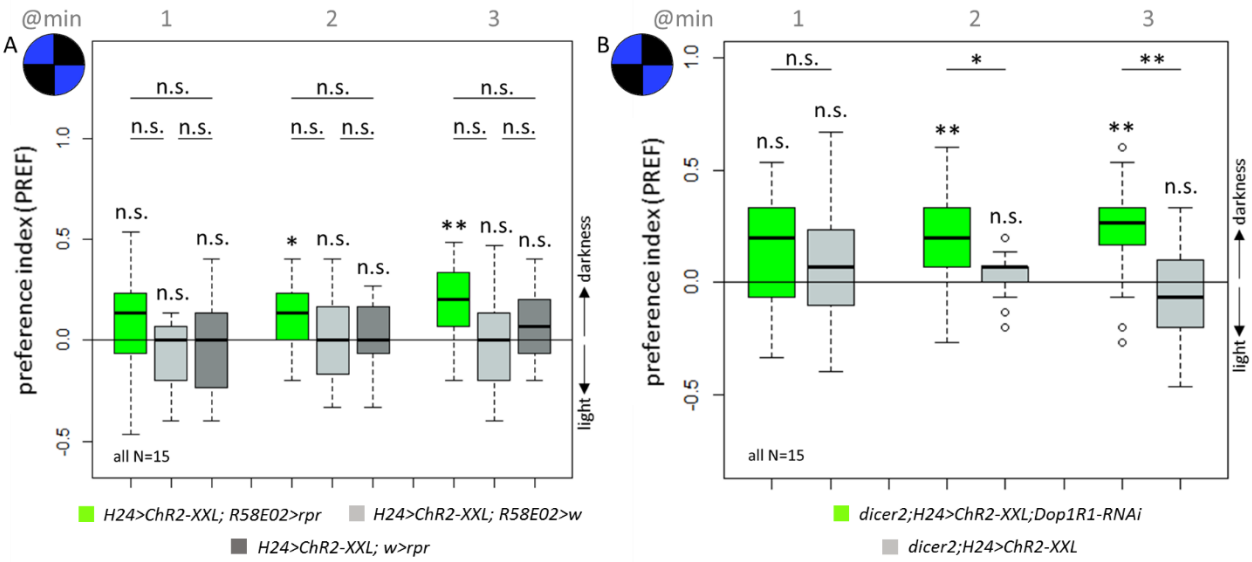

Figure 31: *Optogenetic activation of KCs induces internal rewarding signal. A: Blue light exposure of H24>ChR2-XXL larvae impaired light avoidance within two minutes followed by increase of darkness preference to wild type levels; B: Optogenetic activation of KCs using red shifted cation channel in absence of aversive light stimulus resulted in active action selection of experimental larvae towards illuminated sites.*

To further verify the rewarding effect of KC activation, *H24>ChR2-XXL* larvae were tested in a compound choice assay. One half of a Petri dish containing an odor container was darkened while the other half was illuminated with blue light. Under these conditions, larvae should strongly prefer the dark side based on combination of naïve light avoidance and odor preference. OCT, AM, and BA were used in the compound choice assay. In the OCT and AM tests, control larvae preferred strongly the dark/odor side while experimental larvae showed significantly decreased darkness/odor preference (Fig. 32A, 32B). Using BA in combination with darkness resulted in a significant approach of the control larvae towards the shaded side, while experimental larvae were randomly distributed between dark/odor and illuminated side (Fig. S27). In the odor preference test experimental larvae showed abolished preference for BA upon KC activation (Fig. 27A). By that, it can be assumed that in the compound choice assay *H24>ChR2-XXL* larvae are biased in combining darkness and odor as appetitive stimuli and the comparisson to the genetic controls is untenable.

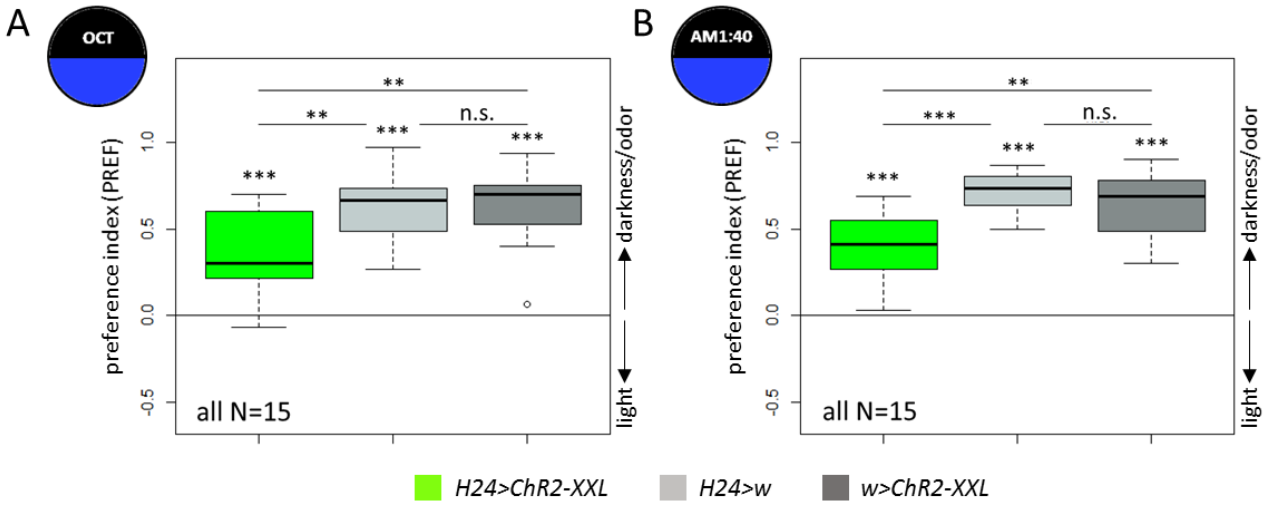

Figure 32: *Optogenetic activation of KCs opposed to simultaneous exposure to two different appetitive stimuli decreases the positive combinatorial effect of the stimuli. A: In a choice assay H24>ChR2-XXL experimental larvae showed decreased darkness/OCT preference compared to genetic control larvae; B: Significantly reduced approach towards dark/AM(1:40) side could be observed after optogenetic activation of KCs.*

In 2016, Rohwedder and colleagues showed that dopaminergic neurons from the primary-lineage protocerebral anterior medial (pPAM) cluster mediate internal reward signals during larval odor-sugar learning [Rohwedder et al. 2016]. Therefore, it was tested whether the KC activation phenotype in the light avoidance assay is based on the activation of these rewarding pPAM neurons and whether it can be reproduced by activating the pPAM neurons. *ChR2-XXL* was expressed in these neurons using the *R58E02-GAL4* driver line and *R58E02>ChR2-XXL* larvae were tested for their darkness preference. In accordance with the previous results, the naïve light avoidance of the experimental larvae was abolished throughout the experiment whereas control larvae showed a significant darkness preference (Fig. 33). Extended data on 30 seconds measurements is depicted in Figure S28.

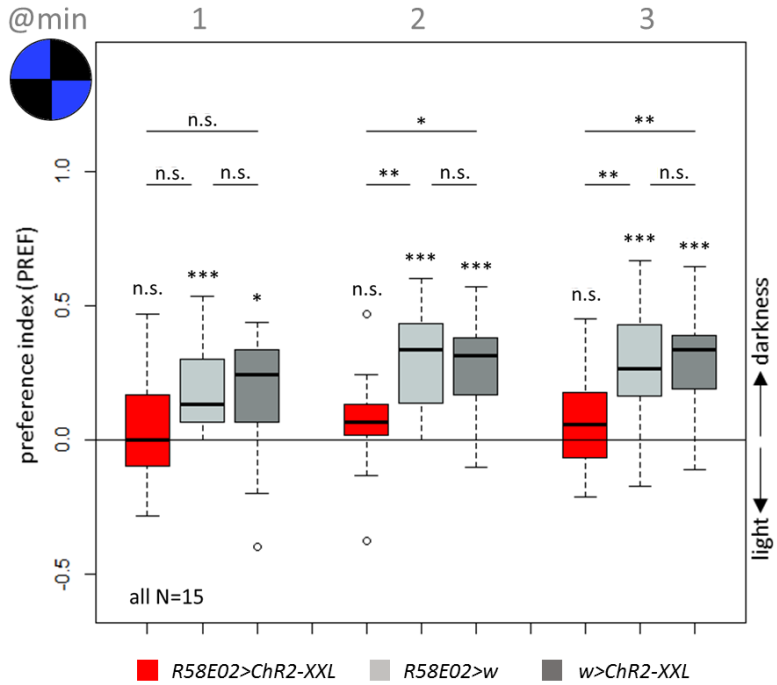

Figure 33: *Optogenetic activation of pPAM neurons results in abolished naïve light avoidance. Throughout three minutes of reccording, experimental larvae were randomly distributed between light and shaded side of a Petri dish and showed no darkness preference.*

As the connectome reconstruction of the larval MB at EM level revealed anatomical KC-to-DAN connections [Eichler et al. 2017], it was assumed that an internal reward signal is induced by the activation of pPAM neurons via recurrent excitatory KC-to-pPAM loop, and thus may serve as appetitive US during substitution learning.

3.7. Does the recurrent KC-to-pPAM loop elicit appetitive memory formation during substitution learning?

It was suggested that the optogenetic activation of KCs results in activation of dopaminergic pPAM neurons which induces a reward signal serving as an appetitive US paired with an odor information. To prove whether this is the underlying mechanism of learning in the substitution assay, the suggested neuronal network was genetically manipulated at different levels. For this purpose, the GAL4/UAS and LexA/LexAop systems were combined (Chapter II). First, the previosly described recombinant line *UAS-ChR2-XXL,LexAop-Kir2.1* was crossed with the combined *R58E02-LexA;H24-GAL4* driver line in order to achieve a concurrent activation of

KCs and silencing of pPAM neurons. As it was expected that the learning phenotype would be abolished in the experimental group, two positive genetic controls lacking either the LexA or the LexAop construct were generated. *H24>ChR2-XXL;R58E02>Kir2.1* larvae did not show memory formation in contrast to *R58E02;H24>ChR2-XXL* control larvae. However, learning behavior was also not observed in *H24>ChR2-XXL,Kir2.1* control larvae (Fig., 34A, S29). Based on the fact that the positive control comprising the recombinant line lacked memory expression too, it was assumed that in this crossing KCs might be not activated as supposed. Therefore, F1 control larvae were tested molacularly for *ChR2-XXL* and *Kir2.1* expression. Indeed, in three out of 10 larvae *ChR2-XXL* expression could not be detected whereas in all larvae *Kir2.1* was expressed (Fig. 34B), suggesting an outcrossing of the *ChR2-XXL* construct in the tested F1 generation. Thus, it could not be exluded that also experimental larvae showed no memory formation due to unordinary KC activation.

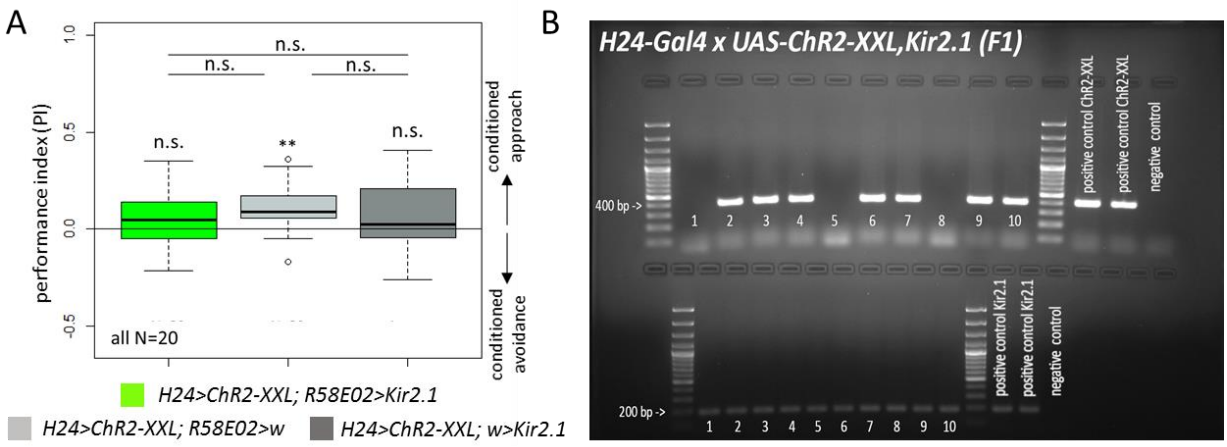

Figure 34: *Silencing of pPAM neurons during substitution learning might result in abolishment of appetitive memory. A: Expression of Kir2.1 in KCs impaired recall of appetitive memory. Larvae from the UAS/LexAop control group dis not express memory as well. However, B: in the tested F1 generation ChR2-XXL was probably outcrossed out of the recombinant effector line as in only 7/10 of the tested F1 larvae ChR2-XXL expression was detected.*

To further test the hypothesis of KC-to-DAN loop inducing appetitive memory during substitution, pPAM neurons were ablated by expressing the apoptotic gene *reaper* (*rpr*): *H24>ChR2-XXL;R58E02>rpr*. Here again, two positive genetic controls were generated as described above. After training, control larvae showed significant memory expression in contrast to experimental larvae (Fig. 35A, S30). The impairment in memory formation in *H24>ChR2-XXL;R58E02>rpr* larvae was not due to altered naïve olfactory behavior, since experimental larvae performed as good as control larvae in an odor preference test (Fig. 35B).

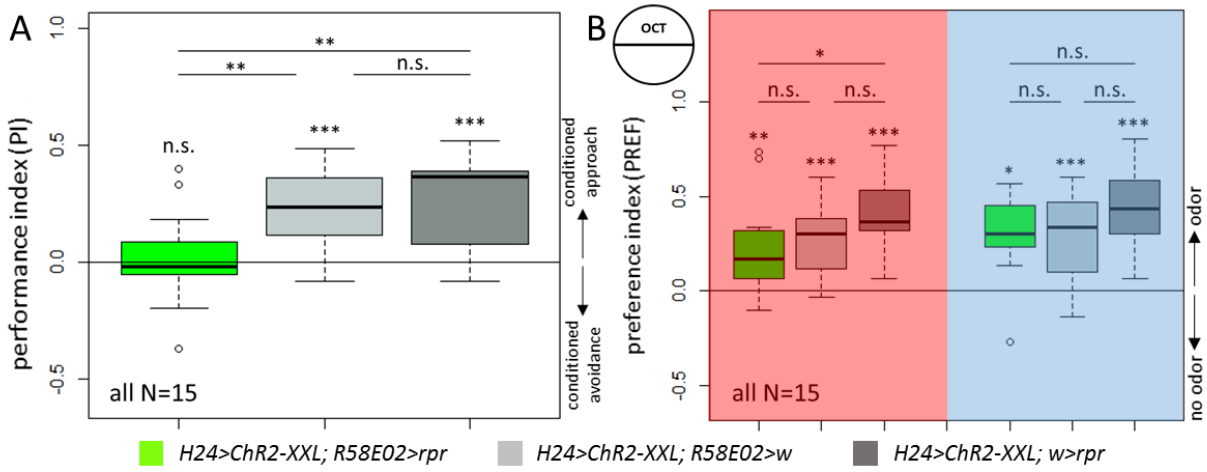

Figure 35: *Ablation of pPAM neurons impairs substitution learning. A: Simultaneous optogenetic activation of KCs and pPAM neuron ablation resulted in abolishment of appetitive memory; B: Experimental larvae did not show impairment in naïve odor preference.*

As the optogenetically-induced appetitive memory formation was abolished after pPAM ablation, the question raised whether experimental larvae would now express an aversive memory. To allow the expression of aversive gustatory memories [Scleyer at al. 2011; Schleyer et al. 2015], larvae were tested on 1.5M salt plates. Interestingly, the experimental group expressed appetitive memory in the presence of the punishing stimulus (Fig. 36A, S31). Consisiting with previous results (Fig. 30C), both positive genetic controls showed no memory expression. In a gustatory preference test, optogenetic activation of KCs enhanced larval 1.5M salt avoidance independent of pPAM ablation (Fig. 36B, S32). Whether the observed appetitive memory in *H24>ChR2-XXL;R58E02>rpr* larvae is due to i) a change in the value, quality or valance of the US, ii) an interference between pPAM signaling pathway and other MBIN pathways involved in aversive learning, iii) a change in internal information balance or iv) developmental effects due to pPAM ablation is still elusive and has to be further investigated.

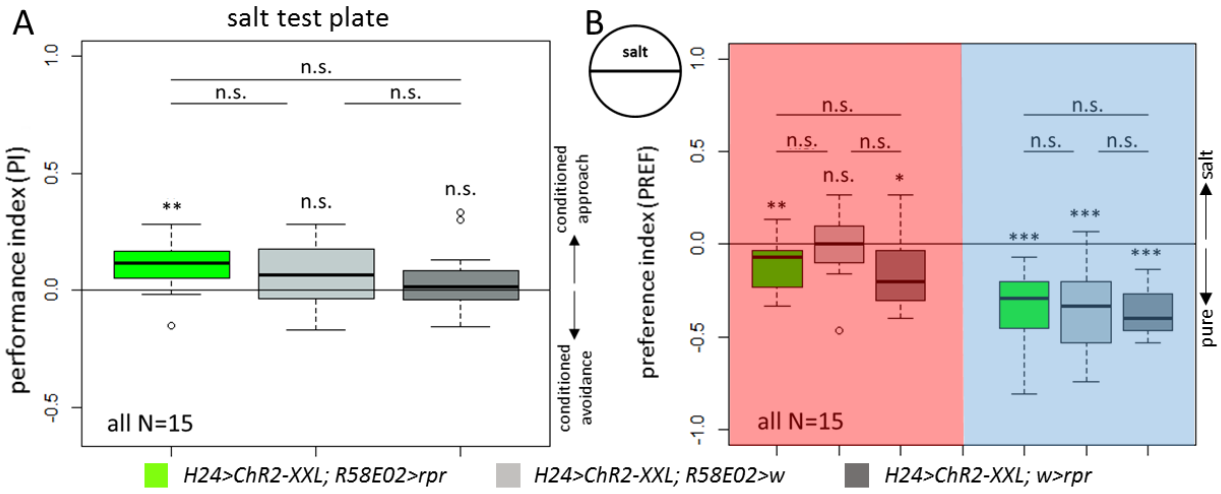

Figure 36: *Simultaneous activation of KCs and ablation of pPAM neurons results in appetitive memory recall on a salt test plate. A: In a substitution learning assay larvae with activated KCs and ablated pPAM neurons showed significant appetitive learning behavior, whereas control larvae did not recall memory on a 1.5 M salt plate; B: Optogenetic activation of KCs resulted in increased salt avoidance independent of pPAM ablation.*

To verify that impaired dopamine (DA) signaling due to pPAM ablation results in an abolishment of appetitive memory formation during substitution, KCs were activated and the dopamine receptor Dop1R1 in KCs was knocked down via RNAi as it is known that Dop1R1 is necessary for appetitive olfactory learning in *Drosophila* larvae [Selcho et al. 2009]. Consistent with the latter results, *dicer2;H24>ChR2-XXL;Dop1R1-RNAi* larvae showed no memory expression in contrast to *dicer2;H24>ChR2* control larvae (Fig. 37A, S33). Here again, the lack of learning behavior was not due to impairment in naïve odor preference (Fig. 37B).

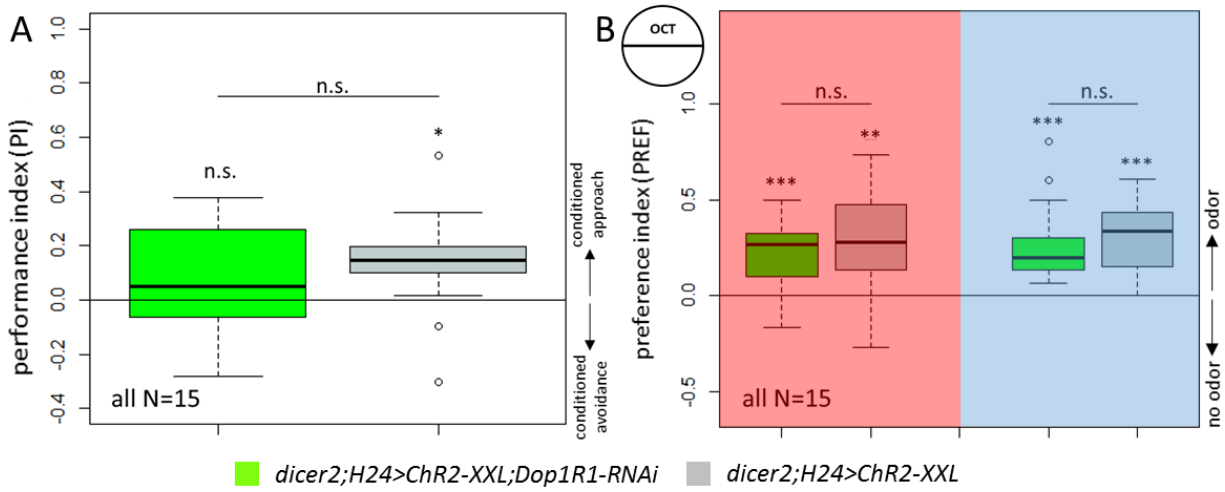

Figure 37: *Downregulation of Dop1R1 in KCs abolishes appetitive learning during substitution conditioning. A: In contrast to control larvae, experimental larvae showed no learning behavior after simultaneous activation of KCs and knock down of the dopaminergic Dop1R1 receptor in MB neurons; B: Impairment in substitution learning was not due to affected naïve odor preference.*

Next, it was tested at the neuronal level whether pPAM neurons respond with intracellular Ca^{2+} increase to KC activation using the Ca^{2+} sensor GCamp6m. Two different cation channels were used to optogenetically activate KCs. First, red-light sensitive *Chrimson* was expressed in *H24-GAL4* positive neurons. Isolated brains were exposed to 620nm red light for base line recording. After 30 seconds, brains were exposed to 475 nm blue light for KC activation and the fluorescence activity of pPAM neurons was monitored. pPAM neurons responded with a significant Ca^{2+} increase upon blue light illumination of the brains (Fig. 38A, 38B).

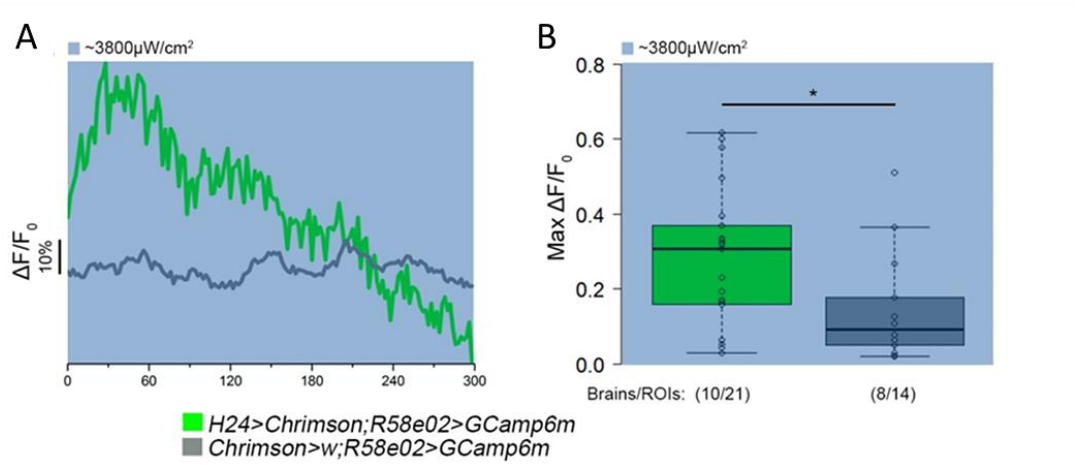

Figure 38: *pPAM neurons respond to optogenetic activation of KCs. A: Activation of H24-GAL4 positive cells using Chrimson resulted in response of pPAM neurons with B: sigificant intracellular Ca^{2+} increase. Figures by D. Pauls*

In a second functional imaging experiment, KCs were activated by expressing *ChR2-XXL* to verify the fluorescence activity of pPAM neurons upon KC activation. Here, brains were first exposed to blue light of low intensity (≈700 µW/cm^2) for base line recording. Then, light intensity was raised up to ≈3800 µW/cm^2. A significant increase of intracellular Ca^{2+} in the pPAM neurons was recorded in response to the higher light intensity (Fig. 39A-C).

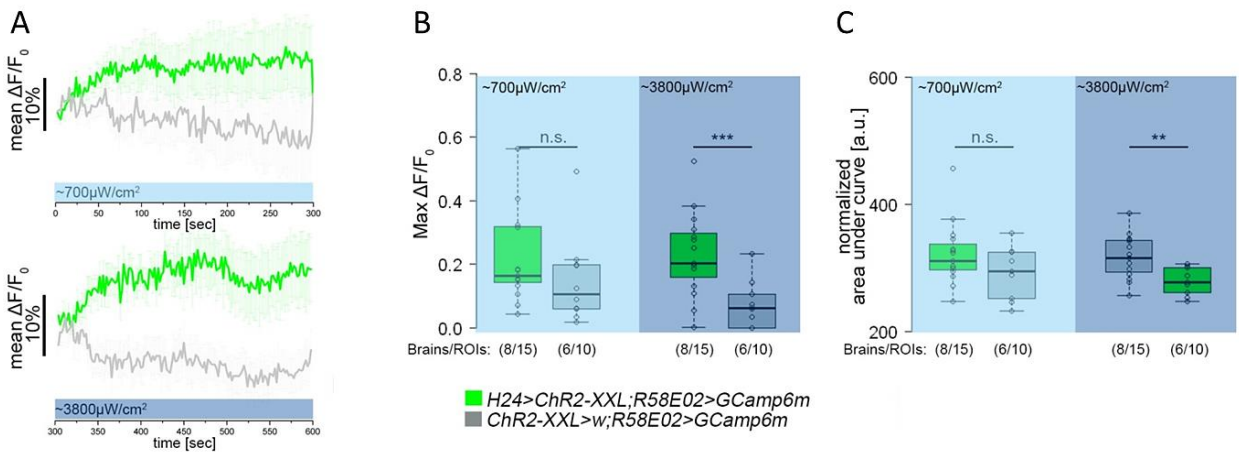

Figure 39: *pPAM neurons respond to optogenetic activation of KCs. A, C: Activation of H24-GAL4 positive cells using ChR2-XXL resulted in response of pPAM neurons with B: sigificant intracellular Ca^{2+} increase. Data and figures by D. Pauls*

These results suggest, that optogenetic activation of KCs is sufficient to increase intracellular Ca^{2+} in pPAM neurons and thus induce neuronal activation. To test whether such feedback activation underlies the internal reward signaling observed before (Fig. 31A, B), light avoidance assays were performed manipulating the KC-to-pPAM loop as previously described (*H24>ChR2-XXL;R58E02>rpr* and *dcr2;H24>ChR2-XXL;Dop1R1-RNAi*). In both experiments larvae from the positive genetic control groups were randomly distributed between dark and illuminated sites (Fig. 40A, B) corresponding to previous results (Fig. 31A). *H24>ChR2-XXL;R58E02>rpr* and *dcr2;H24>ChR2-XXL;Dop1R1-RNAi* experimental larvae showed significant light avoidance behavior by the second and third minute of the measurement (Fig. 40A, B) suggesting that feedback activation of dopamine releasing pPAM neurons is inducing internal reward signal. Extended data on 30 seconds measurements is depicted in Figures S34 and S35.

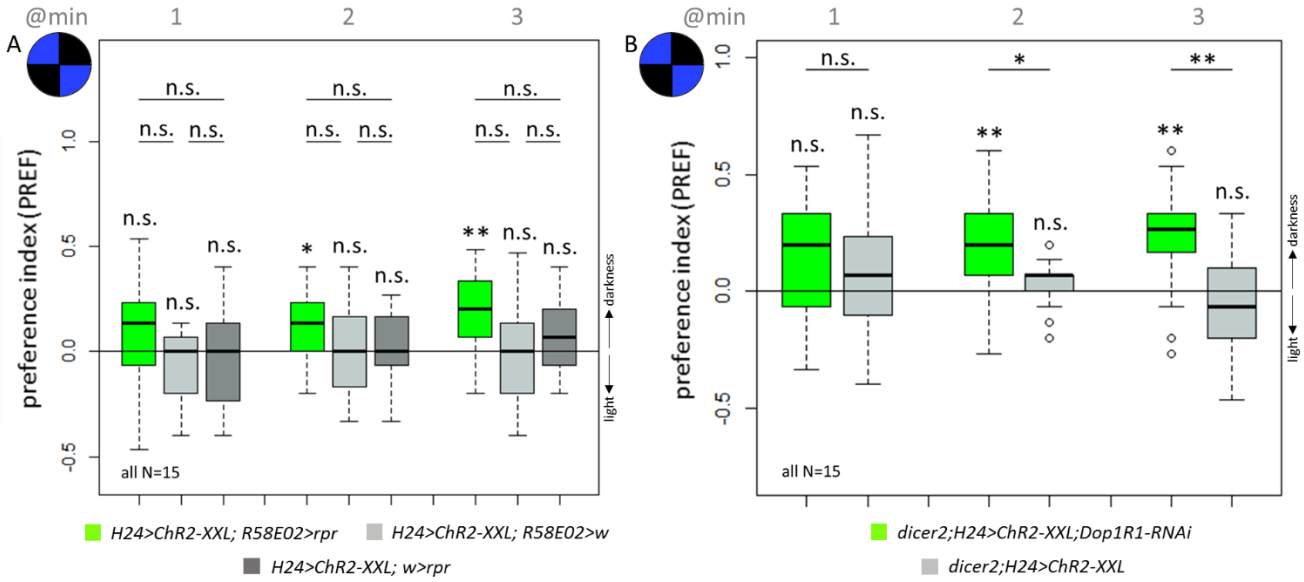

Figure 40: *Internal reward signal is induced by artificial activation of KC-to-pPAM feedback loop. In a light avoidance assay optogenetic activation of KCs resulted in abolishment of negative phototactic behavior while A: simultaneous ablation of pPAM neurons or B: downregulation of Dop1R1 receptor in the KCs restored the naïve larval response to bright light.*

Taken together, these results underpin the hypothesis of a functional positive feedback loop from KCs to pPAM neurons which triggers artificial reward signals during substitution learning and by that induces the formation of appetitive memory.

3.8. Which neurotransmitter is involved in the KC-to-pPAM feedback signaling?

MB Kenyon cells express acetylcholine (ACh) as a classical neurotransmitter and short neuropeptide F (sNPF) as neuromodulator [Croset et al. 2018; Johard et al. 2008] and the role of both neurotransmitters in olfactory learning in adult *Drosophila* has been studied [Barnstedt et al. 2016; Knapek et al. 2013]. Additionally, in 2017 a recurrent feedback loop from KCs to dopaminergic neurons from the protocerebral posterior lateral (PPL) cluster based on ACh signaling was shown to be involved in aversive odor-shock learning in flies [Cervantes-Sandoval et al. 2017]. However, whether these findings apply for larvae is still unknown.

To prove the contribution of ACh in larval olfactory learning and specifically in the KC-to-pPAM feedback signaling, four different subunits of the ACh receptor (AChR) were downregulated via RNAi in the pPAM neurons during odor-sugar learning. Interestingly, knockdown of AChR

subunits did not impair appetitive memory formation in experimental larvae (Fig. 41A-D, S36A-D). Hence, KC-to-pPAM feedback signaling does not depend on acetylcholine in larvae.

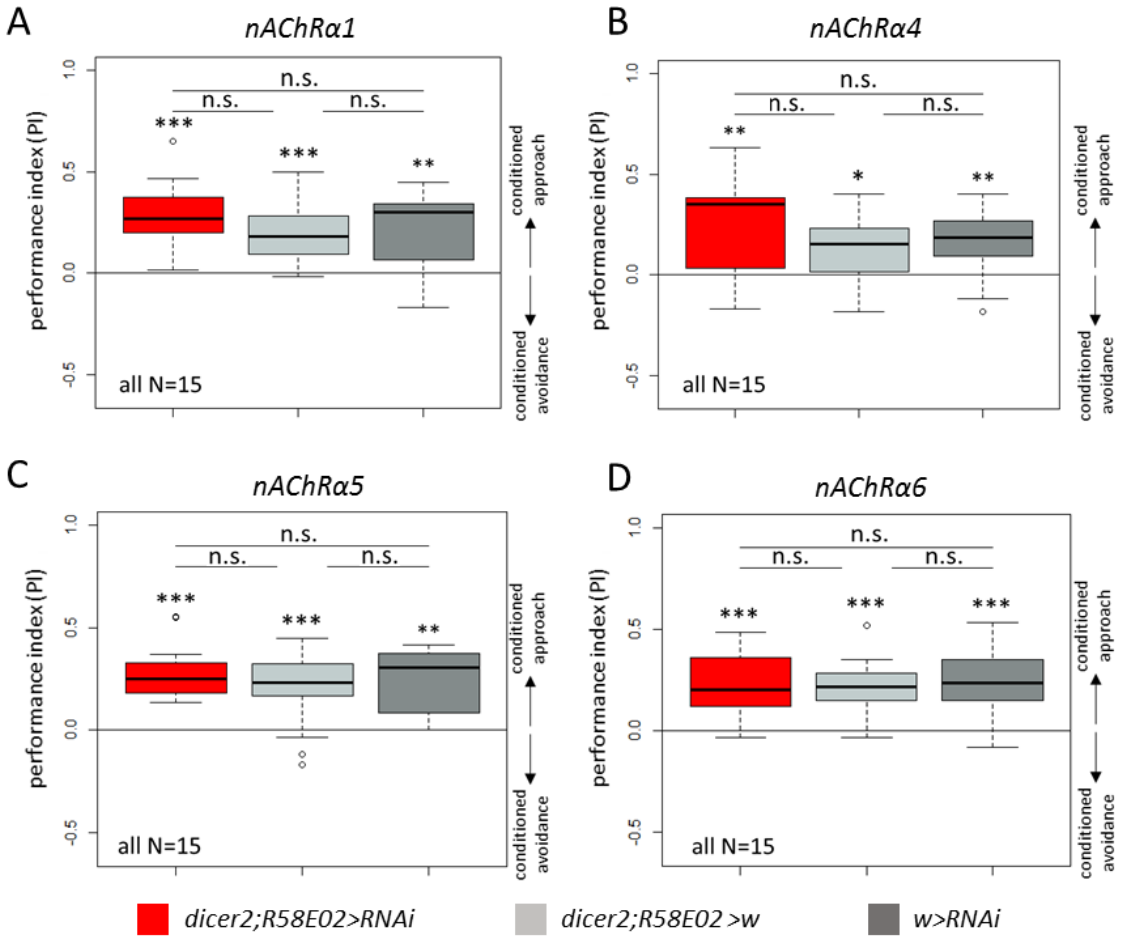

Figure 41: *Odor-sugar learning is not affected by knock down of subunits of the ACh receptor in pPAM neurons. A-D: Larvae with downregulated expression of AChR subunits in the pPAM neurons showed no biased learning behavior in comparisson to genetic controls.*

Next, it was tested whether KCs signal to pPAM neurons via sNPF. For that, the sNPF receptor (sNPFR) was downregulated via RNAi in the pPAM neurons during odor-sugar conditioning. Indeed, although not comletely abolished, significantly reduced learning behavior of experimental larvae compared to both genetic controls was observed (Fig. 42A, S37A). As larvae were still able to form appetitive odor memory, it was suggested that KC-to-pPAM sNPF signaling might not be necessary for memory formation *per se*, but rather for reinforcing the signal within the MB circuit. To examine such possible function of sNPF, the experiment was replicated, however this time larvae were tested five minutes after training (retention time, RT). Significant learning behavior in control larvae was observed five minutes after training

whereas experimental larvae lacked memory expression (Fig. 42B, S37B). The impairment in learning behavior was not caused by affected naïve odor (Fig. 42C) or sugar (Fig. 42D) preference due to sNPFR downregulation. However, it should be proven whether memory decay in the tested groups follows comparable temporal curve progression, as it can be speculated that the memory scores decrease concurrently and independent of sNPF signaling.

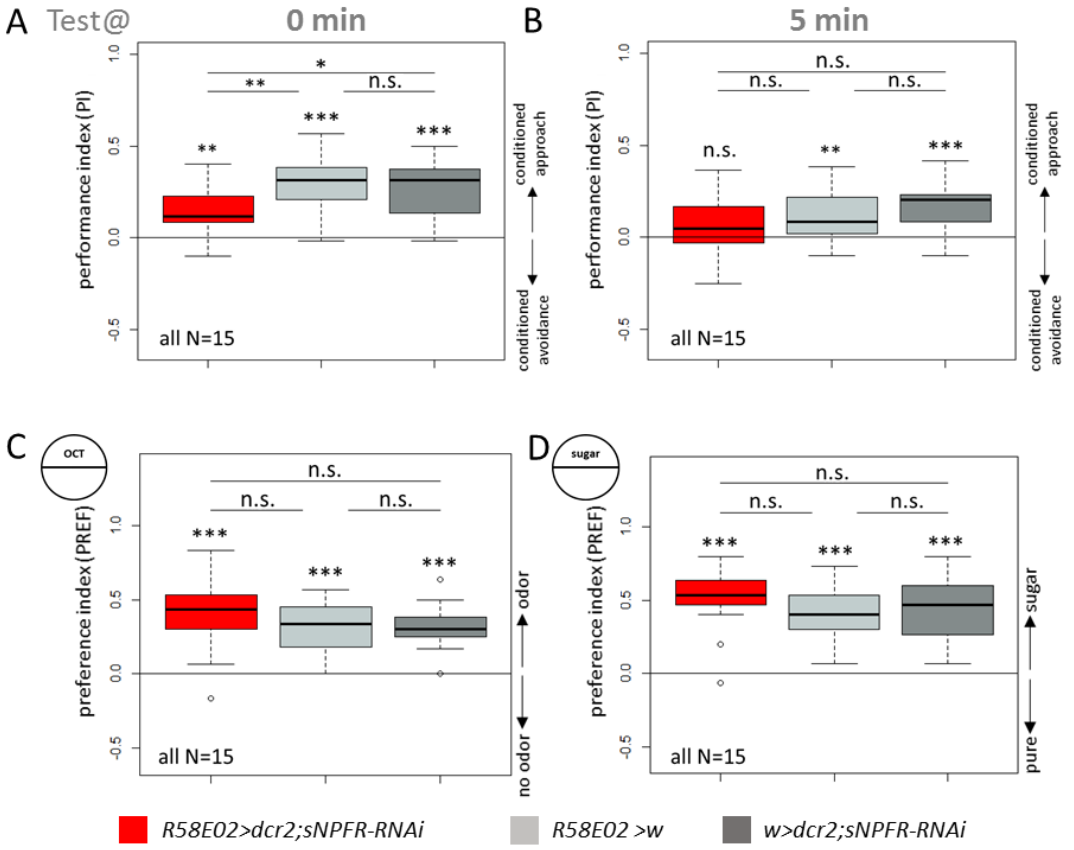

Figure 42: *Odor-sugar learning is affected by knock down of the sNPF receptor in the pPAM neurons. A: Experimental larvae with downregulated expression of sNPFR in the pPAM neurons showed significantly decreased learning performance compared to genetic controls directly after training; B: Memory expression in experimental larvae was completely abolished five minutes after training; Impairment in learning behavior of experimental larvae was not due to biased naive C: odor or D: sugar preference.*

The obtained results indicate a role of sNPF and sNPFR in odor-sugar learning, yet sNPF is not only expressed in the KCs but in various other neurons in the larval CNS [Nassel et al. 2008]. To prove whether sNPF signaling from the KCs underlies the substitution learning phenotype, larvae were challenged to form appetitive memory upon KCs activation while simultaneously neuropeptide maturation in the KCs is altered due to downregulation of *amontillado* [Wegener et al. 2011; Pauls et al. 2015] (*dicer2;H24>ChR2-XXL;amon-RNAi*). As expected,

experimental larvae did not express appetitive memory in contrast to larvae from the positive control group (Fig. 43A, S38). The naïve odor response was not affected by *amon* downregulation (Fig. 43B).

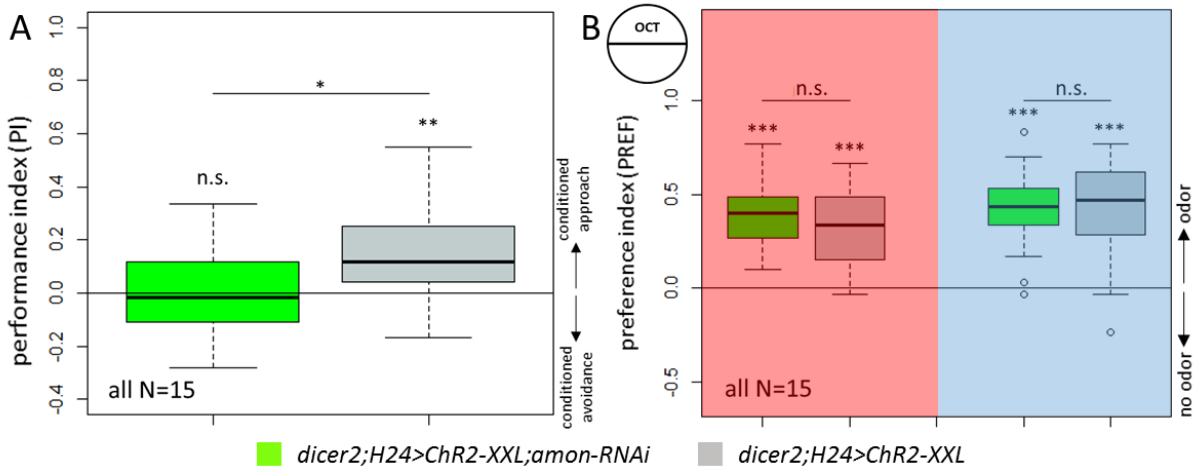

Figure 43: *Disruption of neuropeptide maturation in KCs during substitution learning abolishes appetitive memory. A: Downregulation of amontillado in KCs resulted in significantly decreased learning performance after substitution conditioning compared to genetic control; B: Impairment in substitution lerning was not due to biased naïve odor preference.*

To show the responsivenes of pPAM neurons to sNPF, functional imaging was performed. sNPF was bath applied to isolated brains and the activity of pPAM neurons was monitored. As consequence of sNPF application, intracellular fluorescence activity of pPAM neurons was significantly increased compared to DMSO (vehicle) control (Fig. 44 A-C).

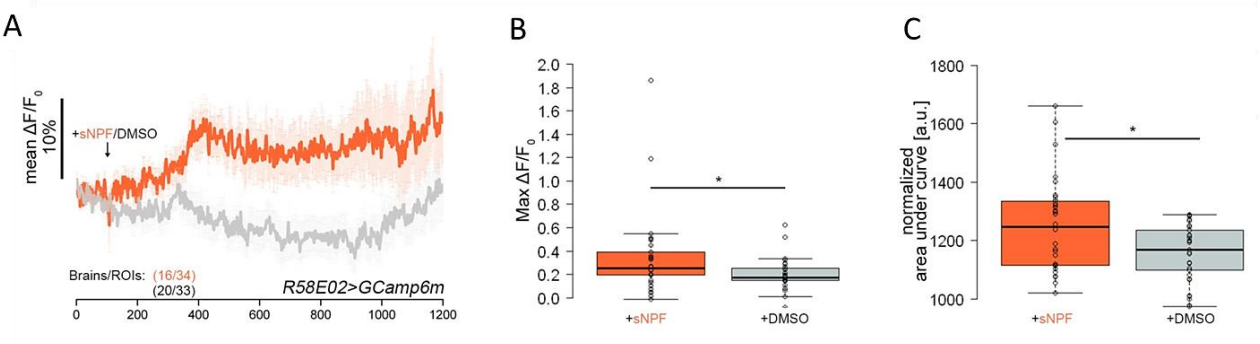

Figure 44: *pPAM neurons respond to sNPF bath application. Application of sNPF on isolated brains resulted in A, C: response in the pPAM neurons with B: significant intracellular Ca^{2+} increase. Data and figures by D. Pauls*

Next, it was to be clarified whether pPAM neurons respond to a neuropeptidergic signal from the KCs. KCs were activated via *Chrimson*, as described above. Additionally, sNPF maturation was impaired by downregulation of *amon* in the KCs and fluorescence activity of the pPAM neurons was monitored. Indeed, pPAM neurons did not respond to KC activation when these lacked mature sNPF. In contrast, activation of KCs expressing mature sNPF resulted in significant increase of intracellular Ca^{2+} in the pPAM neurons (Fig. 45A-C).

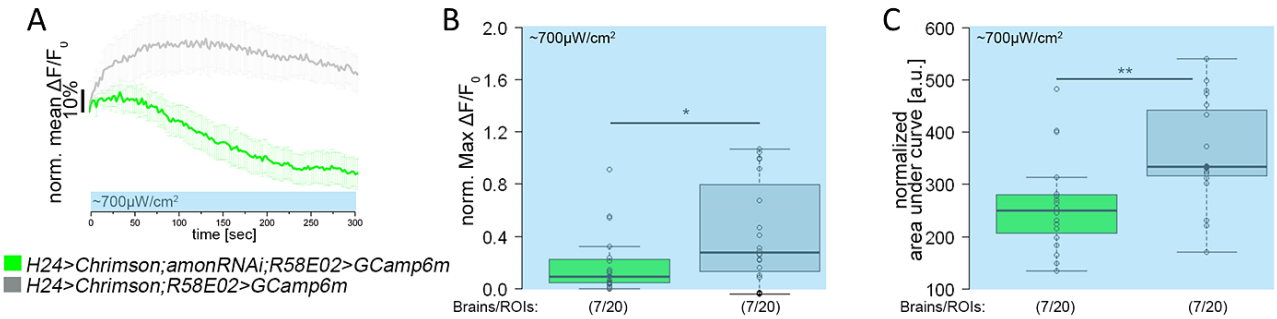

Figure 45: *Disruption of neuropeptide maturation in the KCs inhibits pPAM response to KC activation. A-C: pPAM neurons did not respond to optogenetic activation of KCs if amontillado was downregulated in the latter. Data and figures by D. Pauls*

Since sNPF is the only neuropeptide so far identified to be expressed in the KCs, these results suggest recurrent peptidergig KC-to-pPAM loop based on sNPF signaling.

It was further tested whether the peptidergic signal from the KCs is reponsible for the induction of an internal reward upon optogenetic activation of KCs. A light avoidance assay was performed with simultaneous downregulation of *amon* and KC activation. Larvae from the positive genetic control group were randomly distributed between the dark and illuminated sites (Fig. 46). *dicer2;H24>ChR2-XXL;amon-RNAi* experimental larvae showed significant light avoidance behavior by the third minute of the measurement (Fig. 46) suggesting that peptidergic signaling from the KCs is involved in the activation of internal rewarding pathways. Extended data on 30 seconds measurements is depicted in Figure S39.

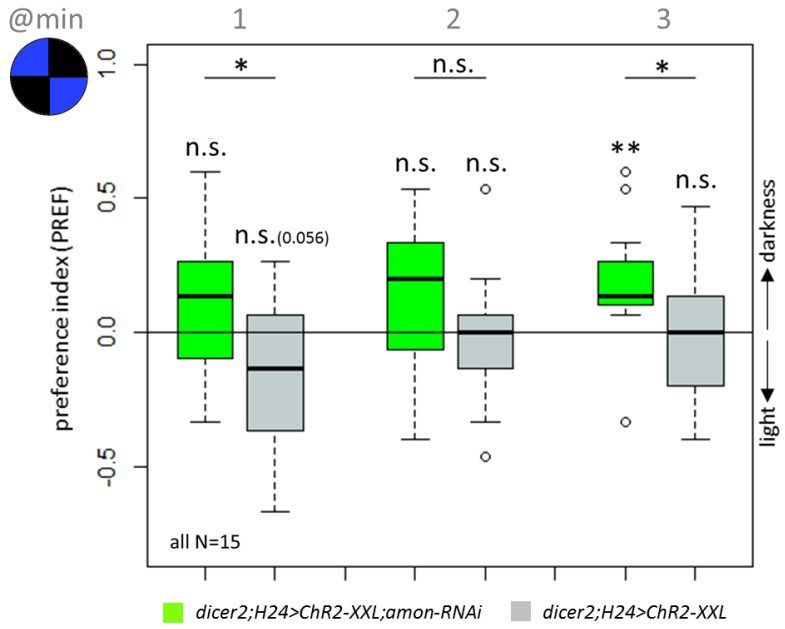

Figure 46: *Internal reward signaling is induced by peptidergic signals from the KCs. In a light avoidance assay optogenetic activation of KCs resulted in abolishment of negative phototactic behavior while simultaneous decrease in neuropeptide levels within the KCs restored the naïve larval response to bright light.*

3.9. Which role may the excitatory feedback loop play within the MB circuitry?

The conventional description of the MB connectivity was significantly expanded by the complete reconstruction of the MB connectome, and, besides the already known MBIN-to-KC and KC-to-MBON connections, additional KC-to-MBIN and MBIN-to-MBON synapses were identified [Eichler et al. 2017]. Here, it could be shown that an anatomical KC-to-pPAM connection is functional and that artificial activation of the feedback loop is sufficient to induce appetitive memory formation. However, the specific role of this feedback signaling was to be unveiled. To test whether the KC-to-pPAM loop biases regular odor-sugar learning, first the naïve sugar preference of larvae was tested. Sugar preference was not affected by KC activation (Fig. 47C). Next, substitution learning was performed pairing KC activation with sugar as physical appetitive US ("*H24>ChR2-XXL*: sugar+blue light"). The same crossing was used in both control experiments: regular odor-sugar learning under red light ("sugar only") and substitution learning assay without sugar exposure ("blue light only"). As there were indications from previous experiments (Fig. 42B) that the feedback loop might be involved in the stabilization of memory, larvae were tested at different time points after training (RT: 0min, 10min, 15min, 30min, 45min). When tested directly or 10 minutes after training, larvae trained under all three different contitions showed comparable significant memory scores. However, 15 minutes after training memory expression was abolished in larvae trained under "sugar only" and "blue light only" condition, respectively. Larvae trained on sugar with simultaneous KC activation showed appetitive memory expression throughout all retention time points, so that positive learning performance was observed even 45 minutes after training (Fig. 47A, 47B). Statistical camparison between the three tested groups at different time points is depicted in Figure S40.

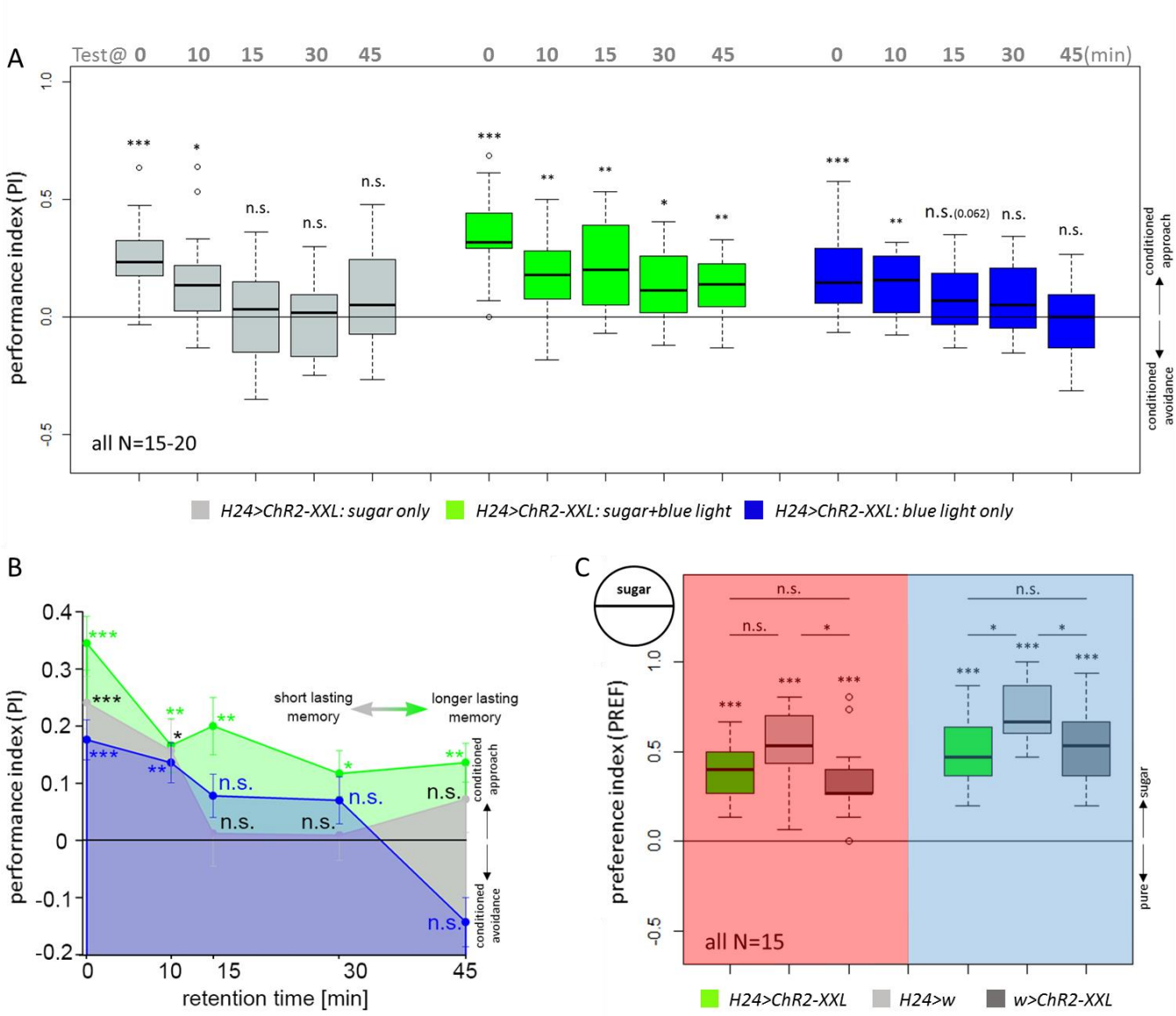

Figure 47: *Optogenetic activation of KCs stabilizes appetitive memory over time. A, B: H24>ChR2-XXL larvae trained with combined blue light and sugar exposure recalled appetitive memory for at least 45 minutes after training featuring stable learning performance thoughout the tested retention period. Larvae tested under control conditions ("sugar only" and "blue light only") showed memory expression immediately after training and 10 minutes after training. After 15 minutes retention time larvae were not able to recall appetitive memory formed during training (figure B by D. Pauls); C: Optogenetic activation of KCs had no effects on sugar preference as experimental and control larvae performed consistently in a sugar preference test both under red and blue light.*

The finding, that artificial activation of a recurrent KC-to-pPAM feedback signaling enhances memory persistance after associative conditioning of larvae gives hints for the function of this newly identified anatomical connection and indicates a potential role for memory stabiliization within the MB circuit.

4. Discussion

4.1. Optogenetic activation of mushroom body Kenyon cells in *Drosophila* larvae is sufficient to induce appetitive olfactory memory during conditioning in absence of rewarding stimulus.

The MB is known to be the "memory center" of insects. Great advantages are achieved in understanding its architecture and way of functioning especially on the strenght of *Drosophila* as model organism. The contribution of the fruit fly larva in unraveling the mechanisms of learning behavior and memory formation is indisputable, as it offeres numerous benefits, e.g. "only" 10 000-neurons nervous system (undergoing single cell reconstruction at synapse level), straightforward handling and behavioral assays, and a huge repertoir of techniques for genetic manipulations. Therefore, this organism was chosen to dissect, at least partially, the neuronal network of memory.

During associative conditioning mushroom body intrinsic neurons, the KCs, receive information for the presence of an US and a CS. In case of larval odor-sugar learning, odor information (CS) is processed via projection neurons, while sugar information is signaled via dopaminergic neurons from the pPAM cluster. As consequence of simultaneous odor-dependent Ca^{2+} influx and dopamine binding at the KCs, cAMP levels in the KCs increase and, following intracellular cascade, synaptic plasticity at the level of KC-to-MBON synapses is induced [Cognigni et al. 2018; Masuda-Nakagawa et al. 2005; Ramaekers et al. 2005; Rohwedder et al. 2016; Saumweber et al. 2018; Selcho et al. 2009; Widmann et al. 2018]. In this study, it was shown that even in the absence of physical reward during training, appetitive memory can be formed in larvae by simultaneous artificial activation of KCs and odor exposure (substitution learning). In adult *Drosophila*, KCs are characterized by cAMP-dependent plasticity, and plasticity in odor-evoked responses, respectively [Louis et al. 2018; Zhang and Roman 2013; Hige et al. 2015]. Hense, artificial activation of KCs with subsequent increase of cAMP may produce MB responses analog to the process of natural reward learning. Further, it could be shown that artificial activation of KCs does not interfere with larval naïve odor

preference for octanol and amyl acetate. Additionally, it was demonstrated that larvae are able to discriminate both odors while KCs are simultaneously activated. On one hand, in motor neurons optogenetic activation of neurons using *ChR2-XXL* results in axonal depolarisation by K^+ and Na^+ increase [Dawydow et al. 2014]. On the other hand, it was shown that Ca^{2+} dynamics in KC somata serves as a substrate for memory coding of odor identity in adult *Drosophila* [Ludke et al. 2018]. Assuming that somatic Ca^{2+} levels are highly dependent on odor signals from the PNs required for associative learning, it can be suggested that indeed subsets of KCs respond odor-specific during substitution learning, and therefore are able to form precise memory for the trained odor. However, an interesting aspect of optogenetic KC activation effects is the change in benzaldehyde preference upon blue light illumination. Spatial map of odor coding within the larval antennal lobe reveals coding of amyl acetate and octanol via *Or85c* while benzaldehyde is represented in *Or30a*, *Or45b*, and *Or67b* AL glomeruli [Kreher et al. 2005]. Such spatial differentiation in odor information processing might be a hint for distinct adaptation of olfactory responses based on internal signals from higher brain centers (e.g. MB or LH). Early olfactory processing is modulated state-dependent (hunger vs. satiety) via serotonergic neurons synapsing onto uPNs (Katrin Vogt, personal communication). Additionally, blocking MB KCs results in inversion of the quality of geranyl acetate from aversive to attractive (Katrin Vogt, personal communication). Further, a mechanism for regulating the processing of olfactory information via inhibitory feedback loops from higher brain regions was described in the olfactory bulb in rats [Balu et al. 2007]. In the *Drosophila* larva, neuromodulatory input via serotonergic and octopaminergic neurons was suggested to have an effect on presynaptic inhibition at the level of AL glomeruli by synapsing onto local interneurons (Broad LN Trio and Keystone LN) [Berck et al. 2016]. However, it is not known whether *Or30a*, *Or45b*, and *Or67b* AL glomeruli are targeted by higher brain centers. It can be speculated that the olfactory signaling pathway involving these ORNs/glomeruli/PNs is modulated by internal signals and by that, the naïve odor response is adjusted dependent on the animal's state. In *Or30a* and *Or45b* glomeruli in total five different odors are processed – benzaldehyde, anisole, acetophenone, 2-methylphenol, and 4-methylphenol [Kreher et al. 2005]. Preliminary results of odor preference tests with anisole reveal comparable to benzaldehyde effect of KC activation on larval naïve anisole preference, as upon optogenetic activation of KCs larvae do not show approach behavior towards the odor (data not shown). Presumed that for the other three odors (acetophenone, 2-methylphenol, and 4-

methylphenol) the same effect can be observed, adaptation of odor-dependent responses based on feedback signaling from e.g. the MBs can be assumed. However, it is still elusive at which level within the olfactory pathway such modulation might intervene and the hypothesis of hierarchical adaptation of odor responses has to be further investigated.

4.2. Appetitive substitution learning depends on dopaminergic pPAM neurons.

As already mentioned, sugar reward is signaled during associative conditioning via dopaminergic pPAM neurons [Rohwedder et al. 2016; Saumweber et al. 2018]. Here, it was demonstrated that appetitive memory formation during substitution learning depends on the activation of dopaminergic pPAM neurons. Memory expression was abolished when pPAM neurons were ablated, or Dop1R1 was downregulated in the KCs, respectively. Considering anatomical data from the MB connectome reconstruction, it was assumed that KCs activate pPAM neurons via feedback signaling, resulting in dopamine release. Thus, binding of dopamine at Dop1R1 receptors mimics the presence of sugar reward and induces association between the odor and the “virtual” reward. This assumption was confirmed, as in a light avoidance tests, larvae with activated KCs, and pPAM neurons respectively, showed a similar response to blue light illumination, namely decreased negative phototactic behavior, suggesting a rewarding effect of the activation of these cells. The functionality of the anatomical KC-to-pPAM connection was verified, as functional imaging experiments revealed an increase of intracellular Ca^{2+} in the pPAM neurons as response to optogenetic activation of KCs. Such functional reciprocal KC-to-DAN connections were already described in adult *Drosophila*. In flies, disrupted cholinergic signaling from KCs to dopaminergic neurons from the PPL cluster impairs aversive odor-electric shock memory [Cervantes-Sandoval et al. 2017]. However, it cannot be excluded that the feedback loop is not direct, but involves intermediary neurons. Particularly, in adult *Drosophila* DANs receive additional excitatory input from MBONs. Consequently, persistant DAN activity results in increased dopamine release during courtship [Zhao et al. 2018] and odor-sugar [Ichinose et al. 2015] training. It is unclear whether the same principle applies for larval learning as well. As there are direct anatomical KC-to-pPAM and MBON-to-MBIN connections [Eichler et al. 2017], it is tempting to speculate that

both patways (direct and indirect) contribute to modulation and/or modification of memory formation and expression. However, no direct connections from MBONs to the rewarding DAN-h1 and DAN-i1 from the pPAM cluster were found so far. Further, contribution of octopaminergic neurons (OANs) to appetitive memory formation during substitution is conceivable. In adults, dopaminergic neurons from the PAM cluster, required for appetitive learning, express the octopamine OAMB receptor. Downregulation of this receptor in PAM neurons affects appetitive learning in flies, suggesting layered OAN-to-DAN-to-KC signaling [Burke et al. 2012]. Furthermore, appetitive motivation relies on octopamine interaction via OCTβ2R receptor with dopaminergic MB MP1 neurons [Burke et al. 2012]. In larvae, similar to KC-to-DAN connections, KCs synapse onto OANs [Eichler et al. 2017]. Additionally, a feed-across motif within the MB vertical and medial lobes was described, which involves OAN-to-MBON-to-DAN connectivity [Eichler et al. 2017]. Thus, hypothetical two-, three- or more-hops feedback loops might further shape learning behavior.

4.3. Appetitive memory expression induced by optogenetic activation of KCs is sugar-specific.

Memory expression is, to certain extent, “motivation”-driven. That is, internal state of the animal in combination with envitonmental information allows computation of what can be expected due to previous experience and memory retrieval. For example, *Drosophila* flies express robust sugar memories after starvation or via mimicking the hungry state by activation of neurons expressing *Drosophila* neuropeptide F (dNPF) [Krashes et al. 2009; Krashes and Waddell 2008]. So far, in *Drosophila* larvae it is not shown whether starvation enhances sugar-memory, however during odor-sugar learning reward information related to sugar-concentration is modulated by NPF as well [Rohwedder et al. 2015], and memory acquisition as well as retreival depends strongly on the value of environmental stimuli. During olfactory learning, a memory trace for an odor is formed. After conditioning, *Drosophila* larvae exhibit outcome expectation-based learned behavior. In this sense, memory is only expressed if the change in behavior, in terms of odor approach or avoidance, predicts a positive outcome [Schleyer et al. 2011; Schleyer et al. 2015]. In a test situation larvae compare the value of the

current situation with the value of the odor memory [Gerber and Hendel 2006; Schleyer et al. 2011]. Therefore, the presence or absence of an US (rewarding or punishing) during test is crucial for memory expression. After appetitive learning, e.g. odor-sugar, larvae show searching behavior and recall olfactory memory only if reward (e.g. sugar) is not available. That is, they expect to find "something good" at the odor site. In contrast, after aversive learning, e.g. odor-high salt, larvae show escape behavior and memory expression only if they are exposed to the punishing stimulus, e.g. high-salt, as in this case they are forced to avoid "something bad" predicted by the learned odor [Gerber and Hendel 2006; Schleyer et al. 2011]. This expectation-based model of action selection was expanded by the finding that larvae remember not only the "good" or "bad" value of a stimulus, but also its quality. For example, sugar memory cannot be recalled on a sugar plate, but exposing the larvae to usually rewarding aspartic acid in a test situation does not affect sugar memory expression. Similarly, salt memory is expressed in the presence of salt, but not in the presence of punishing quinine [Schleyer et al. 2015].

In this study, appetitive memory in *Drosophila* larvae was formed in absence of a rewarding stimulus by optogenetic activation of KCs with simultaneous odor exposure. Testing larvae for memory expression on sugar plates abolished the learned behavior, while testing on amino acid plates resulted in robust memory expression. Having the "match-missmatch" theory, it is argumentative that during substitution learning larvae form an appetitive memory for sugar. This is in line with findings on the function of pPAM neurons, as these signal particularly sugar information [Rohwedder et al. 2016; Saumweber et al. 2018]. However, it is unknown to which extent the memory is specific for fructose used in the experiments. The *R58E02-GAL4* driver line consists of three out of four pPAM neurons, pPAM 1, 3 and 4. Ablation of these three neurons results in impairment of the memory for fructose and sorbitol. Both sugars provide a nutritional value for larvae, but only fructose is perceived as sweet. In contrast, pPAM ablation does not affect memory for sweet but not nutritious arabinose [Rohwedder et al. 2012; Rohwedder et al. 2016]. Thus, memory formation observed during substitution probably relies not only on the gustatory value ("sweet or not"), but involves intern evaluation of the sugar caloric value. As octopamine is assumed to mediate sweetness rather than nutritional value [Selcho et al. 2014; Burke and Waddell 2011], it can be speculated that, in respect to the observed learning behavior using *R58E02-GAL4*, octopamine is not directly involved in the signaling pathway. However, the pPAM2 neuron was shown to be important for odor-

arabinose learning. Thus, it is thrilling to prove whether activation of this neuron would elicit comparable appetitive memory expression, that would suggest involvment of octopaminergic neurons.

A second aspect here is whether an aversive memory – in addition to appetitive memory - is formed during substitution learning. Indeed, there is a hint for simultaneous formation of both types of memory, as when tested on salt after conditioning larvae did not show significant memory expression. However, in such test situation, recall of appetitive memory should not be affected, as larvae were not exposed to a rewarding stimulus. Nevertheless, considering that salt exposure results in the expression of an aversive memory, if such is formed during training, it can be suggested that both types of memory are expressed during test, and by that overall memory expression is nullified. Using the same experimental approach, it should be possible to eliminate the expression of the appetitive memory and simultaneously trigger an aversive memory expression by testing larvae on plates consisiting of both salt and sugar. The assumption of paralell formation of memories of opposing valence would be in line with findings in adult *Drosophila*, as parallel opposing memories (aversive, and appetitive in form of aversive memory extinction) was shown to be formed in the MBON network [Felsenberg et al. 2018]. Unfortunatelly, there is a lack in single-cell studies (comparable to [Saumweber et al. 2018]) on the function of punishment mediating DANs in larvae. Yet, dopaminergic *TH-GAL4* positive neurons were shown to play a role in aversive learning in larvae [Selcho et al. 2009], so deeper analysis of KC-DAN connectivity could provide evidence for further functional loops underlying aversive memory formation. Strikingly, it was observed that larvae express robust appetitive memory on salt test plate after substitution learning when the pPAM neurons are ablated. It is not clear, whether pPAM ablation impairs acquisition of aversive memory during training or its expression during test, however this phenotype is not due to inversion in the quality of salt. Given that rewarding and punishing DANs signal to different MB compartments (punishing DANs from the DL1 cluster -> peduncle and VL, rewarding DANs from the pPAM cluster -> ML [Eichler et al. 2017; Rohwedder et al. 2015; Rohwedder et al. 2016; Saumweber et al. 2018; Selcho et al. 2009]), the complex MB circuitry involving e.g. KC-to-KC connections and feed-across VL-to-ML loops, and the theory of KC-to-MBON synaptic depression, it is tempting to speculate that after ablation of pPAM neurons other so far unidentified functional signaling loops (feedback or feedforward) prevail in order to change the balance in depriving approach/avoidance behavior eliciting synaptic connections, and thus

trigger searching behavior in presence of a punishing stimulus. However, appetitive memory expression during exposure to an aversive stimulus was so far not described, so dissection of the procceses underlyinig such behavior would be of great benefit for understanding the functional connectivity and neuronal mechanisms involved in appetitive vs. aversive learning.

4.4. short neuropeptide F signaling is involved in the KC-to-pPAM feedback loop.

MB KCs express acetylcholine (ACh) as classical neurotransmitter and short neuropeptide F (sNPF) as neuromodulator [Barnstedt et al. 2016; Croset et al. 2018; Johard et al. 2008; Nassel et al. 2008]. In adult *Drosophila*, the function of both signaling substances in learning behavior was investigated. MBON expression of nicotinic ACh receptors is prerequisite for MBON activation, and ACh expression in the KCs is required for appetitive and aversive olfactory memory formation [Barnstedt et al. 2016]. ACh is further involved in KC-to-PPL feedback signaling during aversive learning [Cervantes-Sandoval et al. 2017]. Additionally, sNPF from the KCs modulates appetitive learning in flies [Knapek et al. 2013] and enhances ACh-evoked responses in MBONs [Barnstedt et al. 2016]. So far, in larval MBs only sNPF expression was anatomically described [Nassel et al. 2008], while only one ouf of the three canonical components of the ACh cycle, namely the choline transporter (ChT), was identified [Hamid et al. 2019]. Hamid and colleagues could not detect either Choline acetyltransferase (ChAT) nor vesicular acetylcholine transporter (VAChT) in the larval KCs. However, there is a lack of studies on neurotransmitter function within KCs during conditioning.

Here, first evidence for the role of sNPF in larval odor-sugar learning was provided. Knock down of the sNPF receptor (sNPFR) in the pPAM neurons did not affect naïve behaviors required for memory formation, but impaired appetitive learning. Moreover, downregulation of mature sNPF by RNAi knock down of *amontillado* during substitution learning resulted in a complete abolishment of appetitive memory. These results are in line with the role of sNPF in appetitive learning in adults, as panneuronal knockdown of sNPFR in flies impairs odor-sugar learning as well. It is convincing, that the neuropeptide is released by KCs, since sNPF downregulation in KCs affects appetitive learning [Knapek et al. 2013]. In this thesis, it was shown that pPAM neurons respond to sNPF bath application with significant intracellular Ca^{2+}

increase. To the same extent, optogenetic activation of KCs resulted in pPAM response, while this response was abolished when *amon-RNAi* was expressed in the KCs. Therefore, it is suggested that the intracellular Ca^{2+} increase in the pPAM neurons is a consequence of a neuropeptidergic signal coming from the KCs. These findings underpin the hypothesis of the described KC-to-pPAM feedback loop. However, sNPF is expressed not only in KCs but in high number of different neurons within the larval CNS [Nassel et al. 2008], therefore it cannot be excluded that sNPF signaling acts via additional pathways to modulate odor-driven learned behaviors.

Since ACh was shown to be involved in feedback signaling within the MB circuitry in adult flies [Cervantes-Sandoval et al. 2017], it was inevitable to prove whether this applies also for larvae. Although the same RNAi effector lines as in the study of Cervantes-Sandoval were used to knock down different subunits of the nicotinic ACh receptor (AChR) in the pPAM neurons, no effect on odor-sugar learning was observed in larvae. However, it remains an open question whether ACh plays a role in larval aversive learning, as this is the case in adults [Cervantes-Sandoval et al. 2017]. Moreover, as to date ACh is not detected in larvae [Hamid et al. 2019], it is possible that memory formation is modulated unequaly in adults and larvae. Yet, assuming that larval MBs also express ACh, it is conceivable that not nicotinic but muscarinic AChRs (mAChR-As) are involved in the learning processes. In adult *Drosophila*, mAChR-As at the KC presynaptic terminals are required for aversive olfactory learning and are suggested to be required for KC-to-MBON synaptic depression via KC-KC lateral autoinhibition [Bielopolski et al., 2018]. Given the feed-across connections between the lobes, such mechanism would be plausible in larvae. However, involvement of ACh within the MBs in larval learning remains hypothetical. Unlike in adults, the KC-to-DAN loop described above seems to rely on sNPF and not ACh feedback signaling.

4.5. Recurrent signaling in the MB circuit during associative conditioning increases the persistence of an appetitive odor memory.

Associative memories consist of phases varying in the duration and expression time. So, unconsolidated cAMP-dependent short-term (STM) and middle-term (MTM) memory can be distinguished from consolidated long-term (LTM) and anestesia-resisitent (ARM) memory, whereby LTM and ARM are based on different molecular pathways as LTM formation requires *de novo* protein synthesis, while ARM formation does not [McGaugh 2000; Tomchik and Davis 2009; Tully et al. 1994a; Yin et al. 1994]. In *Drosophila* larvae three different types of memory were identified so far: STM, LTM, and ARM [Honjo and Furukubo-Tokunaga 2005; Khurana et al. 2009; Tully et al. 1994b; Widmann et al. 2016]. The molecular mechanisms within KCs underlying different memory phases in *Drosophila* larvae are well described [Widmann et al. 2016], however little is known about neuronal network components involved in memory consolidation in larvae. In adult *Drosophila*, short- and long-term memory formation relies on cAMP signaling in different KC types [Blum et al. 2009], and is dependent on dopamine signaling from distinct DANs from the PAM cluster [Yamagata et al. 2015]. Memory is formed in MB αβ lobe neurons, while recurrent activity in MB α'β'-DPM (dorsal paired medial) neurons circuit is required for consolidation [Keene et al. 2006; Krashes et al. 2007]. Furthermore, it was shown that ARM formation is modulated by two parallel patways: serotonergic DPM-αβ lobe loop and octopaminergic APL-α'β' lobe circuit [Wu et al. 2013].

In this study, a modulatory KC-to-pPAM neuronal circuit based on sNPF signaling in larvae was identified to be possibly involved in memory stabilization. It was shown that artificial optogenetic activation of KCs in combination with sugar reward during conditioning is sufficient to prolong the period in which memory can be expressed after training. Larvae trained to associate an odor with sugar and simultaneous KC activation showed memory expression 45 minutes after training, whereas if larvae were trained with sugar or KC activation only, memory expression was abolished 15 minutes after training. These findings support the hypothesis that recurrent activity within the MB circuit facilitates aquisition of longer-lasting memories, in line with data from adults. Thus, it is suggested that pPAM neurons are activated during conditioning by i) gustatory signals, and ii) feedback signaling

from the KCs, respectively. By that, difference in pPAM activity, could shape KC responses and potentially induces memories of different types. It should be further pointed out, that DAN activity depends on the internal state, as they are targeted by dNPF neurons in larvae [Rohwedder et al. 2015] as well as in adults [Krashes et al. 2009]. Hense, dopaminergic neurons represent good candidate for evaluation of internal state and external situation, and, by adjusting activity, for triggering formation of short- or long-lasting memory in larvae. In doing so, memory would undergo continual adaptation in the MBs modulated by pPAM neurons, which in turn receive constant feedback from KCs and MBONs. In conclusion, the described KC-to-pPAM feedback loop may act as a signal amplifier in order to stabilize appetitive memory and to induce longer-lasting memories.

It should be further pointed out, that sNPF might play an additional role in establishing different memory phases. sNPF is tightly connected with insulin metabolism, as insulin producing cells (IPCs) express sNPFR, and by that sNPF regulates expression of *Drosophila* insulin like peptides (Dilps) [Lee et al. 2008]. Further, expression of Dilps is increased after ingestion of carbohydrates (e.g. sucrose) [Musselman et al. 2011; Ugrankar et al. 2018]. In *Drosophila* larvae, sucrose consumption blocks lARM formation and enables formation of LTM via insulin signaling and insulin receptors (InRs) within the KCs (Annekathrin Widmann, personal communication). Thus, increased sNPF release after optogenetic activation of KCs might have a dual effect, once by adjusting the pPAM activity via KC-to-pPAM feedback loop, and second by affecting the insulin metabolism.

Nevertheless, it is a long way off to fully understand the neuronal mechanisms of computation during memory formation. In terms of appetitive memory, great progress was done in dissecting the function of MBINs and MBONs at single cell level. However, it is still to be studied i) at single cell level: which neurons are involved in aversive memory acquisition, ii) at circuitry level: how does communication between network components modulate memory formation, consolidation and expression, and iii) to which extent internal and external information contribute to the odor-driven learned behavior of *Drosophila* larvae.

5. Summary

How animals organize behavior in order to adapt to environmental changes is one of the key biological questions. One aspect of behavioral adjustment is learning and memory formation. The functional architecture of memory acquisition, storage and retreival across phyla shares high degree of similarities. For example, in *Drosophila melanogaster* dopamine (DA) signaling is essential for mediating external rewarding and punishing stimuli. In mammals, DA neurons convey also appetitive and aversive information and are involved in learning processes. Here, a dissection of a recurrent signaling from MB KCs to rewarding dopaminergic neurons from the pPAM cluster in *Drosophila* larvae was performed and a novel function of peptidergic KC-to-pPAM feedback loop was identified.

During associative conditioning, fruit fly larvae are trained to pair an olfactory CS with a gustatory US. Previous work has shown that both CS and US can be substituted by artificial activation of the respective signal mediating neurons. In this work, it was demonstrated that in absence of a physical US optogenetic activation of MB KCs is sufficient to induce appetitive memory (substitution learning), suggesting induction of an internal rewarding signaling due to the KC activation. It was hypothesized that the activation of KCs activates in turn dopaminergic pPAM neurons via previously anatomically described KC-to-pPAM feedback loop. To achieve simultaneous manipulation of different components of the neuronal network, different transgenic lines were generated by combining the GAL4/UAS and LexA/LexAop systems. It was observed that the pPAM neurons respond with Ca^{2+} increase to the activation of the KCs, and ablation of the pPAM neurons or downregulation of dopaminergic Dop1R1 receptor in the KCs abolished the learning behavior in larvae in the substitution learning assay. Induction of an internal rewarding signal was further confirmed by a decrease in light avoidance upon KC activation. The activation of KCs did not result in impairment of basic naïve behaviors like crawling speed, sugar preference or preference for certain odors (octanol, amyl acetate). However, an effect on number of stops and turns during locomotion was observed. This hints a change in searching behavior and/or orientation. Interestingly, upon KC activation a loss of naïve preference for benzaldehyde was observed.

As there are findings on influence of the MBs on larval naïve odor avoidance, it can be assumed that the naïve responses to certain odors is regulated by the activity of KCs. However, there is lack of anatomical data on how the MBs could be connected to primary olfactory centers. To dissect the function of the MBs in naïve olfactory behavior, the identification of odors inducing naïve responses that underly regulation by the MBs is required. It is indispensable to investigate possible anatomical connections from the KCs to the LH, PNs, AL and/or ORNs.

By exposing larvae to different test conditions after training, it was assumed that the formed appetitive memory is sugar-specific. However, it could not be excluded that larvae form parallel aversive memories. Testing the larvae on high-concentrated salt resulted in an impaired expression of the acquired appetitive memory. Thus, it was suggested that in the substitution learning assay larvae form memories opposing in their value. Interestingly, after simultaneous KC activation and pPAM ablation larvae showed appetitive memory expression under aversive test conditions. As this finding was completely unexpected and contrary to what is known so far about the mechanisms of memory expression, it is crucial to further investigate the functions of anatomical connections within the MB network.

MB KCs express ACh as classical neurotransmitter and sNPF as neuropeptide. In this work, a function of sNPF in larval learning was evinced. Downregulation of *amontillado* (*amon*) and by that ommision of peptide maturation within the KCs resulted in abolished learning behavior in the substitution assay. Further, downregulation of the sNPF receptor in the pPAM neurons impaired odor-sugar learning, suggesting peptidergic KC-to-pPAM signaling as, additionally, the pPAM neurons did not respond to KC activation after *amon* downregulation in the latter. These result are in line with the function of sNPF in appetitive learning in adult flies. However, the peptidergic KC-to-pPAM signaling opposes findings in adult *Drosophila*, where reccurent MB-to-dopaminergic neurons feedback loop relies on ACh. Yet, in flies such feedback loop was shown to be involved in aversive learning. Whether this applies for larval aversive learning is still elusive. Taken the differences depicted here, it is thrilling to investigate to which extent the functional connectivity underlying memory processes in *Drosophila* flies and larvae is conserved throughout the different developmental stages.

Besides the KC-to-pPAM feedback driven appetitive memory formation during substitution learning assay, the influence of the recurrent peptidergic signaling on memory stability was studied. By testing the larvae at different time points after training it was observed that simultaneous exposure of larvae to sugar and optogenetic activation of KCs results in memory

stabilization. Larvae exposed to only sugar or only KC activation during training showed memory expression up to 10 minutes after trainung. Combining both, natural stimulus with induction of the recurrent signaling, increased the persistance of the acquired appetitive memory, so that larvae showed memory recall 45 minutes after training. These findings were in line with data from adults, showing that dopaminergic neurons are involved in formation of LTM and that recurrent activity within the MB circuit facilitates acquisition of longer-lasting memories. As sNPF, in interplay with *Drosophila* insulin like peptides, is important for carbohydrate metabolism and internal state is decisive for formation of different types of memory (STM, MTM, LTM, and ARM) it can be hypothesized that the MBs regulate the duration and expression time of memory phases at different levels.

Although this work uncovers several functional aspects of the neuronal network underlying memory formation, it opens many questions about different functions of the MBs in modulating behavior. It is still to be investigated how the MBs regulate larval naïve behavioral responses and in how far dopamine, sNPF and other transmitters contribute to their mode of action. Yet,

"the most beautiful thing we can experience is the mysterious. It is the source of all true art and science."

Albert Einstein

6. List of coworkers

Dennis Pauls performed the functional imaging experiments and locomotion assays and generated figures 24A-F, 37A-B, 38A-C, 43A-C, and 44A-C, 46B.

Mareike Selcho performed immunofluorescence studies (Fig. 24B, C, D, and E).

Andreas Thum kindly provided an immunohistochemical image of the *OK107-GAL4* driver line (Fig. 23F).

Maximilian Pfeuffer performed odor preference tests (Fig. 26A-D, 31B, and S27) and a substitution learning assay (Fig. 27A).

Dennis Segebarth performed substitution learning assays (Fig. 24B', C', and F').

Jens Habenstein performed a substitution learning assay (Fig. 24D').

Xenia Stavroulaki performed a substitution learning assay (Fig. 29D).

All other experiments were performed and figures were generated by Radostina Lyutova.

7. References

Aceves-Pina EO, Quinn WG (1979) Learning in normal and mutant *Drosophila* larvae. Science 206:93-96.

Apostolopoulou AA, Widmann A, Rohwedder A, Pfitzenmaier JE, Thum AS (2013) Appetitive associative olfactory learning in *Drosophila* larvae. J Vis Exp.

Aso Y, Sitaraman D, Ichinose T, Kaun KR, Vogt K, Belliart-Guerin G, Placais PY, Robie AA, Yamagata N, Schnaitmann C, Rowell WJ, Johnston RM, Ngo TT, Chen N, Korff W, Nitabach MN, Heberlein U, Preat T, Branson KM, Tanimoto H, Rubin GM (2014a) Mushroom body output neurons encode valence and guide memory-based action selection in *Drosophila*. Elife 3:e04580.

Aso Y, Hattori D, Yu Y, Johnston RM, Iyer NA, Ngo TTB, Dionne H, Abbott LF, Axel R, Tanimoto H, Rubin GM (2014b) The neuronal architecture of the mushroom body provides a logic for associative learning. Elife 3.

Bader R, Colomb J, Pankratz B, Schrock A, Stocker RF, Pankratz MJ (2007) Genetic dissection of neural circuit anatomy underlying feeding behavior in *Drosophila*: Distinct classes of hugin-expressing neurons. J Comp Neurol 502:848-856.

Balu R, Pressler RT, Strowbridge BW (2007) Multiple modes of synaptic excitation of olfactory bulb granule cells. J Neurosci 27:5621-5632.

Barnstedt O, Owald D, Felsenberg J, Brain R, Moszynski JP, Talbot CB, Perrat PN, Waddell S (2016) Memory-relevant mushroom body output synapses are cholinergic. Neuron 89:1237-1247.

Benton R, Sachse S, Michnick SW, Vosshall LB (2006) Atypical membrane topology and heteromeric function of *Drosophila* odorant receptors in vivo. PLoS Biol 4:e20.

Berck ME, Khandelwal A, Claus L, Hernandez-Nunez L, Si G, Tabone CJ, Li F, Truman JW, Fetter RD, Louis M, Samuel AD, Cardona A (2016) The wiring diagram of a glomerular olfactory system. Elife 5.

Bielopolski N, Amin H, Apostolopoulou AA, Rozenfeld E, Lerner H, Huetteroth W, Lin AC, Parnas M (2018) Inhibitory muscarinic acetylcholine receptors enhance 2 aversive olfactory conditioning in adult *Drosophila*. bioRxiv. doi: https://doi.org/10.1101/382440

Blum AL, Li W, Cressy M, Dubnau J (2009) Short- and long-term memory in *Drosophila* require cAMP signaling in distinct neuron types. Curr Biol 19:1341-1350.

Brembs B, Heisenberg M (2000) The operant and the classical in conditioned orientation of *Drosophila melanogaster* at the flight simulator. Learn Mem 7:104-115.

Burke, CJ, Waddell, S. 2011. Remembering nutrient quality of sugar in *Drosophila*. Curr Biol 21: 746– 750.

Burke CJ, Huetteroth W, Owald D, Perisse E, Krashes MJ, Das G, Gohl D, Silies M, Certel S, Waddell S (2012) Layered reward signalling through octopamine and dopamine in *Drosophila*. Nature 492:433-437.

Busch S, Selcho M, Ito K, Tanimoto H (2009) A map of octopaminergic neurons in the *Drosophila* brain. J Comp Neurol 513:643-667.

Campbell RAA, Turner GC (2010) The mushroom body. Curr Biol 20:1:PR11-PR12 doi.org/10.1016/j.cub.2009.10.031

Campbell RAA, Honegger KS, Qin HT, Li WH, Demir E, Turner GC (2013) Imaging a population code for odor identity in the *Drosophila* mushroom body. J Neurosci 33:10568-10581.

Caron SJC, Ruta V, Abbott LF, Axel R (2013) Random convergence of olfactory inputs in the *Drosophila* mushroom body. Nature 497:113-+.

Cervantes-Sandoval I, Phan A, Chakraborty M, Davis RL (2017) Reciprocal synapses between mushroom body and dopamine neurons form a positive feedback loop required for learning. Elife 6.

Clyne PJ, Warr CG, Freeman MR, Lessing D, Kim J, Carlson JR (1999) A novel family of divergent seven-transmembrane proteins: candidate odorant receptors in *Drosophila*. Neuron 22:327-338.

Clyne PJ, Warr CG, Carlson JR (2000) Candidate taste receptors in *Drosophila*. Science 287:1830-1834.

Cognigni P, Felsenberg J, Waddell S (2018) Do the right thing: neural network mechanisms of memory formation, expression and update in *Drosophila*. Curr Opin Neurobiol 49:51-58.

Colomb J, Grillenzoni N, Ramaekers A, Stocker RF (2007) Architecture of the primary taste center of *Drosophila melanogaster* larvae. J Comp Neurol 502:834-847.

Couto A, Alenius M, Dickson BJ (2005) Molecular, anatomical, and functional organization of the *Drosophila* olfactory system. Curr Biol 15:1535-1547.

Crittenden JR, Skoulakis EM, Han KA, Kalderon D, Davis RL (1998) Tripartite mushroom body architecture revealed by antigenic markers. Learn Mem 5:38-51.

Croset V, Treiber CD, Waddell S (2018) Cellular diversity in the *Drosophila* midbrain revealed by single-cell transcriptomics. Elife 7.

Davis RL (1993) Mushroom bodies and *Drosophila* learning. Neuron 11:1-14.

Dawydow A, Gueta R, Ljaschenko D, Ullrich S, Hermann M, Ehmann N, Gao S, Fiala A, Langenhan T, Nagel G, Kittel RJ (2014) Channelrhodopsin-2-XXL, a powerful optogenetic tool for low-light applications. Proc Natl Acad Sci U S A 111:13972-13977.

de Bruyne M, Clyne PJ, Carlson JR (1999) Odor coding in a model olfactory organ: the *Drosophila* maxillary palp. J Neurosci 19:4520-4532.

de Bruyne M, Foster K, Carlson JR (2001) Odor coding in the *Drosophila* antenna. Neuron 30:537-552.

Debelle JS, Heisenberg M (1994) Associative odor learning in *Drosophila* abolished by chemical ablation of mushroom bodies. Science 263:692-695.

Dubnau J, Grady L, Kitamoto T, Tully T (2001) Disruption of neurotransmission in *Drosophila* mushroom body blocks retrieval but not acquisition of memory. Nature 411:476-480.

Dudai Y, Jan YN, Byers D, Quinn WG, Benzer S (1976) dunce, a mutant of *Drosophila* deficient in learning. Proc Natl Acad Sci U S A 73:1684-1688.

Dudai Y, Corfas G, Hazvi S (1988) What is the possible contribution of Ca2+-stimulated adenylate cyclase to acquisition, consolidation and retention of an associative olfactory memory in *Drosophila*. J Comp Physiol A 162:101-109.

Dujardin F. Memoire sur le systeme nerveux des insects. Ann Sci Nat Zool. 1850;14:195–206.

Dunipace L, Meister S, McNealy C, Amrein H (2001) Spatially restricted expression of candidate taste receptors in the *Drosophila* gustatory system. Curr Biol 11:822-835.

Eichler K, Li F, Litwin-Kumar A, Park Y, Andrade I, Schneider-Mizell CM, Saumweber T, Huser A, Eschbach C, Gerber B, Fetter RD, Truman JW, Priebe CE, Abbott LF, Thum AS, Zlatic M, Cardona A (2017) The complete connectome of a learning and memory centre in an insect brain. Nature 548:175-182.

Felsenberg J, Jacob PF, Walker T, Barnstedt O, Edmondson-Stait AJ, Pleijzier MW, Otto N, Schlegel P, Sharifi N, Perisse E, Smith CS, Lauritzen JS, Costa M, Jefferis G, Bock DD, Waddell S (2018) Integration of parallel opposing memories underlies memory extinction. Cell 175:709-722 e715.

Fishilevich E, Domingos AI, Asahina K, Naef F, Vosshall LB, Louis M (2005) Chemotaxis behavior mediated by single larval olfactory neurons in *Drosophila*. Curr Biol 15:2086-2096.

Fishilevich E, Vosshall LB (2005) Genetic and functional subdivision of the *Drosophila* antennal lobe. Curr Biol 15:1548-1553.

Folkers E, Waddell S, Quinn WG (2006) The *Drosophila radish* gene encodes a protein required for anesthesia-resistant memory. Proc Natl Acad Sci U S A 103:17496-17500.

Gao Q, Chess A (1999) Identification of candidate *Drosophil*a olfactory receptors from genomic DNA sequence. Genomics 60:31-39.

Gao Q, Yuan B, Chess A (2000) Convergent projections of *Drosophila* olfactory neurons to specific glomeruli in the antennal lobe. Nat Neurosci 3:780-785.

Gendre N, Luer K, Friche S, Grillenzoni N, Ramaekers A, Technau GM, Stocker RF (2004) Integration of complex larval chemosensory organs into the adult nervous system of *Drosophila*. Development 131:83-92.

Gerber B, Scherer S, Neuser K, Michels B, Hendel T, Stocker RF, Heisenberg M (2004) Visual learning in individually assayed *Drosophila* larvae. J Exp Biol 207:179-188.

Gerber B, Hendel T (2006) Outcome expectations drive learned behaviour in larval *Drosophila*. Proc Biol Sci 273:2965-2968.

Gerber B, Stocker RF (2007) The *Drosophila* larva as a model for studying chemosensation and chemosensory learning: A review. Chemical Senses 32:65-89.

Gerber B, Stocker RF, Tanimura T, Thum AS (2009) Smelling, tasting, learning: *Drosophila* as a study case. Results Probl Cell Differ 47:139-185.

Gervasi N, Tchenio P, Preat T (2010) PKA dynamics in a *Drosophila* learning center: coincidence detection by rutabaga adenylyl cyclase and spatial regulation by dunce phosphodiesterase. Neuron 65:516-529.

Hamid R, Hajirnis N, Kushwaha S, Saleem S, Kumar V, Mishra RK (2019) *Drosophila* Choline transporter non-canonically regulates pupal eclosion and NMJ integrity through a neuronal subset of mushroom body. Dev Biol 446:80-93.

Heimbeck G, Bugnon V, Gendre N, Haberlin C, Stocker RF (1999) Smell and taste perception in *Drosophila melanogaster* larva: toxin expression studies in chemosensory neurons. J Neurosci 19:6599-6609.

Heimbeck G, Bugnon V, Gendre N, Keller A, Stocker RF (2001) A central neural circuit for experience-independent olfactory and courtship behavior in *Drosophila melanogaster*. Proc Natl Acad Sci U S A 98:15336-15341.

Heisenberg M (1980) Mutants of brain structure and function: what is the significance of the mushroom bodies for behavior? Basic Life Sci 16:373-390.

Heisenberg M, Borst A, Wagner S, Byers D (1985) *Drosophila* mushroom body mutants are deficient in olfactory learning. J Neurogenet 2:1-30.

Heisenberg M (1998) What do the mushroom bodies do for the insect brain? an introduction. Learn Mem 5:1-10.

Heisenberg M (2003) Mushroom body memoir: from maps to models. Nat Rev Neurosci 4:266-275.

Hige T, Aso Y, Modi MN, Rubin GM, Turner GC (2015) Heterosynaptic plasticity underlies aversive olfactory learning in Drosophila. Neuron 88:985–998.

Hildebrand JG, Shepherd GM (1997) Mechanisms of olfactory discrimination: converging evidence for common principles across phyla. Annu Rev Neurosci 20:595-631.

Hiroi M, Marion-Poll F, Tanimura T (2002) Differentiated response to sugars among labellar chemosensilla in *Drosophila*. Zoolog Sci 19:1009-1018.

Hiroi M, Meunier N, Marion-Poll F, Tanimura T (2004) Two antagonistic gustatory receptor neurons responding to sweet-salty and bitter taste in *Drosophila*. J Neurobiol 61:333-342.

Honda T, Lee CY, Honjo K, Furukubo-Tokunaga K (2016) Artificial induction of associative olfactory memory by optogenetic and thermogenetic activation of olfactory sensory neurons and octopaminergic neurons in *Drosophila* larvae. Front Behav Neurosci 10:137.

Honegger KS, Campbell RAA, Turner GC (2011) Cellular-resolution population imaging reveals robust sparse coding in the *Drosophila* mushroom body. Journal of Neuroscience 31:11772-11785.

Honjo K, Furukubo-Tokunaga K (2005) Induction of cAMP response element-binding protein-dependent medium-term memory by appetitive gustatory reinforcement in *Drosophila* larvae. J Neurosci 25:7905-7913.

Honjo K, Furukubo-Tokunaga K (2009) Distinctive neuronal networks and biochemical pathways for appetitive and aversive memory in *Drosophila* larvae. J Neurosci 29:852-862.

Huckesfeld S, Schoofs A, Schlegel P, Miroschnikow A, Pankratz MJ (2015) Localization of motor neurons and central pattern generators for motor patterns underlying feeding behavior in *Drosophila* larvae. Plos One 10.

Ichinose T, Aso Y, Yamagata N, Abe A, Rubin GM, Tanimoto H (2015) Reward signal in a recurrent circuit drives appetitive long-term memory formation. Elife 4:e10719.

Ito K, Hotta Y (1992) Proliferation pattern of postembryonic neuroblasts in the brain of *Drosophila melanogaster*. Dev Biol 149:134-148.

Ito K, Awano W, Suzuki K, Hiromi Y, Yamamoto D (1997) The *Drosophila* mushroom body is a quadruple structure of clonal units each of which contains a virtually identical set of neurones and glial cells. Development 124:761-771.

Jefferis GS, Potter CJ, Chan AM, Marin EC, Rohlfing T, Maurer CR, Jr., Luo L (2007) Comprehensive maps of *Drosophila* higher olfactory centers: spatially segregated fruit and pheromone representation. Cell 128:1187-1203.

Johard HA, Enell LE, Gustafsson E, Trifilieff P, Veenstra JA, Nassel DR (2008) Intrinsic neurons of *Drosophila* mushroom bodies express short neuropeptide F: relations to extrinsic neurons expressing different neurotransmitters. J Comp Neurol 507:1479-1496.

Keene AC, Krashes MJ, Leung B, Bernard JA, Waddell S (2006) *Drosophila* dorsal paired medial neurons provide a general mechanism for memory consolidation. Curr Biol 16:1524-1530.

Khurana S, Abu Baker MB, Siddiqi O (2009) Odour avoidance learning in the larva of *Drosophila melanogaster*. J Biosci 34:621-631.

Kim YC, Lee HG, Seong CS, Han KA (2003) Expression of a D1 dopamine receptor dDA1/DmDOP1 in the central nervous system of *Drosophila melanogaster*. Gene Expr Patterns 3:237-245.

Klapoetke NC, Murata Y, Kim SS, Pulver SR, Birdsey-Benson A, Cho YK, Morimoto TK, Chuong AS, Carpenter EJ, Tian Z, Wang J, Xie Y, Yan Z, Zhang Y, Chow BY, Surek B, Melkonian M, Jayaraman V, Constantine-Paton M, Wong GK, Boyden ES (2014) Independent optical excitation of distinct neural populations. Nat Methods 11:338-346.

Knapek S, Kahsai L, Winther AM, Tanimoto H, Nassel DR (2013) Short neuropeptide F acts as a functional neuromodulator for olfactory memory in Kenyon cells of *Drosophila* mushroom bodies. J Neurosci 33:5340-5345.

Kraliz D, Singh S (1997) Selective blockade of the delayed rectifier potassium current by tacrine in *Drosophila*. J Neurobiol 32:1-10.

Krashes MJ, Keene AC, Leung B, Armstrong JD, Waddell S (2007) Sequential use of mushroom body neuron subsets during *Drosophila* odor memory processing. Neuron 53:103-115.

Krashes MJ, Waddell S (2008) Rapid consolidation to a radish and protein synthesis-dependent long-term memory after single-session appetitive olfactory conditioning in *Drosophila*. J Neurosci 28:3103-3113.

Krashes MJ, DasGupta S, Vreede A, White B, Armstrong JD, Waddell S (2009) A neural circuit mechanism integrating motivational state with memory expression in *Drosophila*. Cell 139:416-427.

Kreher SA, Kwon JY, Carlson JR (2005) The molecular basis of odor coding in the *Drosophila* larva. Neuron 46:445-456.

Kwon JY, Dahanukar A, Weiss LA, Carlson JR (2011) Molecular and cellular organization of the taste system in the *Drosophila* larva. J Neurosci 31:15300-15309.

Larsson MC, Domingos AI, Jones WD, Chiappe ME, Amrein H, Vosshall LB (2004) Or83b encodes a broadly expressed odorant receptor essential for *Drosophila* olfaction. Neuron 43:703-714.

Lee KS, Kwon OY, Lee JH, Kwon K, Min KJ, Jung SA, Kim AK, You KH, Tatar M, Yu K (2008) *Drosophila* short neuropeptide F signalling regulates growth by ERK-mediated insulin signalling. Nat Cell Biol 10:468-475.

Lee T, Lee A, Luo L (1999) Development of the *Drosophila* mushroom bodies: sequential generation of three distinct types of neurons from a neuroblast. Development 126:4065-4076.

Levin LR, Han PL, Hwang PM, Feinstein PG, Davis RL, Reed RR (1992) The *Drosophila* learning and memory gene *rutabaga* encodes a Ca2+/Calmodulin-responsive adenylyl cyclase. Cell 68:479-489.

Lin AC, Bygrave AM, de Calignon A, Lee T, Miesenbock G (2014) Sparse, decorrelated odor coding in the mushroom body enhances learned odor discrimination. Nat Neurosci 17:559-568.

Liu C, Placais PY, Yamagata N, Pfeiffer BD, Aso Y, Friedrich AB, Siwanowicz I, Rubin GM, Preat T, Tanimoto H (2012) A subset of dopamine neurons signals reward for odour memory in *Drosophila*. Nature 488:512-516.

Livingstone MS, Sziber PP, Quinn WG (1984) Loss of calcium/calmodulin responsiveness in adenylate cyclase of *rutabaga*, a *Drosophila* learning mutant. Cell 37:205-215.

Louis T, Stahl A, Boto T, Tomchik SM (2018) Cyclic AMP-dependent plasticity underlies rapid changes in odor coding associated with reward learning. P Natl Acad Sci USA 115:E448-E457.

Ludke A, Raiser G, Nehrkorn J, Herz AVM, Galizia CG, Szyszka P (2018) Calcium in Kenyon cell somata as a substrate for an olfactory sensory memory in *Drosophila*. Front Cell Neurosci 12.

Mao Z, Davis RL (2009) Eight different types of dopaminergic neurons innervate the *Drosophila* mushroom body neuropil: anatomical and physiological heterogeneity. Front Neural Circuits 3:5.

Marin EC, Jefferis GSXE, Komiyama T, Zhu HT, Luo LQ (2002) Representation of the glomerular olfactory map in the *Drosophila* brain. Cell 109:243-255.

Marin EC, Watts RJ, Tanaka NK, Ito K, Luo L (2005) Developmentally programmed remodeling of the *Drosophila* olfactory circuit. Development 132:725-737.

Masuda-Nakagawa LM, Tanaka NK, O'Kane CJ (2005) Stereotypic and random patterns of connectivity in the larval mushroom body calyx of *Drosophila*. Proc Natl Acad Sci U S A 102:19027-19032.

Masuda-Nakagawa LM, Gendre N, O'Kane CJ, Stocker RF (2009) Localized olfactory representation in mushroom bodies of *Drosophila* larvae. Proc Natl Acad Sci U S A 106:10314-10319.

Maximilian Pfeuffer (2017) Analysis of odour detection in *Drosophila* larvae with optogenetically activated mushroom body Kenyon cells. Bachelor thesis.

McGaugh JL (2000) Memory--a century of consolidation. Science 287:248-251.

Melcher C, Pankratz MJ (2005) Candidate gustatory Interneurons modulating feeding behavior in the *Drosophila* brain. Plos Biology 3:1618-1629.

Meunier N, Ferveur JF, Marion-Poll F (2000) Sex-specific non-pheromonal taste receptors in *Drosophila*. Curr Biol 10:1583-1586.

Meunier N, Marion-Poll F, Rospars JP, Tanimura T (2003) Peripheral coding of bitter taste in *Drosophila*. J Neurobiol 56:139-152.

Miroschnikow A, Schlegel P, Schoofs A, Hueckesfeld S, Li F, Schneider-Mizell CM, Fetter RD, Truman JW, Cardona A, Pankratz MJ (2018) Convergence of monosynaptic and polysynaptic sensory paths onto common motor outputs in a *Drosophila* feeding connectome. Elife 7.

Monte P, Woodard C, Ayer R, Lilly M, Sun H, Carlson J (1989) Characterization of the larval olfactory response in *Drosophila* and its genetic basis. Behav Genet 19:267-283.

Murthy M, Fiete I, Laurent G (2008) Testing odor response stereotypy in the *Drosophila* mushroom body. Neuron 59:1009-1023.

Musselman LP, Fink JL, Narzinski K, Ramachandran PV, Hathiramani SS, Cagan RL, Baranski TJ (2011) A high-sugar diet produces obesity and insulin resistance in wild-type *Drosophila*. Dis Model Mech 4:842-849.

Nassel DR, Elekes K (1992) Aminergic neurons in the brain of blowflies and *Drosophila*: dopamine- and tyrosine hydroxylase-immunoreactive neurons and their relationship with putative histaminergic neurons. Cell Tissue Res 267:147-167.

Nassel DR, Enell LE, Santos JG, Wegener C, Johard HA (2008) A large population of diverse neurons in the *Drosophila* central nervous system expresses short neuropeptide F, suggesting multiple distributed peptide functions. BMC Neurosci 9:90.

Nayak SV, Singh RN (1983) Sensilla on the tarsal segments and mouthparts of adult *Drosophila melanogaster meigen* (*Diptera*, *Drosophilidae*). Int J Insect Morphol 12:273-291.

Nayak SV, Singh RN (1985) Primary sensory projections from the labella to the brain of *Drosophila melanogaster meigen* (*Diptera*, *Drosophilidae*). Int J Insect Morphol 14:115-129.

Ofstad TA, Zuker CS, Reiser MB (2011) Visual place learning in *Drosophila melanogaster*. Nature 474:204-207.

Olsen SR, Bhandawat V, Wilson RI (2007) Excitatory interactions between olfactory processing channels in the *Drosophila* antennal lobe. Neuron 54:89-103.

Pascual A, Preat T (2001) Localization of long-term memory within the *Drosophila* mushroom body. Science 294:1115-1117.

Pauls D, Selcho M, Gendre N, Stocker RF, Thum AS (2010) *Drosophila* larvae establish appetitive olfactory memories via mushroom body neurons of embryonic origin. J Neurosci 30:10655-10666.

Pauls D, von Essen A, Lyutova R, van Giesen L, Rosner R, Wegener C, Sprecher SG (2015) Potency of transgenic effectors for neurogenetic manipulation in *Drosophila* larvae. Genetics 199:25-37.

Pavlov IP, Anrep GV (1927) Conditioned reflexes; an investigation of the physiological activity of the cerebral cortex. London: Oxford University Press: Humphrey Milford.

Perkins LA, Holderbaum L, Tao R, Hu Y, Sopko R, McCall K, Yang-Zhou D, Flockhart I, Binari R, Shim HS, Miller A, Housden A, Foos M, Randkelv S, Kelley C, Namgyal P, Villalta C, Liu LP, Jiang X, Huan-Huan Q, Wang X, Fujiyama A, Toyoda A, Ayers K, Blum A, Czech B, Neumuller R, Yan D, Cavallaro A, Hibbard K, Hall D, Cooley L, Hannon GJ, Lehmann R, Parks A, Mohr SE, Ueda R, Kondo S, Ni JQ, Perrimon N (2015) The transgenic RNAi project at Harvard Medical School: resources and validation. Genetics 201:843-852.

Putz G, Heisenberg M (2002) Memories in *Drosophila* heat-box learning. Learn Mem 9:349-359.

Python F, Stocker RF (2002) Adult-like complexity of the larval antennal lobe of *D. melanogaster* despite markedly low numbers of odorant receptor neurons. J Comp Neurol 445:374-387.

Quinn WG, Harris WA, Benzer S (1974) Conditioned behavior in *Drosophila melanogaster*. Proc Natl Acad Sci U S A 71:708-712.

Quinn WG, Dudai Y (1976) Memory phases in *Drosophila*. Nature 262:576-577.

Quinn WG, Sziber PP, Booker R (1979) The *Drosophila* memory mutant amnesiac. Nature 277:212-214.

Ramaekers A, Magnenat E, Marin EC, Gendre N, Jefferis GS, Luo L, Stocker RF (2005) Glomerular maps without cellular redundancy at successive levels of the *Drosophila* larval olfactory circuit. Curr Biol 15:982-992.

Radostina Lyutova (2015) Manipulation of sNPF signaling reveals pleiotropic functions in *Drosophila* larvae. Master thesis.

Risse B, Thomas S, Otto N, Lopmeier T, Valkov D, Jiang X, Klambt C (2013) FIM, a novel FTIR-based imaging method for high throughput locomotion analysis. PLoS One 8:e53963.

Robertson HM, Warr CG, Carlson JR (2003) Molecular evolution of the insect chemoreceptor gene superfamily in *Drosophila melanogaster*. Proc Natl Acad Sci U S A 100 Suppl 2:14537-14542.

Rodrigues V (1980) Olfactory behavior of *Drosophila melanogaster*. Basic Life Sci 16:361-371.

Rohwedder A, Pfitzenmaier JE, Ramsperger N, Apostolopoulou AA, Widmann A, Thum AS (2012) Nutritional value-dependent and nutritional value-independent effects on *Drosophila melanogaster* larval behavior. Chem Senses 37:711-721.

Rohwedder A, Selcho M, Chassot B, Thum AS (2015) Neuropeptide F neurons modulate sugar reward during associative olfactory learning of *Drosophila* larvae. J Comp Neurol 523:2637-2664.

Rohwedder A, Wenz NL, Stehle B, Huser A, Yamagata N, Zlatic M, Truman JW, Tanimoto H, Saumweber T, Gerber B, Thum AS (2016) Four individually identified paired dopamine neurons signal reward in larval *Drosophila*. Curr Biol 26:661-669.

Rosenzweig M, Brennan KM, Tayler TD, Phelps PO, Patapoutian A, Garrity PA (2005) The *Drosophila* ortholog of vertebrate TRPA1 regulates thermotaxis. Genes Dev 19:419-424.

Saumweber T, Rohwedder A, Schleyer M, Eichler K, Chen YC, Aso Y, Cardona A, Eschbach C, Kobler O, Voigt A, Durairaja A, Mancini N, Zlatic M, Truman JW, Thum AS, Gerber B (2018) Functional architecture of reward learning in mushroom body extrinsic neurons of larval *Drosophila*. Nat Commun 9:1104.

Sawin-McCormack EP, Sokolowski MB, Campos AR (1995) Characterization and genetic analysis of *Drosophila melanogaster* photobehavior during larval development. J Neurogenet 10:119-135.

Scherer S, Stocker RF, Gerber B (2003) Olfactory learning in individually assayed *Drosophila* larvae. Learn Mem 10:217-225.

Schleyer M, Saumweber T, Nahrendorf W, Fischer B, von Alpen D, Pauls D, Thum A, Gerber B (2011) A behavior-based circuit model of how outcome expectations organize learned behavior in larval *Drosophila*. Learn Mem 18:639-653.

Schleyer M, Miura D, Tanimura T, Gerber B (2015) Learning the specific quality of taste reinforcement in larval *Drosophila*. Elife 4.

Schoofs A, Niederegger S, van Ooyen A, Heinzel HG, Spiess R (2010) The brain can eat: establishing the existence of a central pattern generator for feeding in third instar larvae of *Drosophila virilis* and *Drosophila melanogaster*. J Insect Physiol 56:695-705.

Schroll C, Riemensperger T, Bucher D, Ehmer J, Völler T, Erbguth K, Gerber B, Hendel T, Nagel G, Buchner E, Fiala A (2006) Light-induced activation of distinct modulatory neurons triggers appetitive or aversive learning in *Drosophila* larvae. Curr Biol 16(17):1741-7.

Scott K, Brady R, Jr., Cravchik A, Morozov P, Rzhetsky A, Zuker C, Axel R (2001) A chemosensory gene family encoding candidate gustatory and olfactory receptors in *Drosophila*. Cell 104:661-673.

Selcho M, Pauls D, Han KA, Stocker RF, Thum AS (2009) The role of dopamine in *Drosophila* larval classical olfactory conditioning. PLoS One 4:e5897.

Selcho M, Pauls D, Huser A, Stocker RF, Thum AS (2014) Characterization of the octopaminergic and tyraminergic neurons in the central brain of *Drosophila* larvae. J Comp Neurol 522:3485-3500.

Selcho M, Wegener C (2015) Immunofluorescence and genetic fluorescent labeling techniques in the *Drosophila* nervous system. Immunocytochem. Relat. Tech. 101, 39–62.

Shanbhag SR, Muller B, Steinbrecht RA (1999) Atlas of olfactory organs of *Drosophila melanogaster* - 1. Types, external organization, innervation and distribution of olfactory sensilla. Int J Insect Morphol 28:377-397.

Shanbhag SR, Park SK, Pikielny CW, Steinbrecht RA (2001) Gustatory organs of *Drosophila melanogaster*: fine structure and expression of the putative odorant-binding protein PBPRP2. Cell Tissue Res 304:423-437.

Silbering AF, Galizia CG (2007) Processing of odor mixtures in the *Drosophila* antennal lobe reveals both global inhibition and glomerulus-specific interactions. Journal of Neuroscience 27:11966-11977.

Singh RN, Singh K (1984) Fine-structure of the sensory organs of *Drosophila melanogaster meigen* larva (*Diptera*, *Drosophilidae*). Int J Insect Morphol 13:255-273.

Skinner BF (1950) Are theories of learning necessary? Psychol Rev 57:193-216.

Stocker RF, Schorderet M (1981) Cobalt filling of sensory projections from internal and external mouthparts in *Drosophila*. Cell Tissue Res 216:513-523.

Stocker RF (1994) The organization of the chemosensory system in *Drosophila melanogaster*: a review. Cell Tissue Res 275:3-26.

Stocker RF (2001) *Drosophila* as a focus in olfactory research: mapping of olfactory sensilla by fine structure, odor specificity, odorant receptor expression, and central connectivity. Microsc Res Tech 55:284-296.

Tanaka NK, Awasaki T, Shimada T, Ito K (2004) Integration of chemosensory pathways in the *Drosophila* second-order olfactory centers. Current Biology 14:449-457.

Tanaka NK, Tanimoto H, Ito K (2008) Neuronal assemblies of the *Drosophila* mushroom body. J Comp Neurol 508:711-755.

Technau G, Heisenberg M (1982) Neural reorganization during metamorphosis of the corpora pedunculata in *Drosophila melanogaster*. Nature 295:405-407.

Technau GM (1984) Fiber number in the mushroom bodies of adult *Drosophila melanogaster* depends on age, sex and experience. J Neurogenet 1:113-126.

Thorndike E (1898) Some experiments on animal intelligence. Science 7:818-824.

Thorne N, Chromey C, Bray S, Amrein H (2004) Taste perception and coding in *Drosophila*. Curr Biol 14:1065-1079.

Thum AS, Gerber B (2018) Connectomics and function of a memory network: the mushroom body of larval *Drosophila*. Curr Opin Neurobiol 54:146-154.

Tomchik SM, Davis RL (2009) Dynamics of learning-related cAMP signaling and stimulus integration in the *Drosophila* olfactory pathway. Neuron 64:510-521.

Tully T, Quinn WG (1985) Classical conditioning and retention in normal and mutant *Drosophila melanogaster*. J Comp Physiol A 157:263-277.

Tully T, Preat T, Boynton SC, Del Vecchio M (1994a) Genetic dissection of consolidated memory in *Drosophila*. Cell 79:35-47.

Tully T, Cambiazo V, Kruse L (1994b) Memory through metamorphosis in normal and mutant *Drosophila*. J Neurosci 14:68-74.

Ugrankar R, Theodoropoulos P, Akdemir F, Henne WM, Graff JM (2018) Circulating glucose levels inversely correlate with *Drosophila* larval feeding through insulin signaling and SLC5A11. Commun Biol 1:110.

Ullrich S, Gueta R, Nagel G (2013) Degradation of channelopsin-2 in the absence of retinal and degradation resistance in certain mutants. Biol Chem 394:271-280.

van der Goes van Naters W, Carlson JR (2007) Receptors and neurons for fly odors in *Drosophila*. Curr Biol 17:606-612.

Viswanath V, Story GM, Peier AM, Petrus MJ, Lee VM, Hwang SW, Patapoutian A, Jegla T (2003) Opposite thermosensor in fruitfly and mouse. Nature 423:822-823.

von Essen AMHJ, Pauls D, Thum AS, Sprecher SG (2011) Capacity of Visual Classical Conditioning in *Drosophila* Larvae. Behav Neurosci 125:921-929.

Vosshall LB, Amrein H, Morozov PS, Rzhetsky A, Axel R (1999) A spatial map of olfactory receptor expression in the *Drosophila* antenna. Cell 96:725-736.

Vosshall LB, Wong AM, Axel R (2000) An olfactory sensory map in the fly brain. Cell 102:147-159.

Vosshall LB, Stocker RF (2007) Molecular architecture of smell and taste in *Drosophila*. Annu Rev Neurosci 30:505-533.

Wang Z, Singhvi A, Kong P, Scott K (2004) Taste representations in the *Drosophila* brain. Cell 117:981-991.

Warrick JM, Vakil MF, Tompkins L (1999) Spectral sensitivity of wild-type and mutant *Drosophila melanogaster* larvae. J Neurogenet 13:145-156.

Widmann A, Artinger M, Biesinger L, Boepple K, Peters C, Schlechter J, Selcho M, Thum AS (2016) Genetic dissection of aversive associative olfactory learning and memory in *Drosophila* larvae. PLoS Genet 12:e1006378.

Widmann A, Eichler K, Selcho M, Thum AS, Pauls D (2018) Odor-taste learning in *Drosophila* larvae. J Insect Physiol 106:47-54.

Wilson RI, Laurent G (2005) Role of GABAergic inhibition in shaping odor-evoked spatiotemporal patterns in the *Drosophila* antennal lobe. Journal of Neuroscience 25:9069-9079.

Wolf R, Heisenberg M (1991) Basic organization of operant behavior as revealed in *Drosophila* flight orientation. J Comp Physiol A 169:699-705.

Wong AM, Wang JW, Axel R (2002) Spatial representation of the glomerular map in the *Drosophila* protocerebrum. Cell 109:229-241.

Wu CL, Shih MF, Lee PT, Chiang AS (2013) An octopamine-mushroom body circuit modulates the formation of anesthesia-resistant memory in *Drosophila*. Curr Biol 23:2346-2354.

Wustmann G, Rein K, Wolf R, Heisenberg M (1996) A new paradigm for operant conditioning of *Drosophila melanogaster*. J Comp Physiol A 179:429-436.

Yamagata N, Ichinose T, Aso Y, Placais PY, Friedrich AB, Sima RJ, Preat T, Rubin GM, Tanimoto H (2015) Distinct dopamine neurons mediate reward signals for short- and long-term memories. Proc Natl Acad Sci U S A 112:578-583.

Yao CA, Ignell R, Carlson JR (2005) Chemosensory coding by neurons in the coeloconic sensilla of the *Drosophila* antenna. J Neurosci 25:8359-8367.

Yasuyama K, Meinertzhagen IA, Schurmann FW (2003) Synaptic connections of cholinergic antennal lobe relay neurons innervating the lateral horn neuropile in the brain of *Drosophila melanogaster*. J Comp Neurol 466:299-315.

Yin JC, Wallach JS, Del Vecchio M, Wilder EL, Zhou H, Quinn WG, Tully T (1994) Induction of a dominant negative CREB transgene specifically blocks long-term memory in *Drosophila*. Cell 79:49-58.

Yusuyama K, Meinertzhagen IA, Schurmann FW (2002) Synaptic organization of the mushroom body calyx in *Drosophila melanogaste*r. J Comp Neurol 445:211-226.

Zars T, Fischer M, Schulz R, Heisenberg M (2000) Localization of a short-term memory in *Drosophila*. Science 288:672-675.

Zars T (2000) Behavioral functions of the insect mushroom bodies. Curr Opin Neurobiol 10:790-795.

Zhang S, Roman G (2013) Presynaptic inhibition of gamma lobe neurons is required for olfactory learning in *Drosophila*. Curr Biol 23:2519–2527.

Zhao X, Lenek D, Dag U, Dickson BJ, Keleman K (2018) Persistent activity in a recurrent circuit underlies courtship memory in *Drosophila*. Elife 7.

Appendix

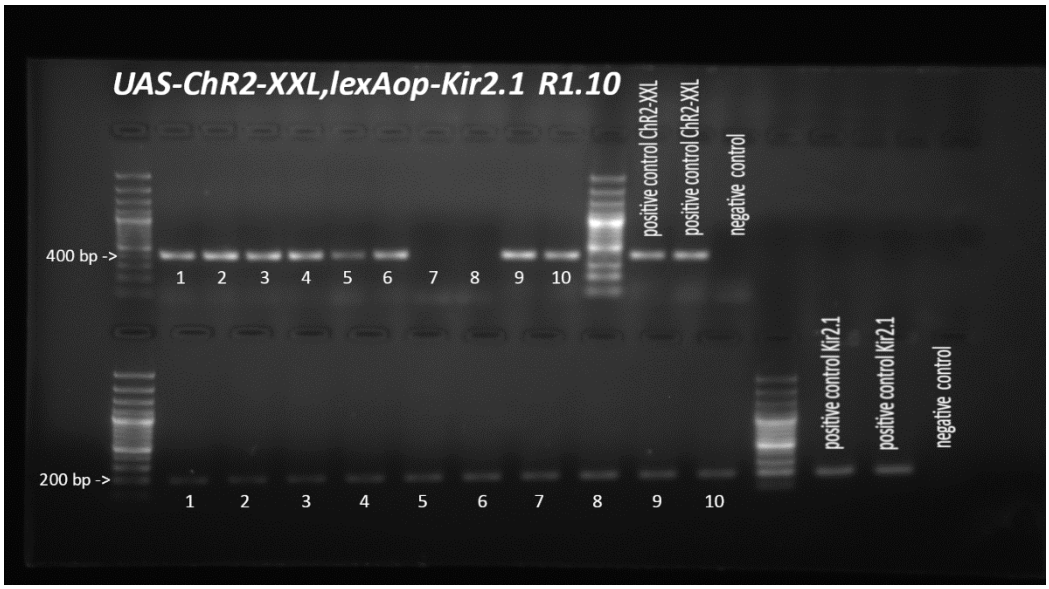

Figure S1: *PCR verification of the transgenes UAS-ChR2-XXL and lexAop-Kir2.1. In R1.10 recombinant line 80% of the flies were ChR2-XXL positive (upper 1 to 10 lanes). The presence of Kir2.1 was proven in 100% of the tested flies (lower 1 to 10 lanes).*

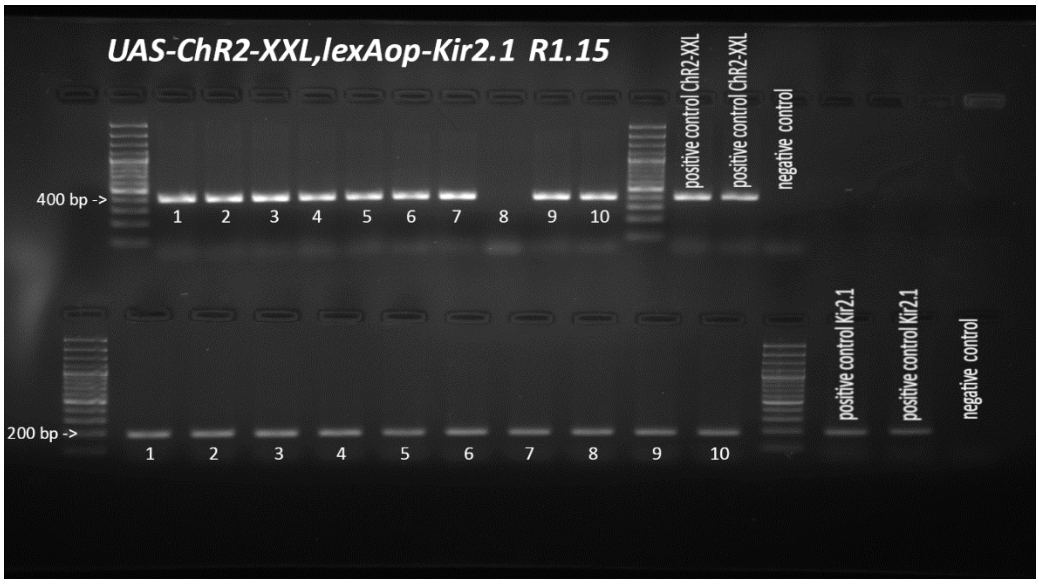

Figure S2: *PCR verification of the transgenes UAS-ChR2-XXL and lexAop-Kir2.1. In R1.15 recombinant line 90% of the flies were ChR2-XXL positive (upper 1 to 10 lanes).The presence of Kir2.1 was proven in 100% of the tested flies (lower 1 to 10 lanes).*

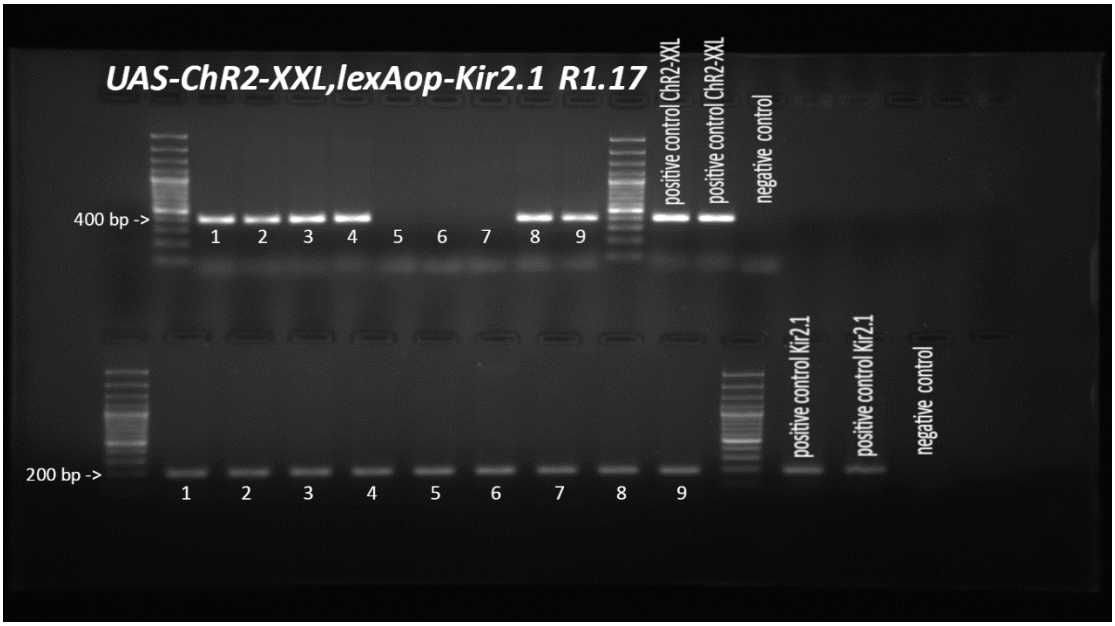

Figure S3: *PCR verification of the transgenes UAS-ChR2-XXL and lexAop-Kir2.1. In R1.10 recombinant line 70% of the flies were ChR2-XXL positive (upper 1 to 10 lanes).The presence of Kir2.1 was proven in 100% of the tested flies (lower 1 to 10 lanes).*

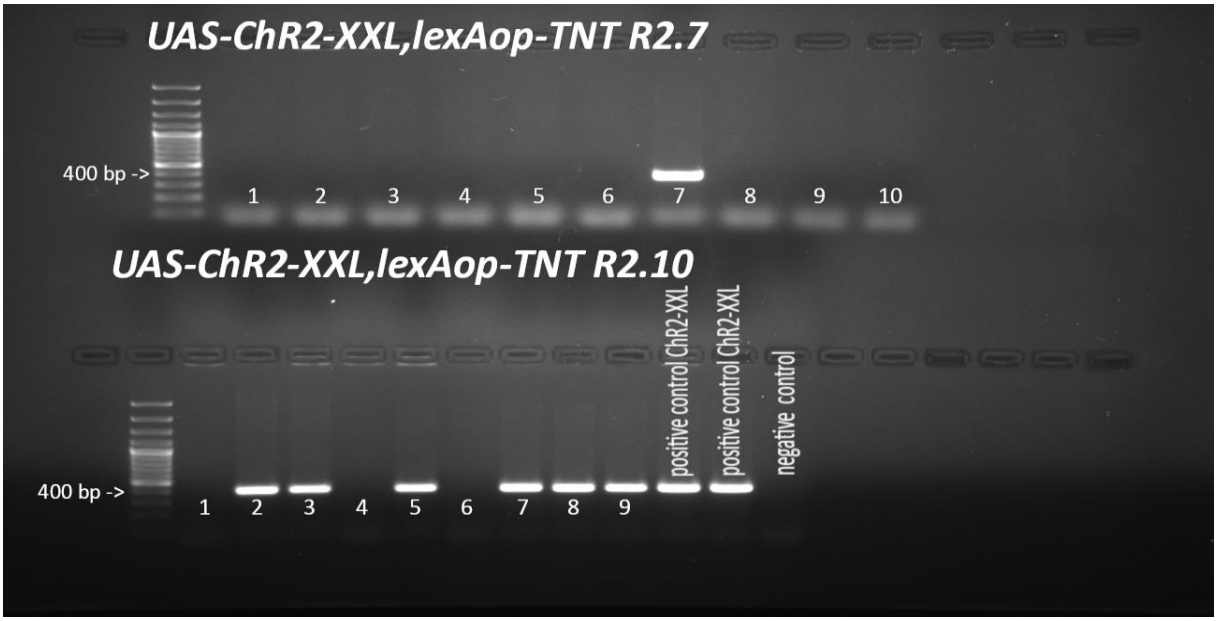

Figure S4: *PCR verification of the transgene UAS-ChR2-XXL. In the tested R2.7 recombinant line 10% of the flies were ChR2-XXL positive (upper 1 to 10 lanes). The expression of ChR2-XXL was proven in 80% of the R2.10 recombinant flies (lower 1 to 10 lanes).*

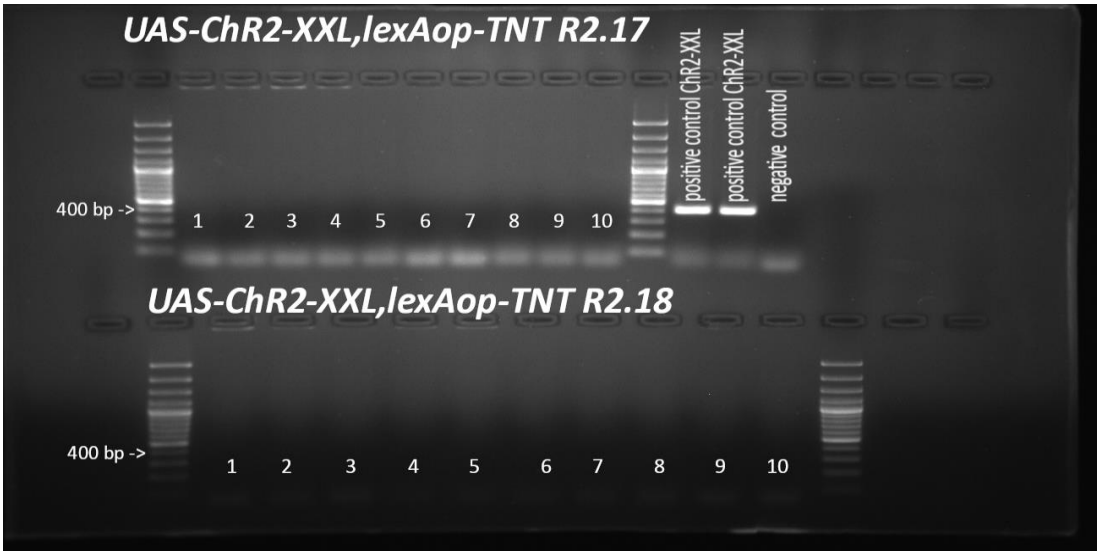

Figure S5: *PCR verification of the transgene UAS-ChR2-XXL. In the tested R2.17 recombinant line none of the flies was ChR2-XXL positive (upper 1 to 10 lanes). The expression of ChR2-XXL could not be proven in none of the R2.18 recombinant flies (lower 1 to 10 lanes).*

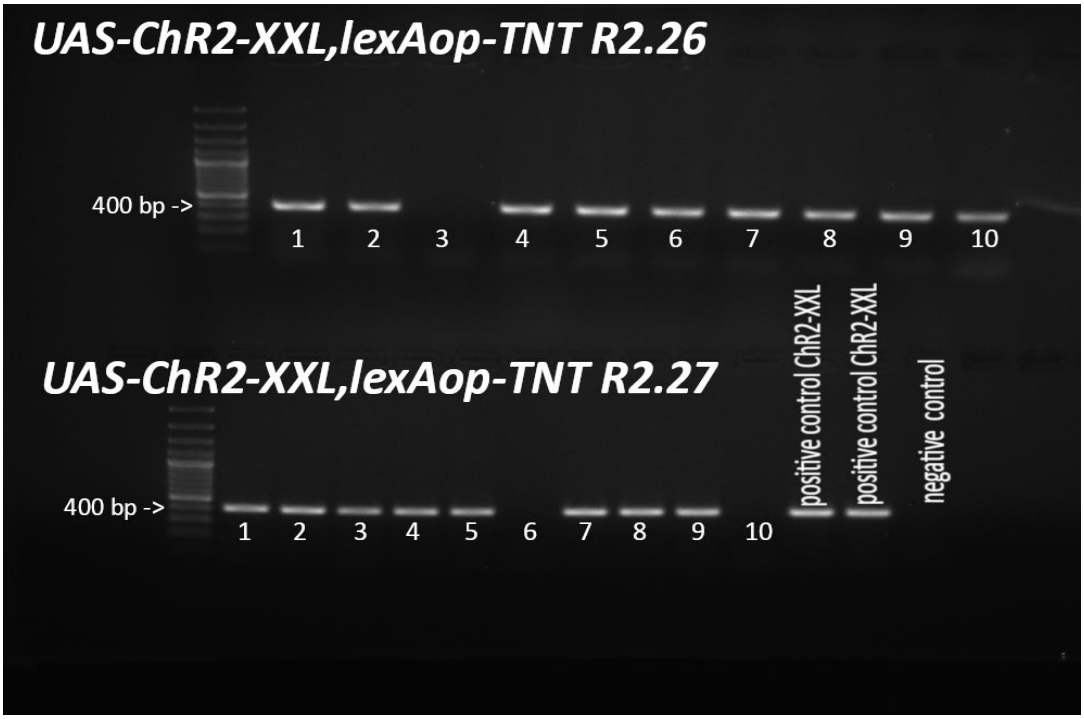

Figure S6: *PCR verification of the transgene UAS-ChR2-XXL. In the tested R2.26 recombinant line 90% of the flies were ChR2-XXL positive (upper 1 to 10 lanes). The expression of ChR2-XXL was proven in 80% of the R2.27 recombinant flies (lower 1 to 10 lanes).*

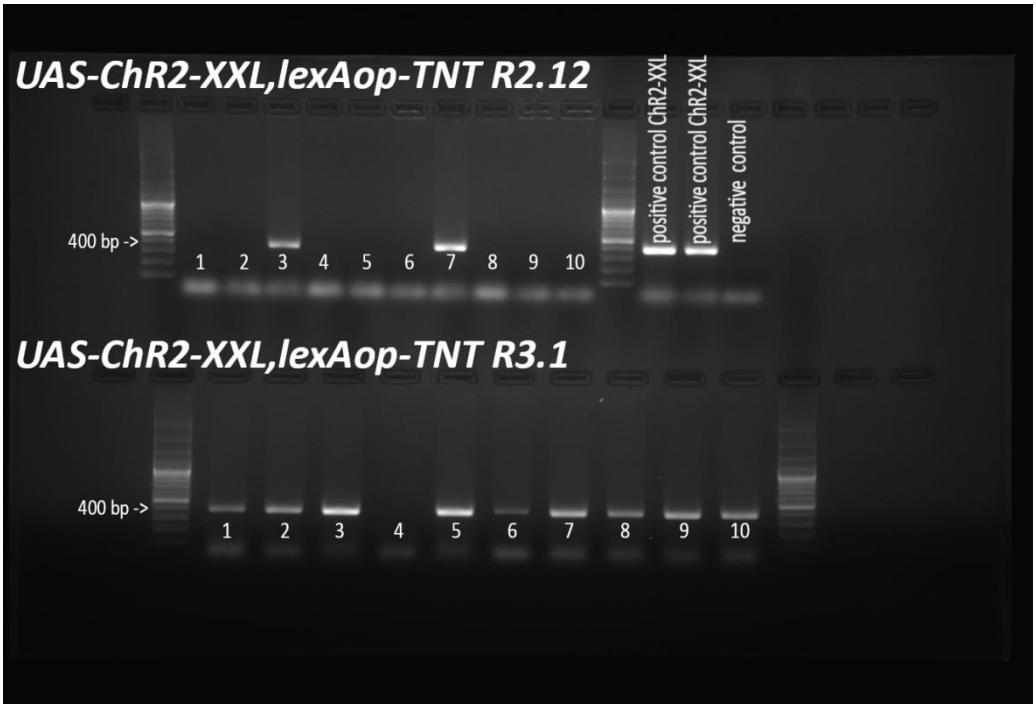

Figure S7: *PCR verification of the transgene UAS-ChR2-XXL. In the tested R2.12 recombinant line 20% of the flies were ChR2-XXL positive (upper 1 to 10 lanes). The expression of ChR2-XXL was proven in 90% of the R3.1 recombinant flies (lower 1 to 10 lanes).*

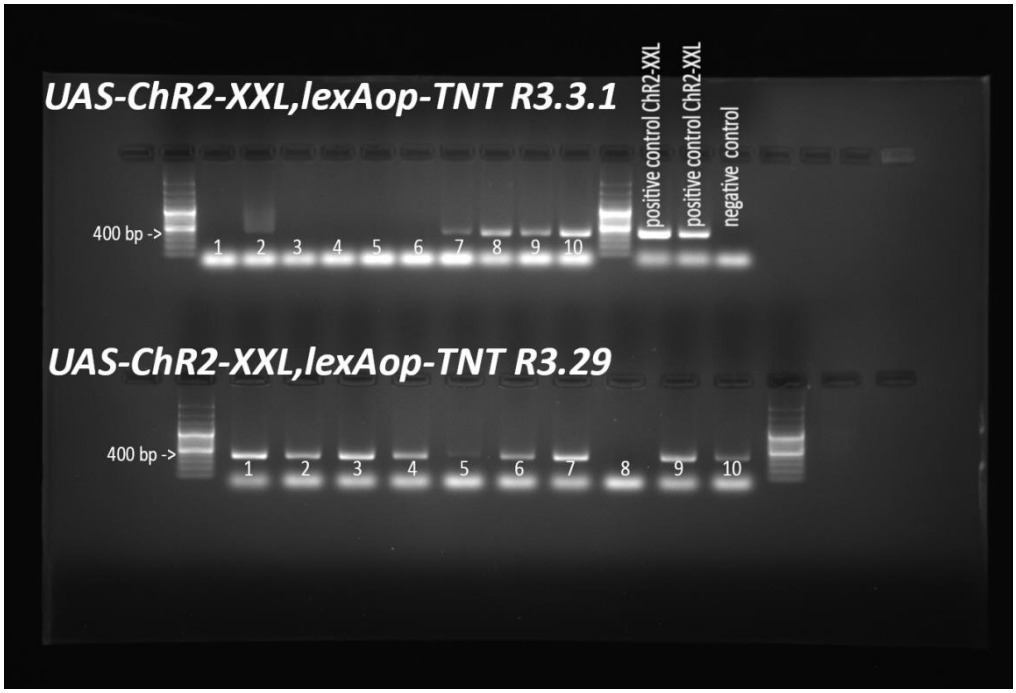

Figure S8: *PCR verification of the transgene UAS-ChR2-XXL. In the tested R3.3.1 recombinant line 50% of the flies were ChR2-XXL positive (upper 1 to 10 lanes). The expression of ChR2-XXL was proven in 90% of the R3.29 recombinant flies (lower 1 to 10 lanes).*

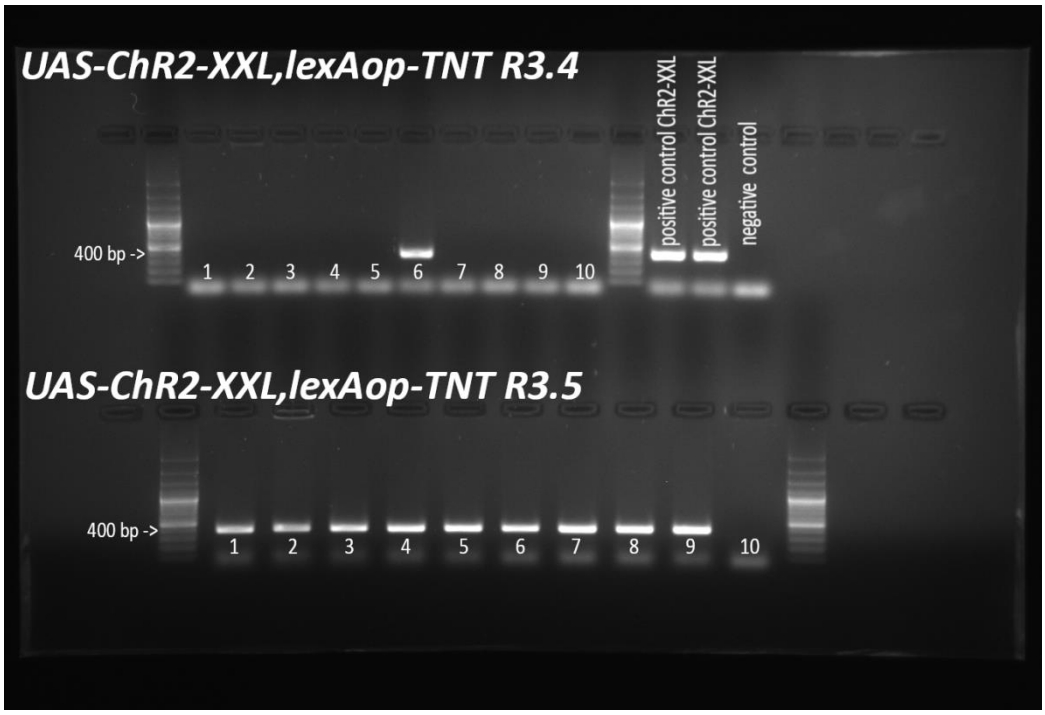

Figure S9: *PCR verification of the transgene UAS-ChR2-XXL. In the tested R3.3 recombinant line 10% of the flies were ChR2-XXL positive (upper 1 to 10 lanes). The expression of ChR2-XXL was proven in 90% of the R3.5 recombinant flies (lower 1 to 10 lanes).*

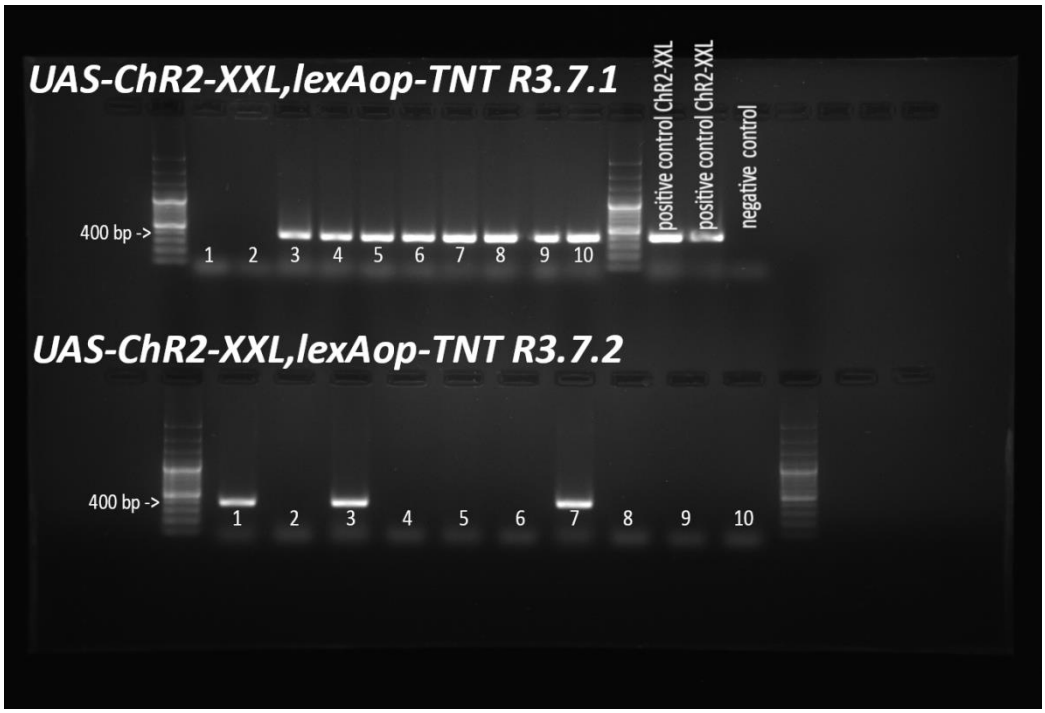

Figure S10: *PCR verification of the transgene UAS-ChR2-XXL. In the tested R3.7.1 recombinant line 80% of the flies were ChR2-XXL positive (upper 1 to 10 lanes). The expression of ChR2-XXL was proven in 30% of the R3.7.2 recombinant flies (lower 1 to 10 lanes).*

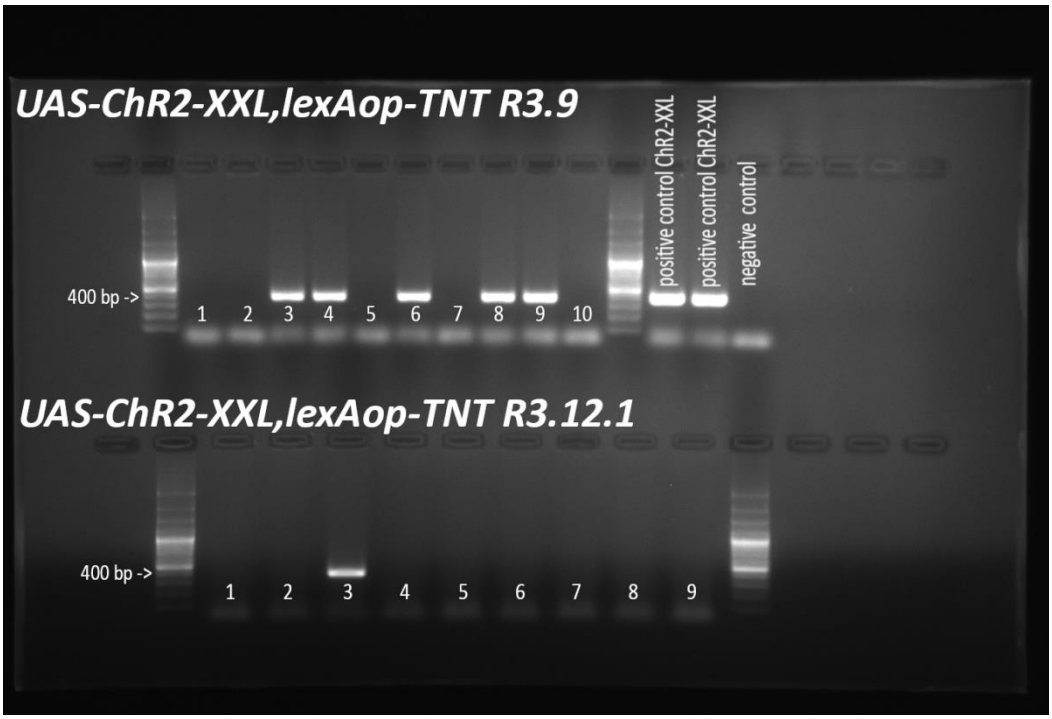

Figure S11: *PCR verification of the transgenes UAS-ChR2-XXL. In the tested R3.9 recombinant line 50% of the flies were ChR2-XXL positive (upper 1 to 10 lanes). The expression of ChR2-XXL was proven in 10% of the R3.12.1 recombinant flies (lower 1 to 10 lanes).*

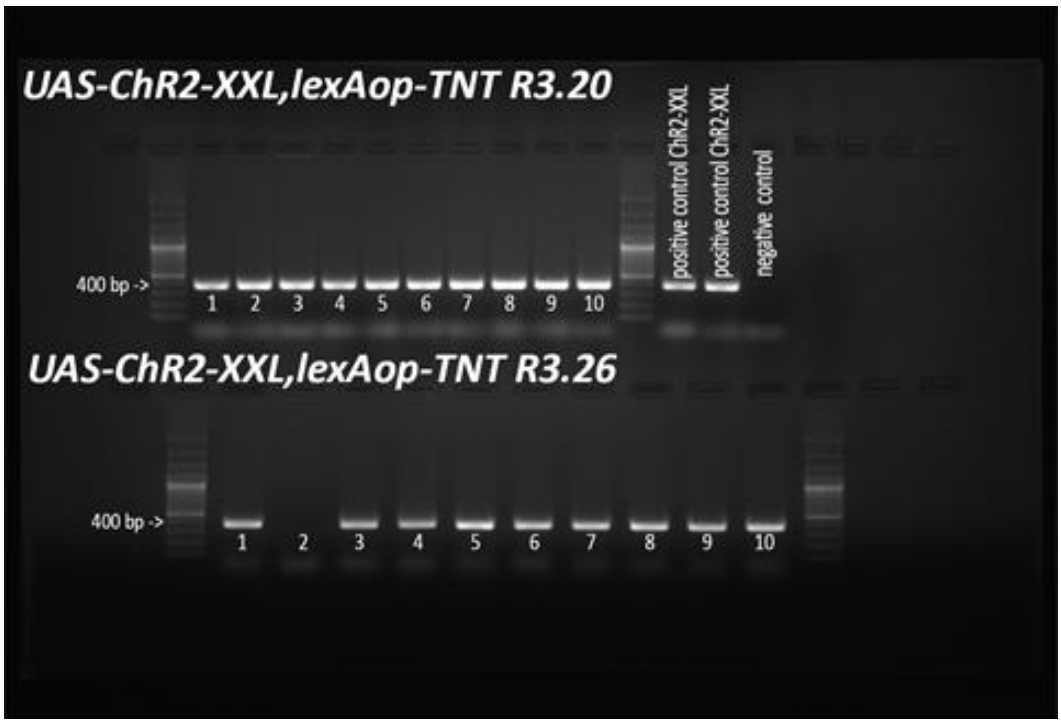

Figure S12: *PCR verification of the transgenes UAS-ChR2-XXL. In the tested R3.20 recombinant line 100% of the flies were ChR2-XXL positive (upper 1 to 10 lanes). The expression of ChR2-XXL was proven in 90% of the R3.26 recombinant flies (lower 1 to 10 lanes).*

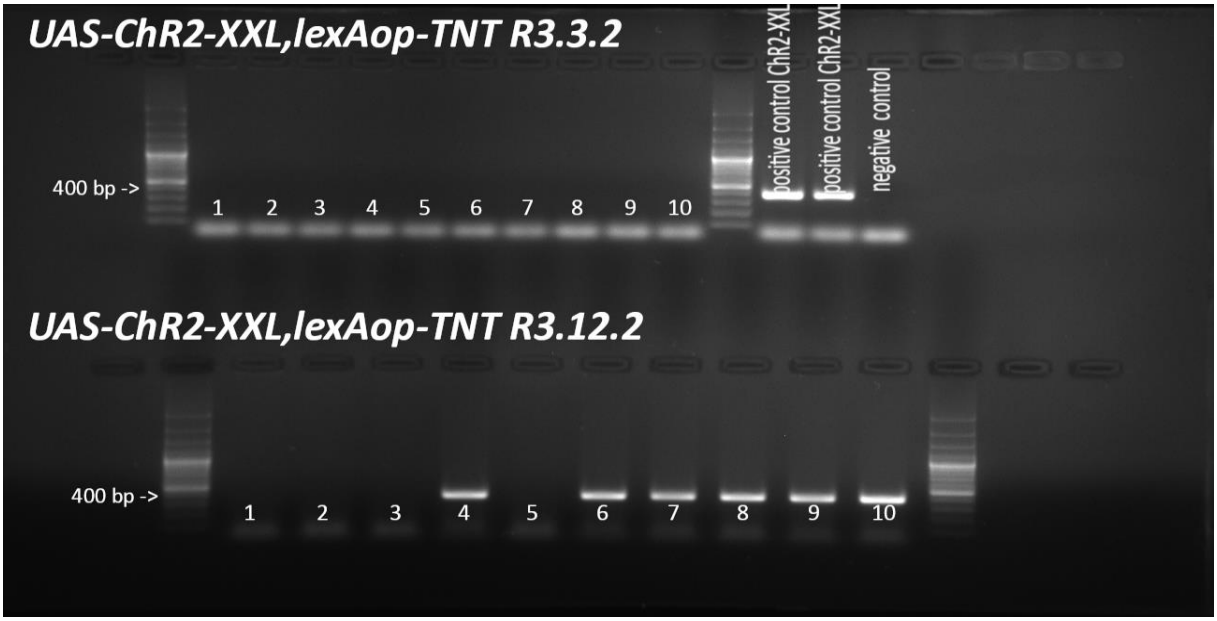

Figure S13: *PCR verification of the transgene UAS-ChR2-XXL. In the tested R3.3.2 recombinant line none of the flies was ChR2-XXL positive (upper 1 to 10 lanes). The expression of ChR2-XXL was proven in 60% of the R3.12.2 recombinant flies (lower 1 to 10 lanes).*

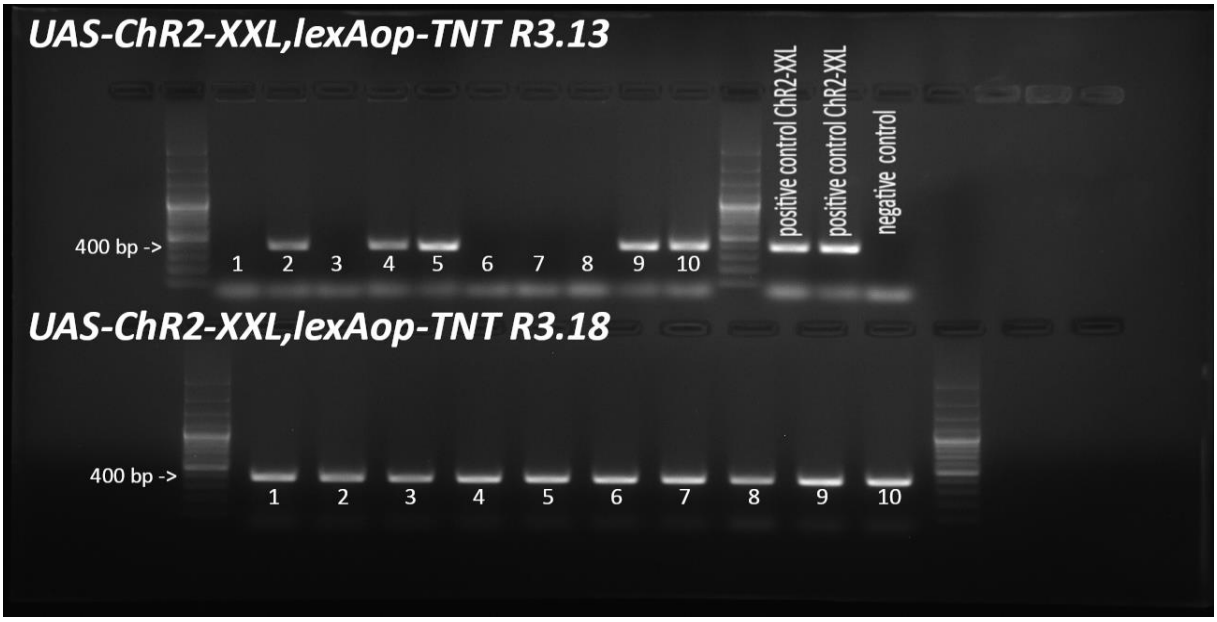

Figure S14: *PCR verification of the transgene UAS-ChR2-XXL. In the tested R3.13 recombinant line 50% of the flies were ChR2-XXL positive (upper 1 to 10 lanes). The expression of ChR2-XXL was proven in 100% of the R3.18 recombinant flies (lower 1 to 10 lanes).*

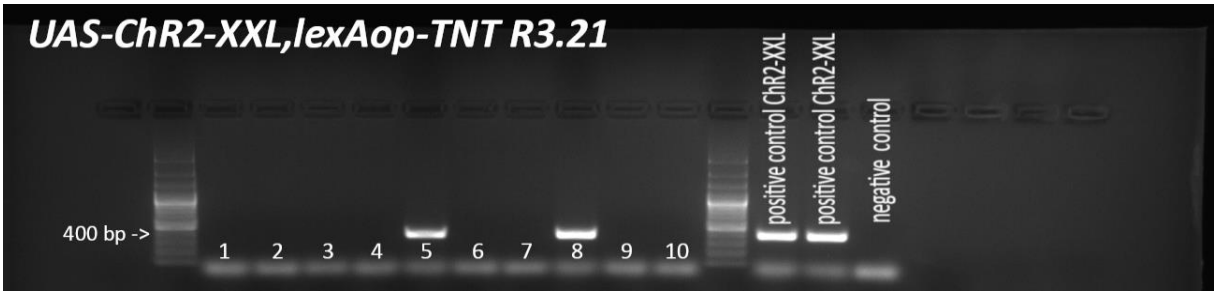

Figure S15: *PCR verification of the transgene UAS-ChR2-XXL. In the tested R3.21 recombinant line 20% of the flies were ChR2-XXL positive.*

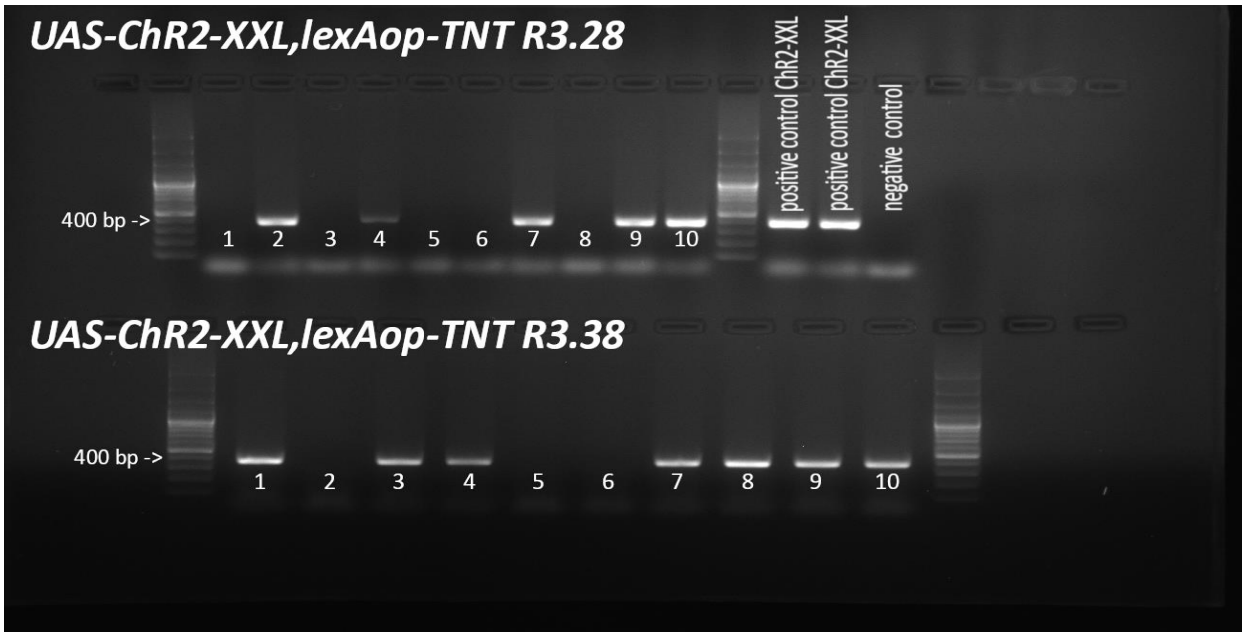

Figure S16: *PCR verification of the transgene UAS-ChR2-XXL. In the tested R3.28 recombinant line 50% of the flies were ChR2-XXL positive (upper 1 to 10 lanes). The expression of ChR2-XXL was proven in 70% of the R3.38 recombinant flies (lower 1 to 10 lanes).*

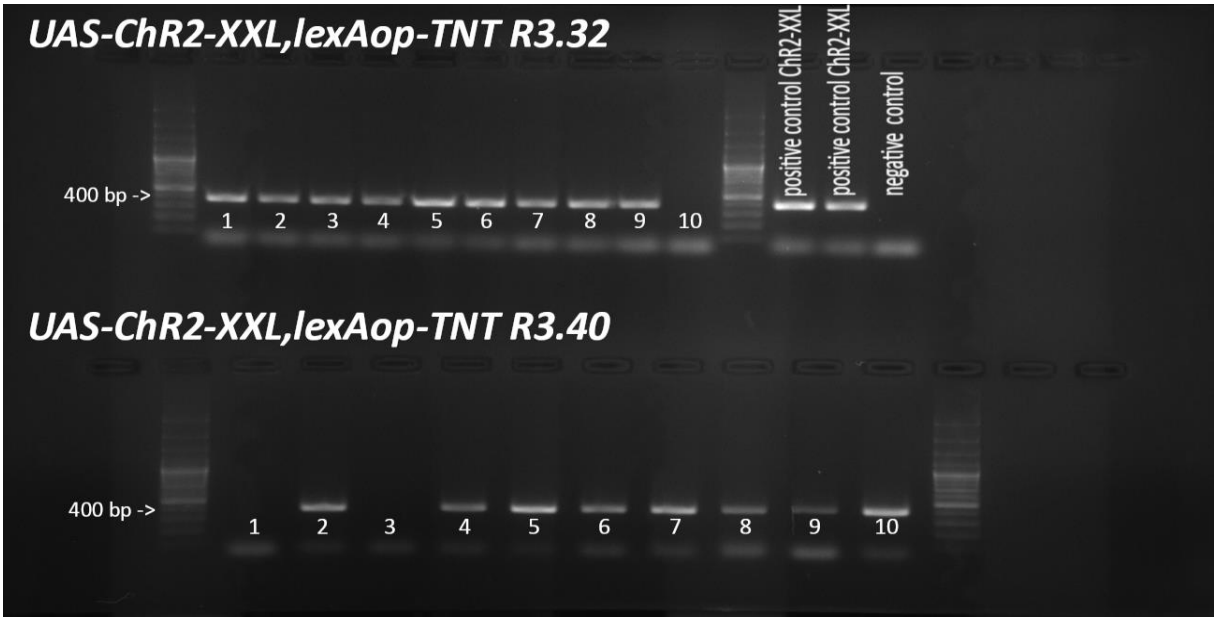

Figure S17: *PCR verification of the transgene UAS-ChR2-XXL. In the tested R3.32 recombinant line 90% of the flies were ChR2-XXL positive upper 1 to 10 lanes). The expression of ChR2-XXL was proven in 80% of the R3.40 recombinant flies (lower 1 to 10 lanes).*

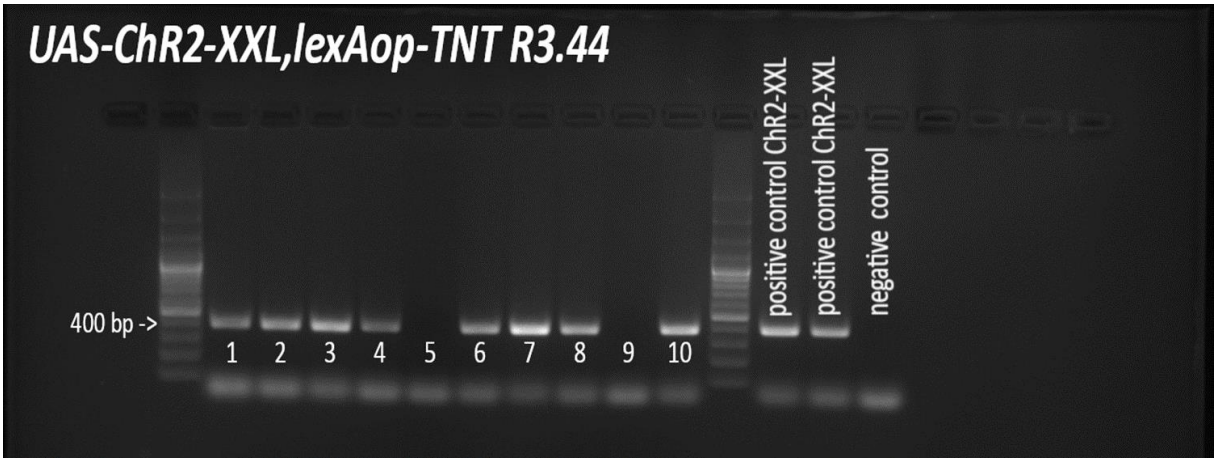

Figure S18: *PCR verification of the transgene UAS-ChR2-XXL. In the tested R3.44 recombinant line 80% of the flies were ChR2-XXL positive.*

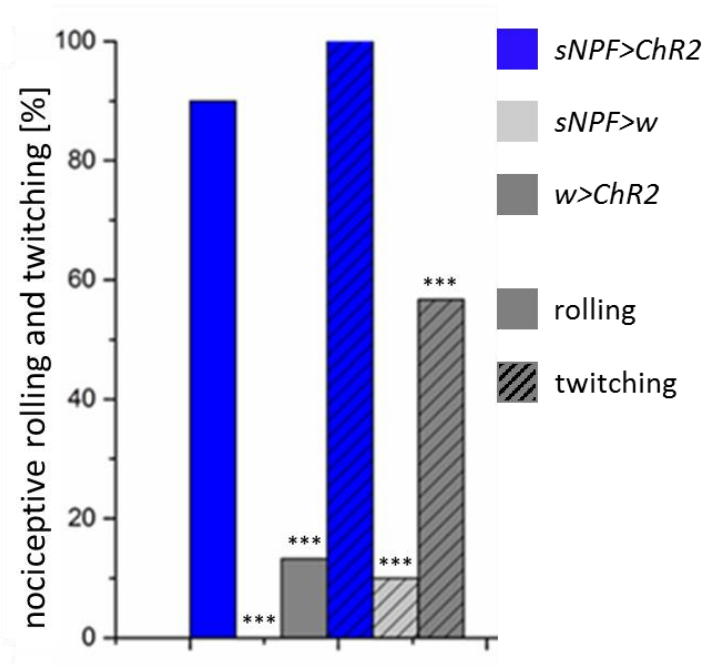

Figure S19: *Optogenetic activation of sNPF-GAL4 positive neurons elicits nociceptive behavior. Experimental larvae show stereotypic rolling and twitching upon blue light illumination. Radostina Lyutova, Master thesis. p-Values: n.s.>0.05, * <0.05, ** <0.01, *** <0.001*

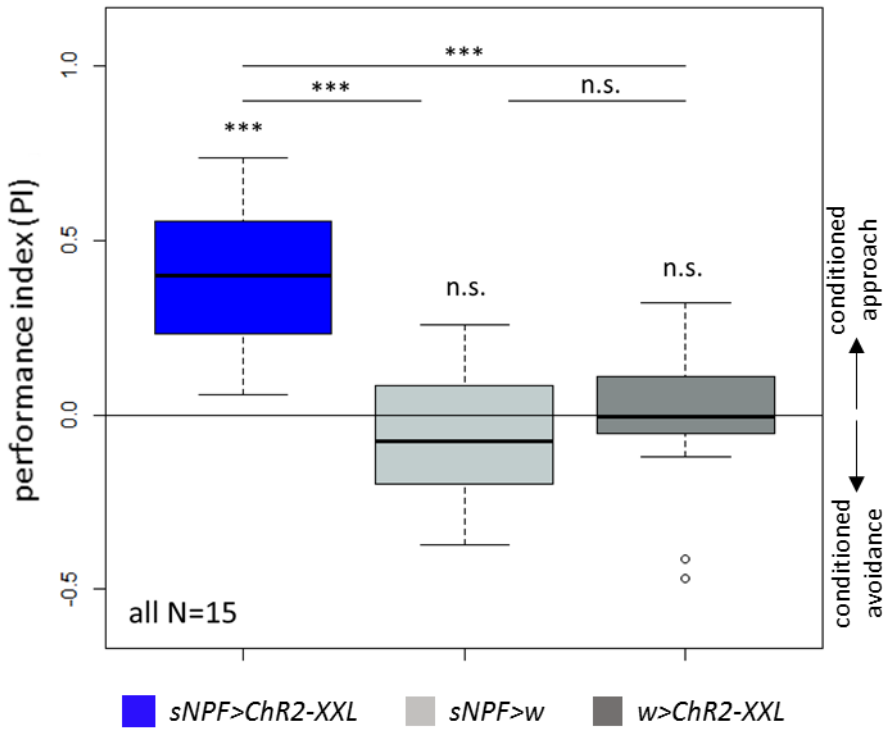

Figure S20: *Optogenetic activation of sNPF-GAL4 positive neurons results in appetitive memory formation. Experimental larvae show significant learning behavior upon blue light illumination whereas learning performance of control larvae is not above chance level. Data by Kamil Guzinski. p-Values: n.s.>0.05, * <0.05, ** <0.01, *** <0.001*

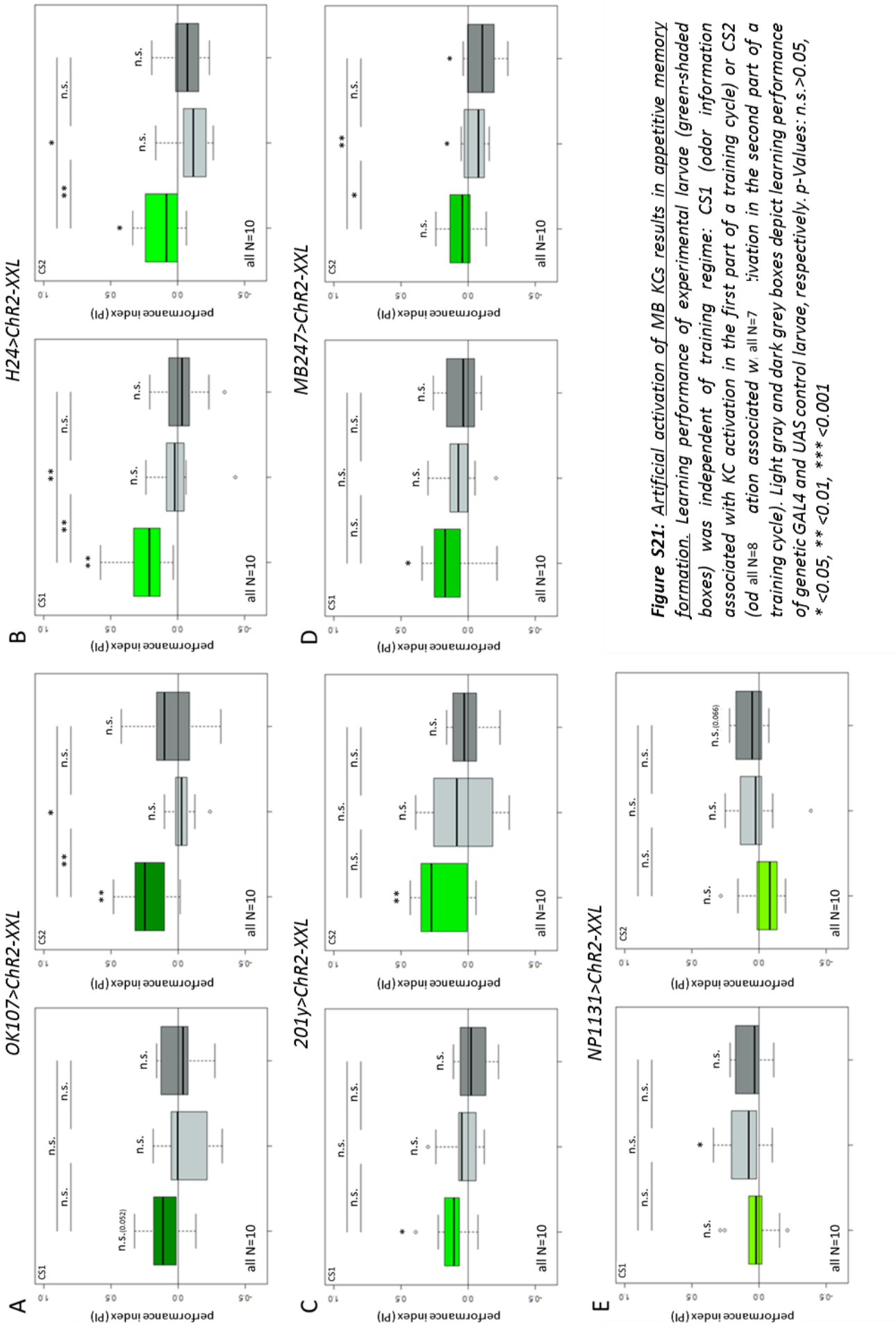

Figure S21: *Artificial activation of MB KCs results in appetitive memory formation. Learning performance of experimental larvae (green-shaded boxes) was independent of training regime: CS1 (odor information associated with KC activation in the first part of a training cycle) or CS2 (odor information associated with KC activation in the second part of a training cycle). Light gray and dark grey boxes depict learning performance of genetic GAL4 and UAS control larvae, respectively. p-Values: n.s.>0.05, * <0.05, ** <0.01, *** <0.001*

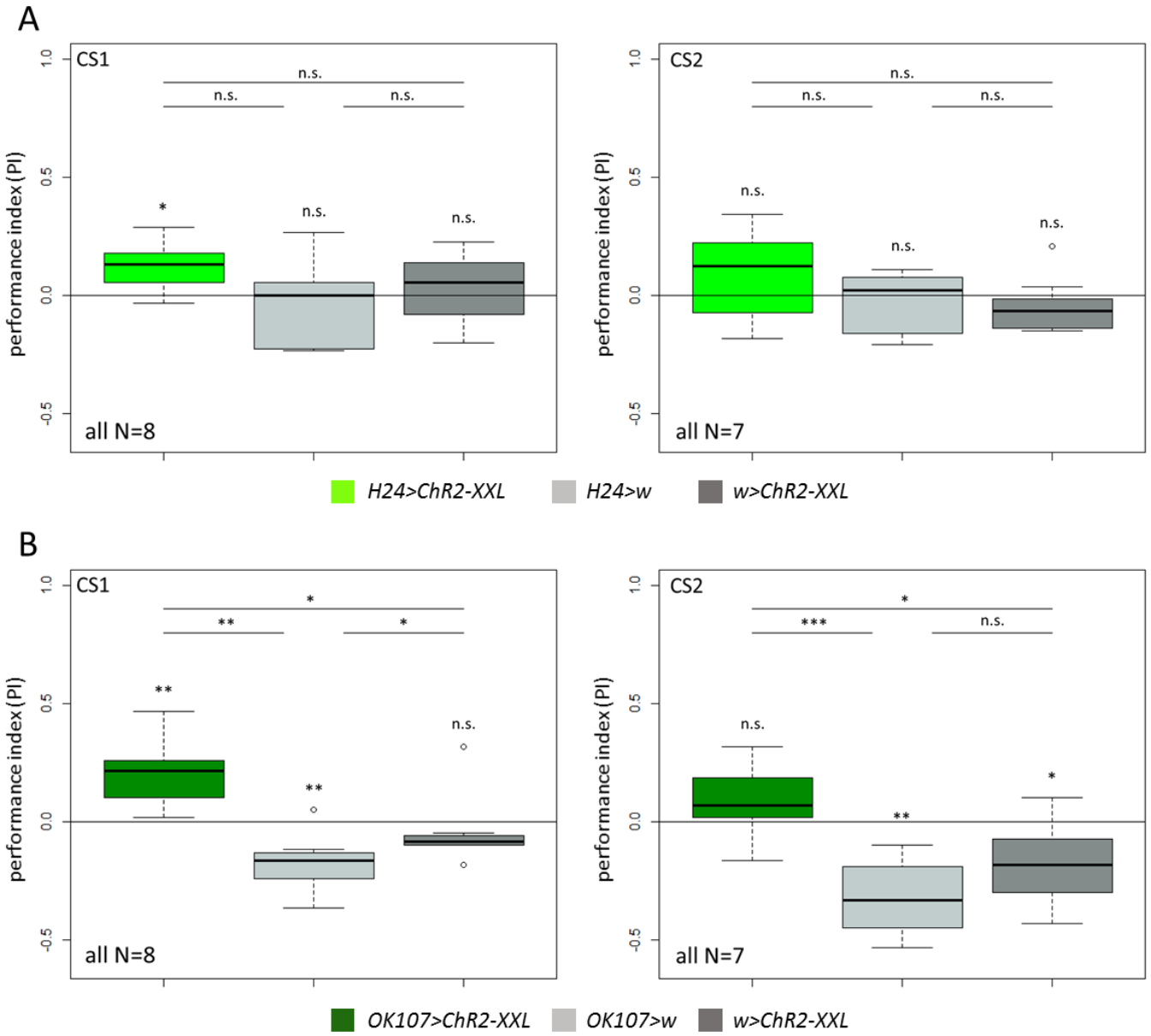

Figure S22: *Artificial activation of MB KCs results in appetitive memory formation in a two-odor (OCT vs. AM (1:40)) substitution paradigm. In both substitution assays experimental larvae showed significant learning performance under CS1 training regime: (odor information associated with KC activation in the first part of a training cycle). Under CS2 training regime (odor information associated with KC activation in the second part of a training cycle) learning behavior of experimental larvae was not above chance level. p-Values: n.s.>0.05, * <0.05, ** <0.01, *** <0.001*

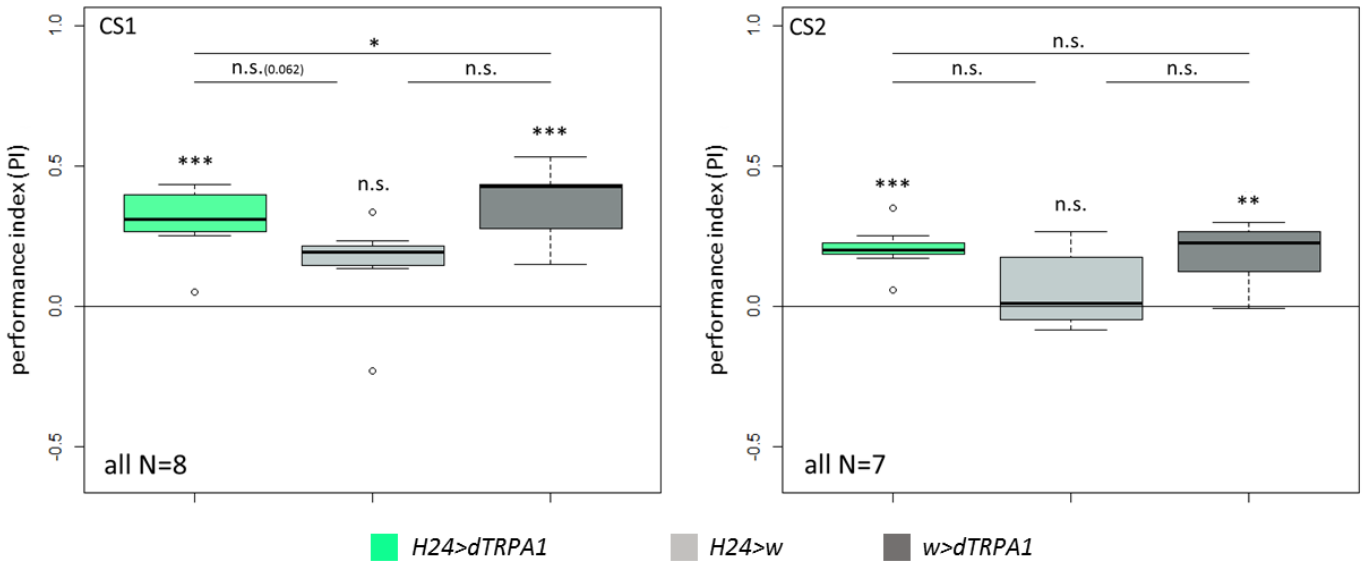

Figure S23: *Odor discrimination at MB level is not disrupted by thermogenetic activation of KCs. In a two-odor (OCT vs. AM (1:40)) substitution paradigm using dTRPA1 for thermogenetic activation of KCs experimental H24>dTRPA1 larvae showed significant learning performance independent of training regime: CS1 (odor information associated with KC activation in the first part of a training cycle) or CS2 (odor information associated with KC activation in the second part of a training cycle). Appetitive memory formation was further observed under both CS1 and CS2 trainings regimes in the UAS genetic control, but not in the GAL4 control larvae. p-Values: n.s.>0.05, * <0.05, ** <0.01, *** <0.001*

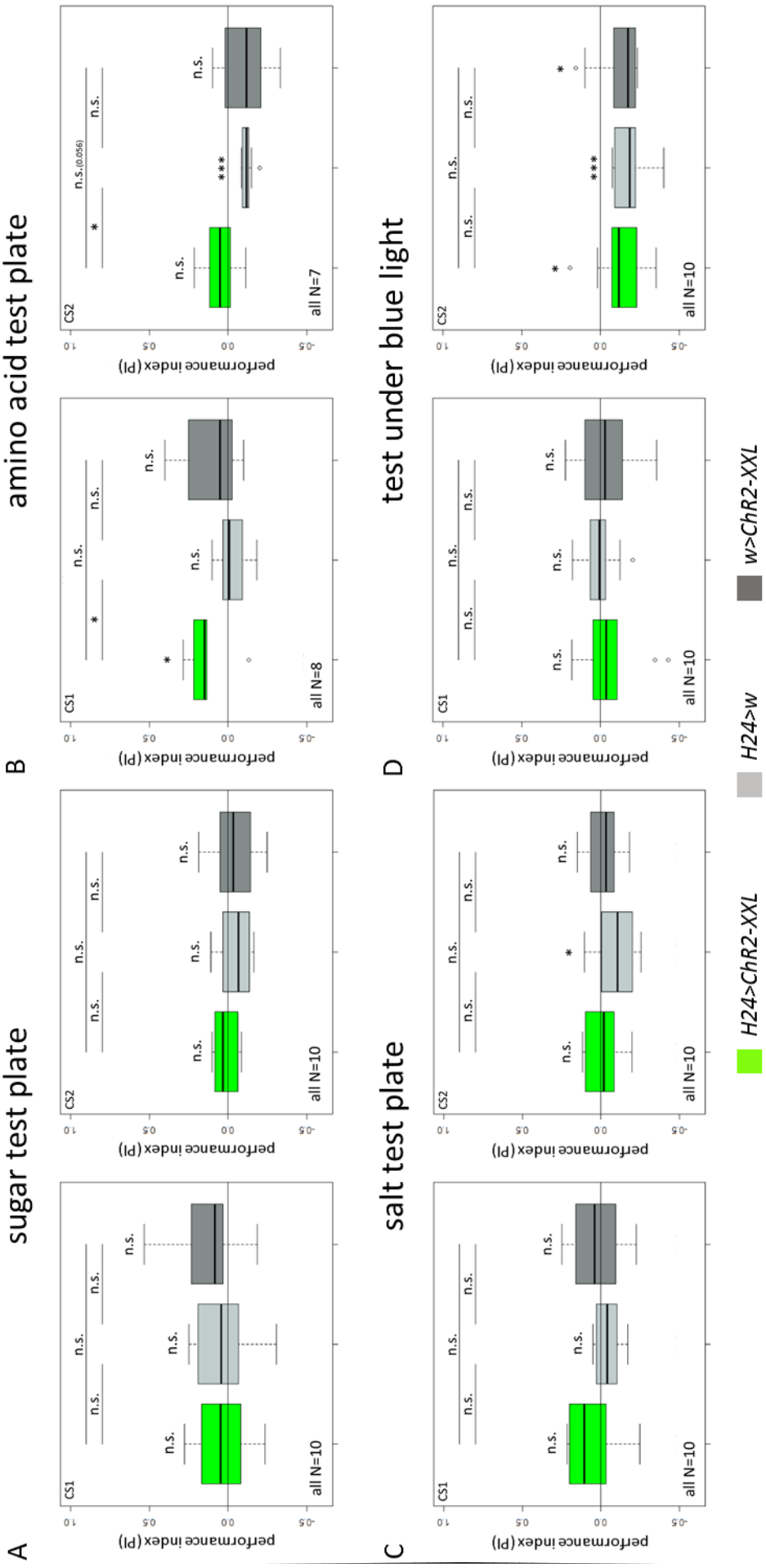

Figure S24: *Optogenetic activation of KCs induces sugar memory formation. A: Sugar exposure of larvae during test abolished appetitive memory expression; B: Amino acid exposure during test did not affect appetitive memory expression; C: Salt exposure of larvae during test inhibited appetitive memory expression; D: When exposed to blue light in a test situation experimental as well as control larvae expressed aversive memory. In all four assays learning performance of experimental larvae was independent of training regime: CS1 (odor information associated with KC activation in the first part of a training cycle) or CS2 (odor information associated with KC activation in the second part of a training cycle). p-Values: n.s.>0.05, * <0.05, ** <0.01, *** <0.001*

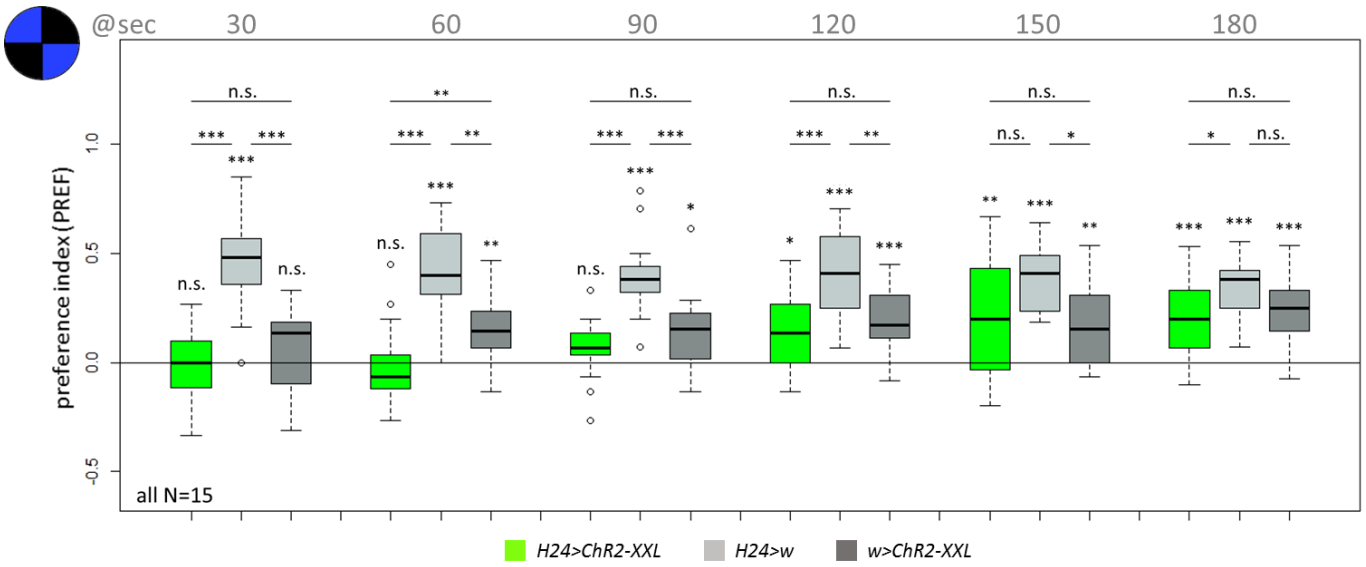

Figure S25: *Optogenetic activation of KCs induces internal rewarding signal. Blue light exposure of H24>ChR2-XXL larvae impaired light avoidance within the first two minutes of blue light exposure followed by progressive increase of darkness preference to wild type levels. p-Values: n.s.>0.05, * <0.05, ** <0.01, *** <0.001*

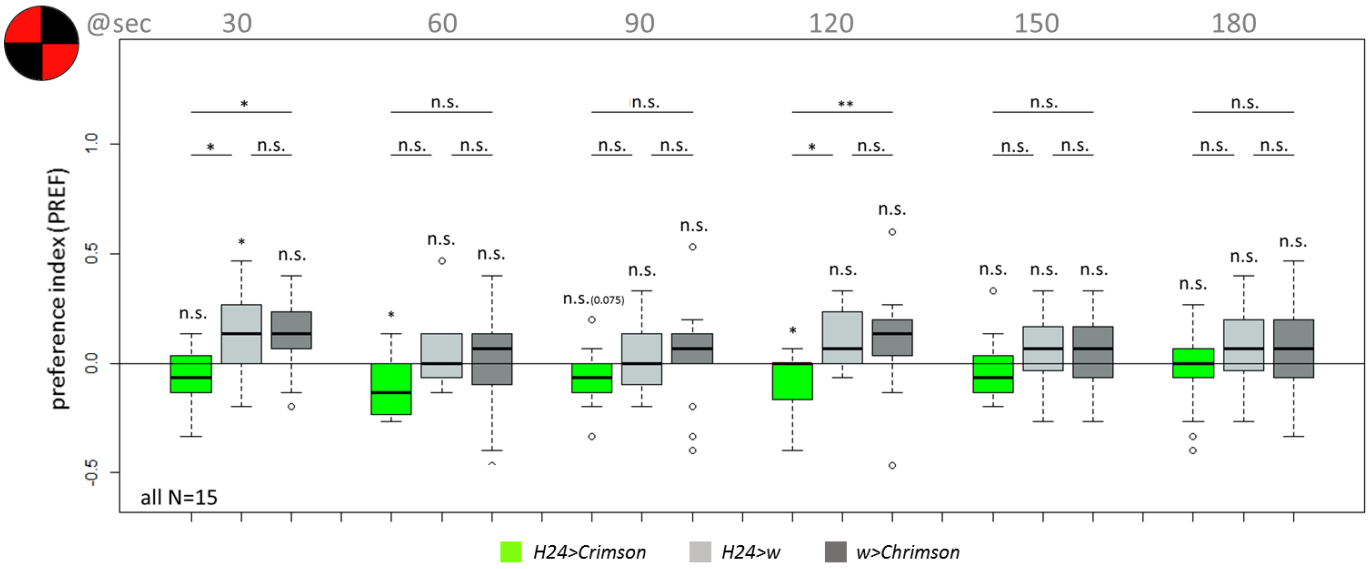

Figure S26: *Optogenetic activation of KCs induces internal rewarding signal. Optogenetic activation of KCs using red shifted cation channel in absence of aversive light stimulus resulted in active action selection of experimental larvae at seconds 60 and 120 during red light exposure towards illuminated sites. The preference of experimental larvae for the illuminated sites of the Petri dish was significantly different from that of the control larvae at seconds 30 and 120 during red light exposure, whereas control larvae were randomly distributed between dark and illuminated sites throughout the three minutes of recording.*
*p-Values: n.s.>0.05, * <0.05, ** <0.01, *** <0.001*

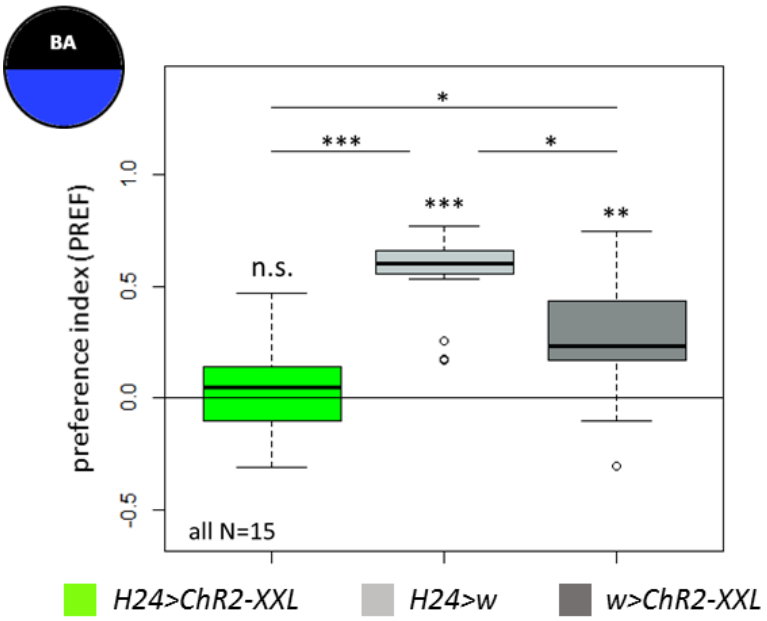

Figure S27: *Optogenetic activation of KCs opposed to simultaneous exposure to two different appetitive stimuli impairs their positive combinatorial effect. In a choice assay experimental larvae showed abolished darkness/BA preference whereas control larvae approached significantly the odor/darkness side. p-Values: n.s.>0.05, * <0.05, ** <0.01, *** <0.001*

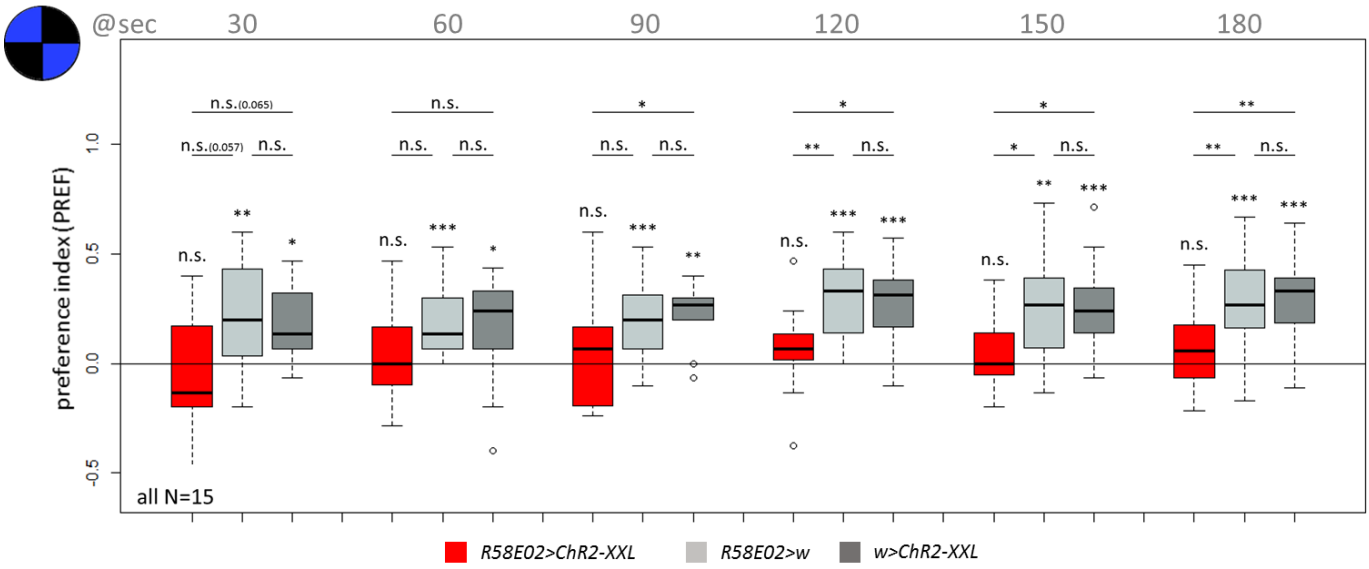

Figure S28: *Optogenetic activation of dopaminergic neurons from the pPAM cluster induces internal rewarding signal. Blue light exposure of experimental larvae biased the naïve light avoidance behavior throughout the three minutes of recording whereas control larvae showed significant negative phototaxis. p-Values: n.s.>0.05, * <0.05, ** <0.01, *** <0.001*

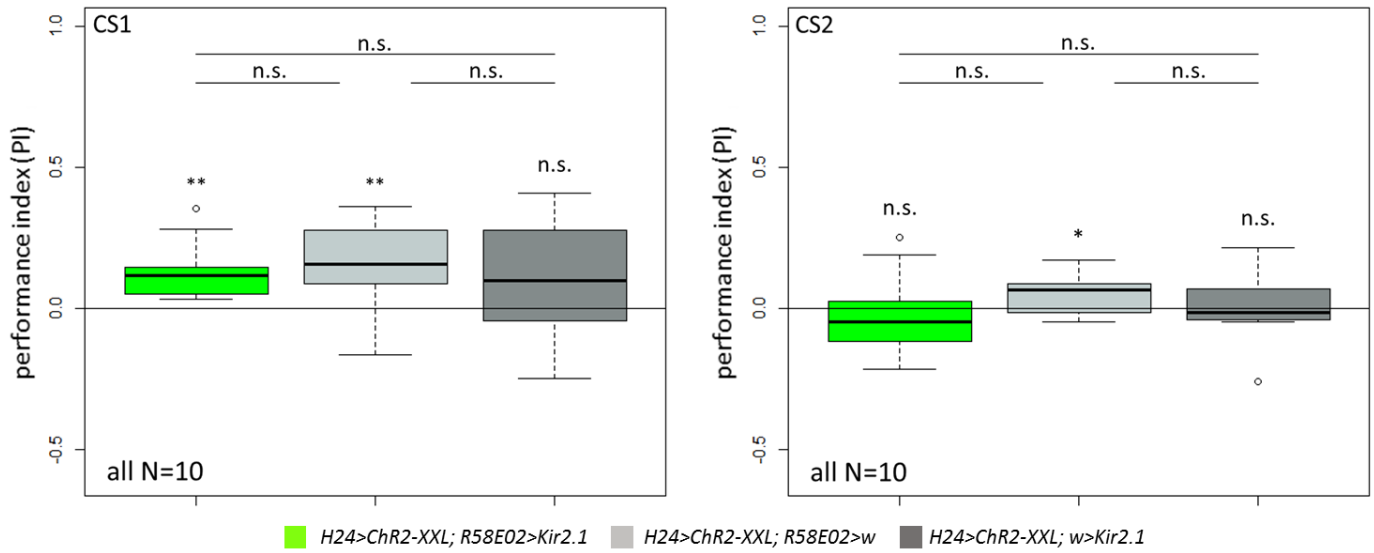

Figure S29: *Silencing of pPAM neurons during substitution learning results in abolishment of appetitive memory. In the substitution assay experimental larvae showed significant learning performance under CS1 training regime: (odor information associated with KC activation in the first part of a training cycle). Under CS2 training regime (odor information associated with KC activation in the second part of a training cycle) learning behavior of experimental larvae was not above chance level. GAL4 control larvae showed significant learning performance independent of training regime whereas the learning performance of the UAS control larvae was not above chance level under CS1 as well as under CS2 training regime. p-Values: n.s.>0.05, * <0.05,*
*** <0.01, *** <0.001*

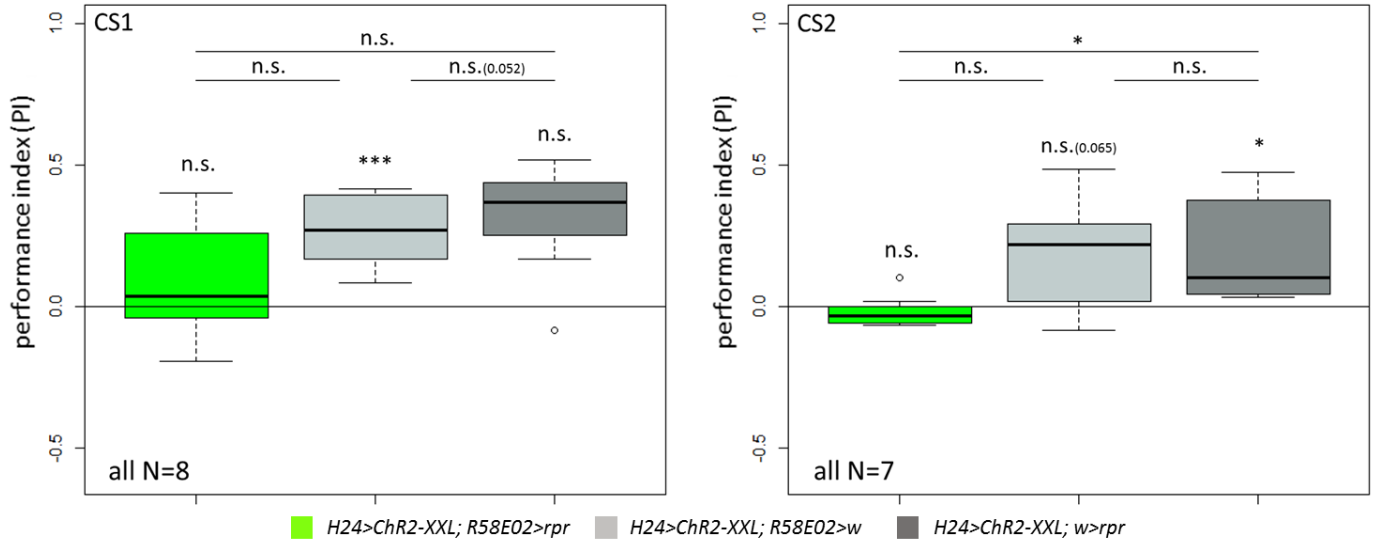

Figure S30: *Ablation of pPAM neurons impairs substitution learning. Simultaneous optogenetic activation of KCs and pPAM neuron ablation resulted in abolishment of appetitive memory independent of training regime: CS1 (odor information associated with KC activation in the first part of a training cycle) or CS2 (odor information associated with KC activation in the second part of a training cycle). p-Values: n.s.>0.05, * <0.05, ** <0.01, *** <0.001*

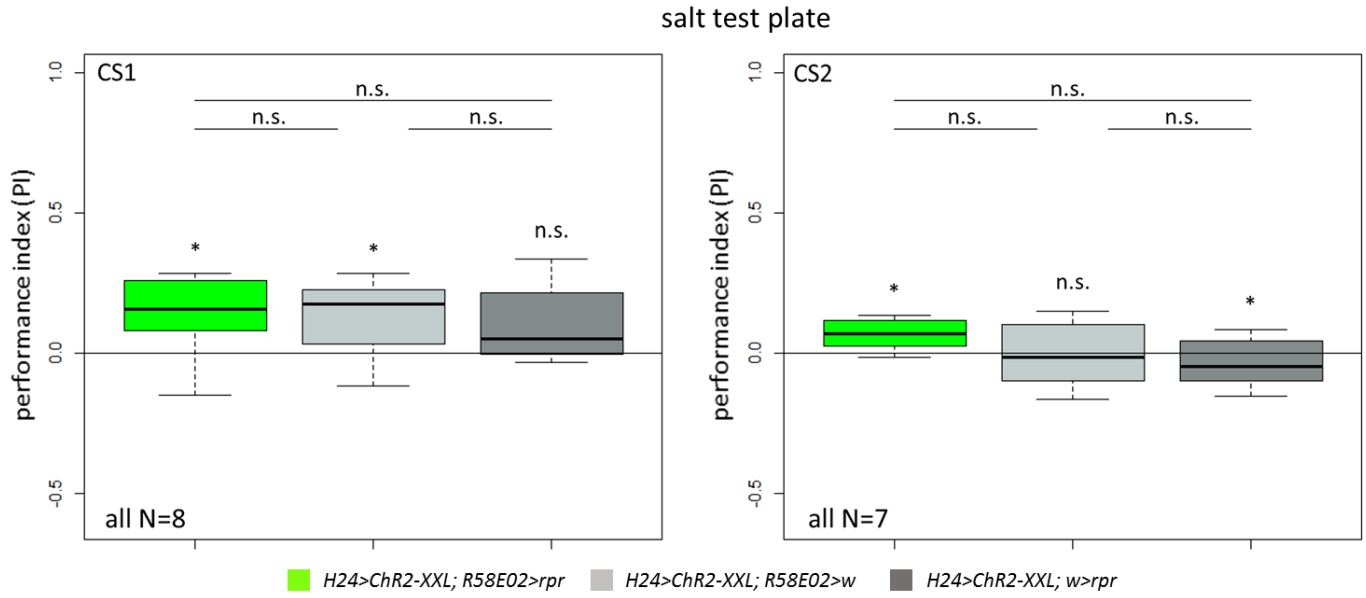

Figure S31: *Simultaneous activation of KCs and ablation of pPAM neurons results in appetitive memory recall on a salt test plate. In a substitution learning assay larvae with activated KCs and ablated pPAM neurons showed significant appetitive learning behavior on a 1.5 M salt plate independent of training regime: CS1 (odor information associated with KC activation in the first part of a training cycle) or CS2 (odor information associated with KC activation in the second part of a training cycle). p-Values: n.s.>0.05, * <0.05, ** <0.01, *** <0.001*

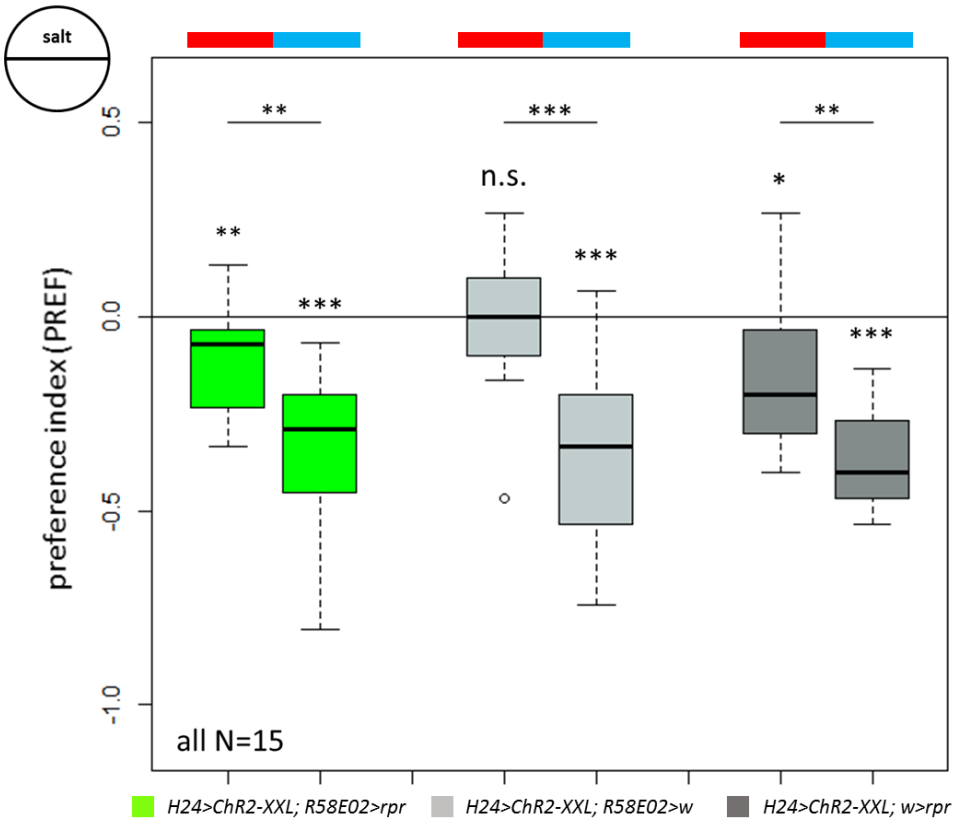

Figure S32: *Blue light exposure enhances naïve larval 1.5M salt avoidance behavior. Simultaneous activation of KCs and ablation of pPAM neurons did not affect naïve salt avoidance. However, exposure to blue light results in a significantly increased salt avoidance. p-Values: n.s.>0.05, * <0.05, ** <0.01, *** <0.001*

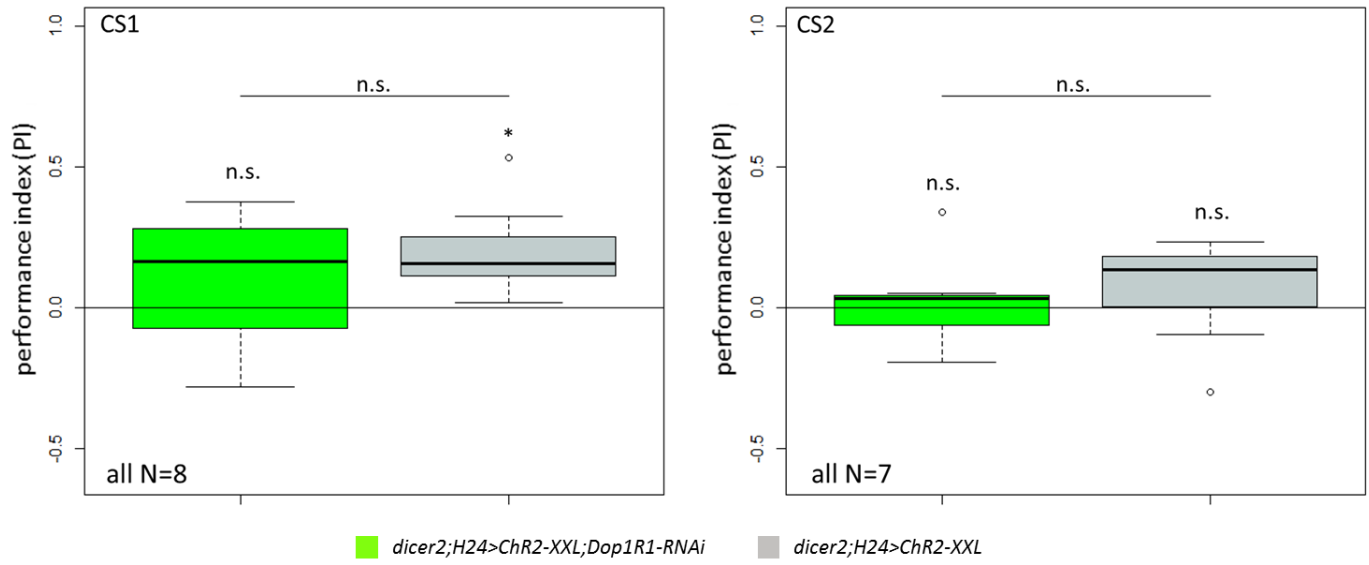

Figure S33: *Downregulation of Dop1R1 in KCs abolishes appetitive learning during substitution conditioning. In contrast to control larvae, experimental larvae showed no learning behavior after simultaneous activation of KCs and knock down of the dopaminergic Dop1R1 receptor in MB neurons under CS1 training regime (odor information associated with KC activation in the first part of a training cycle). Under CS2 (odor information associated with KC activation in the second part of a training cycle) training regime none of the tested groups performed above chance level. p-Values: n.s.>0.05, * <0.05, ** <0.01, *** <0.001*

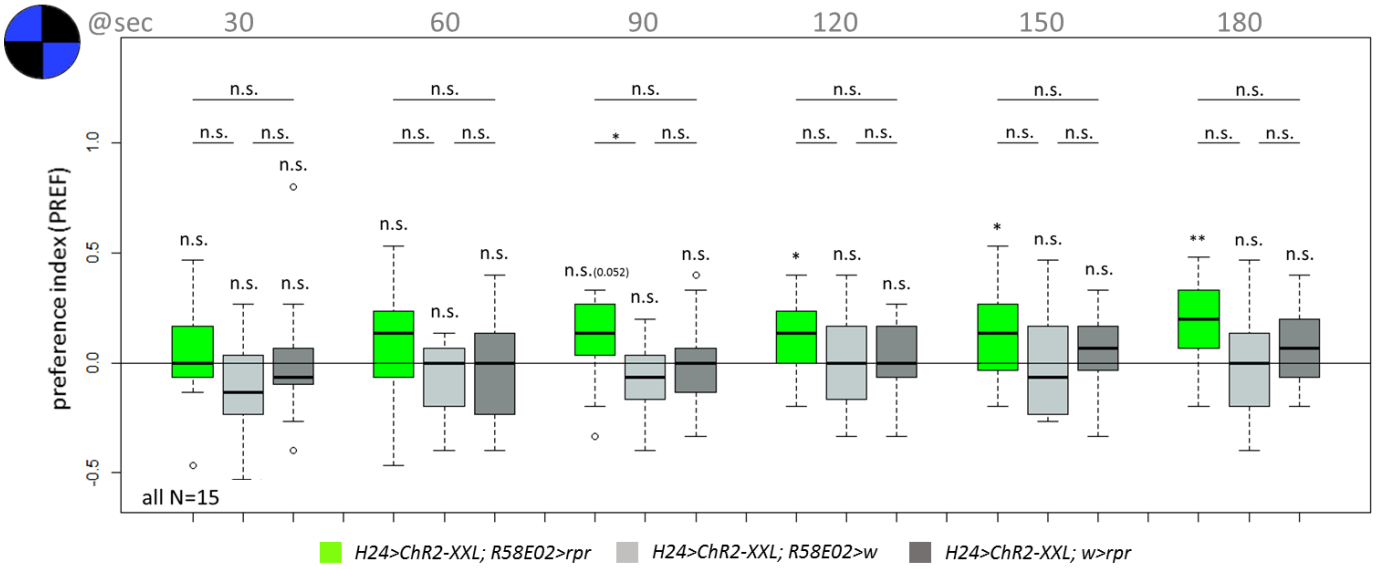

Figure S34: *Internal reward signal is induced by artificial activation of KC-to-pPAM feedback loop. In a light avoidance assay, optogenetic activation of KCs resulted in abolishment of negative phototactic behavior in both control groups throughout the three minutes of recording while simultaneous ablation of pPAM neurons restored the naïve larval response to bright light significantly by the end of the second minute of recording. p-Values: n.s.>0.05, * <0.05, ** <0.01, *** <0.001*

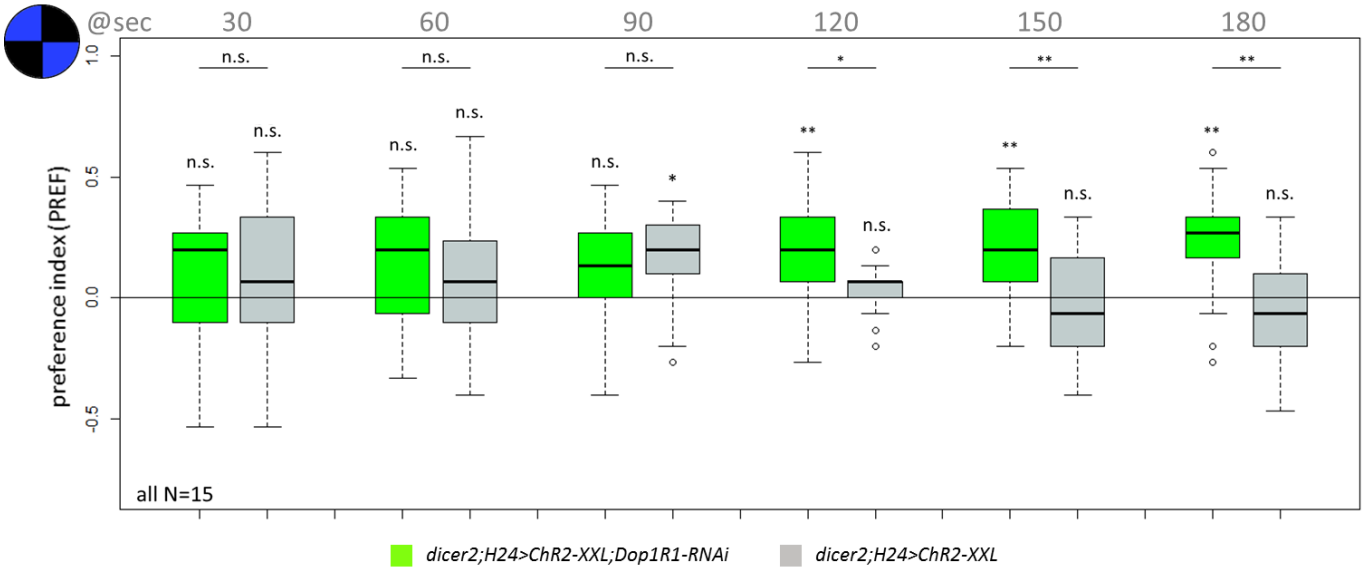

Figure S35: *Internal reward signal relies on dopaminergic input to the MB. In a light avoidance assay, optogenetic activation of KCs resulted in abolishment of negative phototactic behavior in the positive control group while simultaneous downregulation of Dop1R1 receptor in the KCs restored the naïve larval response to bright light by the end of the second minute of recording. p-Values: n.s.>0.05, * <0.05, ** <0.01, *** <0.001*

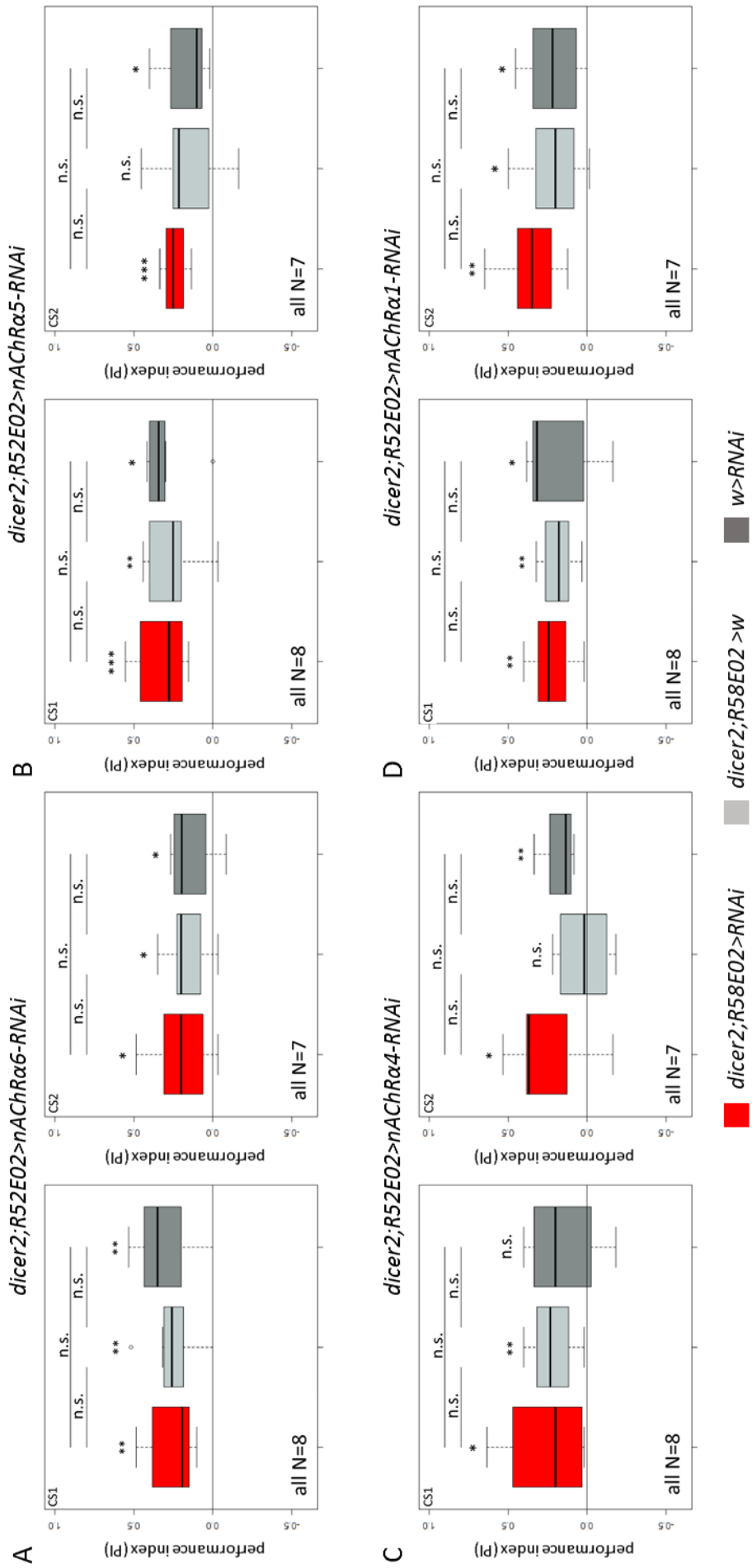

Figure S36: *Odor-sugar learning is not affected by knock down of subunits of the ACh receptor in pPAM neurons. Learning performance of experimental larvae was independent of training regime: CS1 (odor information associated with KC activation in the first part of a training cycle) or CS2 (odor information associated with KC activation in the second part of a training cycle) whereas GAL4 and UAS control larvae showed partially variable regime-dependent learning behavior. p-Values: n.s.>0.05, * <0.05, ** <0.01, *** <0.001*

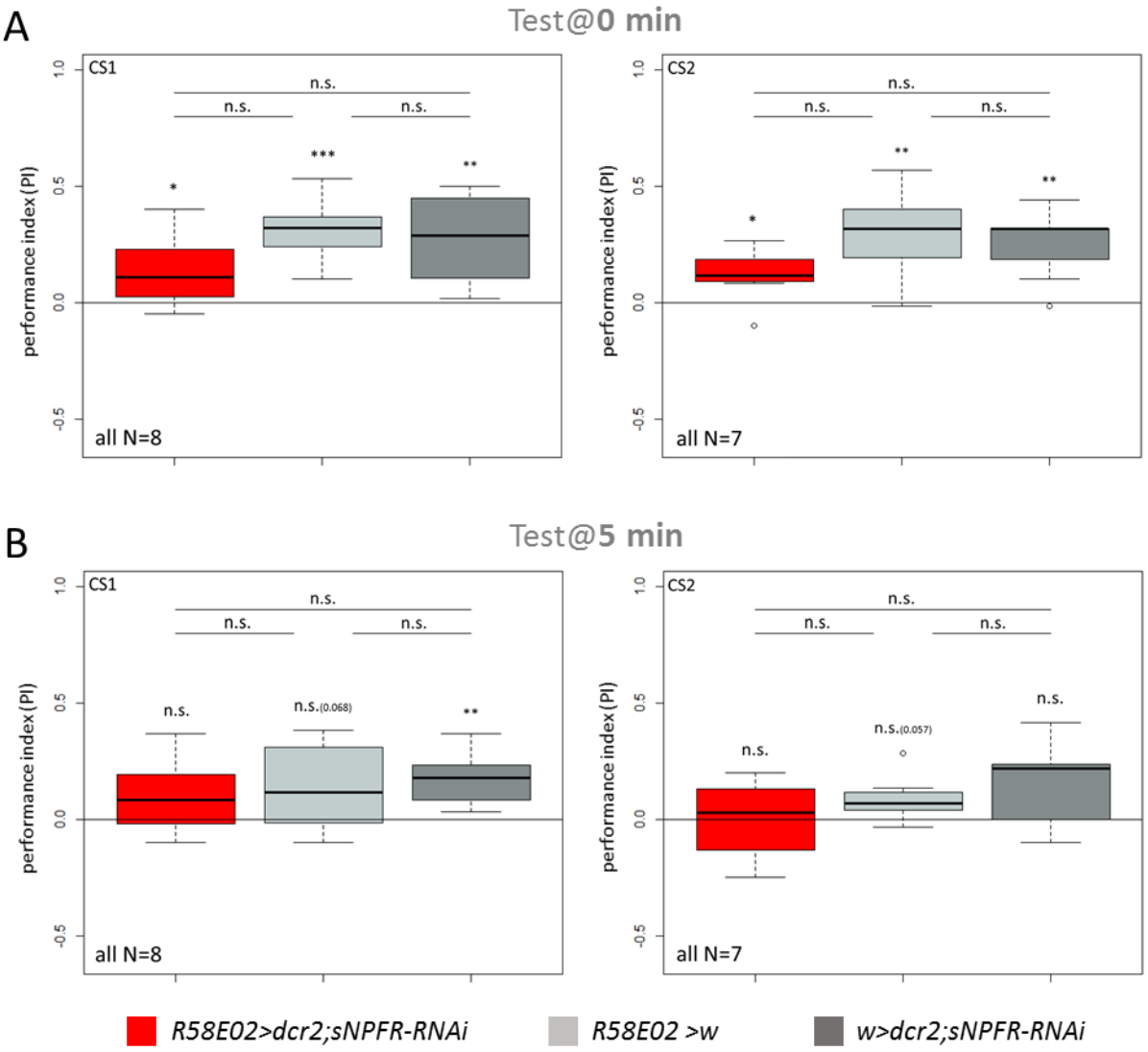

Figure S37: *Odor-sugar learning is affected by knock down of the sNPF receptor in the pPAM neurons. Experimental larvae with downregulated expression of sNPFR in the pPAM neurons showed decrease in learning performance compared to genetic controls independent of training regime: CS1 (odor information associated with KC activation in the first part of a training cycle) or CS2 (odor information associated with KC activation in the second part of a training cycle) as performance indices were lower directly after training and are not above chance level five minutes after CS1 as well as after CS2 training. p-Values: n.s.>0.05,*
** <0.05, ** <0.01, *** <0.001*

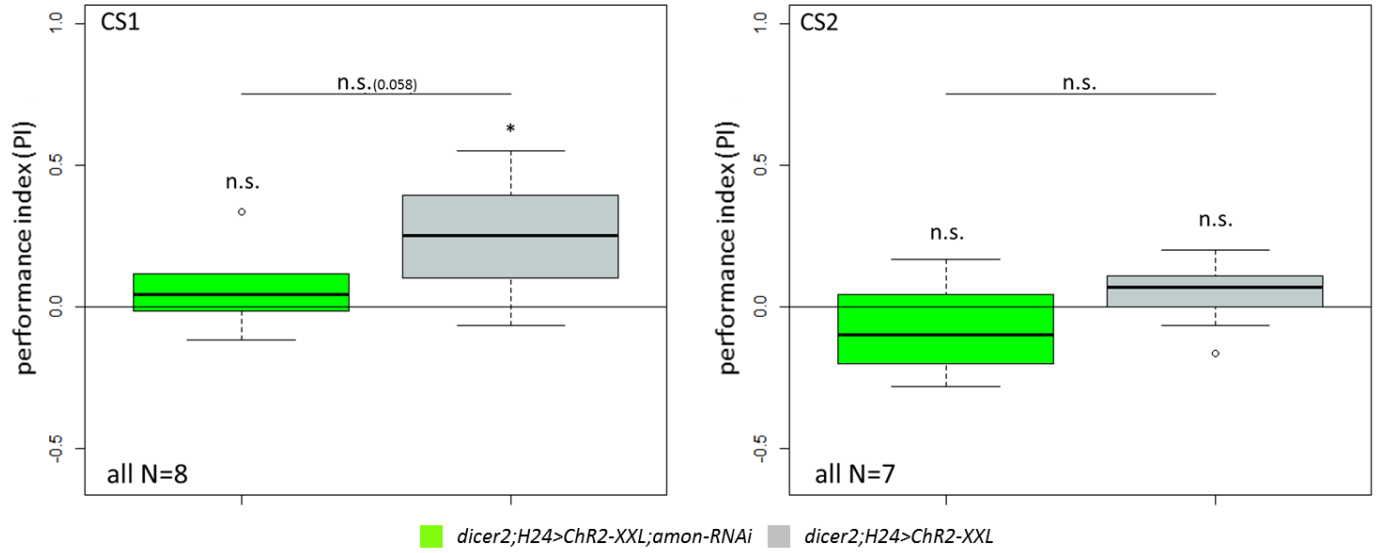

Figure S38: *Disruption of neuropeptide maturation in KCs during substitution learning abolishes appetitive memory. Experimental larvae with downregulated amontillado in KCs showed significantly decreased learning performance after substitution conditioning independent of training regime: CS1 (odor information associated with KC activation in the first part of a training cycle) or CS2 (odor information associated with KC activation in the second part of a training cycle). Significant learning behavior in control larvae was observed only under CS1 but not under CS2 training regime. p-Values: n.s.>0.05, * <0.05, ** <0.01, *** <0.001*

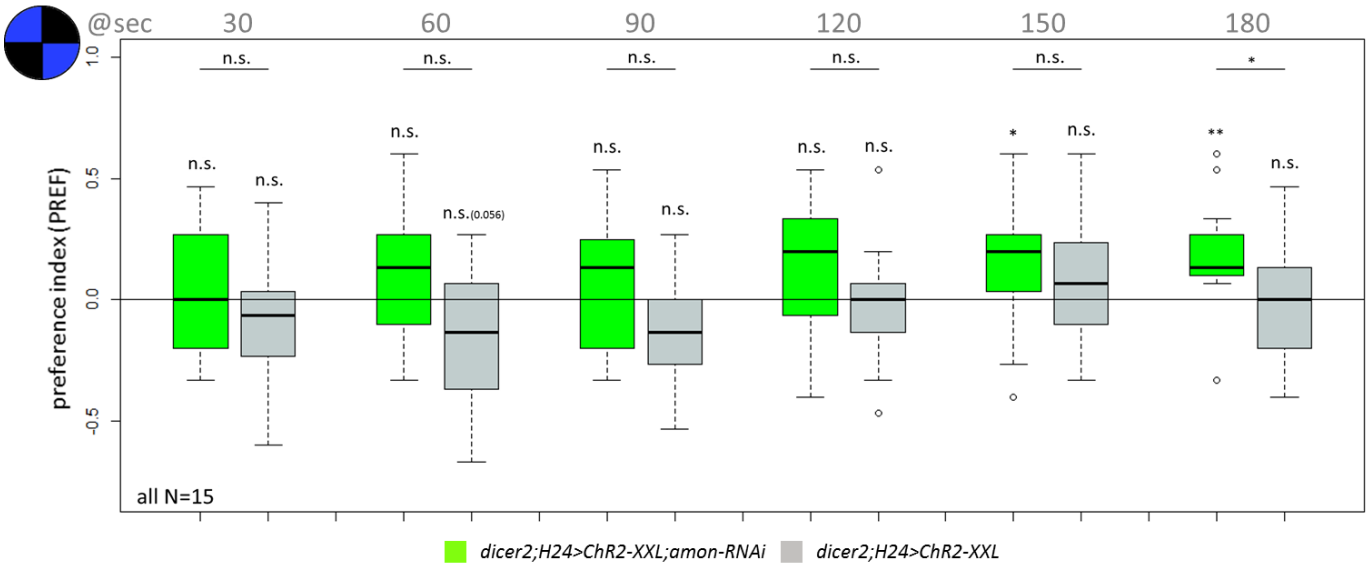

Figure S39: *Internal reward signal is induced by peptidergic signals from the KCs. In a light avoidance assay, optogenetic activation of KCs resulted in abolishment of negative phototactic behavior of control larvae throughout the recording while simultaneous decrease in neuropeptide levels within the KCs restored the naïve larval response to bright light after the second minute of recording. p-Values: n.s.>0.05, * <0.05, ** <0.01, *** <0.001*

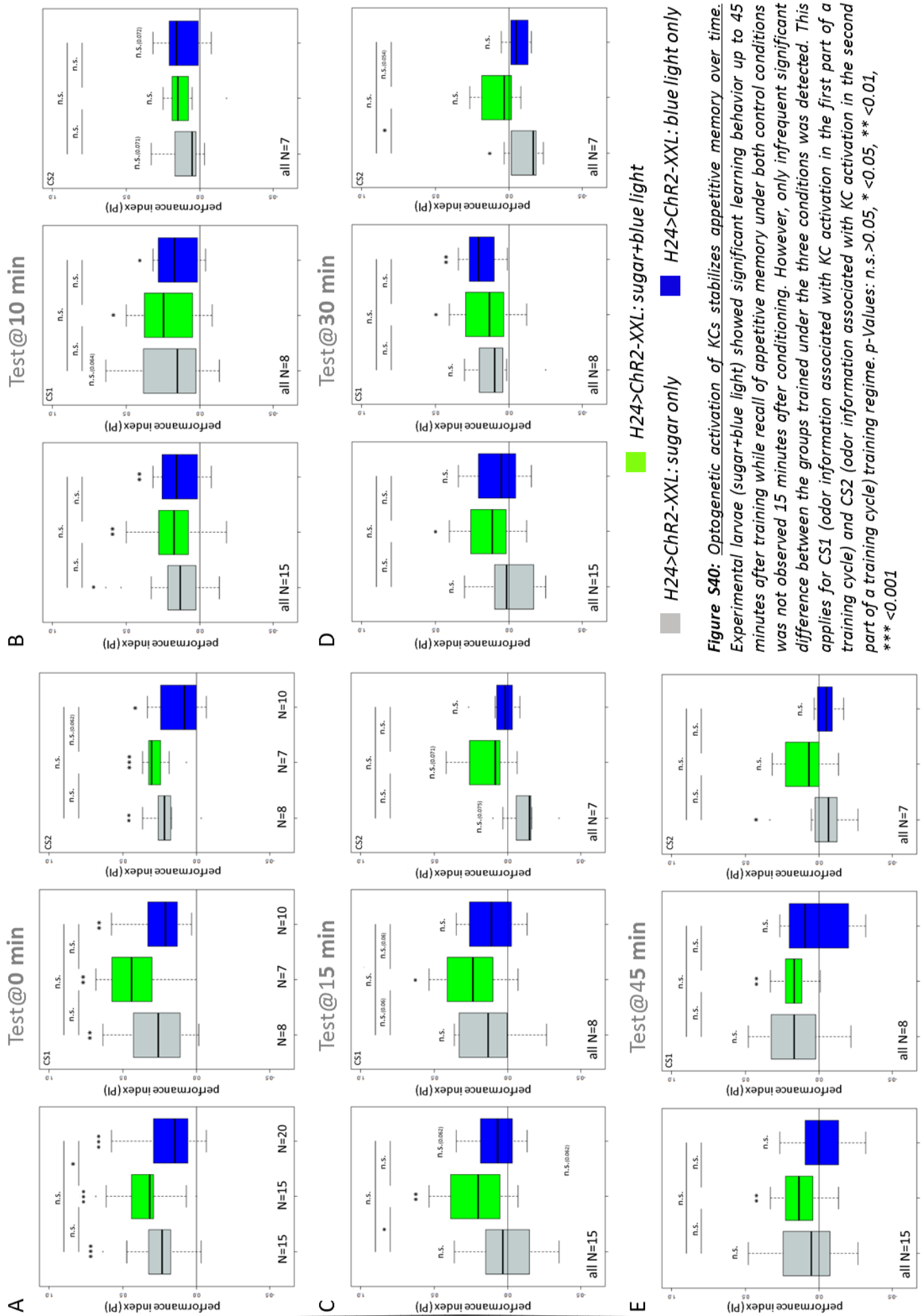

Figure S40: *Optogenetic activation of KCs stabilizes appetitive memory over time. Experimental larvae (sugar+blue light) showed significant learning behavior up to 45 minutes after training while recall of appetitive memory under both control conditions was not observed 15 minutes after conditioning. However, only infrequent significant difference between the groups trained under the three conditions was detected. This applies for CS1 (odor information associated with KC activation in the first part of a training cycle) and CS2 (odor information associated with KC activation in the second part of a training cycle) training regime. p-Values: n.s.>0.05, * <0.05, ** <0.01, *** <0.001*

Table S1: *Summary of significance levels. p-Values: n.s.>0.05, * <0.05, ** <0.01, *** <0.001*

Page	Figure	EXP>GAL4	EXP>UAS	GAL4>UAS
81	24B'	0.48	0.48	0.99
		Null hypothesis	**EXP**	0.964
			GAL4	0.109
			UAS	0.01169
81	24C'	0.0604	0.0026	0.1994
		Null hypothesis	**EXP**	0.000185
			GAL4	0.2139
			UAS	0.6927
81	24D'	0.067	0.015	0.454
		Null hypothesis	**EXP**	0.00499
			GAL4	0.8652
			UAS	0.3985
81	24E'	0.00011	0.00011	0.97845
		Null hypothesis	**EXP**	$7.98e^{-05}$
			GAL4	0.2296
			UAS	0.1632
81	24F'	0.00031	0.01094	0.20483
		Null hypothesis	**EXP**	0.000196
			GAL4	0.1718
			UAS	0.587
83	25B RL	0.754	0.053	0.754
			EXP RL>EXP BL	0.51
83	25B BL	0.35	0.76	0.76
83	25D RL	0.44	0.000016	0.08
			EXP RL>EXP BL	0.51
83	25D BL	0.3	0.67	0.19
83	25E RL	0.38	0.13	0.47
			EXP RL>EXP BL	0.0023
83	25E BL	0.000014	0.0018	0.0249
83	25F RL	0.7743	0.0034	0.0056
			EXP RL>EXP BL	0.0064
83	25F BL	0.000033	0.027	0.041

Page	Figure	EXP>GAL4	EXP>UAS	GAL4>UAS
84	26 RL	0.21	0.21	0.008
		Null hypothesis	**EXP**	0.000008475
			GAL4	$1.361e^{-08}$
			UAS	0.00001477
84	26 BL	0.15	0.69	0.23
		Null hypothesis	**EXP**	0.0001067
			GAL4	$3.23e^{-09}$
			UAS	$6.76e^{-08}$
81	27A RL	1	1	1
		Null hypothesis	**EXP**	0.0006567
			GAL4	0.002031
			UAS	0.004066
86	27A BL	0.272	0.015	0.272
		Null hypothesis	**EXP**	0.3779
			GAL4	0.04783
			UAS	7.34E-06
86	27B RL	1	1	0.72
		Null hypothesis	**EXP**	$2.59e^{-09}$
			GAL4	$2.07e^{-07}$
			UAS	$5.46e^{-10}$
86	27B BL	0.00072	0.17797	0.02296
		Null hypothesis	**EXP**	$1.83e^{-07}$
			GAL4	$8.70e^{-11}$
			UAS	$7.96e^{-06}$
86	27C RL	0.98	0.98	0.98
		Null hypothesis	**EXP**	0.03867
			GAL4	0.06445
			UAS	0.0006325
86	27C BL	1	1	1
		Null hypothesis	**EXP**	0.04248
			GAL4	0.1205
			UAS	0.118
86	27D RL	1	1	1
		Null hypothesis	**EXP**	0.1746
			GAL4	0.00883
			UAS	0.1617

Page	Figure	EXP>GAL4	EXP>UAS	GAL4>UAS
86	27D BL	1	1	1
		Null hypothesis	**EXP**	0.03007
			GAL4	0.4136
			UAS	0.1001
87	28A	0.039	0.115	0.523
		Null hypothesis	**EXP**	0.0188
			GAL4	0.3496
			UAS	0.8885
87	28B	$1.80e^{-07}$	0.00019	0.0284
		Null hypothesis	**EXP**	0.002387
			GAL4	$3.59e^{-05}$
			UAS	0.03179
88	29	0.0139	0.6149	0.0052
		Null hypothesis	**EXP**	$5.56e^{-07}$
			GAL4	0.01718
			UAS	$3.31e^{-06}$
90	30A	1	1	1
		Null hypothesis	**EXP**	0.3856
			GAL4	0.9361
			UAS	0.4182
90	30B	0.0076	0.1824	0.1824
		Null hypothesis	**EXP**	0.008345
			GAL4	0.008185
			UAS	0.8846
90	30C	0.048	0.621	0.104
		Null hypothesis	**EXP**	0.3992
			GAL4	0.00594
			UAS	0.818
90	30D	1	1	1
		Null hypothesis	**EXP**	0.0179
			GAL4	0.009304
			UAS	0.03298
92	31A 60sec	0.00013	0.00722	0.00395
		Null hypothesis	**EXP**	0.4662
			GAL4	$8.21e^{-07}$
			UAS	0.002036

Page	Figure	EXP>GAL4	EXP>UAS	GAL4>UAS
92	31A 120sec	0.00055	0.41529	0.00416
		Null hypothesis	**EXP**	0.01116
			GAL4	$2.89e^{-06}$
			UAS	0.000161
92	31A 180sec	0.028	0.406	0.133
		Null hypothesis	**EXP**	0.000953
			GAL4	$6.58e^{-08}$
			UAS	$3.82e^{-05}$
92	31B 60sec	0.11	0.15	0.75
		Null hypothesis	**EXP**	0.01147
			GAL4	0.3216
			UAS	0.7849
92	31B 120sec	0.0117	0.0062	0.6454
		Null hypothesis	**EXP**	0.02364
			GAL4	0.04628
			UAS	0.09315
92	31B 180sec	0.56	0.56	0.8
		Null hypothesis	**EXP**	0.7192
			GAL4	0.1084
			UAS	0.3027
93	32A	0.006	0.0053	0.8475
		Null hypothesis	**EXP**	0.00006886
			GAL4	$9.604e^{-09}$
			UAS	$2.729e^{-08}$
93	32B	$5.00e^{-05}$	0.0025	0.1694
		Null hypothesis	**EXP**	$2.11e^{-06}$
			GAL4	$6.31e^{-13}$
			UAS	$6.31e^{-09}$
94	33 60sec	0.17	0.25	0.69
		Null hypothesis	**EXP**	0.46
			GAL4	0.0003884
			UAS	0.01506
94	33 120sec	0.0053	0.0101	0.7042
		Null hypothesis	**EXP**	0.2061
			GAL4	$2.52e^{-05}$
			UAS	0.0001149

Page	Figure	EXP>GAL4	EXP>UAS	GAL4>UAS
94	33 180sec	0.0094	0.0087	0.8611
		Null hypothesis	**EXP**	0.219
			GAL4	0.0001677
			UAS	0.0001076
95	34A	0.98	1	0.98
		Null hypothesis	**EXP**	0.09386
			GAL4	0.001439
			UAS	0.1535
96	35A	0.0076	0.0021	0.5586
		Null hypothesis	**EXP**	0.6983
			GAL4	0.000145
			UAS	0.000114
96	35B RL	0.56	0.029	0.08
		Null hypothesis	**EXP**	0.003535
			GAL4	0.0001588
			UAS	$2.27e^{-07}$
96	35B BL	0.88	0.36	0.41
		Null hypothesis	**EXP**	0.01566
			GAL4	0.0004319
			UAS	$1.03e^{-06}$
97	36A	0.86	0.53	0.86
		Null hypothesis	**EXP**	0.003093
			GAL4	0.09446
			UAS	0.2926
97	36B RL	0.16	0.47	0.16
		Null hypothesis	**EXP**	0.006148
			GAL4	0.9027
			UAS	0.04078
97	36B BL	1	1	1
		Null hypothesis	**EXP**	0.00002986
			GAL4	0.00001996
			UAS	4.592E-08
98	37A	0.3415		
		Null hypothesis	**EXP**	0.2544
			GAL4	0.01342

Page	Figure	EXP>GAL4	EXP>UAS	GAL4>UAS
98	37B RL	0.4778		
			EXP	0.0002214
		Null hypothesis	**GAL4**	0.001038
98	37B BL	0.7084		
			EXP	0.0007158
		Null hypothesis	**GAL4**	$4.01e^{-05}$
99	39B LL	0.177		
99	39B HL	0.000858		
100	40A 60sec	0.21	0.59	0.59
			EXP	0.3139
		Null hypothesis	**GAL4**	0.1005
			UAS	0.7706
100	40A 120sec	0.19	0.31	0.65
			EXP	0.01144
		Null hypothesis	**GAL4**	0.8743
			UAS	0.632
100	40A 180sec	0.082	0.436	0.436
			EXP	0.004064
		Null hypothesis	**GAL4**	0.8445
			UAS	0.1061
100	40B 60sec	0.6308		
			EXP	0.07741
		Null hypothesis	**GAL4**	0.2247
100	40B 120sec	0.02174		
			EXP	0.004893
		Null hypothesis	**GAL4**	0.2637
100	40B 180sec	0.007298		
			EXP	0.004285
		Null hypothesis	**GAL4**	0.54
101	41A	0.52	0.52	0.92
			EXP	$1.05e^{-05}$
		Null hypothesis	**GAL4**	$7.47e^{-05}$
			UAS	0.001226

Page	Figure	EXP>GAL4	EXP>UAS	GAL4>UAS
101	41B	0.26	0.44	0.61
		Null hypothesis	**EXP**	0.001324
			GAL4	0.01573
			UAS	0.001921
101	41C	1	1	1
		Null hypothesis	**EXP**	0.000725
			GAL4	0.000739
			UAS	0.001091
101	41D	1	1	1
		Null hypothesis	**EXP**	$7.43e^{-05}$
			GAL4	$6.75e^{-05}$
			UAS	0.000222
102	42A	0.0087	0.0377	0.4753
		Null hypothesis	**EXP**	0.00211
			GAL4	$2.39e^{-06}$
			UAS	$3.01e^{-05}$
102	42B	0.5	0.17	0.5
		Null hypothesis	**EXP**	0.2718
			GAL4	0.008645
			UAS	0.000893
102	42C	0.77	0.77	0.86
		Null hypothesis	**EXP**	$2.44e^{-05}$
			GAL4	$5.50e^{-06}$
			UAS	$6.72e^{-06}$
102	42D	0.58	0.65	0.74
		Null hypothesis	**EXP**	$3.52e^{-07}$
			GAL4	$4.21e^{-06}$
			UAS	$3.05e^{-06}$
103	43A	0.02748		
		Null hypothesis	**EXP**	0.9516
			GAL4	0.009781
103	43B RL	0.3388		
		Null hypothesis	**EXP**	$1.16e^{-06}$
			GAL4	$2.49e^{-05}$

Page	Figure	EXP>GAL4	EXP>UAS	GAL4>UAS
103	43B BL	0.8888		
			EXP	$8.55E^{-06}$
		Null hypothesis	**GAL4**	$7.38E^{-05}$
103	44B	0.015		
104	45B	0.028		
105	46 60sec	0.02421		
			EXP	0.2208
		Null hypothesis	**GAL4**	0.05613
105	46 120sec	0.1564		
			EXP	0.109
		Null hypothesis	**GAL4**	0.8285
105	46 180sec	0.02167		
			EXP	0.004731
		Null hypothesis	**GAL4**	0.7816
107	47A S			
			0min	$1.31e^{-04}$
			10min	0.01145
		Null hypothesis	**15min**	0.8282
			30min	0.95
			45min	0.2346
107	47A S+BL			
			0min	$4.24e^{-06}$
			10min	0.003474
		Null hypothesis	**15min**	0.001366
			30min	0.01168
			45min	0.001402
107	47A BL			
			0min	$7.98e^{-05}$
			10min	0.001895
		Null hypothesis	**15min**	0.06253
			30min	0.1094
			45min	0.7478

Page	Figure	EXP>GAL4	EXP>UAS	GAL4>UAS
107	47C RL	0.09	0.461	0.036
		Null hypothesis	**EXP**	$7.857e^{-07}$
			GAL4	$9.242e^{-08}$
			UAS	0.0009858
107	47C	0.017	0.85	0.019
		Null hypothesis	**EXP**	$5.492e^{-08}$
			GAL4	$1.238e^{-10}$
			UAS	$2.054e^{-07}$

Publications

Publications in connection with this thesis:

Lyutova, R., Selcho, M., Pfeuffer, M., Segebarth, D., Habenstein, J., Rohwedder, A., Frantzmann, F., Wegener, C., Thum, A.S., Pauls, D. (2018). Reward signaling in a recurrent circuit of dopaminergic neurons and peptidergic Kenyon cells. *bioRxiv*. doi:https://doi.org/10.1101/357145. *In revision at Nature Communications*

Other publications, not connected to this thesis:

Pauls, D., von Essen, A., **Lyutova, R.**, van Giesen, L., Rosner, R., Wegener, C. and Sprecher, S.G. (2015). Potency of Transgenic Effectors for Neurogenetic Manipulation in *Drosophila* Larvae. *Genetics*, 199(1), 25-U430. doi:10.1534/genetics.114.172023

Ferry, Q.R.V., **Lyutova, R.** and Fulga, T.A. (2016). Rational design of inducible CRISPR guide RNAs for de novo assembly of transcriptional programs. *Nature Communications*, 8, 14633. doi:10.1038/ncomms14633

Acknowledgments

First and foremost I offer my sincerest gratitude to my supervisor, Dr. Dennis Pauls, who has supported me throughout my thesis with his patience and knowledge whilst allowing me the room to work in my own way. I attribute the level of my doctoral degree to his encouragement and effort and without him this thesis, too, would not have been completed or written.

I wish to express my sincere thanks to Prof. Dr. Christian Wegener for providing me with all the necessary equipment and consumables for the research and his advice and ad-hoc support.

I also thank Prof. Dr. Thomas Raabe and Prof. Dr. Björn Brembs for being members of my thesis committee, and for their regular valuable feedback on my work.

A special thank goes to Prof. Dr. Andreas Thum for the successful collaboration within this project work.

I want to express my gratitude to the Graduate School of Life Sciences at the University of Würzburg for the funding, and for giving me the opportunity to expand my transferrable and scientific skills by offering a wide range of workshops and lectures.

My thanks go also to Prof. Dr. Charlotte Förster for extending my funding at the final stage of preparing this thesis.

I am grateful to Mareike Selcho, Dennis Segebarth, Jens Habenstein, Maximilian Pfeuffer, Xenia Stavroulaki, Astrid Rohwedder and Felix Frantzmann for performing some of the experiments crucial for the outcome of this work.

I give my thanks to Konrad Öchsner and Johann Kaderschabek for the installation of the FIM set up, the LED illumination for the behavioral experiments, the measurements of light intensities at the imaging set up, and the overall technical support.

In my daily work I have been blessed with a friendly and cheerful group of lab colleagues, providing an excellent atmosphere for doing research. For that I would like to thank especially Felix Frantzmann, Benedikt Hofbauer, Susanne Klühspies and Gertrud Gramlich.

I want to give my thanks to my friends Nicole Lange and Clara Heininger for always being there for me and for helping me to zone out after many hours of work, and Saskia Figueroa for proofreading my thesis.

My sincere thanks go to my parents for the unceasing encouragement, support and attention throughout all my studies.

Finally, I want to express my endless gratitude to Georgi for his immense patience, steady support, and for accompanying me on the journey called PhD.

Affidavit

I hereby confirm that my thesis entitled “Functional dissection of recurrent feedback signaling within the mushroom body network of the *Drosophila* larva” is the result of my own work. I did not receive any help or support from commercial consultants. All sources and/or materials applied are listed and specified in the thesis.

Furthermore, I confirm that this thesis has not yet been submitted as part of another examination process neither in identical nor in similar form.

Würzburg, 15.05.2019 Signature

Eidesstattliche Erklärung

gemäß § 4 Absatz 3 der Promotionsordnung der Fakultät für Biologie der Bayerischen Julius-Maximilians-Universität zu Würzburg vom 15. März 1999:

Hiermit erkläre ich an Eides statt, die Dissertation „Funktionelle Analyse einer Rückkopplungsschleife innerhalb der Pilzkörper von *Drosophila* Larven” eigenständig, d.h. insbesondere selbständig und ohne Hilfe eines kommerziellen Promotionsberaters, angefertigt und keine anderen als die von mir angegebenen Quellen und Hilfsmittel verwendet zu haben.

Ich erkläre außerdem, dass die Dissertation weder in gleicher noch in ähnlicher Form bereits in einem anderen Prüfungsverfahren vorgelegen hat.

Würzburg, 15.05.2019 Unterschrift